Testrig optimization by block loads: Remodelling of damage as Gaussian functions and their clustering method

Beim Fachbereich Mathematik
der Universität Kaiserslautern
zur Erlangung des akademischen Grades
Doktor der Naturwissenschaften
(Doctor rerum naturalium, Dr. rer. nat.)
genehmigte

Dissertation

von

Chhitiz Buchasia

Jan 2014

D 386

Contents

Acknowledgements

It is my distinct pleasure to express my deep sense of gratitude and indebtedness to my supervisor, Prof. Dr. Karl-Heinz Küfer, for giving me the opportunity to work at the Fraunhofer ITWM and to write my PhD thesis in this great environment. His invaluable guidance, encouragement and patient review were very helpful in making this thesis a success.

I would also like to thank Dr. Martin Berger for the "coffee breaks" where we had some insightful discussions on several topics and in general for his support through out my thesis. I want to thank Dr. Volker Maag for being a patient listener to what I had to say and always guiding me to the right path. Special thanks to Dr. Uwe Nowak and Dr. Alexander Scherrer for the time we spent together following each other's hobbies.

I want to thank Katrin Stöbener and Alexander Belyaev for proof reading and many useful hints. Thanks a lot to Dimitri Nowak and Katrin Teichert for bearing with me so long in our common PhD struggle. Without you the three years would have been more difficult. I would also like to give my thanks to other members of the optimization department for making the department such a lovely place to work.

I gratefully acknowledge the funding sources that made my PhD work possible. I was honoured to be the recipient of DAAD Scholarship for my first three years and two months and the Fraunhofer ITWM Scholarship for the remaining duration of four months.

I would also like to thank my best friend Anmol and his wife Priyanka for making us feel like home in a foreign country. I will always cherish your words of encouragement and support through out my life.

Lastly, special thanks to my parents and the entire family who did whatever they could to support my education. Thank you for being on my side at the various stages of my life to guide me through all the difficulties that I faced. And most of all for my loving, supportive and encouraging wife Rina whose support and patience during the final stages of this PhD is very much appreciated. Thank you.

1. Introduction

1.1. Fatigue lifetime estimation

Every year millions of automobiles are produced throughout the world. Each of these automobiles have hundreds to thousands of components. The reliability and safety of every automobile component are the main objectives of vehicle design [39]. In case a key component is damaged, automobile may break down and endanger not only the lives of its occupants but also the lives of other people near it. Therefore, automobile component testing is of utmost importance for every automobile manufacturing company.

In other words any component used in an automobile should not fail during its *expected service lifetime*. This requirement is fulfilled when the *estimated fatigue lifetime* of the component is greater than the expected service lifetime. Since Albert [2] in 1837 published the first fatigue-test results, a lot of research has been done in the field of estimating fatigue lifetime for components made of many different materials and surface features. For a detailed history of fatigue and important developments in this field, see Schütz [36].

In the beginning, most of the research on fatigue lifetime estimation was based on the data obtained from the experiments and was used for proposing models, for example, see [2, 23, 29]. This is an expensive procedure. Every time during experiments if a component failed before the expected service life, design changes were made and the newly designed component was tested again. This cycle was repeated until a design that met the requirements was arrived upon. Another approach to test the components of a vehicle is to drive the vehicles on special test tracks that have different kinds of roads to test different aspects of a vehicle design. Testing of components in this way is not only expensive but also time consuming.

Expensive and time consuming tests would lead to increase in the prices of the vehicles and the time to launch a new vehicle in the market. This is not what the automobile manufacturing companies want. It is expected that the tests should not be expensive and take less time to complete. At the same time the results obtained should be very reliable. With the advent of technology, testing of components has changed dramatically.

Technological advancements have led to the use of multi-body simulations for predicting the fatigue life of the components. However, through simulations not every aspect of the component and how it interacts with its environment can be studied. To account for these interactions and to test the component physically, testrigs are built. The reference data for the testrigs is obtained by driving the vehicle on test tracks and through multi-body simulations. Usually, the reference data consists of stress time series or total damage at some points of interest on the surface of the component.

The points of interest are regions of high damage, observed during multi-body simulations and are also called as *hotspots*.

In a testrig, a load time series is applied on the component in regions where it is in contact with other components when assembled inside a vehicle. A load time series at any point of time consists of forces and/or moments that are applied through actuators on the component. The outcome of testing on testrigs should be as close as possible to the reference data. But, the number of points where a component is in contact with other components is usually large. Constructing a testrig which is able to apply load time series at each of these points is expensive and time consuming. Furthermore, any changes to the design of the component would make such testrigs obsolete. To make the testing procedure less expensive, the number of points where actuators are applying load time series is minimized. Additionally, the total duration of testing can be reduced by decreasing the length of the load time series applied through actuators during testing. Despite all these simplifications the results obtained from the testrig are expected to be as close as possible to the reference data.

Therefore, testrig problem can be looked at as an optimization problem where the objective function is defined in such a way that it measures the closeness of the results to the reference data and the variables to be optimized are the load time series, number of the actuators and their locations. Testrig optimization is a relatively new branch of research.

1.2. Scope of this work

In our work we propose a *testrig damage optimization problem*. The approach improves upon the *testrig stress optimization problem* used as a state of the art by industry experts. We assume that the number and location of the actuators is already given so the only free parameter in the optimization is the load time series.

In both the testrig stress optimization problem as well as the testrig damage optimization problem, we optimize the load time series for a given *testrig configuration*. However, in the testrig stress optimization problem the reference data is the stress time series. So, the stress time series computed from the load time series should be as close as possible to the reference stress time series. The detailed behavior of the stresses as functions of time are sometimes not the most important topic. Instead the damage potential of the stress signals are considered. Therefore, in the end we expect that the total damage computed from the stress time series which in turn is computed as a linear superposition of the load time series is also close to the reference damage. Since damage is not part of the objectives in the testrig stress optimization problem the total damage computed from the optimized load time series is not optimal with respect to the reference damage. Additionally, the load time series obtained is as long as the reference stress time series. This makes the testing procedure relatively long. The load time series obtained as a result of the testrig stress optimization problem are general load time series which need cycle counting algorithms and Goodmann corrections before we get the total damage (see Section 2.4.2). The use of cycle counting algorithms makes the damage function from the load time series non-differentiable.

To overcome the issues discussed in the previous paragraph this thesis uses *block loads* as building

block for the load time series. Using block loads makes the damage differentiable with respect to the load time series. Additionally, in some special cases it is shown that damage is convex when block loads are used. This reduces the difficulty arising from a general load time series, as no cycle counting algorithms are required. The differentiability of the damage from the load time series with block loads enables us to use damage in the objective function of the testrig optimization problem. Optimizing load time series using damage in the objective function is what we refer to as the testrig damage optimization problem.

During every iteration of the testrig damage optimization, we have to find the maximum total damage over all plane angles at points of interest on the surface of the component. These points of interest are the regions of high damage computed through simulations or test track data. The plane with the maximum total damage is also called as the *critical plane*. The first testrig damage optimization problem presented uses discretization of the interval for plane angle to find the maximum total damage at each iteration. This however is shown to give unreliable results and makes damage function non-differentiable with respect to the plane angle. To overcome this, the damage function for a given surface stress tensor is remodeled as Gaussian functions (see Chapter 4). The parameters for the Gaussian functions that approximates damage are derived.

Remodeling of damage as Gaussian function gives new insights into the total damage computation required for the optimization. In the new model, the total damage is computed as a sum of Gaussian functions resulting from the load time series acting at each point of time. The plane with the maximum damage is similar to the modes of the Gaussian Mixture Models (GMM). A GMM is a parametric probability density function represented as a weighted sum of Gaussian component densities [31].

The difference between the Gaussian approximation of damage and GMM is that the Gaussian functions used in GMM are probability density functions which is not the case in the damage approximation presented in this work. However, the critical planes in the damage approximation corresponds to the modes of the GMM. Therefore, the mode finding algorithms in [7] for GMM or methods for merging the Gaussian mixture components in [16] can be modified to be used in the case of damage approximation. We derive conditions for a single maximum for general Gaussian functions, similar to the ones given for the unimodality of GMM by Aprausheva et al. in [3].

By using the conditions for a single maximum we give a clustering algorithm that clusters the Gaussian functions in the sum. Each cluster obtained through clustering is such that they give a single maximum in the absence of other Gaussian functions of the sum. The approximate point of maximum of the clusters is used as the starting point for a hill climbing algorithm or fixed point equation on the original damage function to get the actual maximum total damage (see Section 6.2). This actual maximum total damage is then used in the optimization.

We implement the methods on two example problems. The results obtained from the testrig damage optimization problem using discretization is shown to be better than the results obtained from the testrig stress optimization problem. Furthermore, the testrig damage optimization problem using clustering approach to finding the maximum total damage is shown to take less number of iterations and is more reliable than using discretization of the interval for the plane angle.

1.3. Outline

This work is organized as follows. In Chapter 2, we give an overview of a testrig. We introduce the important mathematical aspects involved in testrig optimization, i.e. computing stress time series from load time series and then computing total damage from stress time series. In Chapter 3, we explain the stress optimization that is the current state of the art in testrig problem. We then give a new formulation of testrig problem, using block loads defined in Chapter 2. In the new formulation, we use damage in the objective function unlike in the stress optimization where we use stress in the objective function. The maximum total damage over all plane angles is computed by discretization of the interval. We compare the results of the stress optimization and the damage optimization for two testrig configurations for a steering knuckle. We end Chapter 3 by showing that computing the maximum total damage by discretization of the interval for plane angles makes the results of the optimization less reliable due to the introduction of the discretization errors.

In Chapter 4, we remodel damage as Gaussian functions such that the plane angle is the only unknown parameter. In Chapter 5, we introduce the idea of clustering of Gaussian functions such that each cluster has a single maximum in the absence of all other Gaussian functions. This chapter also gives a clustering algorithm which we use in Chapter 6 to find the planes of maximum damage. We use the new model of damage from Chapter 4 along with the clustering algorithm developed in Chapter 5 to find the planes with maximum damage without introducing any discretization error in the optimization. Chapter 6 ends with a comparison of the two approaches on two examples. In Chapter 7, we recapitulate and discuss our approach, and indicate areas for future research.

2. Mathematical formulation of testrig optimization problem

In an *automotive testrig*, we want to approximate the *reference damage* $D^{(ref)}$ at different points of a component as close as possible to the damage induced during the service life. The points where we want to approximate the reference damage are regions of high stress also called *hotspots* or *critical points*. We approximate the reference damage at the hotspots by applying *load time series* at preselected points (also called *attachment points*) on the component. Load time series are composed of loads acting on the attachment points on the component at different moments of time. Attachment points as the name suggests are the points where the component is attached to other components of the vehicle. When the component is assembled inside the vehicle it is at the attachment points that different forces act.

In a testrig, the component is fixed at one of these attachment points (also called *fixation point*) and at the other attachment points *actuators* may be installed. An actuator enables the application of load time series at the selected attachment points. Building a testrig which is able to apply load time series at each of these attachment points is expensive and time consuming.

Testing of vehicle components in a testrig should be as short and inexpensive as possible but at the same time should reflect the actual damage that will be incurred in the component during service life. To make the testing procedure less expensive we have to minimize the number of attachment points where actuators are installed. Additionally, the total duration of testing can be reduced by decreasing the length of the load time series applied during testing.

Keeping all this in mind this chapter introduces the idea of loads, load time series and describes the computation of stress from load and damage from stress. In Section 2.1, we introduce the notion of testrig configurations. In Section 2.2, we introduce the idea of loads in general and then give a special kind of load known as a block load. The computation of stress time series from load time series is described in Section 2.3. In Section 2.3, we also define *scalar stress* and prove many of its properties which are used in Chapter 4 for approximating damage. In Section 2.4, we see how to compute the total damage from the stress time series due to the application of the load time series at the actuators.

2.1. Testrig configuration

The amount of damage incurred at any point of the component depends on the stress time series at that point due to the load time series applied through the actuators. Stress time series depends

on the attachment points where actuators are installed as well as on the magnitude of the load time series applied through these actuators. As applying load time series at each attachment point is expensive and time consuming, we want to be able to work with a small number of these attachment points. At the same time we want the damage at the selected points to be as close as possible to the reference damage $D^{(ref)}$.

Let us denote by A the total number of available attachment points for fixing or installing of actuators on the component. We denote the index of the fixation point by $A_f \in \{1, 2, \ldots, A\}$ and the index of the attachment points where actuators are installed by the set $A_a \subset \{1, 2, \ldots, A\}$. Additionally, we have $A_f \cap A_a = \emptyset$ and $n_a := |A_a|$. For the testing of a component it is necessary that both $A_f \neq \emptyset$ and $A_a \neq \emptyset$.

At each of the attachment points $\mathfrak{a} \in A_a$ we can apply forces f_x, f_y and f_z acting along x-, y- and z-axis respectively and angular moments m_x, m_y and m_z acting about the x-, y- and z-axis respectively (see in Figure 2.1). The forces can lead to compressive as well as tensile stresses which compress or elongate the component respectively. As per the convention, stresses that are positive are tensile. Positive moments act clockwise and negative moments act counter-clockwise. Altogether we have six possible ways in which we can interact with the component at each attachment point in A_a.

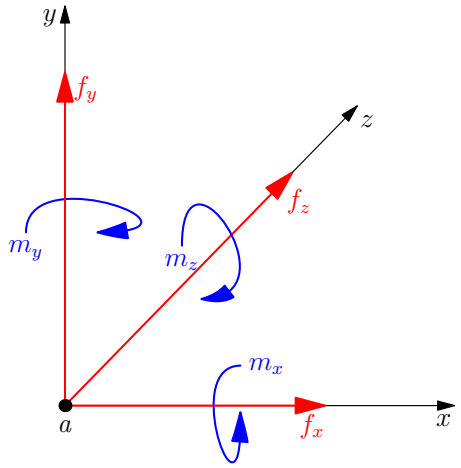

Figure 2.1.: An example of forces and moments at an attachment point $\mathfrak{a} \in A_a$ The forces f_x, f_y and f_z are shown to be acting outwards, however, it is possible to have inwards forces as well. The moments m_y and m_z are clockwise and the moment m_x is counterclockwise.

Again it is expensive to design a testrig where we interact in all six ways with a component at every attachment point in A_a. Therefore, for each attachment point in A_a we choose to apply load time series at a subset of the possible forces and moments. Keeping in mind the complexity of the components and the corresponding testrigs, it is a general belief in the industry that we do not want the total number of such forces and moments to exceed a value of four. The fixation point A_f along with the attachment points for the actuator A_a and the direction of forces and/or the moments acting at these points gives us a testrig configuration.

Definition 2.1.1 (Testrig configuration)**.** We define a testrig configuration $\mathcal{TC}$ as a 3-tuple $(A_f, A_a, \mathcal{F})$. The first element of the tuple, $A_f \in \{1, 2, \ldots, A\}$ is the index of the fixation point.

The second element of the tuple $A_a \subset \{1, 2, \ldots, A\}$ is the set of indices of the points where actuators are installed. The third element of the tuple, $\mathcal{F} := \{(\mathfrak{a}, \mathcal{F}_\mathfrak{a})\}$ is a set of 2-tuples where the first element of the tuple $\mathfrak{a} \in A_a$ is the point where an actuator is installed and the second element $\mathcal{F}_\mathfrak{a} \subset \{f_x, f_y, f_z, m_x, m_y, m_z\}$ gives us the directions of all the chosen forces and/or moments for the attachment point $\mathfrak{a}$. Additionally, we require that $A_f \cap A_a = \emptyset$.

Let us look at an example testrig configuration.

Example 2.1.2. For a component with $A = 4$, a valid testrig configuration $\mathcal{TC}$ can be given as $(1, \{2, 3\}, \{(2, \{f_x, f_y\}), (3, m_z)\})$. The fixation point is $A_f = 1$. The indices of the points where the actuators are attached are given by $A_a = \{2, 3\}$. The set of 2-tuples $\mathcal{F} = \{(2, \{f_x, f_y\}), (3, m_z)\}$ with the first tuple $(2, \{f_x, f_y\})$ meaning that at the attachment point with index 2, we apply forces along the x-axis and the y-axis and the second tuple $(3, \{m_z\})$ meaning that we apply moments around the z-axis at the actuator attached at a point with index 3. There are no forces and moments acting at the attachment point with index 4.

Now that we know what a testrig configuration $\mathcal{TC}$ means we can broadly state the goal of optimization:

For any testrig configuration $\mathcal{TC}$ give a load time series which when applied through the actuators in the testrig configuration $\mathcal{TC}$ incurs at hotspots $\mathbf{x}_i$, a total damage $D_{\mathbf{x}_i}$ as close as possible to the reference damage $D_{\mathbf{x}_i}^{(ref)}$.

However, at this point there are many open questions which need to be answered before we can actually solve the optimization problem. We still do not know how to represent a load time series and compute stress time series and corresponding total damage from it. In the sections that follow we answer these questions. We begin with section 2.2 where we look at different loads and corresponding load time series.

2.2. Load and load time series

From Section 2.1, we know how to describe different testrig configurations. In this section we look at load and load time series. In general the type and number of loads that can be applied through actuators at any point of time will depend on the testrig configuration $\mathcal{TC}$.

Let us denote by tuple $\mathfrak{F}$ all the forces and moments that are to be applied in a given testrig configuration $\mathcal{TC}$. Elements of $\mathfrak{F}$ are of the form $\mathfrak{a}_{\hat{f}}$ where $\mathfrak{a} \in A_a$ and $\hat{f} \in \{f_x, f_y, f_z, m_x, m_y, m_z\}$. At any point of time, for each element in $\mathfrak{F}$ there is a load applied on the component. So at every point of time, the load $\mathbf{l} \in \mathbb{R}^n$ is applied at actuators, where $n = |\mathfrak{F}|$. There is always a one-to-one correspondence between the elements of $\mathfrak{F}$ and $\mathbf{l}$ as highlighted in the example below:

Example 2.2.1. For the testrig configuration $\mathcal{TC}$ in Example 2.1.2, $\mathfrak{F}$ is a 3-tuple $(2_{f_x}, 2_{f_y}, 3_{m_z})$. If we have a load $\mathbf{l} = (10, 20, -5)^T$ at any point in time acting through the actuators, it implies that the forces acting through the actuator at the attachment point with index 2 in the direction of the x-axis and the y-axis are 10 and 20 newtons respectively. The moment about the z-axis at attachment point with index 3 is anticlockwise with a magnitude of 5.

Definition 2.2.2 (General load time series for testrig configuration)**.** A load time series for a testrig configuration $\mathcal{TC}$ is a matrix denoted by $\mathbf{L} \in \mathbb{R}^{n \times N}$ and is given as $\mathbf{L} := (\mathbf{l}_0, \mathbf{l}_1, \ldots, \mathbf{l}_{N-1})$ where $n = |\mathfrak{F}|$, N is the number of points in the time series and $\mathbf{l}_i \in \mathbb{R}^n, i \in \{0, 1, \ldots, N-1\}$ is the i-th column of the general load time series $\mathbf{L}$ and gives the loads acting through the actuators at the i-th point of the load time series.

Furthermore, the rows of the general load time series $\mathbf{L}$ denoted by $\mathbf{l}_j^{'}, j \in \{1, 2, \ldots, n\}$ are the load time series acting at the individual actuators corresponding to the j-th element of $\mathfrak{F}$, i.e., $\mathbf{l}_1^{'}$ corresponds to the load time series at the actuator in the first element of $\mathfrak{F}$ and so on. Before we look at an example we state the assumption on the starting and end point of the load time series.

Assumption 2.2.3. *We start with no loads, i.e.,* $\mathbf{l}_0 = \mathbf{0}_n$ *and we end with no loads, i.e.,* $\mathbf{l}_{N-1} = \mathbf{0}_n$*, where* $\mathbf{0}_n$ *is a vector of size* n *with all of its elements zero.*

Example 2.2.4. An example load time series with $N = 3$ for $\mathcal{TC}$ in Example 2.1.2 can be

$$\mathbf{L} = \begin{pmatrix} 0 & 10 & -5 & 0 \\ 0 & -5 & 10 & 0 \\ 0 & 5 & 7 & 0 \end{pmatrix}. \tag{2.1}$$

We have $\mathbf{l}_0 = (0, 0, 0)^T$, $\mathbf{l}_1 = (10, -5, 7)^T$, $\mathbf{l}_2 = (-5, 10, 5)^T$ and $\mathbf{l}_3 = (0, 0, 0)^T$. While the load time series acting at the actuator installed at the attachment point with index 2 in the direction of the x-axis is $\mathbf{l}_1^{'} = (0, 10, -5, 0)$ and in the direction of the y-axis is $\mathbf{l}_2^{'} = (0, -5, 10, 0)$ and similarly the load time series acting at actuator installed at the attachment point with index 3 about the z-axis is $\mathbf{l}_3^{'} = (0, 5, 7, 0)$.

Another way to represent a load time series is by a *line chart*. A line chart is a type of chart that displays information as a series of data points connected by straight lines. We can draw a line chart for every force/moment at each actuator as seen in Figure 2.2 for Example 2.2.4.

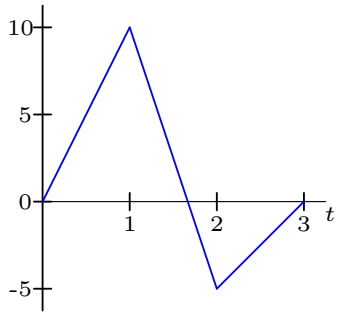

(a) Line chart for $\mathbf{l}_1^{'}$, the load time series at the attachment point with index 2 along the x-axis (2_{f_x}).

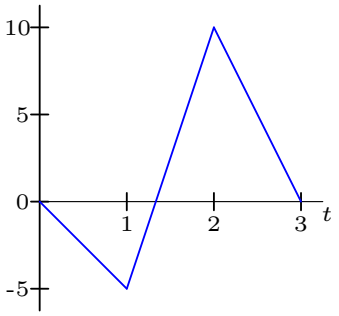

(b) Line chart for $\mathbf{l}_2^{'}$, the load time series at the attachment point with index 2 along the y-axis (2_{f_y}).

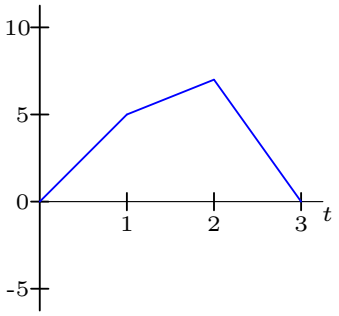

(c) Line chart for $\mathbf{l}_3^{'}$, the load time series at the attachment point with index 3 about the z-axis (3_{m_z}).

Figure 2.2.: Line charts for the rows of general load time series $\mathbf{L}$ as given in Example 2.2.4.

A complete load time series is defined only when we know all the $n(N-2)$ elements of the general

load time series $\mathbf{L}$. The general load time series are much longer and may have thousands of points thereby making the value of $n(N-2)$ large. Each element of the general load time series $\mathbf{L}$ will be a free parameter in the optimization. If we have to work with longer load time series, then the number of free parameters in the optimization problem becomes very large and would require a significant amount of processing time.

To overcome this difficulty we use block loads for each actuator (see Figure 2.3). Using block loads we can construct long load time series without significantly increasing the number of free parameters in the optimization. We define a block load in Definition 2.2.5. Examples of block loads are seen in Figure 2.3.

Definition 2.2.5 (Block load)**.** A block load $\flat \in \mathbb{R}^{4\nu+1}$ is symmetric and is defined by two parameters $\ell \in \mathbb{R}$ and $\nu \in \mathbb{N}$ as

$$\flat(\ell, \nu) = (0, \underbrace{\ell, 0, -\ell, 0, \ldots, \ell, 0, -\ell, 0}_{(\ell, 0, -\ell, 0) \text{ repeated } \nu\text{-times}}) \tag{2.2}$$

where ℓ is the amplitude of the block load and ν is the number of times a single unit of the block load is repeated.

Assumption 2.2.6. *Although we call ℓ as the amplitude of the block load, we assign ℓ to be a positive value if the block load reaches its maximum before its minimum and to be a negative value when the block load reaches its minimum before its maximum.*

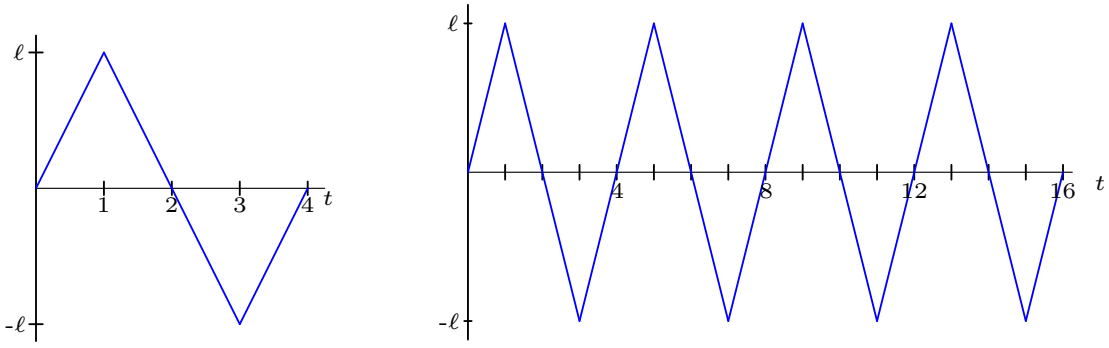

(a) Repeating unit of a block load, $\flat(\ell, 1)$ with $\ell > 0$

(b) Block load $\flat(\ell, 4)$ with $\ell > 0$ with unit $\flat(\ell, 1)$ repeated $\nu = 4$ times.

Figure 2.3.: Block load examples for (a) $\nu = 1$ and (b) $\nu = 4$.

As seen in Figure 2.3, a block load is cyclic and symmetric about the axis. By symmetry we refer to the fact that the minimum and the maximum magnitude of the repeating unit of a block load have the same magnitude. Block loads can be applied more than once to get a longer time series without increasing the number of free parameters in the optimization (see Figure 2.3(b)).

When using block loads we need just two parameters to define arbitrarily long load time series. For the same length of time series, we need $4\nu+1$ parameters to completely define the general load time series while only two parameters are needed to define the block load. Therefore, by using a block load we can considerably reduce the number of free parameters in the optimization.

However, using a single block load in optimization may not be optimal. A load time series for each actuator can be created using different block loads placed one after another acting as a building unit for the load time series. We define a load time series, acting through an actuator, consisting of only block loads as block loading $\mathscr{B}$:

Definition 2.2.7 (Block loading)**.** A block loading $\mathscr{B} \in \mathbb{R}^{n_{\mathscr{B}}}$ is defined by three parameters, $m \in \mathbb{N}$ the number of blocks, $\mathscr{L} = (\ell_1, \ell_2, \ldots, \ell_m) \in \mathbb{R}^m$ the amplitudes of the blocks and $\mathcal{V} = (\nu_1, \nu_2, \ldots, \nu_m) \in \mathbb{N}^m$ the number of times the single unit of block loads is repeated with $n_{\mathscr{B}} = 4\sum_{i=1}^{m} \nu_i + 1$ and is given as

$$\mathscr{B}(m, \mathscr{L}, \mathcal{V}) = (\flat(\ell_i, \nu_i)), i = 1, 2, \ldots, m. \tag{2.3}$$

Assumption 2.2.8. *In a block loading $\mathscr{B}$ more than one continuous points with a magnitude equal to zero are coalesced together into one point.*

Let us see with the help of an example the effect of Assumption 2.2.8 on the length of a block loading $\mathscr{B}$:

Example 2.2.9. If we have $m = 2$, $\mathscr{L} = (5, 10)$ and $\mathcal{V} = (2, 3)$. Then the block loading $\mathscr{B}$ using Assumption 2.2.8 is given as

$$\mathscr{B}(m, \mathscr{L}, \mathcal{V}) = (0, 5, 0, -5, 0, 5, 0, -5, 0, 10, \mathbf{0}, -10, 0, 10, 0, -10, 0, 10, 0, -10, 0) \in \mathbb{R}^{21}$$

and looks like the line chart in Figure 2.4. However, without Assumption 2.2.8 we have the block loading as $(0, 5, 0, -5, 0, 5, 0, -5, \mathbf{0}, \mathbf{0}, 10, 0, -10, 0, 10, 0, -10, 0, 10, 0, -10, 0) \in \mathbb{R}^{22}$. This happens because the block loads in Definition 2.2.5 begin and end with a point having zero magnitude.

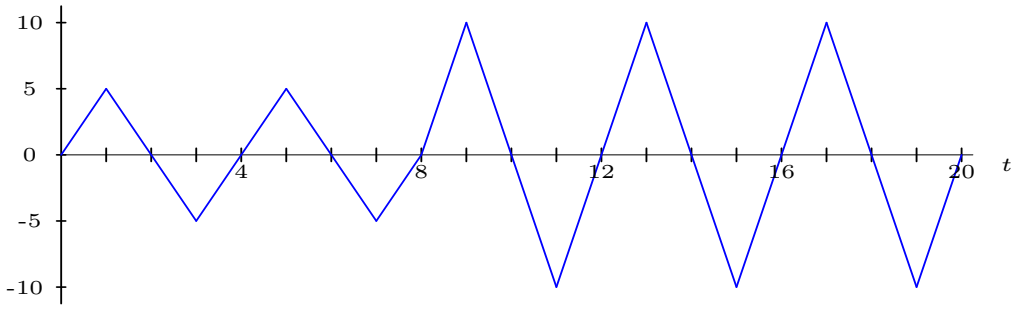

Figure 2.4.: Block loading $\mathscr{B}$ from Example 2.2.9.

For every element in $\mathfrak{F}$ (i.e. for every force/moment at each attachment point in A_a), we can give a block loading. We can redefine the general load time series $\mathbf{L}$ for testrig configuration $\mathcal{TC}$ consisting of block loading $\mathscr{B}$ as $\mathbf{L}_b$.

Remark 2.2.10. It is possible that the number of blocks and the number of repetitions for each element of $\mathfrak{F}$ are different but we can subdivide blocks such that the number of blocks and number of repetitions of a unit block in each block loading is the same. In other words we want $\mathcal{V}$ to be the same for block loadings in a load time series with block loads $\mathbf{L}_b$.

Definition 2.2.11 (Load time series for a testrig configuration with block loads)**.** A load time series for a testrig configuration $\mathcal{TC}$ with block loads is a matrix denoted by $\mathbf{L}_b \in \mathbb{R}^{n \times N}$. Each row

of the matrix is given by a block loading $\mathscr{B}(m, \mathscr{L}_i, \mathcal{V}), i = 1, 2, \ldots, n$ where $\mathscr{L}_i$ are the amplitude of individual blocks for the i-th element of $\mathfrak{F}$, m is the number of blocks and the elements of $\mathcal{V}$ are the number of times the single unit of block loads is repeated.

The loads acting through actuators at any point of time can be given as $\mathbf{l}_j = (\mathscr{B}_{1,j}, \mathscr{B}_{2,j}, \ldots, \mathscr{B}_{n,j})$, $j = 0, 1, 2, \ldots, N$ where $\mathscr{B}_{i,j}$ is the load acting at the i-th element of $\mathfrak{F}$ at the j-th point of time. Next we see a couple of examples to better understand how everything works in the case of load time series with block loads $\mathbf{L}_b$.

Example 2.2.12. We have $m = 2$ with $n = |\mathfrak{F}| = 3$. Then the load time series with block loads $\mathbf{L}_b$ consists of $n = 3$ rows given by the block loadings $\mathscr{B}_1$, $\mathscr{B}_2$ and $\mathscr{B}_3$ all having the same number of cycles for the blocks $\mathcal{V}$. We take $\mathcal{V} = (1, 2)$ and the amplitudes of the blocks is taken as $\mathscr{L}_1 = (5, 8)$, $\mathscr{L}_2 = (10, 5)$ and $\mathscr{L}_3 = (4, 4)$.

Now we can write down our block loadings acting at the elements of $\mathfrak{F}$ as

$$\begin{aligned}
&\mathscr{B}_1(m, \mathscr{L}_1, \mathcal{V}) = (0, 5, 0, -5, 0, 8, 0, -8, 0, 8, 0, -8, 0),\\
&\mathscr{B}_2(m, \mathscr{L}_2, \mathcal{V}) = (0, 10, 0, -10, 0, 5, 0, -5, 0, 5, 0, -5, 0) \text{ and}\\
&\mathscr{B}_3(m, \mathscr{L}_3, \mathcal{V}) = (0, 4, 0, -4, 0, 4, 0, -4, 0, 4, 0, -4, 0).
\end{aligned}$$

Finally, the load time series with block loads $\mathbf{L}_b$ is given as

$$\mathbf{L}_b = \begin{pmatrix} 0 & 5 & 0 & -5 & 0 & 8 & 0 & -8 & 0 & 8 & 0 & -8 & 0 \\ 0 & 10 & 0 & -10 & 0 & 5 & 0 & -5 & 0 & 5 & 0 & -5 & 0 \\ 0 & 4 & 0 & -4 & 0 & 4 & 0 & -4 & 0 & 4 & 0 & -4 & 0 \end{pmatrix} \tag{2.4}$$

The loads acting through the actuators at any point of time can be given as $\mathbf{l}_{2i} = \mathbf{0}_3$ for all $i = 0, 1, \ldots, 6$, $\mathbf{l}_1 = (5, 10, 4)^T$, $\mathbf{l}_3 = (-5, -10, -4)^T$, $\mathbf{l}_5 = (8, 5, 4)^T$, $\mathbf{l}_7 = (-8, -5, -4)^T$ and so on.

Example 2.2.13. In Example 2.2.12, we saw how we get the load time series with block loads $\mathbf{L}_b$ when we are given m, n, $\mathcal{V}$ and $\mathscr{L}_i, i = 1, 2, \ldots, n$. However, we can go the other way round as well, i.e., given the load time series with block loads $\mathbf{L}_b$ we can get all other values. Suppose we have been given $\mathbf{L}_b$ as:

$$\mathbf{L}_b = \begin{pmatrix} 0 & -3 & 0 & 3 & 0 & 6 & 0 & -6 & 0 & 7 & 0 & -7 & 0 & 7 & 0 & -7 & 0 \\ 0 & 7 & 0 & -7 & 0 & 2 & 0 & -2 & 0 & 5 & 0 & -5 & 0 & 5 & 0 & -5 & 0 \\ 0 & 4 & 0 & -4 & 0 & 4 & 0 & -4 & 0 & 4 & 0 & -4 & 0 & 4 & 0 & -4 & 0 \\ 0 & 9 & 0 & -9 & 0 & 1 & 0 & -1 & 0 & 4 & 0 & -4 & 0 & 4 & 0 & -4 & 0 \end{pmatrix}. \tag{2.5}$$

Then we know that the number of rows of $\mathbf{L}_b$ is n which implies $n = 4$. The number of blocks is $m = 3$ with $\mathcal{V} = (1, 1, 2)$ and $\mathscr{L}_1 = (-3, 6, 7)$, $\mathscr{L}_2 = (7, 2, 5)$, $\mathscr{L}_3 = (4, 4, 4)$ and $\mathscr{L}_4 = (9, 1, 4)$.

In this section, we defined a general load time series for a testrig configuration $\mathcal{TC}$ as $\mathbf{L}$ and a load time series for testrig configuration $\mathcal{TC}$ with block loads as $\mathbf{L}_b$. We also made a distinction between the load time series for individual direction of forces/moments applied at an actuator and a load time series for the complete testrig configuration at each point of time. We denoted by $\mathbf{l}_j$ the loads acting through all the actuators at the j-th point in the load time series. In Section 2.3, we see how the load time series can be used to compute the stress time series at any point of the component which in turn can be used to compute the total damage at that point.

2.3. Stress

Computation of the total damage at a hotspot $\mathbf{x}$ on the surface of the component depends on the stress time series at that point. Before we can compute the total damage at any point due to a load time series applied through the actuators, we have to compute the stress time series at that point. In this section, we see how to compute stress acting at any point of time on the component due to a load $\mathbf{l}$ acting through the actuators at that point of time. Specifically, we only consider the points on the surface of the component as it is well known that the fatigue cracks usually initiate from the surface (see [20, p. 58] and [21]).

In general, stress at any point of a component can be specified by the three orthogonal normal stresses (relative to the chosen coordinate system) σ_{xx}, σ_{yy}, σ_{zz} and three orthogonal shear stresses σ_{xy}, σ_{xz}, σ_{yz}. However on the surface of the component only the entries σ_{xx}, σ_{yy} and σ_{xy} are unequal to zero. The stress at any hotspot $\mathbf{x}$ due to load $\mathbf{l}$ can then be given as $\boldsymbol{\sigma}_{\mathbf{x}}(\mathbf{l}) = (\sigma_{\mathbf{x},xx}(\mathbf{l}), \sigma_{\mathbf{x},yy}(\mathbf{l}), \sigma_{\mathbf{x},xy}(\mathbf{l}))^T$. In Figure 2.5, we see the components of $\boldsymbol{\sigma}_{\mathbf{x}}$ acting on a infinitesimal material element around a hotspot $\mathbf{x}$.

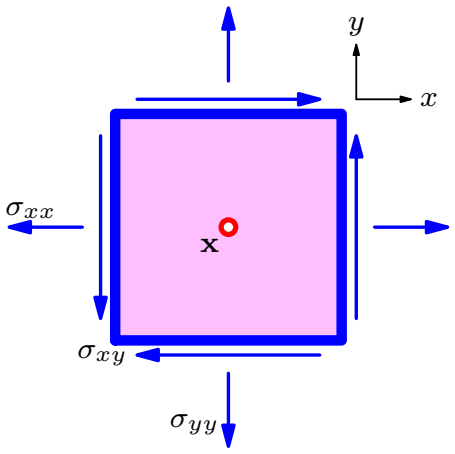

Figure 2.5.: Stress components σ_{xx}, σ_{yy} and σ_{xy} at $\mathbf{x}$ (considering a two-dimensional infinitesimal material element around hotspot $\mathbf{x}$). σ_{xx} and σ_{yy} are the tensile stresses and σ_{xy} is the shear stress.

For every testrig configuration $\mathcal{TC}$, we get from linear Finite Element computations a stress tensor $\tilde{\boldsymbol{\sigma}}_{\mathbf{x}} \in \mathbb{R}^{3\times n}$ with $n = |\mathfrak{F}|$, for every hotspot $\mathbf{x}$ on the surface of the component. The stress tensor $\tilde{\boldsymbol{\sigma}}_{\mathbf{x}}$ encapsulates the application of unit loads at each force/moment and actuator combination that is present in $\mathfrak{F}$. Using the principle of linear superposition as in Vecchio et al. [38], we can then give the stress $\boldsymbol{\sigma}_{\mathbf{x}}$ at hotspot $\mathbf{x}$ due to a load $\mathbf{l}$ through the actuators as

$$\boldsymbol{\sigma}_{\mathbf{x}}(\mathbf{l}) := \tilde{\boldsymbol{\sigma}}_{\mathbf{x}} \cdot \mathbf{l} = \begin{pmatrix} \sigma_{xx,\mathbf{x}}(\mathbf{l}) \\ \sigma_{yy,\mathbf{x}}(\mathbf{l}) \\ \sigma_{xy,\mathbf{x}}(\mathbf{l}) \end{pmatrix}. \tag{2.6}$$

Similarly, the stress time series $\mathbf{\Sigma_x}$ at hotspot $\mathbf{x}$ due to a load time series $\mathfrak{L}$ is given as

$$\mathbf{\Sigma_x}(\mathfrak{L}) = \tilde{\boldsymbol{\sigma}}_\mathbf{x} \cdot \mathfrak{L} = \begin{pmatrix} \sigma_{xx,\mathbf{x}}(\mathbf{l}_i) \\ \sigma_{yy,\mathbf{x}}(\mathbf{l}_i) \\ \sigma_{xy,\mathbf{x}}(\mathbf{l}_i) \end{pmatrix} \tag{2.7}$$

where $i = 0, 1, 2, \ldots, N$ and $\mathfrak{L}$ can be a general load time series $\mathbf{L}$ or a load time series with block loads $\mathbf{L}_b$.

The stress components obtained through linear superposition in Eq. (2.6) are in the coordinate system such that the orientation of the z-axis is normal to the surface. It is however not necessary that the maximum stress is obtained in this coordinate system. So, we are really interested to know the stresses on the planes oriented at an angle α (referred to as plane) to the x-axis (see Figure 2.6). Then, we can compute the maximum stress due to load a $\mathbf{l}$ and the plane α for which the maximum stress is obtained. We need a means to transform the stresses to these new $x'y'$ planes oriented at α to the original x-axis. From Figure 2.6, it can be clearly seen that $\alpha \in [0, \pi)$.

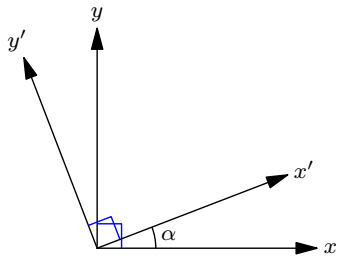

Figure 2.6.: Coordinate axes x' and y' oriented at α to the original x-axis.

In the following discussions, we assume that we have already computed the stress $\boldsymbol{\sigma}$ for any given point and load and therefore, we drop the dependence of $\boldsymbol{\sigma}$ on $\mathbf{x}$ and $\mathbf{l}$. Roylance gives in [34], the following equation for the components of the stress $\boldsymbol{\sigma}$ in the $x'y'$ coordinate axes:

$$\begin{aligned} \sigma_{x'x'}(\boldsymbol{\sigma}, \alpha) &= \sigma_{xx}\cos^2\alpha + \sigma_{yy}\sin^2\alpha + 2\sigma_{xy}\sin\alpha\cos\alpha \\ \sigma_{y'y'}(\boldsymbol{\sigma}, \alpha) &= \sigma_{xx}\sin^2\alpha + \sigma_{yy}\cos^2\alpha - 2\sigma_{xy}\sin\alpha\cos\alpha \\ \sigma_{x'y'}(\boldsymbol{\sigma}, \alpha) &= (\sigma_{yy} - \sigma_{xx})\sin\alpha\cos\alpha + \sigma_{xy}(\cos^2\alpha - \sin^2\alpha) \end{aligned} \tag{2.8}$$

We want to compute the damage for the plane α which has the stress with the largest magnitude. Using any other value of stress gives us an underestimation of the damage and the component will fail before the estimated life. In the next result we show that for a given stress $\boldsymbol{\sigma}$ the maximum absolute value of components $\sigma_{x'x'}$ and $\sigma_{y'y'}$ are the same which is more than the maximum absolute value of $\sigma_{x'y'}$. We therefore use without loss of generality $\sigma_{x'x'}$ for damage computation.

Theorem 2.3.1. *Given stress $\boldsymbol{\sigma}$, the components of stress on the coordinate axes $x'y'$ oriented on a plane α to the original x-axis from Eq.* (2.8) *have the following properties:*

(i) $\max_\alpha |\sigma_{x'x'}(\boldsymbol{\sigma}, \alpha)| = \max_\alpha |\sigma_{y'y'}(\sigma, \alpha)|$ *and*

(ii) $\max_\alpha |\sigma_{x'x'}(\boldsymbol{\sigma}, \alpha)| \geq \max_\alpha |\sigma_{x'y'}(\boldsymbol{\sigma}, \alpha)|$.

Before we prove Theorem 2.3.1, we give a result from Trigonometry which we will use for the proof.

Lemma 2.3.2. *Any linear combination of sine and cosine with same period can be written as a single sine with the same period but with a phase shift and a different amplitude. Mathematically this is equivalent to*

$$y_1 \sin x + y_2 \cos x = b \sin(x + \phi)$$

where $b\cos\phi = y_1$, $b\sin\phi = y_2$ *and* $b = \sqrt{y_1^2 + y_2^2}$.

Proof. For proof see [14, p. 190-191]. Additionally, we know from the equation $b\cos\phi = y_1$ and $b\sin\phi = y_2$ that another representation of ϕ is $sgn(y_2)\cos^{-1}\left(\frac{y_1}{b}\right)$. □

Proof of Theorem 2.3.1. We transform the components of the stress $\boldsymbol{\sigma}$ on the $x'y'$ coordinate axis so that we can use Lemma 2.3.2 to get a simpler form and then look at the maximum absolute value. We begin by simplifying $\sigma_{x'x'}$ first

$$\sigma_{x'x'}(\boldsymbol{\sigma}, \alpha) = \sigma_{xx}\cos^2\alpha + \sigma_{yy}\sin^2\alpha + 2\sigma_{xy}\sin\alpha\cos\alpha$$

Using $\sin^2\alpha = \frac{1}{2}(1 - \cos 2\alpha)$, $\cos^2\alpha = \frac{1}{2}(1 + \cos 2\alpha)$ and $2\sin\alpha\cos\alpha = \sin 2\alpha$ we get

$$= \frac{\sigma_{xx}}{2}(1 + \cos 2\alpha) + \frac{\sigma_{yy}}{2}(1 - \cos 2\alpha) + \sigma_{xy}\sin 2\alpha$$

Collecting $\cos 2\alpha$ and constant terms together

$$= \frac{1}{2}(\sigma_{xx} + \sigma_{yy}) + \frac{1}{2}(\sigma_{xx} - \sigma_{yy})\cos 2\alpha + \sigma_{xy}\sin 2\alpha$$

We define $\hat{a}(\boldsymbol{\sigma}) := \frac{1}{2}(\sigma_{xx} + \sigma_{yy})$ and use Lemma 2.3.2 to get

$$= \hat{a}(\boldsymbol{\sigma}) + b(\boldsymbol{\sigma})\sin(2\alpha + \phi(\boldsymbol{\sigma})) \tag{2.9}$$

where $b(\boldsymbol{\sigma}) := \sqrt{\frac{1}{4}(\sigma_{xx} - \sigma_{yy})^2 + \sigma_{xy}^2}$ and $\phi(\boldsymbol{\sigma}) := sgn(\sigma_{xx} - \sigma_{yy})\cos^{-1}\left(\frac{\sigma_{xy}}{b(\boldsymbol{\sigma})}\right)$. Observing that the sine function is bounded between $[-1, 1]$, the maximum value of $|\sigma_{x'x'}(\boldsymbol{\sigma}, \alpha)|$ with respect to α for a given stress $\boldsymbol{\sigma}$ follows directly from Eq. (2.9) as

$$\max_{\alpha} |\sigma_{x'x'}| = \begin{cases} |\hat{a}(\boldsymbol{\sigma}) + b(\boldsymbol{\sigma})|, & \text{if } \hat{a}(\boldsymbol{\sigma}) \geq 0 \\ |\hat{a}(\boldsymbol{\sigma}) - b(\boldsymbol{\sigma})|, & \text{if } \hat{a}(\boldsymbol{\sigma}) < 0 \end{cases} \tag{2.10}$$

The steps for finding the maximum absolute value of $\sigma_{y'y'}$ are the same as for $\sigma_{x'x'}$ and after simplification we get:

$$\sigma_{y'y'}(\boldsymbol{\sigma}, \alpha) = \hat{a}(\boldsymbol{\sigma}) - b(\boldsymbol{\sigma})\sin(2\alpha + \phi(\boldsymbol{\sigma}))$$

where $b(\boldsymbol{\sigma})$ and $\phi(\boldsymbol{\sigma})$ are the same as in Eq. (2.9). The maximum value of $|\sigma_{y'y'}(\boldsymbol{\sigma}, \alpha)|$ with respect to α for a given $\boldsymbol{\sigma}$ is

$$\max_{\alpha} |\sigma_{y'y'}| = \begin{cases} |\hat{a}(\boldsymbol{\sigma}) + b(\boldsymbol{\sigma})|, & \text{if } \hat{a}(\boldsymbol{\sigma}) \geq 0 \\ |\hat{a}(\boldsymbol{\sigma}) - b(\boldsymbol{\sigma})|, & \text{if } \hat{a}(\boldsymbol{\sigma}) < 0 \end{cases} \tag{2.11}$$

From Eq. (2.10) and Eq. (2.11) statement (i) of the theorem follows.

We can simplify $\sigma_{x'y'}(\boldsymbol{\sigma}, \alpha)$ as below:

$$\sigma_{x'y'}(\boldsymbol{\sigma}, \alpha) = (\sigma_{yy} - \sigma_{xx}) \sin\alpha \cos\alpha + \sigma_{xy}(\cos^2\alpha - \sin^2\alpha)$$

Using $\cos^2\alpha - \sin^2\alpha = \cos 2\alpha$ and $2\sin\alpha\cos\alpha = \sin 2\alpha$ we get

$$= \frac{\sigma_{yy} - \sigma_{xx}}{2} \sin 2\alpha + \sigma_{xy} \cos 2\alpha$$

Using Lemma 2.3.2 to get

$$= b(\boldsymbol{\sigma}) \sin(2\alpha + \psi(\boldsymbol{\sigma}))$$

where $b(\boldsymbol{\sigma})$ is same as in Eq. (2.9) and $\psi(\boldsymbol{\sigma}) = sgn(\sigma_{xy}) \cos^{-1}\left(\frac{\sigma_{yy}-\sigma_{xx}}{2b(\boldsymbol{\sigma})}\right)$. The maximum value of $|\sigma_{x'y'}(\boldsymbol{\sigma}, \alpha)|$ with respect to α is given as

$$\max_{\alpha} |\sigma_{x'y'}(\boldsymbol{\sigma}, \alpha)| = b(\boldsymbol{\sigma}).$$

Hence, if $\hat{a}(\boldsymbol{\sigma}) = 0$ we have $\max_\alpha |\sigma_{x'y'}(\boldsymbol{\sigma}, \alpha)| = \max_\alpha |\sigma_{x'x'}(\boldsymbol{\sigma}, \alpha)|$ and for all other values of $\hat{a}(\boldsymbol{\sigma})$ we have $\max_\alpha |\sigma_{x'y'}(\boldsymbol{\sigma}, \alpha)| < \max_\alpha |\sigma_{x'x'}(\boldsymbol{\sigma}, \alpha)|$. □

From Theorem 2.3.1, we see that the maximum absolute value of $\sigma_{x'x'}$ and $\sigma_{y'y'}$ is equal. Without loss of generality we proceed ahead with $\sigma_{x'x'}$ and rename it as s which denotes the scalar stress.

Definition 2.3.3. The scalar stress s for stress σ on a plane α is defined as

$$s(\boldsymbol{\sigma}, \alpha) := \hat{a}(\boldsymbol{\sigma}) + b(\boldsymbol{\sigma}) \sin\left(2\alpha + \phi(\boldsymbol{\sigma})\right). \tag{2.12}$$

$\hat{a}(\boldsymbol{\sigma})$ can be positive as well as negative. We denote by $a(\boldsymbol{\sigma})$ the absolute value of $\hat{a}(\boldsymbol{\sigma})$, i.e., $a(\boldsymbol{\sigma}) := |\hat{a}(\boldsymbol{\sigma})|$. In the next remark other representations of the scalar stress are given:

Remark 2.3.4. Other representations of $s(\boldsymbol{\sigma}, \alpha)$ as defined in Eq. (2.12) are

(i) $s(\boldsymbol{\sigma}, \alpha) = \dfrac{\sigma_{xx} + \sigma_{yy}\tan^2\alpha + 2\sigma_{xy}\tan\alpha}{1 + \tan^2\alpha}$

(ii) When a load $\mathbf{l}$ is given then the scalar stress s can be computed as

$$s(\boldsymbol{\sigma}(\mathbf{l}), \alpha) = \mathbf{n}(\alpha) \cdot \boldsymbol{\sigma}(\mathbf{l}) = \mathbf{n}(\alpha) \cdot \tilde{\boldsymbol{\sigma}} \cdot \mathbf{l}, \tag{2.13}$$

where

$$\mathbf{n}(\alpha) := \left(\frac{1}{2}\left(1 + \cos 2\alpha\right), \frac{1}{2}\left(1 - \cos 2\alpha\right), \sin 2\alpha\right). \tag{2.14}$$

We use this particular representation from here onwards.

In case of a stress time series $\mathbf{\Sigma}$ we can give a scalar stress time series $\mathbf{S}$ for plane α as

$$\mathbf{S}(\mathbf{\Sigma}, \alpha) = \mathbf{n}(\alpha) \cdot \mathbf{\Sigma}. \tag{2.15}$$

In the next theorem, we prove that the scalar stress s is a periodic function and derive its period length. We show later that the periodicity of the scalar stress s implies that the damage d is also periodic with the same period length. Next we give a definition of a periodic function which we use for the proof of s being periodic.

Definition 2.3.5 (Periodic function)**.** A function f is said to be periodic with period P, ($P > 0$, $P \in \mathbb{R}$) if we have

$$f(x + P) = f(x) \tag{2.16}$$

for all values of x. P is the minimal value for which condition (2.16) holds.

Theorem 2.3.6. *The scalar stress s in Eq. (2.12) is periodic with period π.*

Proof. From Definition 2.3.5, we know that the scalar stress s would be periodic if we can find any $P > 0$ such that $s(\boldsymbol{\sigma}, \alpha + P) = s(\boldsymbol{\sigma}, \alpha)$. Proceeding in this direction, we get from Eq. (2.12)

$$s(\boldsymbol{\sigma}, \alpha + P) = \hat{a}(\boldsymbol{\sigma}) + b(\boldsymbol{\sigma}) \sin(2(\alpha + P) + \phi(\boldsymbol{\sigma}))$$

Using the sum formula for sines $\sin(x + y) = \sin(x)\cos(y) + \cos(x)\sin(y)$ we get

$$= \hat{a}(\boldsymbol{\sigma}) + b(\boldsymbol{\sigma}) \sin(2\alpha + \phi(\boldsymbol{\sigma})) \cos(2P) + b(\boldsymbol{\sigma}) \sin(2P) \cos(2\alpha + \phi(\boldsymbol{\sigma})).$$

Comparing like terms in $s(\boldsymbol{\sigma}, \alpha + P)$ and $s(\boldsymbol{\sigma}, \alpha)$ we get $\cos(2P) = 1$ and $\sin(2P) = 0$. The values of P that simultaneously satisfy these two equations are $P = n\pi, n \in \mathbb{Z}$. From the definition of periodic functions, P is minimal and more than zero. Therefore, we take $n = 1$ to get $P = \pi$. Hence, we have proven that indeed the scalar stress s is a periodic function and its period is $P = \pi$. □

Assumption 2.3.7. *From Theorem 2.3.6 the scalar stress s is periodic with period π and therefore without loss of generality we can assume that all points of maximum and minimum lie in the interval $[0, \pi)$ which has a width of π.*

As a consequence of Theorem 2.3.6, we can now take $\alpha \in [0, \pi)$. We had come to the same conclusion from Figure 2.6. The graph of scalar stress s in one period may lie completely below the horizontal axis, completely above the horizontal axis or may cross the horizontal axis. In Figure 2.7, we can see the three cases. Amount of damage incurred depends on the magnitude of the scalar stress. The maximum absolute value and the minimum absolute value of the scalar stress computation for the first two cases in Figure 2.7 is different from the third case as discussed in the results which follow.

In the next theorem we give conditions which if satisfied, the scalar stress is either always non-negative or always non-positive representing the cases in Figure 2.7(a) and Figure 2.7(b).

Theorem 2.3.8. *For a given stress $\boldsymbol{\sigma}$ whenever $a(\boldsymbol{\sigma}) \geq b(\boldsymbol{\sigma})$, one of the following conditions is true,*

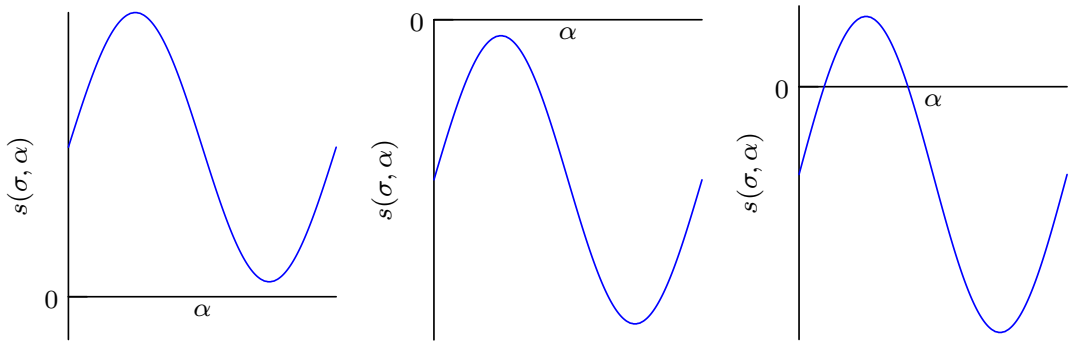

(a) Sample graph for the case $s(\sigma,\alpha) \geq 0, \forall \alpha \in [0,\pi)$.

(b) Sample graph for the case $s(\sigma,\alpha) \leq 0, \forall \alpha \in [0,\pi)$.

(c) Sample graph for the case when scalar stress crosses the horizontal axis.

Figure 2.7.: Possible graphs of scalar stress $s(\boldsymbol{\sigma},\alpha)$ for $\alpha \in [0,\pi)$ for given stress $\boldsymbol{\sigma}$.

(i) If $\hat{a}(\boldsymbol{\sigma}) \geq 0$*, then* $s(\boldsymbol{\sigma},\alpha) \geq 0, \forall\, \alpha \in \mathbb{R}$*,*

(ii) If $\hat{a}(\boldsymbol{\sigma}) < 0$*, then* $s(\boldsymbol{\sigma},\alpha) \leq 0, \forall\, \alpha \in \mathbb{R}$*.*

Proof. (i) If $\hat{a}(\boldsymbol{\sigma}) \geq 0$ we have $a(\boldsymbol{\sigma}) = \hat{a}(\boldsymbol{\sigma})$. The scalar stress s can then be written as

$$s(\boldsymbol{\sigma},\alpha) = a(\boldsymbol{\sigma}) + b(\boldsymbol{\sigma})\sin(2\alpha+\phi).$$

Since, $a(\boldsymbol{\sigma}) \geq b(\boldsymbol{\sigma})$ we get $s(\boldsymbol{\sigma},\alpha) \geq 0, \forall\ \alpha \in \mathbb{R}$.

(ii) If $\hat{a}(\boldsymbol{\sigma}) < 0$ we have $a(\boldsymbol{\sigma}) = -\hat{a}(\boldsymbol{\sigma})$. The scalar stress s can then be written as

$$s(\boldsymbol{\sigma},\alpha) = -a(\boldsymbol{\sigma}) + b(\boldsymbol{\sigma})\sin(2\alpha+\phi).$$

Since, $a(\boldsymbol{\sigma}) \geq b(\boldsymbol{\sigma})$ we get $s(\boldsymbol{\sigma},\alpha) \leq 0, \forall\ \alpha \in \mathbb{R}$. □

The conditions (i) and (ii) in Theorem 2.3.8 when combined, imply that the scalar stress s is always on one side of the horizontal axis if $a(\boldsymbol{\sigma}) \geq b(\boldsymbol{\sigma})$. If $\hat{a}(\boldsymbol{\sigma})$ is non-negative, then the scalar stress s is entirely above the horizontal axis and if $\hat{a}(\boldsymbol{\sigma})$ is negative, then the scalar stress s is entirely below the horizontal axis. We give another representation of the condition $a(\boldsymbol{\sigma}) \geq b(\boldsymbol{\sigma})$ in terms of the components of the stress $\boldsymbol{\sigma}$.

Theorem 2.3.9. *The inequality* $\sigma_{xx}\sigma_{yy} \geq \sigma_{xy}^2$ *holds iff* $a(\boldsymbol{\sigma}) \geq b(\boldsymbol{\sigma})$.

Proof. Using the definition of $a(\boldsymbol{\sigma})$ and $b(\boldsymbol{\sigma})$ the condition $a(\boldsymbol{\sigma}) \geq b(\boldsymbol{\sigma})$ can be written as

$$\frac{1}{2}\left|\sigma_{xx}+\sigma_{yy}\right| \geq \sqrt{\frac{1}{4}\left(\sigma_{xx}-\sigma_{yy}\right)^2+\sigma_{xy}^2}.$$

On squaring the two sides we get

$$\Leftrightarrow \frac{1}{4}(\sigma_{xx}+\sigma_{yy})^2 \geq \frac{1}{4}\left(\sigma_{xx}-\sigma_{yy}\right)^2+\sigma_{xy}^2.$$

We know $(a+b)^2-(a-b)^2=4ab$ which implies

$$\Leftrightarrow \sigma_{xx}\sigma_{yy} \geq \sigma_{xy}^2.$$

Proof is complete as all the relations above are if and only if relations. □

Theorem 2.3.9 equips us with a condition that we can use to check if the scalar stress crosses the axis without having to compute $a(\boldsymbol{\sigma})$ and $b(\boldsymbol{\sigma})$. For computing damage the magnitude of the stress is important. It does not matter if the scalar stress is compressive or tensile, only the magnitude is important. Next we find the maximum and the minimum value of $|s(\boldsymbol{\sigma},\alpha)|$ in case $a(\boldsymbol{\sigma}) \geq b(\boldsymbol{\sigma})$ for $\alpha \in [0,\pi)$. We will use this in the approximation of damage by Gaussian functions in Chapter 4.

Theorem 2.3.10. *For fixed $\boldsymbol{\sigma}$ with $a(\boldsymbol{\sigma}) \geq b(\boldsymbol{\sigma})$ and the scalar stress s as in (2.12) the maximum value of $|s(\boldsymbol{\sigma},\alpha)|$ for $\alpha \in [0,\pi)$ is*

$$s^+_{max}(\boldsymbol{\sigma}) = \max_{\alpha} |s(\boldsymbol{\sigma},\alpha)| = a(\boldsymbol{\sigma}) + b(\boldsymbol{\sigma}), \tag{2.17}$$

at

$$\alpha^+_{max}(\boldsymbol{\sigma}) = \begin{cases} \frac{\pi}{4} - \frac{\phi(\boldsymbol{\sigma})}{2} + n_1\pi, & \text{if } \hat{a} \geq 0 \\ -\frac{\pi}{4} - \frac{\phi(\boldsymbol{\sigma})}{2} + n_1\pi, & \text{if } \hat{a} < 0 \end{cases}, \tag{2.18}$$

and the minimum value of $|s(\boldsymbol{\sigma},\alpha)|$ is

$$s^+_{min}(\boldsymbol{\sigma}) = \min_{\alpha} |s(\boldsymbol{\sigma},\alpha)| = a(\boldsymbol{\sigma}) - b(\boldsymbol{\sigma}), \tag{2.19}$$

at

$$\alpha^+_{min}(\boldsymbol{\sigma}) = \begin{cases} -\frac{\pi}{4} - \frac{\phi(\boldsymbol{\sigma})}{2} + n_2\pi, & \text{if } \hat{a} \geq 0 \\ \frac{\pi}{4} - \frac{\phi(\boldsymbol{\sigma})}{2} + n_2\pi, & \text{if } \hat{a} < 0 \end{cases}, \tag{2.20}$$

where $n_1, n_2 \in \mathbb{Z}$.

Proof. From Eq. (2.12) the scalar stress $s(\boldsymbol{\sigma},\alpha)$ is given by

$$s(\boldsymbol{\sigma},\alpha) = \hat{a}(\boldsymbol{\sigma}) + b(\boldsymbol{\sigma})\sin(2\alpha + \phi(\boldsymbol{\sigma}))$$

We consider the two cases $\hat{a}(\boldsymbol{\sigma}) \geq 0$ and $\hat{a}(\boldsymbol{\sigma}) < 0$ separately:

(i) If $\hat{a}(\boldsymbol{\sigma}) \geq 0$, then $a(\boldsymbol{\sigma}) = \hat{a}(\boldsymbol{\sigma})$. The maximum value of $|s(\boldsymbol{\sigma},\alpha)|$ is computed as

$$s^+_{max}(\boldsymbol{\sigma}) = \max_{\alpha} |a(\boldsymbol{\sigma}) + b(\boldsymbol{\sigma})\sin(2\alpha + \phi(\boldsymbol{\sigma}))|.$$

We have $a(\boldsymbol{\sigma})$ and $b(\boldsymbol{\sigma})$ are positive and do not depend on α. Additionally condition (i) in Theorem 2.3.8 implies that the scalar stress is positive which in turn implies

$$s^+_{max}(\boldsymbol{\sigma}) = a(\boldsymbol{\sigma}) + b(\boldsymbol{\sigma}) \max_{\alpha} \sin(2\alpha + \phi(\boldsymbol{\sigma})).$$

The maximum value of $\sin(2\alpha + \phi(\boldsymbol{\sigma}))$ is one whenever

$$2\alpha + \phi(\boldsymbol{\sigma}) = \frac{\pi}{2} + 2n_1\pi.$$

The maximum occurs at $\alpha^+_{max}(\boldsymbol{\sigma})$ which results in

$$\alpha^+_{max}(\boldsymbol{\sigma}) = \frac{\pi}{4} - \frac{\phi(\boldsymbol{\sigma})}{2} + n_1\pi$$

where $n_1 \in \mathbb{Z}$. Finally we get

$$s^+_{max}(\boldsymbol{\sigma}) = a(\boldsymbol{\sigma}) + b(\boldsymbol{\sigma}).$$

Analogously, the minimum value of $\sin(2\alpha + \phi(\boldsymbol{\sigma}))$ is -1 whenever

$$2\alpha + \phi(\boldsymbol{\sigma}) = -\frac{\pi}{2} + 2n_2\pi.$$

The minimum occurs at $\alpha^+_{min}(\boldsymbol{\sigma})$ which results in

$$\alpha^+_{min}(\boldsymbol{\sigma}) = -\frac{\pi}{4} - \frac{\phi(\boldsymbol{\sigma})}{2} + n_2\pi$$

where $n_2 \in \mathbb{Z}$. In the end we get

$$s^+_{min}(\boldsymbol{\sigma}) = a(\boldsymbol{\sigma}) + b(\boldsymbol{\sigma}) \min_{\alpha} \sin(2\alpha + \phi(\boldsymbol{\sigma})) = a(\boldsymbol{\sigma}) - b(\boldsymbol{\sigma}).$$

(ii) If $\hat{a}(\boldsymbol{\sigma}) < 0$, then $a(\boldsymbol{\sigma}) = -\hat{a}(\boldsymbol{\sigma})$. The proof is similar to the proof of the case $\hat{a}(\boldsymbol{\sigma}) \geq 0$ with the difference that the points of the maximum and the minimum value of $|s(\boldsymbol{\sigma}, \alpha)|$ in the two cases are swapped. Condition (ii) in Theorem 2.3.8 implies that the scalar stress is negative in this case yields

$$\begin{aligned} s^+_{max}(\boldsymbol{\sigma}) &= \max_{\alpha} -\hat{a}(\boldsymbol{\sigma}) - b(\boldsymbol{\sigma}) \sin(2\alpha + \phi) \\ &= \max_{\alpha} a(\boldsymbol{\sigma}) - b(\boldsymbol{\sigma}) \sin(2\alpha + \phi). \end{aligned} \tag{2.21}$$

Both $a(\boldsymbol{\sigma})$ and $b(\boldsymbol{\sigma})$ are positive therefore the maximum value is obtained when we have $\sin(2\alpha + \phi) = -1$ or when $\alpha^+_{max}(\boldsymbol{\sigma}) = -\frac{\pi}{4} - \frac{\phi(\boldsymbol{\sigma})}{2} + n_1\pi, n_1 \in \mathbb{Z}$. Inserting $\sin(2\alpha + \phi) = -1$ in (2.21) we get

$$s^+_{max}(\boldsymbol{\sigma}) = a(\boldsymbol{\sigma}) + b(\boldsymbol{\sigma}). \tag{2.22}$$

Similarly, the minimum value of $|s(\boldsymbol{\sigma}, \alpha)|$ is obtained when we have $\sin(2\alpha + \phi) = 1$ or $\alpha^+_{min}(\boldsymbol{\sigma}) = \frac{\pi}{4} - \frac{\phi(\boldsymbol{\sigma})}{2} + n_2\pi, n_2 \in \mathbb{Z}$ which implies

$$s^+_{min}(\boldsymbol{\sigma}) = a(\boldsymbol{\sigma}) - b(\boldsymbol{\sigma}).$$

This completes the proof. □

From Theorem 2.3.10 we have that $\left|\alpha^+_{max}(\boldsymbol{\sigma}) - \alpha^+_{min}(\boldsymbol{\sigma})\right| = \frac{\pi}{2}$. This implies that if we want an interval of width π centered around $\alpha^+_{max}(\boldsymbol{\sigma})$ then the end points of the interval are $\alpha^-_{min}(\boldsymbol{\sigma})$.

If $a(\boldsymbol{\sigma}) < b(\boldsymbol{\sigma})$, we have for every period two points of minima with value zero and two peaks for the absolute value of scalar stress as in Figure 2.8. In (a) and (b) we see the absolute value of the scalar stress s when $\hat{a}(\boldsymbol{\sigma}) \geq 0$ and $\hat{a}(\boldsymbol{\sigma}) < 0$, respectively. The scalar stress s crosses the horizontal axis and there exist points $\alpha^-_{min}(\boldsymbol{\sigma})$ such that $s(\boldsymbol{\sigma}, \alpha^-_{min}(\boldsymbol{\sigma})) = 0$ (see Figure 2.8). In the next result, we give points of minima $\alpha^-_{min}(\boldsymbol{\sigma})$.

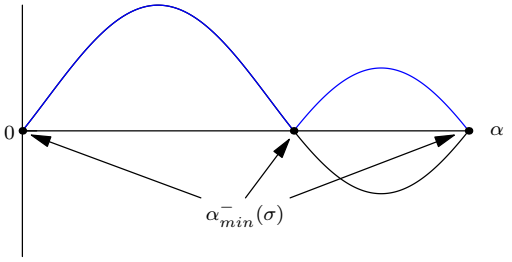

(a) Sample graph for $s(\boldsymbol{\sigma}, \alpha)$ (black) and $|s(\boldsymbol{\sigma}, \alpha)|$ (blue) when $\hat{a}(\boldsymbol{\sigma}) \geq 0$.

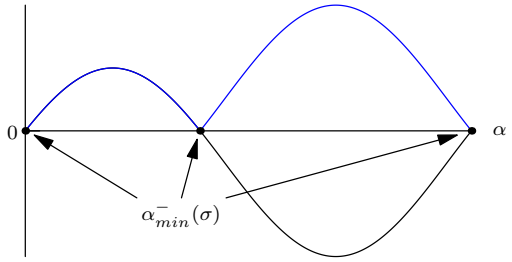

(b) Sample graph for $s(\boldsymbol{\sigma}, \alpha)$ (black) and $|s(\boldsymbol{\sigma}, \alpha)|$ (blue) when $\hat{a}(\boldsymbol{\sigma}) < 0$.

Figure 2.8.: Examples of $|s(\boldsymbol{\sigma}, \alpha)|$ for $\alpha \in [0, \pi)$ when $a(\boldsymbol{\sigma}) < b(\boldsymbol{\sigma})$.

Lemma 2.3.11. *For a fixed stress $\boldsymbol{\sigma}$ with $a(\boldsymbol{\sigma}) < b(\boldsymbol{\sigma})$, the scalar stress $s(\boldsymbol{\sigma}, \alpha)$ from Eq. (2.12) is zero when $\alpha = \alpha^-_{min}(\boldsymbol{\sigma})$ where*

$$\alpha^-_{min}(\boldsymbol{\sigma}) = \begin{cases} -\frac{\theta}{2} - \frac{\phi(\boldsymbol{\sigma})}{2} + n_3\pi, \\ \frac{\theta}{2} - \frac{\phi(\boldsymbol{\sigma})}{2} + \frac{\pi}{2} + n_3\pi, \end{cases} \quad \text{if } \hat{a}(\boldsymbol{\sigma}) \geq 0 \tag{2.23}$$

or

$$\alpha^-_{min}(\boldsymbol{\sigma}) = \begin{cases} \frac{\theta}{2} - \frac{\phi(\boldsymbol{\sigma})}{2} + n_4\pi, \\ -\frac{\theta}{2} - \frac{\phi(\boldsymbol{\sigma})}{2} + \frac{\pi}{2} + n_4\pi, \end{cases} \quad \text{if } \hat{a}(\boldsymbol{\sigma}) < 0 \tag{2.24}$$

with $\theta := \sin^{-1}\left(\frac{a(\boldsymbol{\sigma})}{b(\boldsymbol{\sigma})}\right)$ and $n_3, n_4 \in \mathbb{Z}$.

Proof. If $\hat{a}(\boldsymbol{\sigma}) \geq 0$, we have $a(\boldsymbol{\sigma}) = \hat{a}(\boldsymbol{\sigma})$. Equation (2.12) for the scalar stress s is then given as:

$$s(\boldsymbol{\sigma}, \alpha) = a(\boldsymbol{\sigma}) + b(\boldsymbol{\sigma}) \sin(2\alpha + \phi(\boldsymbol{\sigma})).$$

The scalar stress s is zero if

$$\begin{aligned} a(\boldsymbol{\sigma}) + b(\boldsymbol{\sigma}) \sin(2\alpha + \phi(\boldsymbol{\sigma})) &= 0 \\ \Rightarrow \sin(2\alpha + \phi(\boldsymbol{\sigma})) &= -\frac{a(\boldsymbol{\sigma})}{b(\boldsymbol{\sigma})}. \end{aligned} \tag{2.25}$$

The solutions of the trigonometric equation $\sin(x) = y, -1 \leq y \leq 1$ are given as $x = \sin^{-1} y + 2n\pi$ and $x = \pi - \sin^{-1}(y) + 2n\pi$. Using this we get the solution of the trigonometric equation in (2.25) as

$$2\alpha + \phi(\boldsymbol{\sigma}) = -\theta + 2n_3\pi \tag{2.26}$$

and

$$2\alpha + \phi(\boldsymbol{\sigma}) = \pi + \theta + 2n_3\pi. \tag{2.27}$$

Rewriting Eq. (2.26) and Eq. (2.27) in terms of α gives us Eq. (2.23) and completes first part of the proof.

$$\alpha^-_{min}(\boldsymbol{\sigma}) = \begin{cases} -\frac{\theta}{2} - \frac{\phi(\boldsymbol{\sigma})}{2} + n_3\pi, \\ \frac{\theta}{2} - \frac{\phi(\boldsymbol{\sigma})}{2} + \frac{\pi}{2} + n_3\pi, \end{cases} \quad \text{if } \hat{a}(\boldsymbol{\sigma}) \geq 0 \tag{2.28}$$

Similarly if $\hat{a}(\boldsymbol{\sigma}) < 0$, we have $a(\boldsymbol{\sigma}) = -\hat{a}(\boldsymbol{\sigma})$. Equation (2.12) for the scalar stress s is then given as

$$s(\boldsymbol{\sigma}, \alpha) = -a(\boldsymbol{\sigma}) + b(\boldsymbol{\sigma}) \sin(2\alpha + \phi(\boldsymbol{\sigma})).$$

The scalar stress s is zero if

$$\begin{aligned} -a(\boldsymbol{\sigma}) + b(\boldsymbol{\sigma}) \sin(2\alpha + \phi(\boldsymbol{\sigma})) &= 0 \\ \Rightarrow \sin(2\alpha + \phi(\boldsymbol{\sigma})) &= \frac{a(\boldsymbol{\sigma})}{b(\boldsymbol{\sigma})}. \end{aligned} \tag{2.29}$$

Finally we get the solution to Eq. (2.29) similar to the case $\hat{a}(\boldsymbol{\sigma}) \geq 0$:

$$\alpha^-_{min}(\boldsymbol{\sigma}) = \begin{cases} \frac{\theta}{2} - \frac{\phi(\boldsymbol{\sigma})}{2} + n_4\pi, \\ -\frac{\theta}{2} - \frac{\phi(\boldsymbol{\sigma})}{2} + \frac{\pi}{2} + n_4\pi, \end{cases} \quad \text{if } \hat{a}(\boldsymbol{\sigma}) < 0. \tag{2.30}$$

This completes the proof. □

The values of $\alpha^-_{min}(\boldsymbol{\sigma})$ divide each period of the scalar stress s into two intervals. If $a(\boldsymbol{\sigma}) \neq 0$, the width of one of these intervals is larger than the other. Due to the symmetry of the absolute value of the sine function around its maxima, the midpoint of the interval I_1 with larger width is the point of maximum with a higher absolute scalar stress value. The other interval is represented by I_2. The midpoint of the interval I_1 is the point of maximum $\alpha^-_{max,1}(\boldsymbol{\sigma})$ and the midpoint of the interval I_2 is the point of maximum $\alpha^-_{max,2}(\boldsymbol{\sigma})$.

The width of the interval between the values of $\alpha^-_{min}(\boldsymbol{\sigma})$ in Eq. (2.28) is

$$\left|\frac{\theta}{2} - \frac{\phi(\boldsymbol{\sigma})}{2} + \frac{\pi}{2} + n_3\pi - \left(-\frac{\theta}{2} - \frac{\phi(\boldsymbol{\sigma})}{2} + n_3\pi\right)\right| = \left|\frac{\theta}{2} + \frac{\theta}{2} + \frac{\pi}{2}\right| \tag{2.31a}$$

$$= \theta + \frac{\pi}{2}. \tag{2.31b}$$

Similarly, the width of the interval between the values of $\alpha^-_{min}(\boldsymbol{\sigma})$ in Eq. (2.30) is

$$\left|-\frac{\theta}{2} - \frac{\phi(\boldsymbol{\sigma})}{2} + \frac{\pi}{2} + n_4\pi - \left(\frac{\theta}{2} - \frac{\phi(\boldsymbol{\sigma})}{2} + n_4\pi\right)\right| = \left|-\frac{\theta}{2} - \frac{\theta}{2} + \frac{\pi}{2}\right| \tag{2.32a}$$

We know that $\theta = \sin^{-1}\left(\frac{a(\boldsymbol{\sigma})}{b(\boldsymbol{\sigma})}\right)$ and $a(\boldsymbol{\sigma}) \geq 0$ and $b(\boldsymbol{\sigma}) > 0$. Therefore, $0 \leq \theta \leq \frac{\pi}{2}$, which gives us

$$= \frac{\pi}{2} - \theta. \tag{2.32b}$$

From Theorem 2.3.6, the period of scalar stress is π. The width of interval contained in between the values of $\alpha^-_{min}(\boldsymbol{\sigma})$ in Eq. (2.28) is more than half the period length and is declared as the interval I_1. The width of the interval contained in between the values of $\alpha^-_{min}(\boldsymbol{\sigma})$ in Eq. (2.30) is less than half the period length and is declared as the interval I_2.

Theorem 2.3.12. *The interval I_1 with a larger width is given as*

$$I_1 = \left[\alpha^-_{\max,1}(\boldsymbol{\sigma}) - \frac{\pi}{4} - \frac{\theta}{2},\ \alpha^-_{\max,1}(\boldsymbol{\sigma}) + \frac{\pi}{4} + \frac{\theta}{2}\right] \tag{2.33}$$

where $\alpha^-_{max,1}$ is the midpoint of the interval I_1 and the interval I_2 with a smaller width is given as

$$I_1 = \left[\alpha^-_{\max,2}(\boldsymbol{\sigma}) - \frac{\pi}{4} + \frac{\theta}{2},\ \alpha^-_{\max,2}(\boldsymbol{\sigma}) + \frac{\pi}{4} - \frac{\theta}{2}\right] \tag{2.34}$$

where $\alpha^-_{max,1}$ is the midpoint of the interval I_2.

Proof. From Eq. (2.31) and Eq. (2.32) we see that in both cases $\hat{a}(\boldsymbol{\sigma}) \geq 0$ and $\hat{a}(\boldsymbol{\sigma}) < 0$ the width of interval I_1 is $\theta + \frac{\pi}{2}$ while the width of the interval I_2 is $\frac{\pi}{2} - \theta$. The midpoints of I_1 and I_2 are $\alpha^-_{max,1}(\boldsymbol{\sigma})$ and $\alpha^-_{max,2}(\boldsymbol{\sigma})$ respectively. Using the midpoints and widths of the interval we get Eq. (2.33) and Eq. (2.34). □

Now we can give the maximum absolute value of the scalar stress in the two intervals.

Theorem 2.3.13. *For a fixed stress $\boldsymbol{\sigma}$ with $a(\boldsymbol{\sigma}) < b(\boldsymbol{\sigma})$ and the scalar stress s from (2.12), the maximum value of $|s(\boldsymbol{\sigma}, \alpha)|$ for $\alpha \in I_1$ is*

$$s^-_{max,1}(\boldsymbol{\sigma}) = \max_{\alpha \in I_1} |s(\boldsymbol{\sigma}, \alpha)| = a(\boldsymbol{\sigma}) + b(\boldsymbol{\sigma}), \tag{2.35}$$

at

$$\alpha^-_{max,1}(\boldsymbol{\sigma}) = \begin{cases} \frac{\pi}{4} - \frac{\phi(\boldsymbol{\sigma})}{2} + n_5\pi, & \text{if } \hat{a} \geq 0 \\ -\frac{\pi}{4} - \frac{\phi(\boldsymbol{\sigma})}{2} + n_5\pi, & \text{if } \hat{a} < 0 \end{cases}, \tag{2.36}$$

and the maximum value of $|s(\boldsymbol{\sigma}, \alpha)|$ for $\alpha \in I_2$ is

$$s^-_{max,2}(\boldsymbol{\sigma}) = \min_{\alpha \in I_2} |s(\boldsymbol{\sigma}, \alpha)| = b(\boldsymbol{\sigma}) - a(\boldsymbol{\sigma}), \tag{2.37}$$

at

$$\alpha^-_{max,2}(\boldsymbol{\sigma}) = \begin{cases} -\frac{\pi}{4} - \frac{\phi(\boldsymbol{\sigma})}{2} + n_6\pi, & \text{if } \hat{a} \geq 0 \\ \frac{\pi}{4} - \frac{\phi(\boldsymbol{\sigma})}{2} + n_6\pi, & \text{if } \hat{a} < 0 \end{cases}, \tag{2.38}$$

where $n_5, n_6 \in \mathbb{Z}$.

Proof. From Eq. (2.12) the scalar stress s is given as

$$s(\boldsymbol{\sigma}, \alpha) = \hat{a}(\boldsymbol{\sigma}) + b(\boldsymbol{\sigma}) \sin(2\alpha + \phi(\boldsymbol{\sigma}))$$

We consider the two cases $\hat{a}(\boldsymbol{\sigma}) \geq 0$ and $\hat{a}(\boldsymbol{\sigma}) < 0$ separately:

(i) If $\hat{a}(\boldsymbol{\sigma}) \geq 0$, then $a(\boldsymbol{\sigma}) = \hat{a}(\boldsymbol{\sigma})$. The maximum value of $|s(\boldsymbol{\sigma}, \alpha)|$ for $\alpha \in I_1$ is computed as

$$s^{-}_{max,1}(\boldsymbol{\sigma}) = \max_{\alpha \in I_1} |a(\boldsymbol{\sigma}) + b(\boldsymbol{\sigma}) \sin(2\alpha + \phi(\boldsymbol{\sigma}))|.$$

We have $a(\boldsymbol{\sigma})$ and $b(\boldsymbol{\sigma})$ are positive and do not depend on α. The absolute value of sine function is symmetric about its maximum in both the intervals I_1 and I_2. So, the interval I_1 with larger width has the peak with larger absolute value of the scalar stress. This implies that the maximum value occurs whenever $\sin(2\alpha + \phi(\boldsymbol{\sigma}))$ is one which in turn implies

$$2\alpha + \phi(\boldsymbol{\sigma}) = \frac{\pi}{2} + 2n_5\pi$$

The maximum occurs at the mid point $\alpha^{-}_{max,1}(\boldsymbol{\sigma})$ which results in

$$\alpha^{-}_{max,1}(\boldsymbol{\sigma}) = \frac{\pi}{4} - \frac{\phi(\boldsymbol{\sigma})}{2} + n_5\pi$$

where $n_5 \in \mathbb{Z}$. Finally we get

$$s^{-}_{max,1}(\boldsymbol{\sigma}) = a(\boldsymbol{\sigma}) + b(\boldsymbol{\sigma}).$$

Similarly, the maximum value of $|s(\boldsymbol{\sigma}, \alpha)|$ in the interval I_2 occurs when $\sin(2\alpha + \phi(\boldsymbol{\sigma})) = -1$,

$$2\alpha + \phi(\boldsymbol{\sigma}) = -\frac{\pi}{2} + 2n_6\pi$$

The maximum occurs at the midpoint $\alpha^{-}_{max,2}(\boldsymbol{\sigma})$ which results in

$$\alpha^{-}_{max,2}(\boldsymbol{\sigma}) = -\frac{\pi}{4} - \frac{\phi(\boldsymbol{\sigma})}{2} + n_6\pi$$

where $n_6 \in \mathbb{Z}$. In the end we get

$$s^{-}_{max,2}(\boldsymbol{\sigma}) = |a(\boldsymbol{\sigma}) - b(\boldsymbol{\sigma})| = b(\boldsymbol{\sigma}) - a(\boldsymbol{\sigma}).$$

(ii) If $\hat{a}(\boldsymbol{\sigma}) < 0$, then $a(\boldsymbol{\sigma}) = -\hat{a}(\boldsymbol{\sigma})$. The proof is similar to the proof of the case $\hat{a}(\boldsymbol{\sigma}) \geq 0$ with the difference being that the points of the maximum in the interval I_1 and the points of maximum in the interval I_2 for $|s(\boldsymbol{\sigma}, \alpha)|$ in this case are swapped.

$$\begin{aligned} s^{-}_{max,1}(\boldsymbol{\sigma}) &= \max_{\alpha \in I_1} |\hat{a}(\boldsymbol{\sigma}) + b(\boldsymbol{\sigma}) \sin(2\alpha + \phi) \\ &= \max_{\alpha \in I_1} | - a(\boldsymbol{\sigma}) + b(\boldsymbol{\sigma}) \sin(2\alpha + \phi)|. \end{aligned} \tag{2.39}$$

Both $a(\boldsymbol{\sigma})$ and $b(\boldsymbol{\sigma})$ are positive, therefore, the maximum absolute value is obtained when $\sin(2\alpha + \phi) = -1$ or when $\alpha^{-}_{max,1}(\boldsymbol{\sigma}) = -\frac{\pi}{4} - \frac{\phi(\boldsymbol{\sigma})}{2} + n_5\pi, n_5 \in \mathbb{Z}$. Inserting $\sin(2\alpha + \phi) = -1$ in (2.39) we get

$$s^{-}_{max,1} = a(\boldsymbol{\sigma}) + b(\boldsymbol{\sigma}). \tag{2.40}$$

Similarly, the maximum value of $|s(\boldsymbol{\sigma}, \alpha)|$ in interval I_2 is obtained when $\sin(2\alpha + \phi) = 1$ or $\alpha^{-}_{max,2}(\boldsymbol{\sigma}) = \frac{\pi}{4} - \frac{\phi(\boldsymbol{\sigma})}{2} + n_6\pi, n_6 \in \mathbb{Z}$ which implies

$$s^{-}_{max,2}(\boldsymbol{\sigma}) = b(\boldsymbol{\sigma}) - a(\boldsymbol{\sigma}).$$

This completes the proof. □

Corollary 2.3.14. *The maximum value of the absolute scalar stress $|s(\sigma, \alpha)|$ for a given stress $\boldsymbol{\sigma}$ is $a(\boldsymbol{\sigma}) + b(\boldsymbol{\sigma})$.*

Proof. Follows directly from Theorem 2.3.10 and Theorem 2.3.13. □

In this section, we looked at computation of the scalar stress s from a load $\mathbf{l}$. The points of maximum magnitude of the scalar stress and the corresponding maximum values were derived for the two cases $a(\boldsymbol{\sigma}) \geq b(\boldsymbol{\sigma})$ and $a(\boldsymbol{\sigma}) < b(\boldsymbol{\sigma})$. For every period, in the case of $a(\boldsymbol{\sigma}) \geq b(\boldsymbol{\sigma})$ there is one maximum and one minimum. However, in the case of $a(\boldsymbol{\sigma}) < b(\boldsymbol{\sigma})$ for every period there are two maximums and two minimums. In Section 2.4, we see how to compute the damage d from the scalar stress s. The section also gives a comparison of the damage computation for a general load time series $\mathbf{L}$ and a load time series with block loads $\mathbf{L}_b$.

2.4. Damage

Damage occurs when a component is subjected to repeated loading and unloading. Microscopic crack formation starts at the regions of high stress concentrations when these repeated loads are above a certain threshold [18]. Over time after many repetitions of loading and unloading the crack reaches a critical size, and the component fails suddenly [21]. Therefore, it is important to be able to compute the damage due to these repeated loading and unloading for estimating the fatigue life of a component.

In testrigs, we apply a load time series to mimic the actual repeated loading and unloading during service life. When we apply a constant load time series then there is no damage incurred in the component. For a load time series to incur damage on a component it must have turning points (i.e. there exist points where the stress due to the load time series changes from increasing to decreasing and vice versa).

In Section 2.4.1, we describe damage computation for the case when the load time series leads to a stress time series with alternating stress. By alternating stress we mean that there always exist pairs of non-zero continuous points in the time series such that the magnitude of stress above and below the horizontal axis is the same. An example time series with alternating stress is shown in Figure 2.9.

Section 2.4.2 describes additional steps we need to take before we can compute the damage from a general load time series $\mathbf{L}$. After these additional steps damage computation can be done as in the case of load time series with alternating stresses. In Section 2.4.3, we show that the stress

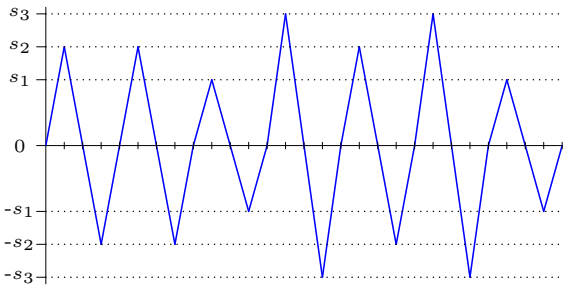

Figure 2.9.: Example of a stress time series with alternating stress. Alternating stress s_1 is repeated twice, i.e. $\nu_1 = 2$, for s_2 we have $\nu_2 = 3$ and for s_3 we have $\nu_3 = 2$.

time series obtained from a load time series with block loads $\mathbf{L}_b$ is similar to a stress time series with alternating stress. We modify the damage computation to take into account the properties of block loads.

2.4.1. Damage for time series with alternating stress

For damage calculations from alternating stress values we use the linear damage accumulation rule also called as Miner's rule or the Palmgren-Miner linear damage hypothesis (see [23, 26]).

Definition 2.4.1 (Palmgren-Miner rule)**.** Given a stress time series with m different alternating stress amplitudes, $s_i \in \mathbb{R}_+$ with $\mathbf{S}_a = (s_1, s_2, \cdots, s_m)$, each contributing ν_i cycles with $\mathcal{V} = (\nu_1, \nu_2, \ldots, \nu_m)$. Palmgren-Miner rule states that if N_i is the number of cycles to failure of a constant stress reversal s_i, then the total damage D is given as

$$D = \sum_{i=1}^{m} \frac{\nu_i}{N_i}. \tag{2.41}$$

The number of cycles to failuer N_i of a constant alternating stress amplitude s_i are experimentally determined and presented in the form of curves called Wöhler's curve or S-N curves. S-N curves are graphs of the amplitude of cyclic stress (S) against the logarithmic scale of cycles to failure (N). S-N Curves are characteristic of the material used in the experiments and are valid for uni-axial stress cycles with mean zero (ratio R of minimum to maximum stress as -1). Most S-N curves have a single uniform slope k until it becomes a horizontal line for the high cycles. However, some materials have two slopes k_1 and k_2 which divides the S-N curve into two regions one with a slope k_1 and another with a slope k_2. In Figure 2.10, we see examples for S-N curve with one slope and two-slopes.

By σ_1 and N_1, we denote the values of the stress and the corresponding number of cycles required for failure at the point where the slope changes from a value of k_1 to a value of k_2 in the S-N curve with two slopes. In general, the fatigue strength zone of the S-N curve can be described as a straight line in the log co-ordinate system with the following equation (see [24])

$$N_i = N_D \left(\frac{s_i}{\sigma_D} \right)^{-k} \tag{2.42}$$

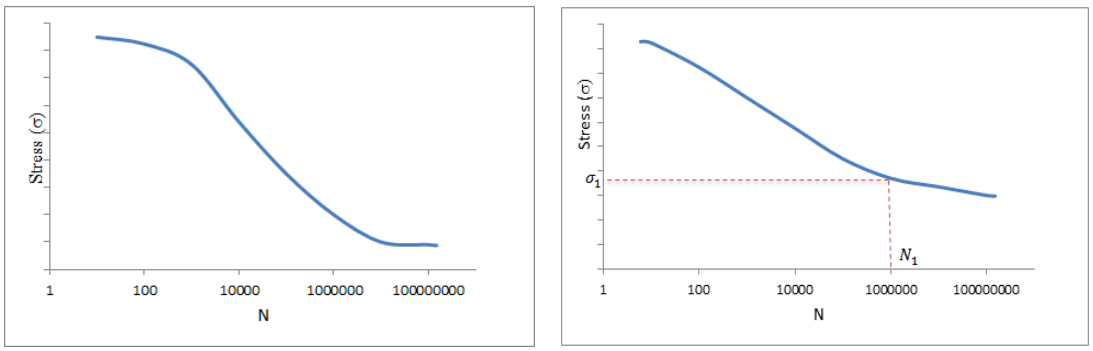

(a) S-N curve with one slope (b) S-N curve with two slopes

Figure 2.10.: Schematics of S-N Curves. The horizontal axis is the number of cycles to failure and the vertical axis is the magnitude of the alternating stress. The linear part of the S-N curve in (a) and the two liner parts of the S-N curve in (b) are called fatigue strength zone.

where N_i is the number of cycles required for failure when alternating stress with amplitude s_i is applied repeatedly. The exponent k determines the slope of the S-N curve in the fatigue strength zone. The parameters N_D and σ_D are material dependent. In case of one slope, we substitute σ_D and N_D by a reference stress σ_e and its corresponding number of cycles to failure N_e respectively. Similarly in the case of two slopes we substitute $\sigma_D = \sigma_1$ and $N_D = N_1$. In the fatigue strength zone with a slope k_1 we have $k = k_1$ and similarly for the fatigue strength zone with a slope k_2 we have $k = k_2$.

Definition 2.4.2 (Damage for one slope)**.** The damage d in the case of one slope with a constant alternating stress $s_i \in \mathbb{R}$ contributing ν_i cycles is given as

$$d(s_i, \nu_i) = \frac{\nu_i}{N_i} \overset{Eq.(2.42)}{=} \frac{\nu_i}{N_e} \left(\frac{|s_i|}{\sigma_e} \right)^k . \tag{2.43}$$

Definition 2.4.3 (Damage for two slopes)**.** The damage d in the case of two slopes with a constant alternating stress $s_i \in \mathbb{R}$ contributing $\nu_i \in \mathbb{N}$ cycles is given as

$$d(s_i, \nu_i) = \frac{\nu_i}{N_i} \overset{Eq.(2.42)}{=} \begin{cases} \frac{\nu_i}{N_1} \left(\frac{|s_i|}{\sigma_1} \right)^{k_1}, & \text{if } |s_i| > \sigma_1, \\ \frac{\nu_i}{N_1} \left(\frac{|s_i|}{\sigma_1} \right)^{k_2}, & \text{if } |s_i| \leq \sigma_1. \end{cases} \tag{2.44}$$

In Figure 2.11, we see the damage for the two cases for increasing value of s and $\nu = 1$. In (a) we see the damage for one slope with $k = 5$ and in (b) we see the damage for two slopes, $k_1 = 5$ and $k_2 = 15$.

Using the Palmgren-Miner rule from Definition 2.4.1, the total damage is then given as

$$D(\mathbf{S}_a, \mathcal{V}) = \sum_{i=1}^{m} d(s_i, \nu_i) \tag{2.45}$$

where m is the number of different stress amplitudes in the stress time series, $\mathbf{S}_a$ has all the stress

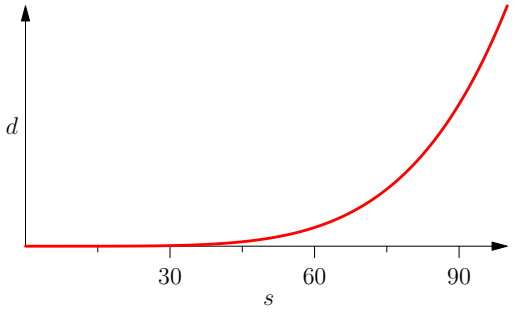

(a) Profile of damage d for stress amplitude s with $\nu = 1$ for one slope case with $k = 5$, $\sigma_e = 55$, $N_e = 10^8$.

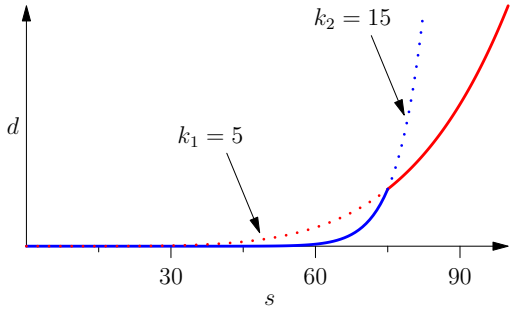

(b) Profile of damage d for stress amplitude s with $\nu = 1$ for two slope case with $k_1 = 5$, $k_2 = 15$, $\sigma_1 = 75$, $N_1 = 10^6$.

Figure 2.11.: Example plots for the damage for one slope and two slopes . In (b) we see the damage for the two slopes with solid lines and the damage for individual slopes extended with dotted lines.

amplitudes in the time series in an order which corresponds to that of the number of repetitions in $\mathcal{V}$ and the damage d is as defined in Eq. (2.43) if one slope and as defined in Eq. (2.44) if two slopes.

Example 2.4.4. For the stress time series in Figure 2.9 with $\mathbf{S}_a = (s_1, s_2, s_3)$, $\mathcal{V} = (2, 3, 2)$, one slope and material properties k, σ_e and N_e, the total damage can be computed as

$$\begin{aligned} D(\mathbf{S}_a, \mathcal{V}) &= \sum_{i=1}^{3} d(s_i, \nu_i) \\ &= \frac{\nu_1}{N_e}\left(\frac{s_1}{\sigma_e}\right)^k + \frac{\nu_2}{N_e}\left(\frac{s_2}{\sigma_e}\right)^k + \frac{\nu_3}{N_e}\left(\frac{s_3}{\sigma_e}\right)^k \\ &= \frac{1}{\sigma_e^k N_e}\left(2s_1^k + 3s_2^k + 2s_3^k\right) \end{aligned}$$

In the next section, we show how to compute damage for a general load time series $\mathbf{L}$. We explain additional steps that have to be taken before we can compute damage from $\mathbf{L}$.

2.4.2. Damage for general load time series

The loads that a vehicle experiences in service life are given by a general load time series $\mathbf{L}$ and are multi-axial, i.e., at each point of time we have the stress $\boldsymbol{\sigma}$ with components σ_{xx}, σ_{yy} and σ_{xy} acting on the surface points. However, the S-N curves generated from experiments are typically for uni-axial loading. Therefore, some transformation is needed whenever the loading is multi-axial to give an equivalent uni-axial loading. The critical plane analysis is widely used in engineering to account for the effects of cyclic, multi-axial load histories on the fatigue life of materials and structures (for more details see [10, 13, 27, 37]). A critical plane is defined as a plane with the maximum damage after the application of a load time series. In Section 2.3, we showed how to compute scalar stress s on a particular plane α from the components σ_{xx}, σ_{yy} and σ_{xy} of the stress $\boldsymbol{\sigma}$.

The scalar stress time series $\mathbf{S}$ obtained for a plane angle α and $\mathbf{L}$ is generally not alternating. However, the S-N curves are best suited for cyclic alternating stresses. One way to deal with such stress time series is to count stress cycles and then use the damage accumulation methods on the counted cycles. The load cycles are formed by pairing the local maxima with the local minima, using some kind of cycle counting algorithm. For several cycle counting procedures see Collins [8].

The rainflow counting method presented by Endo in 1967 ([12, 22]), is generally accepted as being the best cycle counting procedure. For the definition of rainflow cycle we use the definition by Rychlik [35]. Figure 2.12 illustrates the definition of a rainflow cycle by Rychlik. The rainflow cycles can be identified with the help of a 4-point algorithm presented in de Jonge [9], Brokate et al. [6] and Johannesson and Speckert [17]. The 4-point algorithm is presented in Appendix C.1. We observe that due to the application of 4-point algorithm or any cycle counting algorithm in general the resulting damage is non-differentiable.

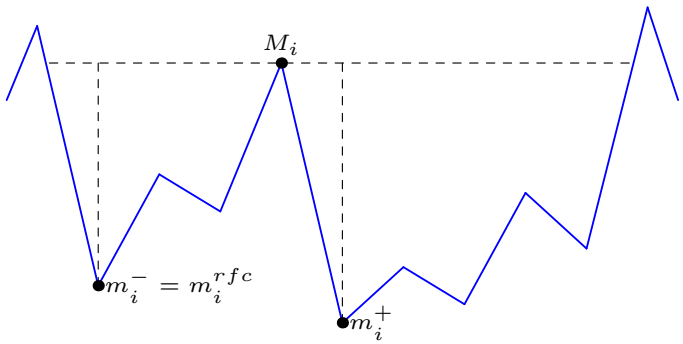

Figure 2.12.: The definition of rainflow cycle by Rychlik [35]. From every local maximum M_i we try to reach above or at the same level, in the forward and the backward directions. While doing so we try to minimize the downward excursion, i.e. we choose from m_i^- and m_i^+, which gives the smallest deviation from the maximum M_i and call it the rainflow minimum m_i^{rfc}. Then the i-th rainflow cycle is defined as (m_i^{rfc}, M_i).

The rainflow cycles obtained by the 4-point algorithm may not have a mean stress value of zero. The S-N curves are obtained after substantial amount of testing for the simple case of alternating loading and it is practically impossible to determine S-N curves for every combination of mean and alternating stress. If the mean stress is not zero, then we need to apply corrections to get the stress amplitude s_a corresponding to the case when the mean stress is zero. A preferred correction method is through the Goodman diagrams which is the cycles-to-failure plotted as a function of mean stress s_m and alternating stress s along lines of constant R-values, $R = \frac{s_{min}}{s_{max}}$. An example Goodman diagram is shown in Figure 2.13 and the mathematical representation is given as:

$$s_{goodman} = \sigma_{fat}\left(1 - \frac{\sigma_m}{\sigma_u}\right) \tag{2.46}$$

where $s_{goodman}$ is the stress amplitude after applying Goodman correction, σ_{fat} is the fatigue limit for completely reversed loading, σ_m is the mean stress and σ_u is the ultimate tensile stress. For more details about Goodman diagrams see [25].

In Algorithm 2.4.1, we give steps to compute the total damage D for a general load time series $\mathbf{L}$ on a plane α for any point on the surface. The testrig configuration $\mathcal{TC}$ is given through the

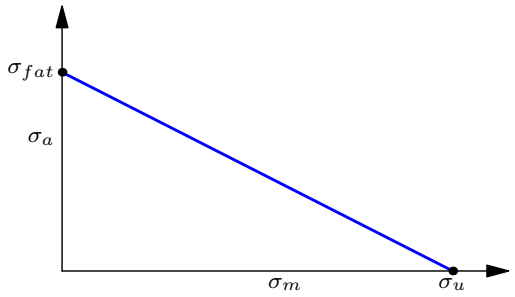

Figure 2.13.: An example Goodman diagram. The area below the curve is the region where the material should not fail for the given mean stress.

input parameter $\tilde{\boldsymbol{\sigma}}$. The material parameters are part of the damage computation function $d(s, \nu)$ where s is the alternating stress magnitude and ν is the number of cycles of the alternating stress s. The output of the algorithm is the damage D.

Algorithm 2.4.1: Computing total Damage D from a general load time series $\mathbf{L}$ on plane α

Data: $\tilde{\boldsymbol{\sigma}}$, $\mathbf{L}$, α, $d(s, \nu)$
Result: D

```
begin
    Σ ⟵ σ̃ · L
    S ⟵ n(α) · Σ
    S^rfc, V^rfc ⟵ 4PointAlgorithm(S)                ▷ From Appendix C.1
    S_a^{rfc,corrected} ⟵ GoodmanCorrection(S^rfc)
    i ⟵ 1
    while i ≤ |S_a^{rfc,corrected}| do
        D ⟵ D + d(s_i^{rfc,corrected}, ν_i^rfc)
        i ⟵ i + 1
    end
    return D
end
```

In Algorithm 2.4.1, $\boldsymbol{\Sigma} \in \mathbb{R}^{3\times N}$ is the stress time series at a given point due to a load times series $\mathbf{L}$. $\mathbf{S} \in \mathbb{R}^N$ is the scalar stress time series on the plane α. From the $4PointAlgorithm$ we get all the cycles $\mathbf{S}^{rfc}$ as defined by Rychlik in [35] and the number of times each cycle appears $\mathcal{V}^{rfc}$. Next the function $GoodmanCorrection$ returns the magnitude of the alternating stresses as $\mathbf{S}_a^{rfc,corrected}$ corresponding to each cycle in $\mathbf{S}^{rfc}$. Finally, the damage for each alternating stress is computed with the help of the damage function d.

We observe that the damage from a general load time series $\mathbf{L}$ is non-differentiable due to the cycle counting algorithm like the rainflow counting method as well as corrections of the mean stress by the help of the Goodman diagrams. This makes it difficult to use the damage from $\mathbf{L}$ in the optimization of the load time series for testrigs. In Section 2.4.3, we see that in the case of load time series with block loads $\mathbf{L}_b$, the computation of the damage is straight forward. Neither a cycle counting algorithm nor a mean correction method is required because our block loads have a zero mean stress and consist of alternating stresses.

2.4.3. Damage from load time series with block loads

When using the stress time series due to a load time series with block loads $\mathbf{L}_b$, the damage at any point $\mathbf{x} \in \mathbb{R}^3$ on the surface depends only on the amplitude $\ell_{i,j}$, for the j-th block at the i-th element in $\mathfrak{F}$ and the number of cycles ν_j (from Remark 2.2.10 the j-th block for all the actuators have the same number of cycles ν_j) of the individual block loads in $\mathbf{L}_b$ when using Palmgren-Miner rule for damage accumulation. Therefore, by using a load time series with block loads we eliminate the need for the cycle counting algorithms and do not need any corrections. Using Remark 2.2.10, we define the load $\mathbf{l}_{b,j}$ as the amplitudes of the j-th block for each force/moment acting at actuators in A_a as

$$\mathbf{l}_{b,j} := (\ell_{1,j}, \ell_{2,j}, \dots, \ell_{n,j})^T \tag{2.47}$$

where $j \in \{1, 2, \dots, m\}$. We can define by $\mathbf{L}_{b,a}$ the matrix of amplitudes of block loads in $\mathbf{L}_b$ with columns $\mathbf{l}_{b,j}, j = 1, 2, \dots, m$ as:

$$\mathbf{L}_{b,a} := (\mathbf{l}_{b,1}, \mathbf{l}_{b,2}, \dots, \mathbf{l}_{b,m}) \in \mathbb{R}^{n \times m}. \tag{2.48}$$

The stress due to the matrix of amplitudes $\mathbf{L}_{b,a}$ at hotspot $\mathbf{x}$ is computed as

$$\mathbf{\Sigma}_\mathbf{x}(\mathbf{L}_{b,a}) = \tilde{\boldsymbol{\sigma}}_\mathbf{x} \mathbf{L}_{b,a} = (\sigma_\mathbf{x}(\mathbf{l}_{b,1}), \dots, \sigma_\mathbf{x}(\mathbf{l}_{b,m})) \in \mathbb{R}^{3 \times m}. \tag{2.49}$$

where $\mathbf{\Sigma}_\mathbf{x}$ is from Eq. (2.7). In this case $\mathbf{\Sigma}_\mathbf{x}$ is a condensed time series where each point on the time series represents the amplitude of alternating stresses at hotspot $\mathbf{x}$. By $\mathbf{S}_\mathbf{x}$ we denote the magnitudes of the scalar stresses on plane α acting at the hotspot $\mathbf{x}$ due to all the block loads and is the same as $\mathbf{S}_a$ in Eq. (2.45) and is given as:

$$\mathbf{S}_\mathbf{x}(\mathbf{L}_{b,a}, \alpha) := \mathbf{n}(\alpha) \mathbf{\Sigma}_\mathbf{x}(\mathbf{L}_{b,a}) = \left(s\left(\boldsymbol{\sigma}_\mathbf{x}(\mathbf{l}_{b,1}), \alpha\right), \dots, s\left(\boldsymbol{\sigma}_\mathbf{x}(\mathbf{l}_{b,m}), \alpha\right)\right)^T \tag{2.50}$$

where s is the scalar stresses on plane α from Eq. (2.12). Then the total damage from the amplitude matrix $\mathbf{L}_{b,a}$ due to the load time series with block loads $\mathbf{L}_b$ for plane α at hotspot $\mathbf{x}$ and the testrig configuration $\mathcal{TC}$ is computed as

$$\begin{aligned} D_\mathbf{x}(\mathbf{L}_{b,a}, \mathcal{V}, \alpha) :=& D(\mathbf{S}_\mathbf{x}(\mathbf{L}_{b,a}, \alpha)), \mathcal{V}) && \text{(2.51a)} \\ =& D(\mathbf{n}(\alpha) \mathbf{\Sigma}_\mathbf{x}(\mathbf{L}_{b,a}, \mathcal{V}) && \text{(2.51b)} \\ \text{Eq. (2.7)} \Rightarrow =& D(\mathbf{n}(\alpha) \tilde{\boldsymbol{\sigma}}_\mathbf{x} \mathbf{L}_{b,a}, \mathcal{V}) && \text{(2.51c)} \end{aligned}$$

where $\tilde{\boldsymbol{\sigma}}_\mathbf{x} \in \mathbb{R}^{3 \times n}$ is from the testrig configuration and depends on the hotspot $\mathbf{x}$ and the total damage D from Eq. (2.45). In Algorithm 2.4.2, we describe the complete process of computation of total damage from a load time series with block loads $\mathbf{L}_b$. We provide $\mathbf{L}_{b,a}$ and $\mathcal{V}$ to the algorithm as these two are sufficient to describe $\mathbf{L}_b$ completely.

We look at an example to better understand how everything works.

Example 2.4.5. From Example 2.2.12, we get $m = 2$, $n = 3$, $\mathcal{V} = (1, 2)$, $\mathscr{L}_1 = (5, 8)$, $\mathscr{L}_2 = (10, 5)$ and $\mathscr{L}_3 = (4, 4)$. Now we can write the amplitudes of the j-th block applied through the actuators $\mathbf{l}_{b,j}$ as $\mathbf{l}_{b,1} = (5, 10, 4)^T$ and $\mathbf{l}_{b,2} = (8, 5, 4)^T$. The matrix of amplitudes of block loads $\mathbf{L}_{b,a}$ in $\mathbf{L}_b$ is

Algorithm 2.4.2: Computing total Damage D at hotspot $\mathbf{x}$ from a load time series with block loads $\mathbf{L}_b$ on a plane α

Data: $\tilde{\boldsymbol{\sigma}}_{\mathbf{x}}$, $\mathbf{L}_{b,a}$, $\mathcal{V}$, α, $D(\mathbf{S}_a, \mathcal{V})$
Result: $D_{\mathbf{x}}$
begin
  $\boldsymbol{\Sigma}_{\mathbf{x}} \longleftarrow \tilde{\boldsymbol{\sigma}}_{\mathbf{x}} \mathbf{L}_{b,a}$
  $\mathbf{S}_{a,\mathbf{x}} \longleftarrow \mathbf{n}(\alpha)\boldsymbol{\Sigma}_{\mathbf{x}}$
  $D_{\mathbf{x}} \longleftarrow D(\mathbf{S}_{a,\mathbf{x}}, \mathcal{V})$
  return $D_{\mathbf{x}}$
end

given as

$$\mathbf{L}_{b,a} = \begin{pmatrix} 5 & 8 \\ 10 & 5 \\ 4 & 4 \end{pmatrix} \tag{2.52}$$

and the stress due to the matrix of amplitudes $\mathbf{L}_{b,a}$ at a hotspot $\mathbf{x}$ with stress tensor $\tilde{\boldsymbol{\sigma}}_{\mathbf{x}}$ is given as

$$\boldsymbol{\Sigma}_{\mathbf{x}}(\mathbf{L}_{b,a}) = \tilde{\boldsymbol{\sigma}}_{\mathbf{x}} \begin{pmatrix} 5 & 8 \\ 10 & 5 \\ 4 & 4 \end{pmatrix} \tag{2.53}$$

And similarly, the scalar stresses $\mathbf{S}_{\mathbf{x}}$ on plane α due to the block loads in the load time series with block load $\mathbf{L}_b$ can be computed as in Eq. (2.50), which can then be used in Eq. (2.51) to compute the total damage at hotspot $\mathbf{x}$.

Not only is it easy to compute the damage from the load time series with block loads $\mathbf{L}_b$ but also it is easy to apply the block loads through actuators in an actual testrig. The number of parameters required to specify a load time series with the same number of points is less in the case of load time series with block loads $\mathbf{L}_b$ as compared to the number of parameters required to specify the general load time series $\mathbf{L}$.

In Theorem 2.4.7, we see that for any hotspot $\mathbf{x}$, the total damage computation for a load time series with block loads $\mathbf{L}_b$ is convex for the case of one slope. Before we state and prove Theorem 2.4.7 we give a result on convexity that is used in the proof:

Lemma 2.4.6. *If $q \in \mathbb{R}^m$, $r \in \mathbb{R}$ and $\eta : \mathbb{R}^m \to \mathbb{R}$ is convex, then the function $\zeta : \mathbb{R}^m \to \mathbb{R}$ with values $\zeta(y) = \eta\left(q^T y + r\right)$ is convex.*

Proof. For any y^1, y^2 and $\lambda \in [0, 1]$, we have

$$\begin{aligned} \zeta(\lambda y^1 + (1-\lambda)y^2) &= \eta\left(q^T\left(\lambda y^1 + (1-\lambda)y^2\right) + r\right) \\ &= \eta\left(q^T\lambda y^1 + q^T(1-\lambda)y^2 + (\lambda + 1 - \lambda)r\right) \\ &= \eta\left(\lambda\left(q^T y^1 + r\right) + (1-\lambda)\left(q^T y^2 + r\right)\right) \\ \eta \text{ convex } \Rightarrow &\leq \lambda\eta\left(q^T y^1 + r\right) + (1-\lambda)\eta\left(q^T y^2 + r\right) \\ &= \lambda\zeta(y^1) + (1-\lambda)\zeta(y^2) \end{aligned}$$

Hence, composition with an affine function preserves convexity. □

Theorem 2.4.7. *For a given $\alpha \in [0, \pi)$ and load time series with block loads $\mathbf{L}_b$ consisting of amplitude matrix $\mathbf{L}_{b,a}$ and fixed number of cycles $\mathcal{V}$. If the material has one slope in the S-N curve, then the total damage $D_{\mathbf{x}}$ from Eq. (2.51) at hotspot $\mathbf{x}$ is convex.*

Proof. In case of one slope, the total damage at a hotspot $\mathbf{x}$ on the plane α is given by Eq. (2.43). Using vector of scalar stresses $\mathbf{S}_{\mathbf{x}}$ on plane α from Eq. (2.50) the total damage is:

$$D_{\mathbf{x}}(\mathbf{L}_{b,a}, \mathcal{V}, \alpha) = \sum_{j=1}^{m} \frac{\nu_j}{N_e} \left(\frac{|s\left(\sigma_{\mathbf{x}}(\mathbf{l}_{b,j}), \alpha\right)|}{\sigma_e} \right)^k = \frac{1}{N_e \sigma_e^k} \sum_{j=1}^{m} \nu_j |\mathbf{n}(\alpha) \cdot \tilde{\boldsymbol{\sigma}}_{\mathbf{x}} \cdot \mathbf{l}_{b,1}|^k \tag{2.55}$$

The scalar stress due to the j-th block loads in $\mathbf{L}_b$ is an affine function which maps the block amplitudes to the stresses. Additionally, the powers of absolute value function $|y|^p$ is convex for $p \geq 1$. Hence, from Lemma 2.4.6, $|s\left(\sigma_{\mathbf{x}}(\mathbf{l}_{b,j}), \alpha\right)|^k$ is convex with $k > 1$. Similarly, $\nu_j |s\left(\sigma_{\mathbf{x}}(\mathbf{l}_{b,j}), \alpha\right)|^k$ is convex. Finally, the sum of convex functions is convex as well. Hence, $D_{\mathbf{x}}$ is convex if the material has one slope. □

The total damage $D_{\mathbf{x}}$ for two slopes is not convex over the entire domain. This is because of the change in the slope at σ_1 on the S-N curve. However, as in Theorem 2.4.7, it can be easily proven that for each slope alone the total damage is convex. The convexity does not hold when we move from one slope to the other slope.

Another formulation

We give another formulation for computing damage that us used as a free parameter in the optimization in Chapter 3. In Eq. (2.48) we gave the amplitudes of each block load in the load time series $\mathbf{L}_b$ as an amplitude matrix $\mathbf{L}_{b,a}$. We can give another formulation for the the amplitudes of each block load, but this time in the form of a vector. Let us denote by $\hat{\mathbf{L}}$ the amplitudes of the block loads in the load time series $\mathbf{L}_b$ arranged one after another, i.e., all the j-th block loads acting through the actuators are followed by all the $(j+1)$-th block loads acting through the actuators:

$$\hat{\mathbf{L}} := \begin{pmatrix} \mathbf{l}_{b,1} \\ \mathbf{l}_{b,2} \\ \vdots \\ \mathbf{l}_{b,m} \end{pmatrix} \tag{2.56}$$

where $\mathbf{l}_{b,1}$ is from Eq. (2.47) and m is the number of blocks. The vector of scalar stress $\hat{\mathbf{S}}_{\mathbf{x}}$ at hotspot $\mathbf{x} \in \mathfrak{X}$ from $\hat{\mathbf{L}}$ in the new formulation is given as:

$$\hat{\mathbf{S}}_{\mathbf{x}}(\hat{\mathbf{L}}, \alpha) = \mathbf{N}(\alpha) \hat{\boldsymbol{\Sigma}}_{\mathbf{x}} \hat{\mathbf{L}} \tag{2.57}$$

where

$$\mathbf{N}(\alpha) = \begin{pmatrix} \mathbf{n}(\alpha) & \mathbf{0}_3^T & \cdots & \mathbf{0}_3^T \\ \mathbf{0}_3^T & \mathbf{n}(\alpha) & \cdots & \mathbf{0}_3^T \\ \vdots & \vdots & \ddots & \vdots \\ \mathbf{0}_3^T & \mathbf{0}_3^T & \cdots & \mathbf{n}(\alpha) \end{pmatrix}_{m \times 3m} \tag{2.58}$$

and

$$\hat{\boldsymbol{\Sigma}}_{\mathbf{x}} = \begin{pmatrix} \tilde{\boldsymbol{\sigma}}_{\mathbf{x}} & \mathbf{0}_{3\times n} & \cdots & \mathbf{0}_{3\times n} \\ \mathbf{0}_{3\times n} & \tilde{\boldsymbol{\sigma}}_{\mathbf{x}} & \cdots & \mathbf{0}_{3\times n} \\ \vdots & \vdots & \ddots & \vdots \\ \mathbf{0}_{3\times n} & \mathbf{0}_{3\times n} & \cdots & \tilde{\boldsymbol{\sigma}}_{\mathbf{x}} \end{pmatrix}_{3m\times nm} \tag{2.59}$$

with $\mathbf{n}(\alpha)$ from Eq. (2.14), $\mathbf{0}_3^T$ is row vector with three zeros, $\mathbf{0}_{3\times n}$ is matrix with all zero entries and $\tilde{\boldsymbol{\sigma}}_{\mathbf{x}}$ is the stress tensor from Eq. (2.6). In the next result, we show that the scalar stress vectors, $\mathbf{S}_{\mathbf{x}}$ from Eq. (2.50) and $\hat{\mathbf{S}}_{\mathbf{x}}$ from Eq. (2.57) are the same.

Lemma 2.4.8. *For a given load time series with block loads $\mathbf{L}_b$, the scalar stress vectors $\mathbf{S}_{\mathbf{x}}$ from Eq.* (2.50) *and $\hat{\mathbf{S}}_{\mathbf{x}}$ from Eq.* (2.57) *are the same.*

Proof. We know from Eq. (2.50) that each element of the scalar stress vector $\mathbf{S}_{\mathbf{x}}$ is given as:

$$s(\boldsymbol{\sigma}_{\mathbf{x}}(\mathbf{l}_{b,j}), \alpha) = \mathbf{n}(\alpha) \cdot \tilde{\boldsymbol{\sigma}}_{\mathbf{x}} \cdot \mathbf{l}_{b,j} = \mathbf{n}(\alpha) \cdot \boldsymbol{\sigma}_{\mathbf{x},j}, j \in \{1, 2, \ldots, m\}. \tag{2.60}$$

where stress $\boldsymbol{\sigma}_{\mathbf{x},j} = \tilde{\boldsymbol{\sigma}}_{\mathbf{x}} \cdot \mathbf{l}_{b,j}$ is the stress developed by the j-th block acting through all the actuators. Similarly, we observe in Eq. (2.57) that the matrices $\mathbf{N}(\alpha)$ and $\hat{\boldsymbol{\Sigma}}_{\mathbf{x}}$ are block diagonal matrices. Therefore, each element of the scalar stress vector $\hat{\mathbf{S}}$ is given in exactly the same way as the elements of $\mathbf{S}_{\mathbf{x}}$. □

Lemma 2.4.8 implies that the total damage computed from the two scalar stress vectors will be the same. In the case of one slope, the total damage at a hotspot $\mathbf{x}$ for the plane α is given by Eq. (2.43). Using the vector of scalar stresses $\hat{\mathbf{S}}_{\mathbf{x}}$ on plane α, the total damage $\hat{D}_{\mathbf{x}}$ is:

$$\hat{D}_{\mathbf{x}}(\hat{\mathbf{L}}, \mathcal{V}, \alpha) = D_{\mathbf{x}}(\mathbf{L}_{b,a}, \mathcal{V}, \alpha) = \frac{1}{N_e \sigma_e^k} \sum_{j=1}^{m} \nu_j |\mathbf{n}(\alpha) \cdot \tilde{\boldsymbol{\sigma}}_{\mathbf{x}} \cdot \mathbf{l}_{b,j}|^k = \frac{1}{N_e \sigma_e^k} \sum_{j=1}^{m} \nu_j |\mathbf{n}(\alpha) \cdot \boldsymbol{\sigma}_{\mathbf{x},j}|^k \tag{2.61}$$

where the total damage function $D_{\mathbf{x}}$ is from Eq. (2.55) and the number of cycles $\mathcal{V}$ for each block in the load time series is fixed before the optimization. Next, we prove that the total damage is differentiable with respect to the amplitude vector $\hat{\mathbf{L}}$ in the case of one slope.

Theorem 2.4.9. *The total damage function $\hat{D}_{\mathbf{x}}$ from Eq.* (2.61) *is differentiable with respect to the amplitude vector $\hat{\mathbf{L}}$ in the case of one slope.*

Proof. Contribution of the j-th block load to the total damage $\hat{D}_{\mathbf{x}}$ is

$$\nu_j |\mathbf{n}(\alpha) \cdot \tilde{\boldsymbol{\sigma}}_{\mathbf{x}} \cdot \mathbf{l}_{b,j}|^k$$

We know that $|x|^k$ is differentiable for $k > 1$ and a linear mapping $\mathbf{l}_{b,j} \mapsto \mathbf{n}(\alpha) \cdot \tilde{\boldsymbol{\sigma}}_{\mathbf{x}} \cdot \mathbf{l}_{b,j}$ is also differentiable. Therefore, the contribution of j-th block to the total damage is differentiable with respect to the amplitudes of the j-th block loads $\mathbf{l}_{b,j}$ in the load time series, as it is a composition of two differentiable functions. Total damage $\hat{D}_{\mathbf{x}}$ is a sum of differentiable functions and therefore, it is also differentiable. □

The derivative of total damage with respect to amplitudes of the j-th block loads $\mathbf{l}_{b,j}$ in the load

time series can be computed by using the chain rule of differentiation. Total damage $\hat{D}_{\mathbf{x}}$ is also convex:

Corollary 2.4.10. *Given plane α and fixed number of cycles of repetitions $\mathcal{V}$ in the load time series with block loads $\mathbf{L}_b$. If the material has one slope in the S-N curve, then the total damage $\hat{D}_{\mathbf{x}}$ from Eq.* (2.61) *at hotspot $\mathbf{x}$ is convex*

Proof. We compute from the load time series with block loads $\mathbf{L}_b$ the amplitude vector $\hat{\mathbf{L}}$ and the number of cycles of each block $\mathcal{V}$. The result follows directly from Theorem 2.4.7 observing that the vector of scalar stresses $\hat{\mathbf{S}}_{\mathbf{x}}$ and $\mathbf{S}_{\mathbf{x}}$ are the same from Lemma 2.4.8. □

For parameters $\mathbf{l}_{b,j}$ for all $j \in \{1, 2, \ldots, m\}$ and $\mathcal{V}$ fixed total damage $\hat{D}_{\mathbf{x}}$ is a trigonometric equation in α and is therefore differentiable for α. The first derivative of the total damage $\hat{D}_{\mathbf{x}}$ with respect to α in this case is given below:

Theorem 2.4.11. *If the S-N curve has one slope and parameters $\hat{\mathbf{L}}$, $\mathcal{V}$ are fixed, then the first derivative of the total damage $\hat{D}_{\mathbf{x}}$ from Eq.* (2.61) *with respect to α is given as*

$$\frac{d\hat{D}_{\mathbf{x}}(\hat{\mathbf{L}}, \mathcal{V}, \alpha)}{d\alpha} = \frac{k}{N_e \sigma_e^k} \sum_{j=1}^{m} \nu_j |\mathbf{n}(\alpha) \cdot \boldsymbol{\sigma}_{\mathbf{x},j}|^{k-2} \left(\mathbf{n}(\alpha) \cdot \boldsymbol{\sigma}_{\mathbf{x},j}\right) \left(\mathbf{n}'(\alpha) \cdot \boldsymbol{\sigma}_{\mathbf{x},j}\right) \tag{2.62}$$

where $\mathbf{n}'(\alpha) = (-\cos(2\alpha), \cos(2\alpha), 2\sin(2\alpha))$.

Proof. Replacing $|\mathbf{n}(\alpha) \cdot \boldsymbol{\sigma}_{\mathbf{x},j}|$ by $\sqrt{(\mathbf{n}(\alpha) \cdot \boldsymbol{\sigma}_{\mathbf{x},j})^2}$ and taking the first derivative of the total damage $\hat{D}_{\mathbf{x}}$ after simplification gives us the result. □

This chapter described various aspects of a testrig such as testrig configurations, different types of loads, computation of the stress and the damage. We also proved that the total damage function is convex and differentiable in the case of materials with one slope in the S-N curve. In the next chapter, we use these ideas and formulate two variations of testrig optimization problem. We compare the results of the two optimization problems for two testrig configurations for a steering knuckle of a vehicle.

3. Testrig optimization problem

The goal of the testrig optimization is to come as close as possible to the so-called reference stresses and/or reference damages at every hotspot $\mathbf{x}_i \in \mathfrak{X}$ where $\mathfrak{X} = \{\mathbf{x}_1, \mathbf{x}_2, \ldots, \mathbf{x}_{n_h}\}$ is the set of all hotspots. For the optimization we assume that the section forces (loads) of the component under service loading have been either measured or calculated by multi-body simulation techniques. From the loads we obtain reference stress signals $\sigma^{(ref)} \in \mathbb{R}^{3n_h \times N_f}$, where n_h is the number of hotspots and N_f is the number of points in the reference stress time series, by using Finite Element Analysis (FEA) and $D^{(ref)} \in \mathbb{R}^{n_h}$ by using damage computation from Section 2.4. In Figure 3.1, we see a knuckle with hotspots marked with yellow dots.

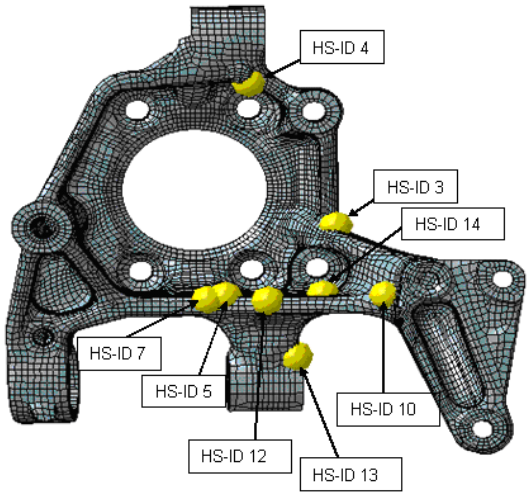

Figure 3.1.: A knuckle with hotspots marked in yellow dots [1].

However, the detailed behavior of the stresses as functions of time are sometimes not the most important topic. Instead the damage potential of the stress signals are considered. As seen in Section 2.4, the damage computation is rather complex non-linear non-differentiable for even simplest of cases when using general load time series $\mathbf{L}$ (Definition 2.2.2). In Section 3.1 we formulate the optimization problem of finding the load time series in two ways. We describe the measure of closeness to the reference data that is used as the objective functions in the optimization. We also prove properties of the possible objective functions in this section. Then Section 3.2 gives numerical results and discusses the issues arising in the optimization. In Section 3.2, we also compare the two approaches to optimizing testrigs described in Section 3.1. Finally, we end the chapter with a discussion on some of the drawbacks of discretization in the testrig optimization how to overcome them.

3.1. Optimization problem for testrigs

Before we can start doing optimization we need to be able to formulate the physical aspects of our requirements in terms of an optimization problem. In this section, we give two different approaches for testrig optimization problem. The first formulation is the current state of the art and we do not directly use damage in the optimization. Instead we try to find a load time series that gives stress time series that is as close as possible to the reference stress time series $\sigma^{(ref)}$ obtained from FEA. We hope that the damage computed at the hotspots from the stress time series obtained from the optimization is also close to the reference damage values at the hotspots. We name the first formulation as stress optimization. In the second formulation we use damage directly in the optimization but with load time series consisting of only block loads $\mathbf{L}_b$ (Definition 2.2.11) and name it as damage optimization. We make the following assumption for the optimization:

Assumption 3.1.1. *We have been given a testrig configuration $\mathcal{TC}$ (Definition 2.1.1) and we have to find the load time series that when applied at the actuator positions in $\mathcal{TC}$ leads to a damage at the hot spots as close as possible to the reference damage.*

3.1.1. Stress Optimization

In this formulation of the optimization problem, the free parameters are the loads at actuators in the given testrig configuration $\mathcal{TC}$. We want to the compute loads at each point of the time series that lead to stresses which are as close as possible to the reference stresses at the given hotspots. Therefore, for each point of the reference stress time series we have to solve an optimization problem. The number of points in the stress time series is N_f, so we have to solve N_f optimization problems.

To tackle the testrig stress optimization problem the first step is to represent the search space as a subset of the Euclidean space. From Section 2.2 we know that the load $\mathbf{l}_i$ at i-th point of time is a n-dimensional vector

$$\mathbf{l}_i = (l_{i,1}, l_{i,2}, \ldots, l_{i,n})^T$$

where $l_{i,j}$ is the load acting at the j-th element of $\mathfrak{F}$ (from Section 2.2) at i-th point of time. In the next definition, we limit the design space of the applied loads to ones that make sense for the testrig.

Definition 3.1.2. (Design space of the testrig stress optimization problem) Let $l_{min} \leq l_l < l_u \leq l_{max}$ where l_{min} and l_{max} are the minimum and the maximum load that can be applied through the actuators in the testrig configuration $\mathcal{TC}$. We call

$$\mathscr{D}_\sigma = \{\mathbf{l} \in \mathbb{R}^n | \mathbf{l} \in [l_l, l_u]^n\}$$

the *design space* of the testrig stress optimization problem.

The optimization would want to answer with the most preferable solution out of the set of all the feasible solutions. The set of all feasible solutions is a subset of the design space. In what follows, every element of the design space is considered feasible whenever the magnitude of the stress due

to the element are below some maximum stress σ_{max}, usually the ultimate tensile strength σ_u of the material used in the component. The ultimate tensile strength is the maximum stress that a material can withstand without failing. Before we can give the definition of a feasible solution we denote by $\mathcal{S} \in \mathbb{R}^{3n_h}$ the stress vector consisting of stress $\boldsymbol{\sigma}$ (from Eq. (2.6)) at all the hotspots when a load $\mathbf{l}$ is applied through actuators as:

$$\mathcal{S}(\mathfrak{X}, \mathbf{l}) := \begin{pmatrix} \boldsymbol{\sigma}(\mathbf{x}_1, \mathbf{l}) \\ \boldsymbol{\sigma}(\mathbf{x}_2, \mathbf{l}) \\ \vdots \\ \boldsymbol{\sigma}(\mathbf{x}_{n_h} \mathbf{l}) \end{pmatrix} \tag{3.1}$$

where $\boldsymbol{\sigma}(\mathbf{x}_i, \mathbf{l})$ are the stresses due to a load $\mathbf{l}$ acting at the hotspots $\mathbf{x}_i, i = 1, 2, \ldots, n_h$ and $\mathfrak{X} = \{\mathbf{x}_1, \mathbf{x}_2, \ldots, \mathbf{x}_{n_h}\}$ is the set of all hotspots. We can reformulate the stress vector $\mathcal{S}$ as a matrix-vector product:

Theorem 3.1.3. *The stress vector $\mathcal{S}$ from Eq. (3.1) due to load a $\mathbf{l}$ at all the hotspots in $\mathfrak{X}$ is given as*

$$\mathcal{S}(\mathfrak{X}, \mathbf{l}) = \widetilde{\boldsymbol{\Sigma}}(\mathfrak{X}) \cdot \mathbf{l} \tag{3.2}$$

where

$$\widetilde{\Sigma}(\mathfrak{X}) = \begin{pmatrix} \tilde{\sigma}_{\mathbf{x}_1} \\ \tilde{\sigma}_{\mathbf{x}_2} \\ \vdots \\ \tilde{\sigma}_{\mathbf{x}_{n_h}} \end{pmatrix} \in \mathbb{R}^{3n_h \times n}, \tag{3.3}$$

and $\tilde{\sigma}_{\mathbf{x}_i}$ from Eq. (2.6).

Proof. Using the stress $\boldsymbol{\sigma}$ from Eq. (2.6) and inserting into Eq. (3.1) we get

$$\mathcal{S}(\mathfrak{X}, \mathbf{l}) = \begin{pmatrix} \boldsymbol{\sigma}(\mathbf{x}_1, \mathbf{l}) \\ \boldsymbol{\sigma}(\mathbf{x}_2, \mathbf{l}) \\ \vdots \\ \boldsymbol{\sigma}(\mathbf{x}_{n_h} \mathbf{l}) \end{pmatrix} = \begin{pmatrix} \tilde{\sigma}_{\mathbf{x}_1} \cdot \mathbf{l} \\ \tilde{\sigma}_{\mathbf{x}_2} \cdot \mathbf{l} \\ \vdots \\ \tilde{\sigma}_{\mathbf{x}_{n_h}} \cdot \mathbf{l} \end{pmatrix} = \begin{pmatrix} \tilde{\sigma}_{\mathbf{x}_1} \\ \tilde{\sigma}_{\mathbf{x}_2} \\ \vdots \\ \tilde{\sigma}_{\mathbf{x}_{n_h}} \end{pmatrix} \cdot \mathbf{l} = \widetilde{\boldsymbol{\Sigma}}(\mathfrak{X}) \cdot \mathbf{l}. \tag{3.4}$$

□

In other words from Theorem 3.1.3 we see that each row of $\mathcal{S}$ is a linear superposition of load $\mathbf{l}$.

Assumption 3.1.4. *The i-th column of the matrix $\widetilde{\boldsymbol{\Sigma}}(\mathfrak{X})$ encapsulates the contribution to the stresses developed at all the hotspots when applying a unit load at the i-th element of $\mathfrak{F}$. In general we assume that the unit loads at different elements of $\mathfrak{F}$ do not affect the hotspots in exactly the same way. In other words the columns of the matrix $\widetilde{\boldsymbol{\Sigma}}$ are linearly independent.*

Using Assumption 3.1.4, we can prove that matrix $\widetilde{\boldsymbol{\Sigma}}(\mathfrak{X})^T \widetilde{\boldsymbol{\Sigma}}(\mathfrak{X})$ is a positive definite matrix.

Lemma 3.1.5. *Given a matrix $\widetilde{\boldsymbol{\Sigma}}(\mathfrak{X})$ as in Eq. (3.3), then the matrix $\widetilde{\boldsymbol{\Sigma}}(\mathfrak{X})^T \widetilde{\boldsymbol{\Sigma}}(\mathfrak{X})$ is a positive definite matrix.*

Proof. We know from Assumption 3.1.4 that the columns of the matrix $\widetilde{\mathbf{\Sigma}}(\mathfrak{X})$ are linearly independent. Therefore, in order to prove that the matrix $\widetilde{\mathbf{\Sigma}}(\mathfrak{X})^T\widetilde{\mathbf{\Sigma}}(\mathfrak{X})$ is positive semi-definite matrix we have to show that for any non-zero column vector $\mathbf{z} \in \mathbb{R}^n$, $z^T\widetilde{\mathbf{\Sigma}}(\mathfrak{X})^T\widetilde{\mathbf{\Sigma}}(\mathfrak{X})z$ is positive. However, $z^T\widetilde{\mathbf{\Sigma}}(\mathfrak{X})^T\widetilde{\mathbf{\Sigma}}(\mathfrak{X})z = \left\|\widetilde{\mathbf{\Sigma}}(\mathfrak{X})z\right\|_2^2 > 0$. Hence, $\widetilde{\mathbf{\Sigma}}(\mathfrak{X})^T\widetilde{\mathbf{\Sigma}}(\mathfrak{X})$ is a positive definite matrix. □

Next we give the definition of the feasible set of the testrig stress optimization problem.

Definition 3.1.6 (Feasible set of the testrig stress optimization problem)**.** For a given testrig configuration $\mathcal{TC}$, a solution $\mathbf{l} \in \mathscr{D}_\sigma$ is *feasible* if and only if

$$\|\mathcal{S}(\mathfrak{X}, \mathbf{l})\|_\infty \leq \sigma_{max}.$$

The set of all feasible solutions for testrig stress optimization problem is denoted by $\mathcal{L}_\sigma$.

Not all feasible solutions are preferable. We use *objective functions* to measure the *preferability* of one feasible solution compared to another. In the context of stress optimization in testrig this implies that we want the stress vector $\mathcal{S}$ obtained at any point of time for all the hotspots to be as close as possible to the corresponding reference stress values. Let us denote by η a function that measures for reference stress at any point i of the time series, its closeness with stress vector $\mathcal{S}(\mathfrak{X}, \mathbf{l})$. If $\eta(\mathfrak{X}, \mathbf{l}_1) < \eta(\mathfrak{X}, \mathbf{l}_2)$, then load $\mathbf{l}_1$ is preferable to load $\mathbf{l}_2$ with respect to η. The function η is called an *objective function*, and the image $\eta(\mathscr{D}_\sigma) \subset \mathbb{R}$ of the design space is called the *objective space*. The optimization problem at the i-th point of the reference stress time series is then given as

$$\min_{\mathbf{l}_i \in \mathcal{L}_\sigma} \eta(\mathfrak{X}, \mathbf{l}_i). \tag{TSOP}$$

A simple choice for objective function η is the square of the Euclidean norm or the 2-norm. Then for the i-th point on the reference stress time series we get

$$\eta(\mathfrak{X}, \mathbf{l}_i) = \left\|\sigma_i^{(ref)} - \mathcal{S}(\mathfrak{X}, \mathbf{l}_i)\right\|_2^2. \tag{3.5}$$

The testrig stress optimization problem (TSOP) consists of both box constraints and inequality constraints. Additionally, it can be easily shown that problem (TSOP) with the objective function η from Eq. (3.5) is a convex quadratic optimization problem with both box constraints and inequality constraints (BOINCQP):

Definition 3.1.7. A convex quadratic optimization problem with both box constraints and inequality constraints can be expressed in the form

$$\begin{aligned} \text{minimize } & \frac{1}{2}\mathbf{y}^T\mathbf{P}\mathbf{y} + \mathbf{q}^T\mathbf{y} + r \\ \text{subject to } & \mathbf{A}\mathbf{y} \leq \mathbf{b} \\ & u_i \leq y_i \leq v_i, i = 1, 2, \ldots, n \end{aligned} \tag{BOINCQP}$$

where $\mathbf{P}$ is a symmetric, positive definite $n \times n$ matrix, $\mathbf{A} \in \mathbb{R}^{m \times n}$ and u_i are the lower bounds and v_i are the upper bounds on y_i.

Theorem 3.1.8. *The testrig stress optimization problem* (TSOP) *with the objective function* η

from Eq. (3.5) *is a convex quadratic optimization problem with both box constraints and inequality constraints* (BOINCQP).

Proof. The only thing to prove is that the objective function η from Eq. (3.5) is convex and has a quadratic form similar to the objective function in (BOINCQP). We can rewrite the objective function η as shown below:

$$\eta(\mathfrak{X}, \mathbf{l}_i) = \left\| \sigma_i^{(ref)} - \mathcal{S}(\mathfrak{X}, \mathbf{l}_i) \right\|_2^2 \tag{3.6a}$$

$$\overset{Eq.(3.2)}{=} \left(\sigma_i^{(ref)} - \widetilde{\mathbf{\Sigma}}(\mathfrak{X})\mathbf{l} \right)^T \left(\sigma_i^{(ref)} - \widetilde{\mathbf{\Sigma}}(\mathfrak{X})\mathbf{l} \right) \tag{3.6b}$$

Expanding the two products we get

$$= \left(\sigma_i^{(ref)} \right)^T \sigma_i^{(ref)} - \left(\sigma_i^{(ref)} \right)^T \widetilde{\mathbf{\Sigma}}(\mathfrak{X})\mathbf{l} - \left(\widetilde{\mathbf{\Sigma}}(\mathfrak{X})\mathbf{l} \right)^T \sigma_i^{(ref)} + \left(\widetilde{\mathbf{\Sigma}}(\mathfrak{X})\mathbf{l} \right)^T \widetilde{\mathbf{\Sigma}}(\mathfrak{X})\mathbf{l} \tag{3.6c}$$

We see that both $\left(\sigma_i^{(ref)} \right)^T \widetilde{\mathbf{\Sigma}}(\mathfrak{X})\mathbf{l}$ and $\left(\widetilde{\mathbf{\Sigma}}(\mathfrak{X})\mathbf{l} \right)^T \sigma_i^{(ref)}$ are scalar and equal which simplifies to

$$= \left(\sigma_i^{(ref)} \right)^T \sigma_i^{(ref)} - 2 \left(\sigma_i^{(ref)} \right)^T \widetilde{\mathbf{\Sigma}}(\mathfrak{X})\mathbf{l} + \left(\widetilde{\mathbf{\Sigma}}(\mathfrak{X})\mathbf{l} \right)^T \widetilde{\mathbf{\Sigma}}(\mathfrak{X})\mathbf{l} \tag{3.6d}$$

$$= \left(\sigma_i^{(ref)} \right)^T \sigma_i^{(ref)} - 2 \left(\sigma_i^{(ref)} \right)^T \widetilde{\mathbf{\Sigma}}(\mathfrak{X})\mathbf{l} + \mathbf{l}^T \widetilde{\mathbf{\Sigma}}(\mathfrak{X})^T \widetilde{\mathbf{\Sigma}}(\mathfrak{X})\mathbf{l} \tag{3.6e}$$

Equation (3.6e) has the same form as the objective function in the problem (BOINCQP) with $P = 2\widetilde{\mathbf{\Sigma}}(\mathfrak{X})^T \widetilde{\mathbf{\Sigma}}(\mathfrak{X})$, $q = -2 \left(\sigma_i^{(ref)} \right)^T \widetilde{\mathbf{\Sigma}}(\mathfrak{X})$ and $r = \left(\sigma_i^{(ref)} \right)^T \sigma_i^{(ref)}$. Additionally, from Lemma 3.1.5 we have that $\widetilde{\mathbf{\Sigma}}(\mathfrak{X})^T \widetilde{\mathbf{\Sigma}}(\mathfrak{X})$ is positive definite matrix. Hence, the objective function η is convex. □

The solution method to this convex quadratic optimization problem with both linear inequality constraints and box constraints is already implemented in MATLAB by *quadprog* and is ready to use. The *quadprog* method is used with the *interior-point-convex* algorithm. From the load time series resulting from the optimization we compute corresponding stress time series. The stress time series is then used to compute the total damage at the hotspots and we hope that the computed total damage is as close as possible to the reference damage at every hotspot. We see in Section 3.2 the results of the optimization on two testrig configurations in the case of a steering knuckle.

In this section, we looked at testrig stress optimization problem. We showed that testrig stress optimization problem is a special case of convex quadratic optimization problem when we choose the objective function η as in Eq. (3.5). So far we did not involve damage directly in the optimization. In the next section, we see how we can use damage in the optimization by the help of block loads.

3.1.2. Damage Optimization

In this formulation of the testrig optimization problem, we involve damage directly in the objective function. However, when using a general load time series $\mathbf{L}$, the total damage is computed from the Algorithm 2.4.1 and the relation from load to the damage is non-differentiable due to the cycle counting algorithms like Rainflow counting. Additionally, if the mean value of the cycles obtained through Rainflow counting is not zero, then we have to additionally apply some form of correction to get the equivalent stress amplitude for the case of zero mean. Therefore, general load time series for damage optimization cannot be used with optimization algorithms that need first or higher order derivatives.

By using a load time series with block loads $\mathbf{L}_b$ we eliminate the need for counting cycles as well as corrections. Section 2.4.3 described the total damage computation on plane α at hotspot $\mathbf{x}$ from the amplitude vector $\hat{\mathbf{L}}$ and number of cycles for each block load in $\mathbf{L}_b$ given by $\mathcal{V}$ as

$$\hat{D}_{\mathbf{x}}(\hat{\mathbf{L}}, \mathcal{V}, \alpha) = D(\mathbf{N}(\alpha) \cdot \hat{\mathbf{\Sigma}}_{\mathbf{x}} \cdot \hat{\mathbf{L}}, \mathcal{V}) = \frac{1}{N_e \sigma_e^k} \sum_{j=1}^{m} \nu_j |\mathbf{n}(\alpha) \cdot \tilde{\boldsymbol{\sigma}}_{\mathbf{x}} \cdot \mathbf{l}_{b,j}|^k$$

where D is the total damage from alternating stresses from Eq. (2.45), $\mathbf{N}(\alpha)$ is from Eq. (2.58) and $\hat{\mathbf{\Sigma}}_{\mathbf{x}}$ is from Eq. (2.59).

Damage computation discussed in Section 2.4.3 was for a single hotspot. When we have more than one hotspots $\mathfrak{X} = \{\mathbf{x}_1, \mathbf{x}_2, \ldots, \mathbf{x}_{n_h}\}$ we need to compute the scalar stress from each block for every hotspot. For every hotspot $\mathbf{x}_i \in \mathfrak{X}$ we have a different stress tensor $\tilde{\boldsymbol{\sigma}}_{\mathbf{x}_i}$ which maps the loads to the stresses for that hotspot. The stress tensors $\tilde{\boldsymbol{\sigma}}_{\mathbf{x}_i}$ are already given and depend only on the testrig configuration $\mathcal{TC}$ used and the hotspot $\mathbf{x}_i$. The total damage at hotspot $\mathbf{x}_i, i = 1, 2, \ldots, n_h$ can then be computed as

$$\hat{D}_{\mathbf{x}_i}(\hat{\mathbf{L}}, \mathcal{V}, \alpha) = D(\mathbf{N}(\alpha) \cdot \hat{\mathbf{\Sigma}}_{\mathbf{x}_i} \cdot \hat{\mathbf{L}}, \mathcal{V}) = \frac{1}{N_e \sigma_e^k} \sum_{j=1}^{m} \nu_j |\mathbf{n}(\alpha) \cdot \tilde{\boldsymbol{\sigma}}_{\mathbf{x}_i} \cdot \mathbf{l}_{b,1}|^k \tag{3.7}$$

In the testrig damage optimization we fix the number of cycles for the block loads $\mathcal{V}$ before the optimization. We want to find the maximum total damage at each hotspot over all planes α. For every hotspot $\mathbf{x}_i$ the plane $\alpha^*_{\mathbf{x}_i}$ which has the maximum total damage may be different. Therefore, the only free parameters for the optimization are the elements of the amplitude vector $\ell_{ij}, i = 1, 2, \ldots, n, j = 1, 2, \ldots, m$, where ℓ_{ij} is the amplitude of the j-th block load at the i-th element of $\mathfrak{F}$. Again to tackle the testrig damage optimization problem the first step is to represent the search space as a subset of the Euclidean space.

Definition 3.1.9. (Design space of the testrig damage optimization problem) Let $l_{min} \leq l_l < l_u \leq l_{max}$ where l_{min} and l_{max} are the minimum and the maximum load that can be applied through the actuators in the testrig configuration $\mathcal{TC}$ respectively. We call

$$\mathscr{D}_D = \left\{ \hat{\mathbf{L}} \in \mathbb{R}^{nm} | \ell_{ij} \in [l_l, l_u], \forall i, j \right\}$$

the *design space* of the testrig damage optimization problem.

The optimization would want to answer with the most preferable solution out of the set of all

feasible solutions. The set of all feasible solutions is a subset of the design space. In what follows, every element of the design space is considered feasible whenever the magnitude of the maximum stress due to the element at all the hotspots is below some maximum stress σ_{max} as in the case of testrig stress optimization problem. Feasible set of the testrig optimization problem is:

Definition 3.1.10 (Feasible set of the testrig damage optimization problem)**.** For a given testrig configuration $\mathcal{TC}$, a solution $\hat{\mathbf{L}} \in \mathscr{D}_D$ is *feasible* if and only if

$$\left\| \hat{\mathbf{\Sigma}}_{\mathbf{x}_i} \cdot \hat{\mathbf{L}} \right\|_\infty \leq \sigma_{max}, \forall \mathbf{x}_i \in \mathfrak{X}$$

where $\hat{\mathbf{\Sigma}}_{\mathbf{x}_i}$ is from Eq. (2.59). The set of all feasible solutions for testrig damage optimization problem is denoted by $\mathcal{L}_D$.

However, not all feasible solutions are equally preferable. As in the case of testrig stress optimization we use *objective functions* to measure the preferability of one feasible solution compared to another feasible solution. In the context of testrig damage optimization this implies that we want the maximum of the total damage $\hat{D}_{\mathbf{x}_i}$ among all the planes α to be as close as possible to the reference damage $D^{(ref)}_{\mathbf{x}_i}$. We look on all the planes α because the component fails along the plane with the maximum damage. Let us denote by $\widetilde{D}_{\mathbf{x}_i}$ the maximum total damage at hotspot $\mathbf{x}_i$ with respect to planes α for the amplitude vector $\hat{\mathbf{L}}$:

$$\widetilde{D}_{\mathbf{x}_i}\left(\hat{\mathbf{L}}, \mathcal{V}\right) = \max_{\alpha \in [0,\pi)} \hat{D}_{\mathbf{x}_i}\left(\hat{\mathbf{L}}, \mathcal{V}, \alpha\right). \tag{3.8}$$

Generally it is not possible that the maximum total damage at every hotspot is equal to the reference damage at these hotspots. This forms the basis for the multi-objective nature of the testrig damage optimization problem. Let us denote by $\zeta_i : \mathscr{D}_D \to \mathbb{R}$ a function that measures the closeness of maximum total damage $\widetilde{D}_{\mathbf{x}_i}$ at hotspot $\mathbf{x}_i$ and reference damage $D^{(ref)}_{\mathbf{x}_i}$. This gives us a vector of functions $Z_{\mathcal{V}}$:

$$Z_{\mathcal{V}}(\hat{\mathbf{L}}) = \begin{pmatrix} \zeta_1\left(D^{(ref)}_{\mathbf{x}_1}, \widetilde{D}_{\mathbf{x}_1}\left(\hat{\mathbf{L}}, \mathcal{V}\right)\right) \\ \zeta_2\left(D^{(ref)}_{\mathbf{x}_2}, \widetilde{D}_{\mathbf{x}_2}\left(\hat{\mathbf{L}}, \mathcal{V}\right)\right) \\ \vdots \\ \zeta_{n_h}\left(D^{(ref)}_{\mathbf{x}_1}, \widetilde{D}_{\mathbf{x}_{n_h}}\left(\hat{\mathbf{L}}, \mathcal{V}\right)\right) \end{pmatrix} \tag{3.9}$$

We have to minimize $Z_{\mathcal{V}}$ in each of its component. As stated before $\mathcal{V}$ is fixed for each instance of the optimization problem. The set of objective function vectors $Z_{\mathcal{V}}(\mathscr{D}_D)$ is - as a subset of $\mathbb{R}^{n_h}$ - ordered by the *component wise order relation*:

$$y^1 \leq y^2 \implies y^1_i \leq y^2_i \ \forall i = 1, 2, \ldots, n_h.$$

However, this ordering is not *total*: it may occur that for some y^1, $y^2 \in Z_{\mathcal{V}}(\mathscr{D}_D)$ neither $y^1 \leq y^2$ nor $y^2 \leq y^1$ holds. As a consequence, usually there is no single feasible solution $\hat{\mathbf{L}}$ which is best in every objective function. Rather, there is a set of "minimal" solutions which are called *Pareto efficient*.

Definition 3.1.11 (Pareto efficient in Def 2.1 in [11])**.** A feasible solution $\hat{\mathbf{L}} \in \mathcal{L}_D$ is called Pareto efficient if there is no other $\widetilde{\mathbf{L}} \in \mathcal{L}_D$ such that $\zeta_i(\widetilde{\mathbf{L}}) \leq \zeta_i(\hat{\mathbf{L}})$ for all $i \in \{1, 2, \ldots, n_h\}$ and $\zeta_j(\hat{\mathbf{L}}) < \zeta_j(\widehat{\mathbf{L}})$ for some $j \in \{1, 2, \ldots, n_h\}$

Definition 3.1.12 (weakly Pareto efficient, Def. 2.24 in [11])**.** A feasible solution $\hat{\mathbf{L}} \in \mathcal{L}_D$ is called weakly Pareto efficient if there is no other $\widetilde{\mathbf{L}} \in \mathcal{L}_D$ such that $\zeta_i(\widetilde{\mathbf{L}}) < \zeta_i(\hat{\mathbf{L}})$ for all $i \in \{1, 2, \ldots, n_h\}$.

Definition 3.1.13 (Multi-objective optimization problem)**.** Let $Z : \mathscr{D}_D \to \mathbb{R}^{n_h}$. We call

$$\begin{aligned} Z(\hat{\mathbf{L}}) &\to \min \\ \hat{\mathbf{L}} &\in \mathcal{L}_D \end{aligned} \tag{MOOP}$$

a *multi-objective optimization problem*, where minimizing indicates the search for Pareto efficient solutions.

There are different ways to tackle (MOOP). Each Pareto efficient point is obtained as a solution to a weighted-sum-of-objective-functions problem:

$$\begin{aligned} Z_{\mathcal{V},W}(\hat{\mathbf{L}}) := \sum_{i=1}^{n_h} w_i \zeta_i \left(D_{\mathbf{x}_i}^{(ref)}, \widetilde{D}_{\mathbf{x}_i} \left(\mathbf{\Sigma}_{\mathbf{x}_i} \left(\hat{\mathbf{L}} \right), \mathcal{V} \right) \right) &\to \min \\ \hat{\mathbf{L}} &\in \mathcal{L}_D \end{aligned} \tag{WSDP}$$

where $W = (w_1, w_2, \ldots, w_{n_h})$ is the weight vector and the weights must respect the following relations: $w_i \geq 0$ for all $i \in \{1, 2, \ldots, n_h\}$ and

$$\sum_{i=1}^{n_h} w_i = 1.$$

Different choices of the weight vector W leads to different Pareto efficient solutions.

So far we have not discussed about the function ζ_i that measures the closeness of maximum total damage $\widetilde{D}_{\mathbf{x}_i}$ at hotspot $\mathbf{x}_i$ and reference damage $D_{\mathbf{x}_i}^{(ref)}$. From engineering point of view it is better that the total damage $\widetilde{D}_{\mathbf{x}_i}$ at different hotspots $\mathbf{x}_i$ are not underestimating the reference damage $D_{\mathbf{x}_i}^{(ref)}$. Underestimating reference damage would lead to overestimating fatigue life of the component which is not desirable. Therefore, the function ζ_i must penalize more the damage values at hotspots that underestimate the reference damage compared to the damage values that overestimate the reference damage by the same amount. Keeping this in mind we define the function ζ_i as:

$$\zeta_i \left(D_{\mathbf{x}_i}^{(ref)}, \widetilde{D}_{\mathbf{x}_i} \left(\hat{\mathbf{L}}, \mathcal{V} \right) \right) := \frac{D_{\mathbf{x}_i}^{(ref)}}{\widetilde{D}_{\mathbf{x}_i} \left(\hat{\mathbf{L}}, \mathcal{V} \right)} + \frac{\widetilde{D}_{\mathbf{x}_i} \left(\hat{\mathbf{L}}, \mathcal{V} \right)}{D_{\mathbf{x}_i}^{(ref)}}. \tag{3.10}$$

The function ζ_i from Eq. (3.10) is in the form of $\frac{1}{y} + y$ which has the minimum value when $y = 1$, i.e. $\widetilde{D}_{\mathbf{x}_1} \left(\hat{\mathbf{L}}, \mathcal{V} \right) = D_{\mathbf{x}_1}^{(ref)}$. We also observe that ζ_i penalizes the underestimation of the reference damage more than the overestimation. In the next results we give properties of the general ζ function

Lemma 3.1.14. *Let us define a function*

$$\zeta : \mathbb{R}_+ \to \mathbb{R}, y \mapsto \frac{1}{y} + y. \tag{3.11}$$

For $y_1, y_2 \in \mathbb{R}_+$, if we have $1 \geq y_1 > y_2$, then $\zeta(y_1) < \zeta(y_2)$.

Proof. The property stated above is true if we can show, that the function ζ is decreasing in the interval $(0, 1)$. A function is decreasing on an interval if the first derivative of the function is negative on this interval. We take the first derivative of the function ζ to get

$$\zeta'(y) = -\frac{1}{y^2} + 1 \tag{3.12}$$

For all values of $y \in (0, 1)$ we see that $\frac{1}{y^2} > 1$ and the sum $-\frac{1}{y^2} + 1$ is negative. Therefore, the function ζ is decreasing on the interval $(0, 1)$. This implies that for any $y_1, y_2 \in \mathbb{R}_+$ with $1 \geq y_1 > y_2$ we have $\zeta(y_1) < \zeta(y_2)$. □

Lemma 3.1.15. *The function ζ from Eq.* (3.11) *is increasing on the interval* $(1, \infty)$.

Proof. We know that the value of $\frac{1}{y^2}$ is less than one when $y > 1$. Therefore, the first derivative of the function ζ from (3.12) is positive and ζ is increasing on the interval $(1, \infty)$. □

In the next result we prove that the function ζ from Eq. (3.11) is convex on the interval $(0, \infty)$.

Theorem 3.1.16. *The function ζ from Eq.* (3.11) *is convex on the interval* $(0, \infty)$.

Proof. The second derivative of the function ζ is given as

$$\zeta''(y) = \frac{2}{y^3}. \tag{3.13}$$

Since the value of $\frac{2}{y^3} > 0$ for all $y \in (0, \infty)$ therefore, the function ζ is convex on the interval $(0, \infty)$. □

The solution method to the non-linear constrained optimization problem (WSDP) is already implemented in MATLAB by *fmincon* and is ready to use. The *fmincon* method is used with the *interior-point* algorithm. We see in Section 3.2 the results of the optimization on a real world example.

The following result holds for the optimal solution of the damage optimization problem (WSDP) with objective function $Z_{\mathcal{V},W}$:

Lemma 3.1.17. *If $\hat{\mathbf{L}}^* \in \mathcal{L}_D$ is an optimal solution to the damage optimization problem* (WSDP) *with functions ζ_i from Eq.* (3.10) *and fixed number of cycles $\mathcal{V}$, then $\exists i \in \{1, 2, \ldots, m\}$ such that*

$$\frac{\widetilde{D}_{\mathbf{x}_i}(\hat{\mathbf{L}}^*, \mathcal{V})}{D_{\mathbf{x}_i}^{(ref)}} \geq 1 \tag{3.14}$$

Proof. Let to the contrary that $\hat{\mathbf{L}}^* \in \mathcal{L}_D$ is an optimal solution to the damage optimization problem (WSDP) such that $\nexists i \in \{1, 2, \ldots, m\}$ satisfying Eq. (3.14). This implies

$$\forall i, \frac{\widetilde{D}_{\mathbf{x}_i}(\hat{\mathbf{L}}^*, \mathcal{V})}{D_{\mathbf{x}_i}^{(ref)}} < 1.$$

Let us choose $\hat{\mathbf{L}} = \alpha\hat{\mathbf{L}}^*$, $\alpha \in \mathbb{R}$ and $\alpha > 1$. We select α such that

$$\max\left(\frac{\widetilde{D}_{\mathbf{x}_1}(\hat{\mathbf{L}}^*,\mathcal{V})}{D^{(ref)}_{\mathbf{x}_1}},\ldots,\frac{\widetilde{D}_{\mathbf{x}_{n_h}}(\hat{\mathbf{L}}^*,\mathcal{V})}{D^{(ref)}_{\mathbf{x}_{n_h}}}\right) = 1.$$

Therefore, we have $\forall i \in \{1,2,\ldots,n_h\}$

$$1 \geq \frac{\widetilde{D}_{\mathbf{x}_i}(\hat{\mathbf{L}},\mathcal{V})}{D^{(ref)}_{\mathbf{x}_i}} > \frac{\widetilde{D}_{\mathbf{x}_i}(\hat{\mathbf{L}}^*,\mathcal{V})}{D^{(ref)}_{\mathbf{x}_i}}. \tag{3.15}$$

This is true because if we multiply all the elements of a amplitude vector by a positive scalar value, then the damage value changes by the k-th power of this scalar value, where k is the slope of the part of the S-N curve which is to be used. Using Lemma 3.1.14 for Eq. (3.15) we get $\forall i \in \{1,2,\ldots,n_h\}$

$$\frac{D^{(ref)}_{\mathbf{x}_i}}{\widetilde{D}_{\mathbf{x}_i}(\hat{\mathbf{L}},\mathcal{V})} + \frac{\widetilde{D}_{\mathbf{x}_i}(\hat{\mathbf{L}},\mathcal{V})}{D^{(ref)}_{\mathbf{x}_i}} < \frac{D^{(ref)}_{\mathbf{x}_i}}{\widetilde{D}_{\mathbf{x}_i}(\hat{\mathbf{L}}^*,\mathcal{V})} + \frac{\widetilde{D}_{\mathbf{x}_i}(\hat{\mathbf{L}}^*,\mathcal{V})}{D^{(ref)}_{\mathbf{x}_i}}. \tag{3.16}$$

This implies

$$\sum_{i=1}^{n_h} w_i \frac{D^{(ref)}_{\mathbf{x}_i}}{\widetilde{D}_{\mathbf{x}_i}(\hat{\mathbf{L}},\mathcal{V})} + \frac{\widetilde{D}_{\mathbf{x}_i}(\hat{\mathbf{L}},\mathcal{V})}{D^{(ref)}_{\mathbf{x}_i}} < \sum_{i=1}^{n_h} w_i \frac{D^{(ref)}_{\mathbf{x}_i}}{\widetilde{D}_{\mathbf{x}_i}(\hat{\mathbf{L}}^*,\mathcal{V})} + \frac{\widetilde{D}_{\mathbf{x}_i}(\hat{\mathbf{L}}^*,\mathcal{V})}{D^{(ref)}_{\mathbf{x}_i}}. \tag{3.17}$$

This is a contradiction to the optimality of $\hat{\mathbf{L}}^*$ and therefore the assumption made is not correct and proves the result. □

Next, we give an analytical representation of the maximum total damage when S-N curve has one slope and a load time series with one block is acting through the actuators.

Lemma 3.1.18. *If the number of blocks in a load time series with block load is one and S-N curve has one slope, the value of $\widetilde{D}_{\mathbf{x}_i}$ defined in Eq.* (3.8) *is given as*

$$\widetilde{D}_{\mathbf{x}_i}\left(\hat{\mathbf{L}},\mathcal{V}\right) = \frac{\nu_1}{\sigma_e^k N_e}\left(\frac{1}{2}\sqrt{\left(\tilde{\boldsymbol{\sigma}}^1_{\mathbf{x}_i}\hat{\mathbf{L}} + \tilde{\boldsymbol{\sigma}}^2_{\mathbf{x}_i}\hat{\mathbf{L}}\right)^2} + \sqrt{\frac{1}{4}\left(\tilde{\boldsymbol{\sigma}}^1_{\mathbf{x}_i}\hat{\mathbf{L}} - \tilde{\boldsymbol{\sigma}}^2_{\mathbf{x}_i}\hat{\mathbf{L}}\right)^2 + \left(\tilde{\boldsymbol{\sigma}}^3_{\mathbf{x}_i}\hat{\mathbf{L}}\right)^2}\right)^k \tag{3.18}$$

where ν_1 is the number of cycles of the first and only block, σ_e, N_e and k depend on the material properties.

Proof. We have one block therefore $\hat{\boldsymbol{\Sigma}}_{\mathbf{x}_i}\cdot\hat{\mathbf{L}}$ is a column vector with three components corresponding to $\sigma_{\mathbf{x}_i,xx}$, $\sigma_{\mathbf{x}_i,yy}$ and $\sigma_{\mathbf{x}_i,xy}$ respectively. If $\tilde{\boldsymbol{\sigma}}^j_{\mathbf{x}_i}$ represents the j-th row of the stress tensor $\tilde{\boldsymbol{\sigma}}_{\mathbf{x}_i}$ then we have $\sigma_{\mathbf{x}_i,xx} = \tilde{\boldsymbol{\sigma}}^1_{\mathbf{x}_i}\hat{\mathbf{L}}$, $\sigma_{\mathbf{x}_i,yy} = \tilde{\boldsymbol{\sigma}}^2_{\mathbf{x}_i}\hat{\mathbf{L}}$ and $\sigma_{\mathbf{x}_i,xy} = \tilde{\boldsymbol{\sigma}}^3_{\mathbf{x}_i}\hat{\mathbf{L}}$. Again from Corollary 2.3.14 we know that the maximum absolute value of scalar stress is given as $a(\boldsymbol{\sigma}) + b(\boldsymbol{\sigma})$ where $a(\boldsymbol{\sigma}) = \frac{1}{2}\left|\sigma_{xx} + \sigma_{yy}\right| = \frac{1}{2}\sqrt{\left(\sigma_{xx} + \sigma_{yy}\right)^2}$ and $b(\boldsymbol{\sigma}) = \sqrt{\frac{1}{4}\left(\sigma_{xx} - \sigma_{yy}\right)^2 + \sigma_{xy}^2}$. In the current context this gives us

$$\widetilde{D}_{\mathbf{x}_i}\left(\hat{\mathbf{L}},\mathcal{V}\right) = \frac{\nu_1}{\sigma_e^k N_e}\left(\frac{1}{2}\sqrt{\left(\tilde{\boldsymbol{\sigma}}^1_{\mathbf{x}_i}\hat{\mathbf{L}} + \tilde{\boldsymbol{\sigma}}^2_{\mathbf{x}_i}\hat{\mathbf{L}}\right)^2} + \sqrt{\frac{1}{4}\left(\tilde{\boldsymbol{\sigma}}^1_{\mathbf{x}_i}\hat{\mathbf{L}} - \tilde{\boldsymbol{\sigma}}^2_{\mathbf{x}_i}\hat{\mathbf{L}}\right)^2 + \left(\tilde{\boldsymbol{\sigma}}^3_{\mathbf{x}_i}\hat{\mathbf{L}}\right)^2}\right)^k. \qquad \square$$

3.2. Numerical results

For the damage optimization we have to compute the maximum total damage $\widetilde{D}_{\mathbf{x}_i}$ at every hotspot $\mathbf{x}_i \in \mathfrak{X}$ for every iteration in the optimization. For more than one block in the load time series, there is no analytical representation which we can use to do so. Therefore, we discretize the interval $[0, \pi)$ for the plane angle α into eighteen points. We compute the total damage at each of these points. The maximum damage at these eighteen points is taken as the value of $\widetilde{D}_{\mathbf{x}_i}$. We do this for each hotspot. We discuss in Section 3.3, the issues relating to computing maximum total damage through discretization.

3.2.1. Example: Knuckle

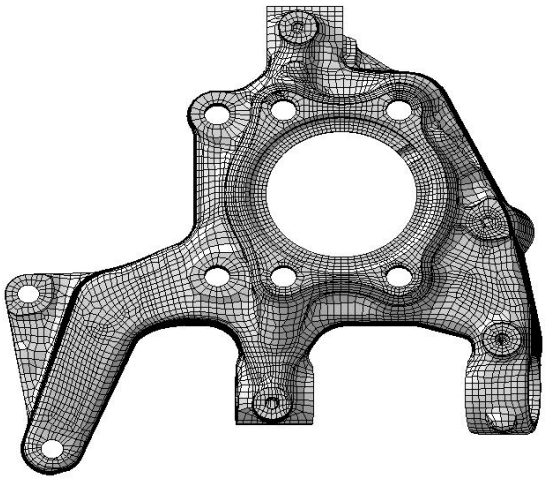

Figure 3.2.: A knuckle [1].

The example we look at is a knuckle. A knuckle connects the steering wheel to the suspension and wheels of the vehicle. So, we can say that a knuckle connects the steering wheel to the rest of the vehicle, allowing the driver to direct the vehicle. As the driver turns the wheel, the motion is transferred through the knuckles. Knuckle is one of the most often used components of a vehicle. Therefore, precise estimation of fatigue lifetime of a knuckle is important. In Figure 3.2, we see the knuckle which we use as the component under testing.

The knuckle in Figure 3.2 has seven possible attachment points. We use one of these attachment point as the fixation point A_f to fix the component in the testrig. We do not want the number of force/moment n acting through the actuators to be more than three so in all the results presented we have $n = 3$. The number of hotspots n_h is given to be ten. The location of the ten hotspots is given by $\mathfrak{X} = \{\mathbf{x}_1, \mathbf{x}_2, \ldots, \mathbf{x}_{10}\}$. We have been given the reference stress time series and the the reference damage values for each hotspot. The reference damage values $D^{(ref)}$ for the hotspots are given in Table 3.1:

The material of the knuckle has two slopes in the S-N curve. The value of the alternating stress where the slope changes is $\sigma_1 = 74.8kPa$ and the corresponding value of the number of cycles

i	$D_{\mathbf{x}_i}^{(ref)}$
1	3.2×10^{-5}
2	5.4×10^{-5}
3	4.0×10^{-5}
4	5.2×10^{-5}
5	2.2×10^{-5}
6	2.2×10^{-5}
7	1.8×10^{-5}
8	3.8×10^{-6}
9	3.6×10^{-5}
10	2.8×10^{-5}

Table 3.1.: The reference damage values for the ten hotspots on the knuckle.

is $N_1 = 1 \times 10^6$. The ultimate tensile stress and the maximum allowed stress value is given as $\sigma_u = 190.5kPa$ and $\sigma_{max} = 190.5kPa$, respectively. The slope $k_1 = 5$ and the slope $k_2 = 15$.

We compare the results obtained from the stress optimization problem (TSOP) and damage optimization problem (WSDP) for different testrig configurations $\mathcal{TC}$. At the end of this section, we compare the results from the different instances of the testrig damage optimization problem.

Stress and Damage optimization results

There are 17400 points in the reference stress time series. Therefore, the general load time series that is obtained from the stress optimization also has 17400 points. This is different in the case of damage optimization. The number of points in the load time series with block loads depend only on the number of block loads and the number of cycles of each block load. We use the inbuilt function *quadprog* of MATLAB with the *interior-point-convex* algorithm for the stress optimization and the inbuilt function *fmincon* of MATLAB with the *interior-point* algorithm for the damage optimization. We see the results obtained from the stress and damage optimization on two different configurations.

First Configuration: The first testrig configuration we consider is given as:

$$\mathcal{TC}_1 = (3, \{2, 4, 5\}, \{(2, \{f_x\}), (4, \{f_y\}), (5, \{f_y\})\}). \tag{3.19}$$

The index of the fixation point is $A_f = 3$. We apply load time series at $\mathfrak{F} = (2_{f_x}, 4_{f_y}, 5_{f_y})$, i.e., at the attachment point with index 2 we apply forces along the x-axis, at the attachment points with index 4 and 5 we apply forces along the y-axis. For the damage optimization problem we additionally fix the number of block loads m to 50, the number of cycles for each block load $\nu_i = 5, i = 1, 2, \ldots, m$ and the weights w_i to be all equal. The constraints on the maximum and minimum loads that can be applied through the actuators is given as $l_l = -18000$ Newtons and $l_u = 18000$ Newtons, respectively. We are also given the stress tensor $\tilde{\boldsymbol{\sigma}}_{\mathbf{x}_i}$ for the ten hotspots.

For the damage optimization we used a random vector with maximum magnitude half the maximum allowed load l_u in the testrig. All calculations are done on an Intel Core i3 CPU with 2.53 GHz and 4 GB RAM. Calculating a solution using stress optimization takes 35.67 seconds.

Calculating a solution using damage optimization takes 148.03 second for 182 iterations. This corresponds to an average of 0.81 second for each iteration. We see in what follows that although the time taken for damage optimization is larger compared to the stress optimization we get better results with damage optimization.

Since, we want to be as close as possible to the reference damage at the hotspots we compare the results obtained from the stress optimization problem and the damage optimization problem in terms of the maximum total damage at each hotspot in Figure 3.3. We also present the function values ζ_i from Eq. (3.9) for each hotspot $\mathbf{x}_i$ for the two optimization problems in Figure 3.4.

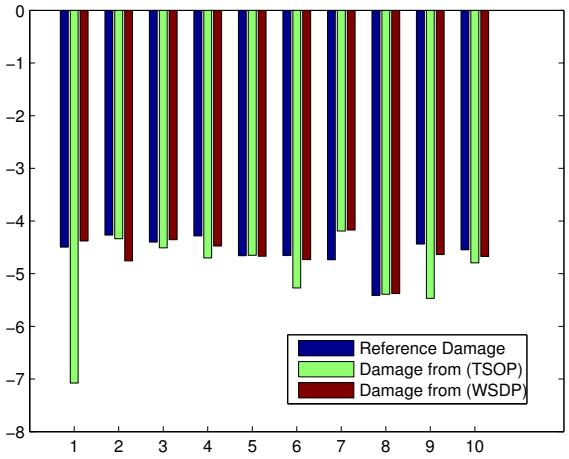

Figure 3.3.: Maximum total damage from the stress optimization (green) and the damage optimization (brown) compared with the reference damage (blue). The horizontal axis is the index of the hotspots and the vertical axis is the damage values on the logarithmic scale.

In Figure 3.3, we see as expected the maximum total damage from damage optimization is closer to the reference damage at more than half the hotspots. At the hotspot with index 2 the maximum total damage from stress optimization is closer to the reference damage. The number of points in the load time series with block loads $\mathbf{L}_b$ from damage optimization is $4\sum_{i=1}^{50}\nu_i + 1 = 1001$. We see that with only one-seventeenth number of points in the load time series, damage optimization gives maximum total damage which is closer to the reference damage at more than half of the hotspots when compared with the maximum total damage from the load time series resulting from stress optimization.

In Table 3.2, we see the magnitude of the relative error for the total maximum damage at all the hotspots for the stress optimization and the damage optimization. We see that the maximum magnitude of relative error in the stress optimization is higher than that in the case of damage optimization. This again implies that maximum total damage obtained by the damage optimization is closer to the reference damage values.

i	$\frac{\lvert D^{(ref)}_{\mathbf{x}_i} - D_{\mathbf{x}_i} \rvert}{D_{\mathbf{x}_i}}$ for (TSOP)	$\frac{\lvert D^{(ref)}_{\mathbf{x}_i} - \tilde{D}_{\mathbf{x}_i} \rvert}{\tilde{D}_{\mathbf{x}_i}}$ for (WSDP)
1	379.32	0.234
2	0.175	2.084
3	0.287	0.098
4	1.620	0.558
5	0.014	0.024
6	3.115	0.192
7	0.716	0.727
8	0.056	0.084
9	9.738	0.582
10	0.764	0.333

Table 3.2.: The relative error in damage for maximum total damage computed from the load time series obtained as a result of the two optimization.

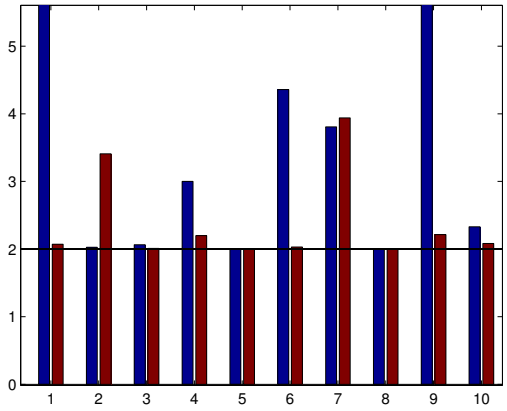

Figure 3.4.: Results for evaluating function ζ for the damage from the stress optimization (blue) and the damage optimization (brown). The black horizontal line with a value of 2 is the minimum value for the function ζ. The horizontal axis is the index of the hotspots and the vertical axis is the values of the function ζ.

In Figure 3.4, we see that at eight out of ten hotspots the value of the function ζ_i is close to its minimum value for the damage optimization. But, this is true only for five hotspots for the stress optimization. The maximum value among the functions ζ_i for the damage optimization is for hotspot with index 7 and has a value of 3.940. The maximum value among the functions ζ_i for the stress optimization is for hotspot with index 1 and has a value of 380.33. Optimally we want the value of the functions ζ_i to be two for all the hotspots.

In Figure 3.5, we see the load time series obtained from the stress optimization and in Figure 3.6 we see the load time series with block load obtained from the damage optimization. The general load time series $\mathbf{L}$ from the stress optimization (TSOP) is very irregular and difficult to use in a testrig when compared to the load time series with block loads $\mathbf{L}_b$ from the damage optimization (WSDP) that is easier to use and has considerably small number of points. Additionally, we see that the load time series at hotspot with index 2 resulting from the stress optimization (TSOP) has a magnitude of 80000 Newtons which is approximately four times the maximum magnitude

allowed in the damage optimization. The box constraint put on the amplitude of the block loads is active only for two blocks as seen in Figure 3.6 (a).

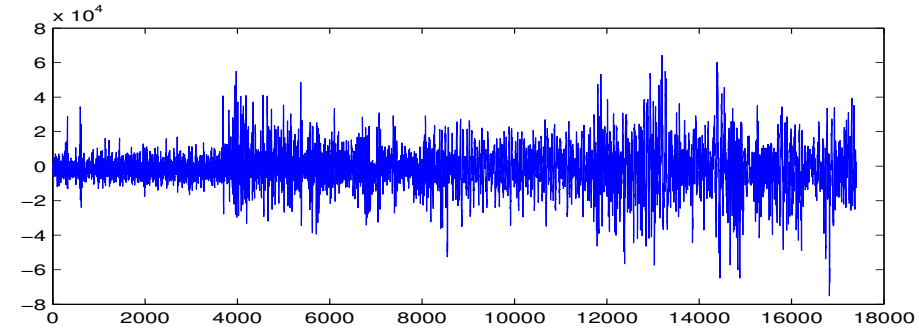

(a) Load time series at hotspot with index 2 acting along the x-axis.

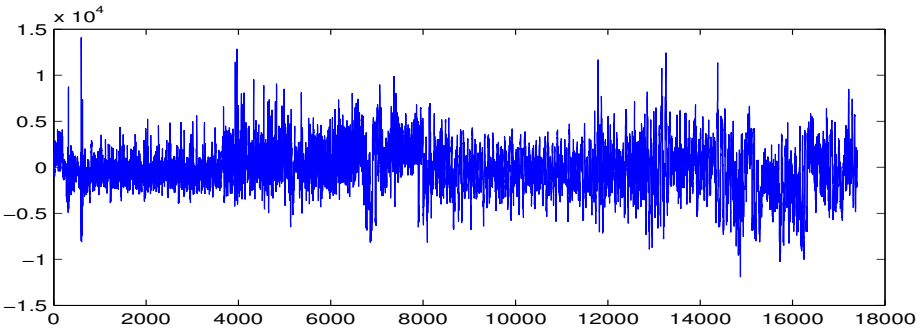

(b) Load time series at hotspot with index 4 acting along the y-axis.

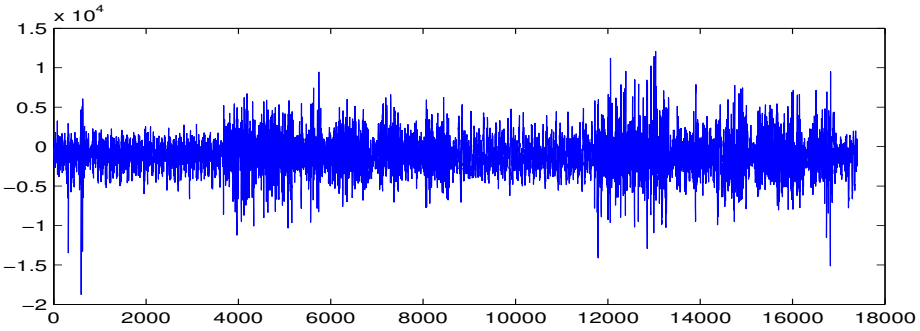

(c) Load time series at hotspot with index 5 acting along the y-axis.

Figure 3.5.: General load time series $\mathbf{L}$ obtained from stress optimization (TSOP) for testrig configuration $\mathcal{TC}_1$ from Eq. (3.19).

One thing to point out here is that not all the points in the load time series obtained in the case of stress optimization (TSOP) contributes to the damage contribution. This is because many of the points are removed when computing damage using 4-Point algorithm for counting cycles in the stress time series. In case of the load time time series with block loads obtained from damage optimization every block load has a contribution in the total damage.

We saw for the testrig configuration $\mathcal{TC}$ in Eq. (3.19) that the load time series obtained as a result of the damage optimization (WSDP) incurs damage at the hotspot that is closer to the reference

damage at eight hotspots as compared to the damage from the load time series obtained as a result of the stress optimization (TSOP).

Second Configuration
Next, we give results for the testrig configuration which has the best results in the context that stress optimization fives maximum total damage value close to the reference damage values at all except one hotspot:

$$\mathcal{TC}_2 = (3, \{5, 4, 2\}, \{(5, \{f_x\}), (4, \{f_y\}), (2, \{f_z\})\}) \tag{3.20}$$

The index of the fixation point is $A_f = 3$. We apply load time series at $\mathfrak{F} = (5_{f_x}, 4_{f_y}, 2_{f_z})$, i.e., at the attachment point with index 5 we apply forces along the x-axis, at the attachment point with index 4 we apply forces along the y-axis and at the attachment point with index 2 we apply forces along the z-axis. For the damage optimization problem we additionally fix the number of block loads m to 50, the number of cycles for each block load $\nu_i = 5, i = 1, 2, \ldots, m$ and the weights w_i to be all equal. The constraints on the maximum and minimum loads that can be applied through the actuators is given as $l_l = -14000$ Newtons and $l_u = 14000$ Newtons. We are also given the stress tensor $\tilde{\boldsymbol{\sigma}}_{\mathbf{x}_i}$ for the ten hotspots.

For the damage optimization we used a random vector with maximum magnitude half the maximum allowed load l_u in the testrig. All calculations are done on an Intel Core i3 CPU with 2.53 GHz and 4 GB RAM. Calculating a solution using stress optimization takes 37.49 seconds. Calculating a solution using damage optimization takes 174.08 second for 213 iterations. This corresponds to an average of 0.817 seconds for each iteration.

In Figure 3.7, we see that the maximum total damage at the ten hotspots resulting from the load time series obtained through stress optimization (TSOP) and damage optimization (WSDP). In Figure 3.8, we see the function values ζ_i from Eq. (3.9) for each hotspot $\mathbf{x}_i$ for the two optimization problems.

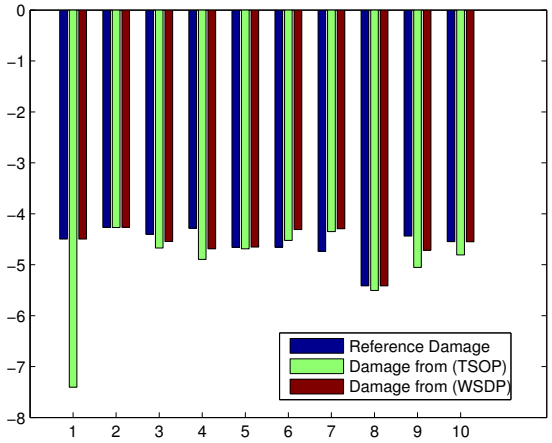

Figure 3.7.: Maximum total damage from stress optimization (green) and damage optimization (brown) compared with the reference damage (blue). The horizontal axis is the index of the hotspots and the vertical axis is the damage values on the logarithmic scale.

In this case as well, maximum total damage due to the load time series as a result of the damage optimization is closer to the reference damage at six hotspots. At other hotspots, the difference between the damages incurred by the load time series from the two optimization problems is small. The advantage of the damage optimization is that the maximum relative error is comparatively less for all the hotspots which is not true for the stress optimization. Again, the number of points in the load time series with block loads $\mathbf{L}_b$ from damage optimization is $4\sum_{i=1}^{50}\nu_i + 1 = 1001$.

In Table 3.3, we see the magnitude of the relative error for the total maximum damage at all the hotspots for the stress optimization and the damage optimization. Similar to the observation made from Table 3.2, we see that the maximum magnitude of relative error in the stress optimization is higher than that in the case of damage optimization. This implies that maximum total damage obtained by the damage optimization is closer to the reference damage values.

i	$\frac{\lvert D^{(ref)}_{\mathbf{x}_i} - D_{\mathbf{x}_i}\rvert}{D_{\mathbf{x}_i}}$ for (TSOP)	$\frac{\lvert D^{(ref)}_{\mathbf{x}_i} - \widetilde{D}_{\mathbf{x}_i}\rvert}{\widetilde{D}_{\mathbf{x}_i}}$ for (WSDP)
1	809.078	0.042
2	0.004	0.019
3	0.862	0.410
4	3.094	1.567
5	0.072	0.021
6	0.245	0.572
7	0.590	0.635
8	0.228	0.005
9	3.125	0.803
10	0.186	0.020

Table 3.3.: The magnitude of the relative error in damage for maximum total damage computed from the load time series obtained as a result of the two optimization. Here, $D_{\mathbf{x}_i}$ denotes the maximum total damage from the load time series resulting from the stress optimization (TSOP) at hotspot $\mathbf{x}_i$.

In Figure 3.8, we see that at seven out of the ten hotspots a value close to the minimum value of the ζ function is obtained for the damage optimization. However, this is true only for four hotspots for the stress optimization. The maximum value among the functions ζ_i for the damage optimization is for hotspot with index 7 and has a value of 3.138. The maximum value among the functions ζ_i for the stress optimization is for hotspot with index 1 and has a value of 810.08. We observe that the maximum value among the functions ζ_i for damage optimization is less than the maximum value of among the functions ζ_i in the previous testrig configuration. This means that the maximum relative error is smaller in this testrig configuration. But, the maximum value of ζ_i for stress optimization is approximately twice the value of the maximum value of ζ_i in the previous testrig configuration. However, we observe that the value of the function ζ_i at other hotspots is all less than 4.5 in this testrig configuration unlike the previous testrig configuration.

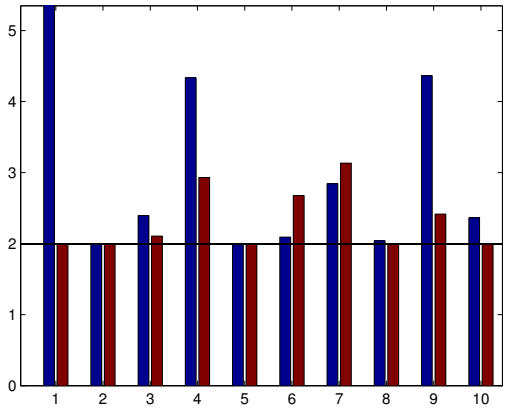

Figure 3.8.: Results for evaluating function ζ for the damage from the stress optimization (blue) and the damage optimization (brown). The black horizontal line with a value of 2 is the minimum value for the function ζ. The horizontal axis is the index of the hotspots and the vertical axis is the values of the function ζ.

In Figure 3.9, we see the load time series obtained from the testrig stress optimization and in Figure 3.10 we see the load time series with block load obtained from the damage optimization. The general load time series $\mathbf{L}$ from the stress optimization (TSOP) is very similar to that obtained in the stress optimization from the previous testrig configuration. The box constraint put on the amplitude of the block loads is not active on any of the block loads in all the three load time series as seen in Figure 3.10 (a).

From Table 3.2 and Table 3.3 we see that the maximum magnitude of the relative error in the case of testrig damage optimization problem (WSDP) is very small compared to the maximum relative error in the case of testrig stress optimization problem (TSOP). Also, the function ζ_i for hotspots $\mathbf{x}_i, i = 1, 2, \ldots, n_h$, when evaluated for total maximum damage from testrig damage optimization problem (WSDP) is closer to the minimum value of 2 in comparison to the values of the function ζ_i when evaluated for the total maximum damage from testrig stress optimization problem (WSDP). The length of the load time series obtained in the stress optimization is always equal to the reference stress time series which usually has thousands of points, however, the length of the load time series obtained by damage optimization depends on the number of chosen blocks and corresponding number of cycles. The cost and time for applying the load time series through actuators in damage optimization can be controlled which is not possible for the load time series obtained by the stress optimization. Therefore, we see that damage optimization is a better alternative to the stress optimization which is the current state of the art.

So far we have not investigated the effect of the number of times a unit of the block load is repeated on the optimal objective function value resulting from the damage optimization. In the next section we discuss this aspect of the damage optimization. We end the next section by looking at the consequences of using discretization in finding the maximum total damage over all planes.

3.3. Discussion

In Figure 3.11, we see the optimal value of the objective function $Z_{\mathcal{V},W}$ for load time series with one block when ν_1 is increasing. When the value of ν_i is increasing we see that the optimal value of $Z_{\mathcal{V},W}$ is also increasing. This trend is also observed when we have more than one block in the load time series. However, the slope of the curve in higher number of blocks is not as steep as seen in Figure 3.11. Therefore, from what has been observed it is not optimal to take the value of ν_i very large.

In the previous section, we gave results for the damage optimization which used discretization of the plane angles α for finding the maximum total damage at each iteration in the optimization. Discretization as expected leads to discretization error when computing maximum total damage. This error is introduced at each iteration of the optimization and therefore, may lead to solutions that do not estimate the fatigue life of the component as precisely as required. In Figure 3.12, we see the actual total damage $\hat{D}_{\mathbf{x}_i}$ on the interval $[0, \pi)$ and the total damage on the 18 planes into which we discretized the interval $[0, \pi)$. In (a), we see the plots for the results presented for the testrig configuration $\mathcal{TC}_1$ from Eq. (3.19) and in (b), we see the plots for the results presented for the testrig configuration $\mathcal{TC}_2$ from Eq. (3.20). In both the plots we only show the total damage for those hotspots where the discretization error is more than 3%. The discretization error could go as high as 10%.

Therefore, we want to be able to compute the maximum total damage on the planes α as accurately as possible. However, there is no direct method that can be used to do so. Therefore, in the next chapter we remodel damage from a block load as Gaussian functions such that the plane angle α is the only independent variable in the case of one slope in the S-N curve. Total damage is then given as the sum of Gaussian functions. In Chapter 5, we derive conditions that when satisfied the Gaussian functions in the sum leads to a single maximum. We use these conditions to give a clustering algorithm. The clustering algorithm is used to approximate the point of maximum total damage for each hotspot. Finally, we use the theory developed in Chapter 6 for computing the exact maximum total damage at each iteration during the optimization.

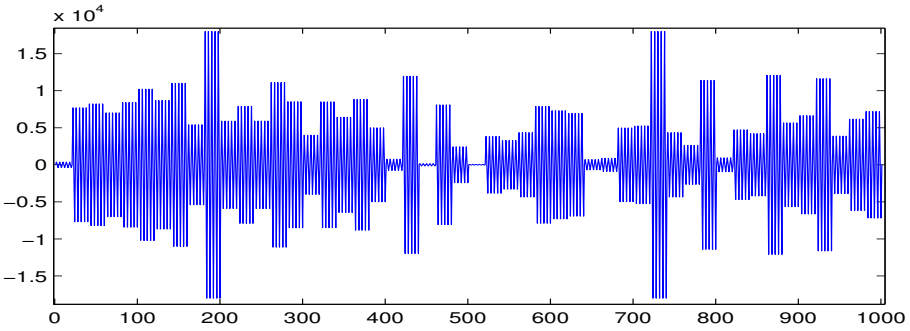

(a) Load time series with block loads at hotspot with index 2 acting along the x-axis.

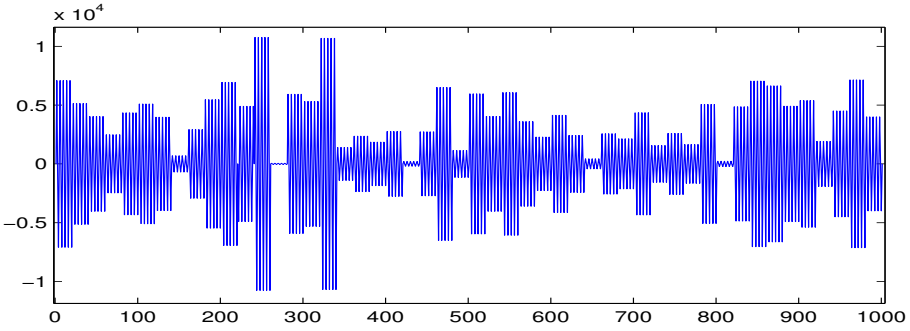

(b) Load time series with block loads at hotspot with index 4 acting along the y-axis.

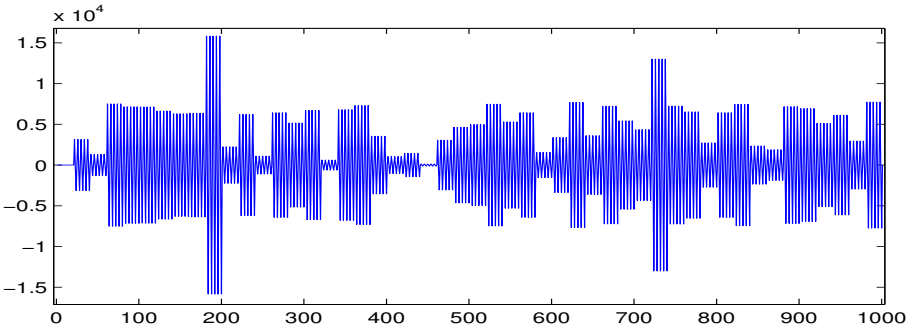

(c) Load time series with block loads at hotspot with index 5 acting along the y-axis.

Figure 3.6.: Load time series with block loads $\mathbf{L}_b$ obtained from damage optimization (WSDP) for testrig configuration $\mathcal{TC}_1$ from (3.19).

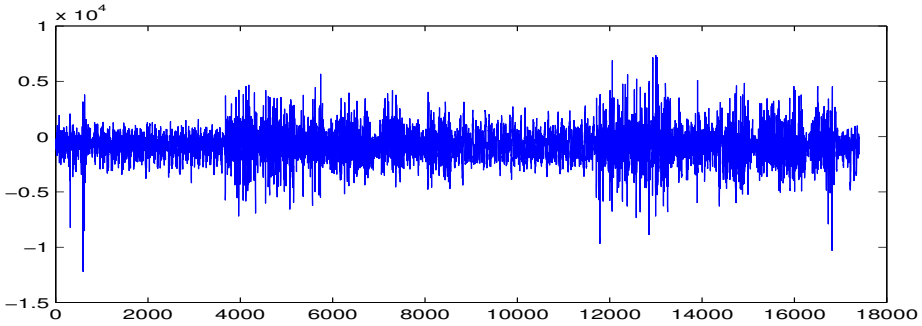

(a) Load time series at hotspot with index 5 acting along the x-axis.

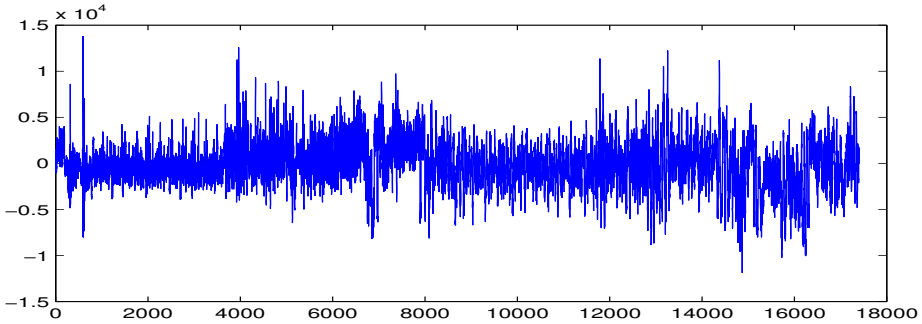

(b) Load time series at hotspot with index 4 acting along the y-axis.

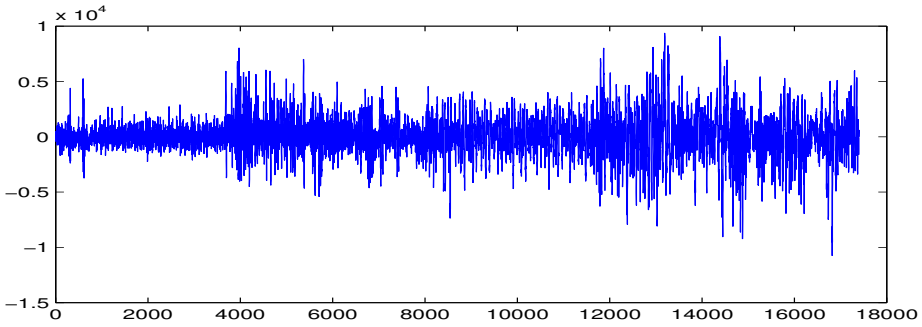

(c) Load time series at hotspot with index 2 acting along the z-axis.

Figure 3.9.: General load time series $\mathbf{L}$ obtained from stress optimization (TSOP) for testrig configuration $\mathcal{TC}_2$ from (3.20).

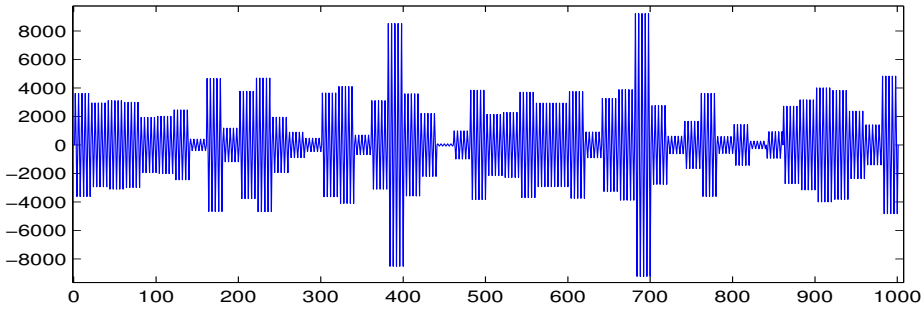

(a) Load time series with block loads at hotspot with index 5 acting along the x-axis.

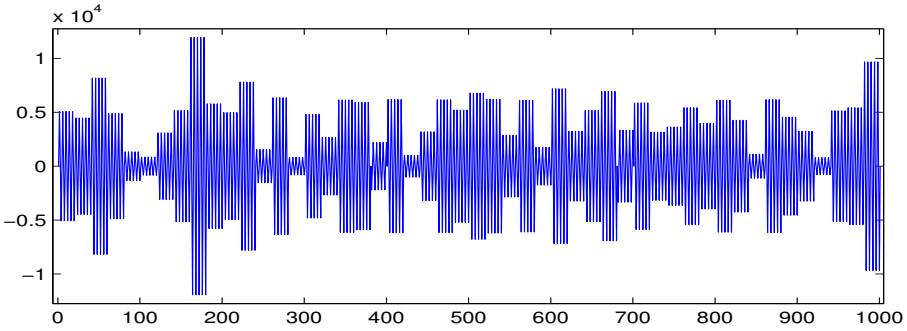

(b) Load time series with block loads at hotspot with index 4 acting along the y-axis.

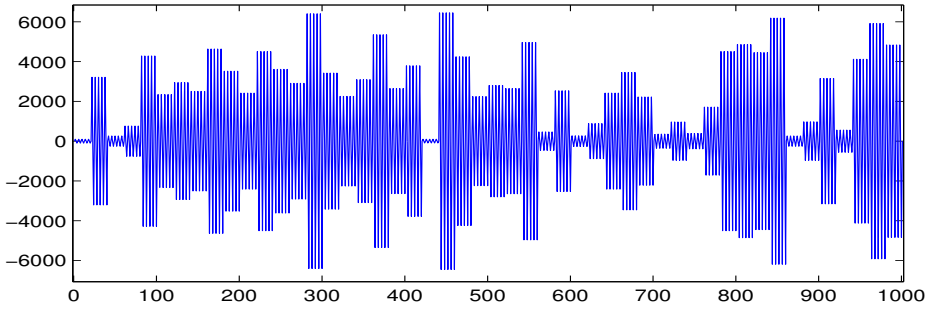

(c) Load time series with block loads at hotspot with index 2 acting along the z-axis.

Figure 3.10.: Load time series with block loads $\mathbf{L}_b$ obtained from damage optimization (WSDP) for testrig configuration $\mathcal{TC}_2$ from (3.20).

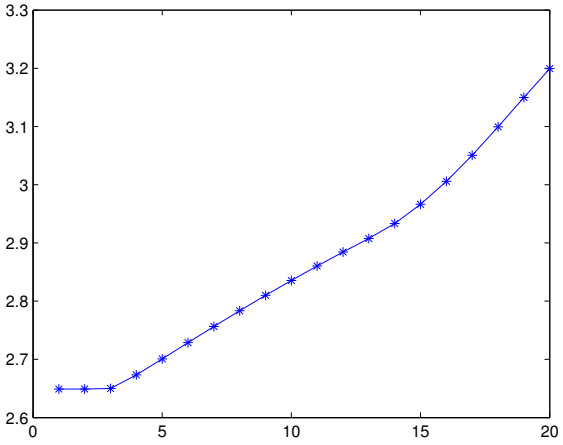

Figure 3.11.: Optimal value of objective function $Z_{\mathcal{V},W}$ for testrig configuration $\mathcal{TC}_2$ for load time series with one block for different values of ν_1. The horizontal axis gives the value of ν_1 and the vertical axis gives the optimal value of the objective function $Z_{\mathcal{V},W}$.

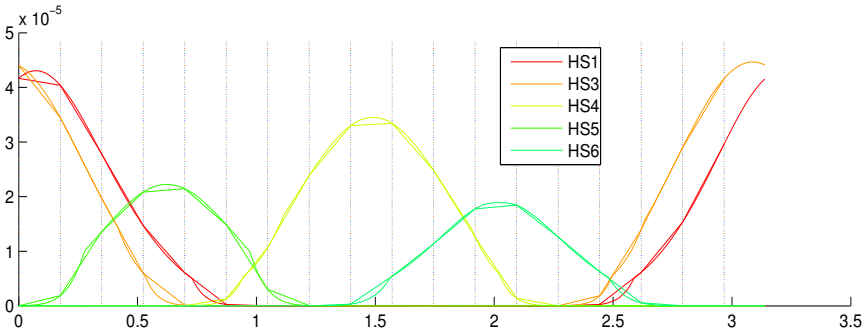

(a) Testrig configuration $\mathcal{TC}_1$

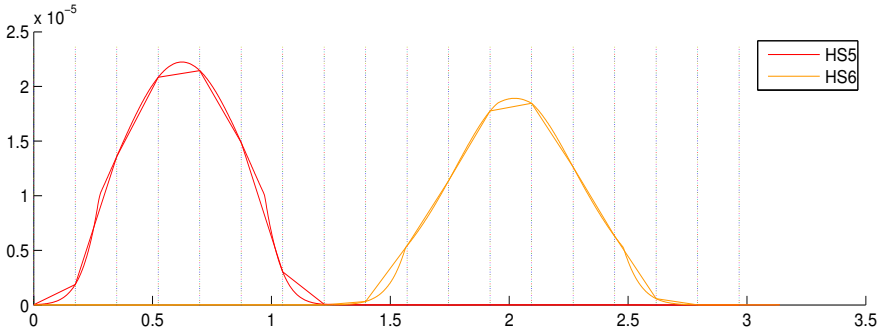

(b) Testrig configuration $\mathcal{TC}_2$

Figure 3.12.: Total damage on 18 planes (dotted lines) and actual damage on the interval $[0, \pi)$. (a) plots for hotspots with index 1, 3, 4, 5, and 6 in the case of testrig configuration $\mathcal{TC}_1$. (b) plots for hotspots with index 5 and 6 from the results obtained in the case of testrig configuration $\mathcal{TC}_2$. We see the discretization error by taking the maximum total damage from the 18 planes shown as dotted lines.

4. Gaussian approximation of damage: one slope

In the previous chapter we saw that the maximum damage computed from the discretization of the plane angle α can introduce discretization errors. Due to the discretization errors the optimal load time series computed by the optimization algorithm is not the actual optimal and the component may fail before its estimated fatigue life. We discretized the plane angle α as there is no direct method which gives the maximum damage for a given block loading. Before we can deal with the discretization errors we must be able to represent the damage in terms of the plane angle α as the only independent variable. In this chapter the damage is approximated by the Gaussian functions with α as the independent variable for load time series with one block having just one cycle. Since, we want to find the maximum damage for a given load time series with block loads it is important that the approximation is very close to the damage in the neighborhood of its maximum.

Definition 4.0.1 (Gaussian function)**.** A Gaussian function is defined as

$$f_{\breve{a},\breve{b},\breve{c}} : \mathbb{R} \to \mathbb{R}, \alpha \mapsto \breve{a} \exp\left(-\left(\frac{\alpha - \breve{b}}{\breve{c}}\right)^2\right) \tag{4.1}$$

where $\breve{a} \in \mathbb{R}_+$ is the maximum value of $f_{\breve{a},\breve{b},\breve{c}}$ at $\alpha = \breve{b}$, $\breve{b} \in \mathbb{R}$ and $\breve{c} \in \mathbb{R}_+$ such that $\breve{b} \pm \frac{\breve{c}}{\sqrt{2}}$ are the inflexion points of $f_{\breve{a},\breve{b},\breve{c}}$.

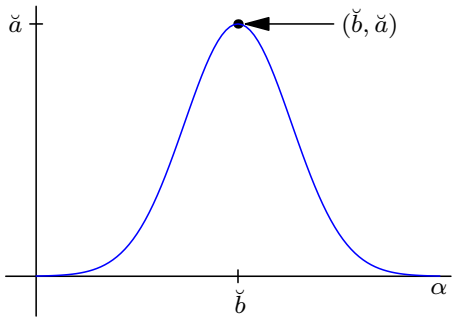

Figure 4.1.: General form of the graph of a Gaussian function $f_{\breve{a},\breve{b},\breve{c}}$.

Section 4.1 recapitulates the computation of the damage for one slope. We also see that the damage is a periodic function with period π. In Section 4.2, the idea of approximation of damage around the point of maximum is introduced and the parameters $\breve{a}$, $\breve{b}$ and $\breve{c}$ of the approximation are derived while formulating a result on the quality of the approximation. In other words in Section 4.2, we derive the approximate model for one period of damage. In Section 4.3, an approximate model for damage for $\alpha \in \mathbb{R}$ is developed. For more than one block load, the damage from each block can

have different points of maximum. Keeping this in mind, Section 4.4 gives an approximation of the damage for one block on the interval $[0, \pi]$. In Section 4.4, the interval $[0, \pi]$ becomes the common interval for the approximation of the damage for different block loads and is chosen because the damage function is periodic with period π. The chapter concludes with the comparison of the damage and the approximated model in Section 4.5. Numerical results are presented to show that the error of approximation is small in the neighborhood of the maximum value.

4.1. Damage for one slope

The failure of a component starts by the formation of microscopic cracks in the high stress regions on the surface. When these microscopic cracks reach a critical size the component suddenly fails [21]. We therefore want to compute the damage on the surface. In this chapter we approximate damage from a load time series with one block having just one cycle. For computing the damage at any point $\mathbf{x} \in \mathbb{R}^3$ on the surface due to a load time series with one block load $\mathbf{L}_b$, we need to know the stress $\boldsymbol{\sigma}_\mathbf{x} = (\sigma_{xx}, \sigma_{yy}, \sigma_{xy})^T$, at that point and the angle of the plane ($\alpha \in \mathbb{R}$) that we are interested in. We know from Section 2.4.3 that the damage is computed in terms of the matrix of amplitudes $\mathbf{L}_{b,a} = (\mathbf{l}_{b,1})$ of the block loads in the load time series with block loads $\mathbf{L}_b$:

$$\begin{aligned} D_\mathbf{x}(\mathbf{L}_{b,a}, \mathcal{V}, \alpha) &= D(\mathbf{n}(\alpha)\tilde{\boldsymbol{\sigma}}_\mathbf{x}\mathbf{L}_{b,a}, \mathcal{V}) \\ &= D(\mathbf{n}(\alpha)\boldsymbol{\sigma}_\mathbf{x}(\mathbf{l}_{b,1})) \\ &\overset{Eq.2.55}{=} \frac{1}{N_e\sigma_e^k}\nu_1 \left|s\left(\sigma_\mathbf{x}(\mathbf{l}_{b,1}), \alpha\right)\right|^k \end{aligned} \tag{4.2}$$

where $s\left(\sigma_\mathbf{x}(\mathbf{l}_{b,1}), \alpha\right) = \mathbf{n}(\alpha)\sigma_\mathbf{x}(\mathbf{l}_{b,1})$ is the scalar stress for the one and only block, k is the slope of the S-N curve for the material, and σ_e is the stress at any point on the S-N curve with N_e the corresponding number of loading cycles required for the component under loading to fail. The parameters k, σ_e and N_e are material properties and are obtained from experiments.

We approximate the damage $D_\mathbf{x}$ for a single cycle of block load. Hence, for the development of the model, block length do not make any difference and, therefore, we assume that $\nu_1 = 1, \mathcal{V} = (\nu_1)$:

$$D_\mathbf{x}(\mathbf{L}_{b,a}, \mathcal{V}, \alpha) = \frac{1}{N_e\sigma_e^k}\left|s\left(\sigma_\mathbf{x}(\mathbf{l}_{b,1}), \alpha\right)\right|^k \tag{4.3}$$

From Theorem 2.3.6 we know that scalar stress s is periodic with period π, which implies from Eq. (4.3) that damage $D_\mathbf{x}$ is also periodic with period π.

Assumption 4.1.1. *For the approximation of damage with respect to the plane angle α we assume that the stress vector $\boldsymbol{\sigma}_\mathbf{x}(\mathbf{l}_{b,1})$ is constant and in the development of the model drop the parameters $\mathbf{x}$ and $\mathbf{l}_{b,1}$ on which stress $\boldsymbol{\sigma}$ and damage D depends .*

We define by $\hat{d}$ damage for one block with stress $\boldsymbol{\sigma}$ and plane angle α as

$$\hat{d}(\boldsymbol{\sigma}, \alpha) := d(s(\boldsymbol{\sigma}, \alpha), 1) \tag{4.4}$$

where damage from alternating stress d is given in Eq. (2.43).

Figure 4.2 shows some sample plots for one period of damage $\hat{d}$ for a block load with one cycle in the case of one slope. The damage in (a) represents the case when $s(\boldsymbol{\sigma}, \alpha) \geq 0$ or $s(\boldsymbol{\sigma}, \alpha) \leq 0$ for all α, or in other words, the stress is completely on one side of the axis. From Theorem 2.3.9 the two conditions are equivalent to $a(\boldsymbol{\sigma}) \geq b(\boldsymbol{\sigma})$. The damage $\hat{d}$ has one peak in this case. The damage in (b) represents the case $a(\boldsymbol{\sigma}) < b(\boldsymbol{\sigma})$ and has two peaks. We observe that the damage profiles in Figure 4.2 look like a Gaussian function. For approximating the damage in (a) we need one Gaussian function while for the damage in (b) we need two Gaussian functions.

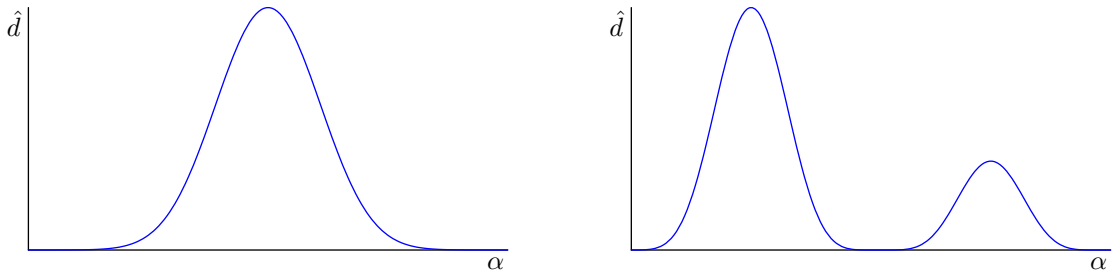

(a) A sample plot of damage for $a(\boldsymbol{\sigma}) \geq b(\boldsymbol{\sigma})$. (b) A sample plot of damage for $a(\boldsymbol{\sigma}) < b(\boldsymbol{\sigma})$.

Figure 4.2.: Sample damage plots for one slope and single block with one cycle.

4.2. Approximation of the damage in the neighborhood of the maximum

In this section, we introduce the idea of approximation of the damage, for a block load with $\nu = 1$, by Gaussian functions in an interval centered around the point of maximum. The requirements we enforce on all our approximations are that they must be accurate at the points of minimum and maximum damage in the interior of the interval of approximation and the approximation error has to be small in the neighborhood of the maximum.

In Section 4.2.1, we look at the case when $a(\boldsymbol{\sigma}) \geq b(\boldsymbol{\sigma})$. From Figure 4.2(a) we see that we require one Gaussian function for the approximation of the damage. We derive the parameters of the Gaussian function and give a result on the quality of the approximation. We do a similar analysis in Section 4.2.2 for the case $a(\boldsymbol{\sigma}) < b(\boldsymbol{\sigma})$. From Figure 4.2(b) we see that we need two Gaussian functions for the approximation of the damage when $a(\boldsymbol{\sigma}) < b(\boldsymbol{\sigma})$.

4.2.1. Case $a(\boldsymbol{\sigma}) \geq b(\boldsymbol{\sigma})$

The stress vector $\boldsymbol{\sigma} = (\sigma_{xx}, \sigma_{yy}, \sigma_{xy})^T$ is the stress induced at some point due to the application of a load time series with a single block at the actuators. We denote by g the approximation of damage around the maximum damage and define it as

$$g(\boldsymbol{\sigma}, \alpha) := f_{\breve{a}(\boldsymbol{\sigma}), \breve{b}(\boldsymbol{\sigma}), \breve{c}(\boldsymbol{\sigma})}(\alpha) + \breve{d}(\boldsymbol{\sigma}), \tag{4.5}$$

where $f_{\breve{a}(\boldsymbol{\sigma}),\breve{b}(\boldsymbol{\sigma}),\breve{c}(\boldsymbol{\sigma})}$ is the Gaussian function with the parameters $\breve{a}$, $\breve{b}$ and $\breve{c}$ as functions of $\boldsymbol{\sigma}$ and $\alpha \in I := \left[\breve{b}(\boldsymbol{\sigma}) - \frac{\pi}{2}, \breve{b}(\boldsymbol{\sigma}) + \frac{\pi}{2}\right]$. The interval I is centered around the point of maximum $\breve{b}(\boldsymbol{\sigma})$. A Gaussian function starts decreasing to zero symmetrically on both sides as we move away from its maximum. However, when $a(\boldsymbol{\sigma}) > b(\boldsymbol{\sigma})$ the minimum damage due to a block load is not zero on the interval I. This difference in two functions is accounted for by using a shift parameter $\breve{d}$ in the definition of approximation function g.

The maximum damage occurs at $\alpha^+_{max}(\boldsymbol{\sigma})$ in Eq. 2.18. When the damage and its approximation are evaluated at $\alpha = \alpha^+_{max}(\boldsymbol{\sigma})$ we get

$$f_{\breve{a}(\boldsymbol{\sigma}),\breve{b}(\boldsymbol{\sigma}),\breve{c}(\boldsymbol{\sigma})}(\alpha^+_{max}(\boldsymbol{\sigma})) + \breve{d}(\boldsymbol{\sigma}) = \frac{(a(\boldsymbol{\sigma}) + b(\boldsymbol{\sigma}))^k}{\sigma_e^k N_e}. \tag{4.6}$$

The Gaussian function $f_{\breve{a}(\boldsymbol{\sigma}),\breve{b}(\boldsymbol{\sigma}),\breve{c}(\boldsymbol{\sigma})}$ has its maximum at $\alpha = \breve{b}(\boldsymbol{\sigma})$. For the approximation to be maximum as well, $\breve{b}(\boldsymbol{\sigma})$ must be equal to $\alpha^+_{max}(\boldsymbol{\sigma})$. Equating $\breve{b}(\boldsymbol{\sigma})$ to $\alpha^+_{max}(\boldsymbol{\sigma})$ from Eq. (2.18) we get

$$\breve{b}(\boldsymbol{\sigma}) = \alpha^+_{max}(\boldsymbol{\sigma}) = \begin{cases} \frac{\pi}{4} - \frac{\phi(\boldsymbol{\sigma})}{2} + n_1\pi, & \text{if } \hat{a}(\boldsymbol{\sigma}) \geq 0 \\ -\frac{\pi}{4} - \frac{\phi(\boldsymbol{\sigma})}{2} + n_1\pi, & \text{if } \hat{a}(\boldsymbol{\sigma}) < 0 \end{cases}. \tag{4.7}$$

This simplifies Eq. (4.6) to

$$\breve{a}(\boldsymbol{\sigma}) + \breve{d}(\boldsymbol{\sigma}) = \frac{(a(\boldsymbol{\sigma}) + b(\boldsymbol{\sigma}))^k}{\sigma_e^k N_e}. \tag{4.8}$$

Then, the Gaussian function is centred around $\alpha = \alpha^+_{max}(\boldsymbol{\sigma})$. Additionally, in the interval I the minimum damage occurs at $\alpha^+_{min}(\boldsymbol{\sigma})$ with

$$\left|\alpha^+_{max}(\boldsymbol{\sigma}) - \alpha^+_{min}(\boldsymbol{\sigma})\right| = \frac{\pi}{2}. \tag{4.9}$$

Since, Interval I is centered around $\alpha^+_{max}(\boldsymbol{\sigma})$ and has a width of π both the end points of the interval I due to symmetry of the Gaussian function correspond to $\alpha^+_{min}(\boldsymbol{\sigma})$. Since, $a(\boldsymbol{\sigma}) \geq b(\boldsymbol{\sigma})$ from Theorem 2.3.10 the minimum value of $|s(\boldsymbol{\sigma}, \alpha)|$ is $a(\boldsymbol{\sigma}) - b(\boldsymbol{\sigma})$ which implies that the minimum damage is $\frac{(a(\boldsymbol{\sigma}) - b(\boldsymbol{\sigma}))^k}{\sigma_e^k N_e}$. Evaluating the damage and its approximation at $\alpha = \alpha^+_{min}(\boldsymbol{\sigma})$ and using Eq. (4.9) we get

$$\breve{a}(\boldsymbol{\sigma}) \exp\left(-\frac{\pi^2}{4\breve{c}^2(\boldsymbol{\sigma})}\right) + \breve{d}(\boldsymbol{\sigma}) = \frac{(a(\boldsymbol{\sigma}) - b(\boldsymbol{\sigma}))^k}{\sigma_e^k N_e}. \tag{4.10}$$

Parameters $\breve{a}(\boldsymbol{\sigma})$, $\breve{c}(\boldsymbol{\sigma})$, and $\breve{d}(\boldsymbol{\sigma})$ must satisfy Eq. (4.8) and Eq. (4.10) for approximating maximum and minimum damage accurately. Figure 4.3 gives a visual representation of Eq. (4.8) and Eq. (4.10).

In the next Theorem we investigate the quality of our approximation.

Theorem 4.2.1. *Given stress vector $\boldsymbol{\sigma} = (\sigma_{xx}, \sigma_{yy}, \sigma_{xy})^T$ and $\nu = 1$ with $a(\boldsymbol{\sigma}) \geq b(\boldsymbol{\sigma})$. If the approximation function g is as defined in Eq. (4.5) with parameters $\breve{a}(\boldsymbol{\sigma})$, $\breve{b}(\boldsymbol{\sigma})$ and $\breve{d}(\boldsymbol{\sigma})$ satisfying Eq. (4.7), Eq. (4.8) and Eq. (4.10), and additionally if*

$$\breve{c}(\boldsymbol{\sigma}) = \sqrt{\frac{\breve{a}(\boldsymbol{\sigma})\sigma_e^k N_e}{2kb(\boldsymbol{\sigma})(a(\boldsymbol{\sigma}) + b(\boldsymbol{\sigma}))^{k-1}}}, \tag{4.11}$$

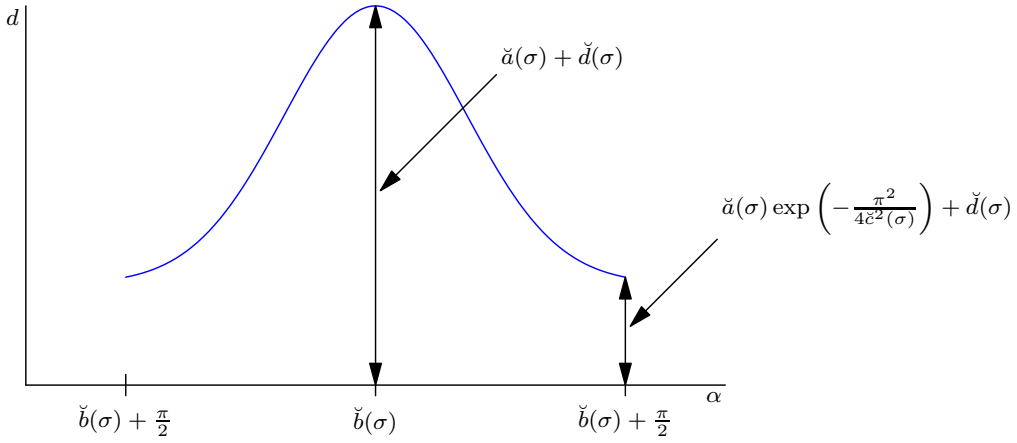

Figure 4.3.: Explanation of approximation around maximum for one slope and $a(\boldsymbol{\sigma}) \geq b(\boldsymbol{\sigma})$.

then for $\alpha \in \left[\breve{b}(\boldsymbol{\sigma}) - \frac{\pi}{2}, \breve{b}(\boldsymbol{\sigma}) + \frac{\pi}{2}\right]$*, function* g *is an approximation to the damage function* $\hat{d}$ *from Eq.* (4.4) *of order 4, i.e.,*

$$\left|\hat{d}(\boldsymbol{\sigma}, \alpha) - g(\boldsymbol{\sigma}, \alpha)\right| = O((\alpha - \breve{b}(\boldsymbol{\sigma}))^4). \tag{4.12}$$

Proof. For the proof we use Taylor's expansion for the damage and the Gaussian function. From Theorem 2.3.8, When $a(\boldsymbol{\sigma}) \geq b(\boldsymbol{\sigma})$ then the following is true

(i) If $\hat{a}(\boldsymbol{\sigma}) \geq 0$ then $s(\boldsymbol{\sigma}, \alpha) \geq 0, \forall\, \alpha \in [0, \pi)$,

(ii) If $\hat{a}(\boldsymbol{\sigma}) < 0$ then $s(\boldsymbol{\sigma}, \alpha) \leq 0, \forall\, \alpha \in [0, \pi)$.

From Definition 2.4.2 and Eq. (4.4), the damage for the two cases with $\nu = 1$ is

$$\hat{d}(\boldsymbol{\sigma}, \alpha) = \frac{1}{\sigma_e^k N_e} \begin{cases} \left(\hat{a}(\boldsymbol{\sigma}) + b(\boldsymbol{\sigma}) \sin(2\alpha + \phi(\boldsymbol{\sigma}))\right)^k, & \text{if } \hat{a}(\boldsymbol{\sigma}) \geq 0 \\ \left(-\hat{a}(\boldsymbol{\sigma}) - b(\boldsymbol{\sigma}) \sin(2\alpha + \phi(\boldsymbol{\sigma}))\right)^k, & \text{if } \hat{a}(\boldsymbol{\sigma}) < 0 \end{cases} \tag{4.13}$$

We have $a(\boldsymbol{\sigma}) = |\hat{a}(\boldsymbol{\sigma})|$ which simplifies Eq. (4.13) to

$$= \frac{1}{\sigma_e^k N_e} \begin{cases} \left(a(\boldsymbol{\sigma}) + b(\boldsymbol{\sigma}) \sin(2\alpha + \phi(\boldsymbol{\sigma}))\right)^k, & \text{if } \hat{a}(\boldsymbol{\sigma}) \geq 0 \\ \left(a(\boldsymbol{\sigma}) - b(\boldsymbol{\sigma}) \sin(2\alpha + \phi(\boldsymbol{\sigma}))\right)^k, & \text{if } \hat{a}(\boldsymbol{\sigma}) < 0 \end{cases} \tag{4.14}$$

Rewriting Eq. (4.7) in terms of $\phi(\boldsymbol{\sigma})$ yields

$$\phi(\boldsymbol{\sigma}) = \begin{cases} \frac{\pi}{2} - 2\breve{b}(\boldsymbol{\sigma}) + 2n_1\pi, & \text{if } \hat{a}(\boldsymbol{\sigma}) \geq 0 \\ -\frac{\pi}{2} - 2\breve{b}(\boldsymbol{\sigma}) + 2n_1\pi, & \text{if } \hat{a}(\boldsymbol{\sigma}) < 0 \end{cases}. \tag{4.15}$$

Inserting $\phi(\boldsymbol{\sigma})$ from Eq. (4.15) into Eq. (4.14) and observing that $\sin(\frac{\pi}{2} + \theta + 2n_1\pi) = \cos\theta$ and $\sin(-\frac{\pi}{2} + \theta + 2n_1\pi) = -\cos\theta$ to obtain

$$\hat{d}(\boldsymbol{\sigma}, \alpha) = \frac{1}{\sigma_e^k N_e} \left(a(\boldsymbol{\sigma}) + b(\boldsymbol{\sigma}) \cos(2\alpha - 2\breve{b}(\boldsymbol{\sigma}))\right)^k. \tag{4.16}$$

The Taylor series expansion of the damage at $\breve{b}(\boldsymbol{\sigma})$ is given from Eq. (A.1) in Theorem A.1.1 as

$$\hat{d}(\boldsymbol{\sigma},\alpha) = \hat{d}(\boldsymbol{\sigma},\breve{b}(\boldsymbol{\sigma})) + \frac{2kb(\boldsymbol{\sigma})}{\sigma_e^k N_e}\left(a(\boldsymbol{\sigma})+b(\boldsymbol{\sigma})\right)^{k-1}(\alpha-\breve{b}(\boldsymbol{\sigma}))^2 + O\left((\alpha-\breve{b}(\boldsymbol{\sigma}))^4\right), \alpha \in I. \quad (4.17)$$

Damage is maximum at $\breve{b}(\boldsymbol{\sigma})$ so we can replace $\hat{d}(\boldsymbol{\sigma},\breve{b}(\boldsymbol{\sigma}))$ by $\frac{(a(\boldsymbol{\sigma})+b(\boldsymbol{\sigma}))^k}{\sigma_e^k N_e}$ in Eq. (4.17) to get

$$\hat{d}(\boldsymbol{\sigma},\alpha) = \frac{\left(a(\boldsymbol{\sigma})+b(\boldsymbol{\sigma})\right)^k}{\sigma_e^k N_e} + \frac{2k\left(a(\boldsymbol{\sigma})+b(\boldsymbol{\sigma})\right)^{k-1}}{\sigma_e^k N_e}(\alpha-\breve{b}(\boldsymbol{\sigma}))^2 + O\left((\alpha-\breve{b}(\boldsymbol{\sigma}))^4\right). \quad (4.18)$$

Now we want to compute the Taylor series representation of the approximation function g. We use the Taylor series representation of the exponential function:

$$\exp(x) = \sum_{i=0}^{\infty}\frac{x^i}{i!} \text{ for all x.} \quad (4.19)$$

Replacing x by $-\left(\frac{\alpha-\breve{b}(\boldsymbol{\sigma})}{\breve{c}(\boldsymbol{\sigma})}\right)^2$ in Eq (4.19) and inserting in the approximation function g and after reordering we get:

$$g(\boldsymbol{\sigma},\alpha) = \breve{a}(\boldsymbol{\sigma}) + \breve{d}(\boldsymbol{\sigma}) + \breve{a}(\boldsymbol{\sigma})\sum_{i=1}^{\infty}(-1)^i\frac{1}{i!}\left(\frac{\alpha-\breve{b}(\boldsymbol{\sigma})}{\breve{c}(\boldsymbol{\sigma})}\right)^{2i}, \alpha \in I. \quad (4.20)$$

Inserting the value of $\breve{a}(\boldsymbol{\sigma}) + \breve{d}(\boldsymbol{\sigma})$ from Eq. (4.8) into Eq. (4.20) leads to

$$g(\boldsymbol{\sigma},\alpha) = \frac{\left(a(\boldsymbol{\sigma})+b(\boldsymbol{\sigma})\right)^k}{\sigma_e^k N_e} + \breve{a}(\boldsymbol{\sigma})\sum_{i=1}^{\infty}(-1)^i\frac{1}{i!}\left(\frac{\alpha-\breve{b}(\boldsymbol{\sigma})}{\breve{c}(\boldsymbol{\sigma})}\right)^{2i}. \quad (4.21)$$

Subtracting Eq (4.21) from Eq (4.18) yields

$$\left|\hat{d}(\boldsymbol{\sigma},\alpha) - g(\boldsymbol{\sigma},\alpha)\right| = \left(\frac{\breve{a}(\boldsymbol{\sigma})}{\breve{c}(\boldsymbol{\sigma})^2} - \frac{2kb(\boldsymbol{\sigma})(a(\boldsymbol{\sigma})+b(\boldsymbol{\sigma}))^{k-1}}{\sigma_e^k N_e}\right)(\alpha-\breve{b}(\boldsymbol{\sigma}))^2 + O((\alpha-\breve{b}(\boldsymbol{\sigma}))^4)$$

Choosing $\breve{c}(\boldsymbol{\sigma})$ such that the term $(\alpha-\breve{b}(\boldsymbol{\sigma}))^2$ vanishes gives us Eq. (4.11).

$$\begin{aligned} \frac{\breve{a}(\boldsymbol{\sigma})}{\breve{c}(\boldsymbol{\sigma})^2} &- \frac{2kb(\boldsymbol{\sigma})(a(\boldsymbol{\sigma})+b(\boldsymbol{\sigma}))^{k-1}}{\sigma_e^k N_e} = 0 \\ \Rightarrow \breve{c}(\boldsymbol{\sigma}) &= \sqrt{\frac{\breve{a}(\boldsymbol{\sigma})\sigma_e^k N_e}{2kb(\boldsymbol{\sigma})(a(\boldsymbol{\sigma})+b(\boldsymbol{\sigma}))^{k-1}}} \end{aligned}$$

This completes the proof. □

In Theorem 4.2.1, we proved that the Gaussian approximation g is very close to the damage $\hat{d}$ in the neighborhood of the point of maximum. This is good as eventually we want to find the point of maximum when more than one block loads are acting on the component. Hence, it is important that error in the neighborhood of the point of maximum is small and at the same time the ratio of maximum error to the maximum damage should also be small. In Section 4.5, we give a comparison of the damage $\hat{d}$ and the approximation function g as well as a comparison of the

maximum error and maximum damage.

In the next lemma we give the equations to compute the parameters $\breve{a}(\boldsymbol{\sigma})$ and $\breve{d}(\boldsymbol{\sigma})$ in the definition of the approximation function g from Eq. (4.5).

Lemma 4.2.2. *The parameters $\breve{a}(\boldsymbol{\sigma})$ and $\breve{d}(\boldsymbol{\sigma})$ in Eq. (4.5) are given as*

$$\breve{a}(\boldsymbol{\sigma}) = \frac{(a(\boldsymbol{\sigma}) + b(\boldsymbol{\sigma}))^k - (a(\boldsymbol{\sigma}) - b(\boldsymbol{\sigma}))^k}{\sigma_e^k N_e \left(1 - \exp\left(-\frac{\pi^2}{4\breve{c}^2(\boldsymbol{\sigma})}\right)\right)} \text{ and} \tag{4.22}$$

$$\breve{d}(\boldsymbol{\sigma}) = \frac{(a(\boldsymbol{\sigma}) - b(\boldsymbol{\sigma}))^k - (a(\boldsymbol{\sigma}) + b(\boldsymbol{\sigma}))^k \exp\left(-\frac{\pi^2}{4\breve{c}^2(\boldsymbol{\sigma})}\right)}{\sigma_e^k N_e \left(1 - \exp\left(-\frac{\pi^2}{4\breve{c}^2(\boldsymbol{\sigma})}\right)\right)}. \tag{4.23}$$

Proof. The two equations, Eq. (4.8) and Eq. (4.10) have three unknowns. We can use these two equations to give $\breve{a}(\boldsymbol{\sigma})$ and $\breve{d}(\boldsymbol{\sigma})$ in terms of $\breve{c}(\boldsymbol{\sigma})$. Subtracting Eq. (4.10) from Eq. (4.8) we get a equation in $\breve{a}(\boldsymbol{\sigma})$ and $\breve{c}(\boldsymbol{\sigma})$:

$$\breve{a}(\boldsymbol{\sigma}) \left(1 - \exp\left(-\frac{\pi^2}{4\breve{c}^2(\boldsymbol{\sigma})}\right)\right) = \frac{(a(\boldsymbol{\sigma}) + b(\boldsymbol{\sigma}))^k - (a(\boldsymbol{\sigma}) - b(\boldsymbol{\sigma}))^k}{\sigma_e^k N_e}. \tag{4.24}$$

Rearranging Eq. (4.24) gives us Eq. (4.22) for computing $\breve{a}(\boldsymbol{\sigma})$. Inserting the value of $\breve{a}(\boldsymbol{\sigma})$ into Eq. (4.8) and further simplification gives us Eq. (4.23) for computing $\breve{d}(\boldsymbol{\sigma})$. □

The value of $\breve{a}(\boldsymbol{\sigma})$ is always positive but the value of $\breve{d}(\boldsymbol{\sigma})$ can be positive as well as negative. An example when $\breve{d}(\boldsymbol{\sigma})$ is negative is when $a(\boldsymbol{\sigma}) = b(\boldsymbol{\sigma})$.

The next corollary gives us an equation for computing $\breve{c}(\boldsymbol{\sigma})$.

Corollary 4.2.3. *The parameter $\breve{c}(\boldsymbol{\sigma})$ in the definition of the approximation function g in Eq. (4.5) is given as*

$$\breve{c}(\boldsymbol{\sigma}) = \sqrt{\frac{(a(\boldsymbol{\sigma}) + b(\boldsymbol{\sigma}))^k - (a(\boldsymbol{\sigma}) - b(\boldsymbol{\sigma}))^k}{2kb(\boldsymbol{\sigma})(a(\boldsymbol{\sigma}) + b(\boldsymbol{\sigma}))^{k-1} \left(1 - \exp\left(-\frac{\pi^2}{4\breve{c}^2(\boldsymbol{\sigma})}\right)\right)}} \tag{4.25}$$

Proof. Inserting $\breve{a}(\boldsymbol{\sigma})$ from Eq. (4.22) into Eq. (4.11) gives us $\breve{c}(\boldsymbol{\sigma})$. □

We can rewrite Eq. (4.25) as a product of two factors as

$$\breve{c}(\boldsymbol{\sigma}) = \sqrt{\frac{(a(\boldsymbol{\sigma}) + b(\boldsymbol{\sigma}))^k - (a(\boldsymbol{\sigma}) - b(\boldsymbol{\sigma}))^k}{2kb(\boldsymbol{\sigma})(a(\boldsymbol{\sigma}) + b(\boldsymbol{\sigma}))^{k-1}}} \frac{1}{\sqrt{1 - \exp\left(-\frac{\pi^2}{4\breve{c}^2(\boldsymbol{\sigma})}\right)}} \tag{4.26}$$

The first factor in Eq. (4.26) is constant while the second factor depends on $\breve{c}(\boldsymbol{\sigma})$ itself. Such equations are also known as fixed point equations. Since the parameters $\breve{a}(\boldsymbol{\sigma})$ and $\breve{d}(\boldsymbol{\sigma})$ depend on the parameter $\breve{c}(\boldsymbol{\sigma})$, the fixed point equation for $\breve{c}(\boldsymbol{\sigma})$ has to be solved first before parameters $\breve{a}(\boldsymbol{\sigma})$ and $\breve{d}(\boldsymbol{\sigma})$ can be computed. In order to use the approximation we have to show that there

exists at least one solution to the Eq. (4.25). We introduce some standard definitions and results that is used to prove that Eq. (4.25) has a unique fixed point.

Definition 4.2.4 (Fixed point)**.** Let $T : X \to X$ be a map of a metric space to itself. A point $x_0 \in X$ is called the fixed point of T if $T(x_0) = x_0$.

Definition 4.2.5 (Contraction Mapping)**.** Let (X, d) be a complete metric space. A function $T : X \to X$ is said to be a contraction mapping if there is a constant q with $0 \leq q < 1$ such that

$$d(T(x), T(y)) \leq qd(x, y) \text{ for all } x, y \in \mathbb{R}$$

Theorem 4.2.6 (Contraction mapping theorem)**.** *Every contraction mapping has a unique fixed point.*

Proof. For proof see [4]. □

We use Definitions 4.2.4, Definition 4.2.5 and Theorem 4.2.6 to prove that Eq. (4.25) has a unique fixed point for every $\boldsymbol{\sigma}$. For the proof we define

$$T : \mathbb{R} \to \mathbb{R}, y \longmapsto \frac{1}{\sqrt{1 - \exp\left(-\frac{\pi^2}{4y^2}\right)}}. \tag{4.27}$$

The mapping T is the second factor in Eq. (4.26) replacing $\breve{c}(\sigma)$ by y. Since the mapping T is once continuously differentiable, the smallest q to fulfill condition in Theorem 4.2.6 is $q = \sup_{y' \in \mathbb{R}} |T'(y')|$. Therefore, $q < 1$ is equivalent to $|T'(y)| < 1 - \epsilon$, for all $y \in \mathbb{R}$ and $0 < \epsilon < 1$. The following lemma proves a general result that we use to show $|T'(y)| < 1 - \epsilon$ for all $y \in \mathbb{R}$ and $0 < \epsilon < 1$.

Lemma 4.2.7. *We have*

$$\frac{\mathfrak{t}^2 \exp\left(-\frac{\mathfrak{t}^2}{\mathfrak{s}^2\mathfrak{p}^2}\right)}{\mathfrak{r}\mathfrak{s}^2\mathfrak{p}^3\left(1 - \exp\left(-\frac{\mathfrak{t}^2}{\mathfrak{s}^2\mathfrak{p}^2}\right)\right)^{\frac{3}{2}}} < \frac{\mathfrak{s}}{\mathfrak{r}\mathfrak{t}}$$

for all $\mathfrak{r}$, $\mathfrak{s}$, $\mathfrak{t} \in \mathbb{R}_+$ *and* $\mathfrak{p} \in \mathbb{R}$.

Proof. Multiplying both the numerator and the denominator by $\exp\left(\frac{3\mathfrak{t}^2}{2\mathfrak{s}^2\mathfrak{p}^2}\right)$ and further simplification leads to

$$\frac{\mathfrak{t}^2 \exp\left(-\frac{\mathfrak{t}^2}{\mathfrak{s}^2\mathfrak{p}^2}\right)}{\mathfrak{r}\mathfrak{s}^2\mathfrak{p}^3\left(1 - \exp\left(-\frac{\mathfrak{t}^2}{\mathfrak{s}^2\mathfrak{p}^2}\right)\right)^{\frac{3}{2}}} \frac{\exp\left(\frac{3\mathfrak{t}^2}{2\mathfrak{s}^2\mathfrak{p}^2}\right)}{\exp\left(\frac{3\mathfrak{t}^2}{2\mathfrak{s}^2\mathfrak{p}^2}\right)} = \frac{\mathfrak{t}^2 \exp\left(\frac{\mathfrak{t}^2}{2\mathfrak{s}^2\mathfrak{p}^2}\right)}{\mathfrak{r}\mathfrak{s}^2\mathfrak{p}^3\left(\exp\left(\frac{\mathfrak{t}^2}{\mathfrak{s}^2\mathfrak{p}^2}\right) - 1\right)^{\frac{3}{2}}}$$

Now using the series expansion of the exponential function to get

$$\frac{\mathfrak{t}^2 \exp\left(-\frac{\mathfrak{t}^2}{\mathfrak{s}^2\mathfrak{p}^2}\right)}{\mathfrak{r}\mathfrak{s}^2\mathfrak{p}^3\left(1 - \exp\left(-\frac{\mathfrak{t}^2}{\mathfrak{s}^2\mathfrak{p}^2}\right)\right)^{\frac{3}{2}}} = \frac{\mathfrak{t}^2 \sum_{i=0}^{\infty} \frac{1}{2^i} \cdot \left(\frac{\mathfrak{t}^2}{\mathfrak{s}^2\mathfrak{p}^2}\right)^i \cdot \frac{1}{i!}}{\mathfrak{r}\mathfrak{s}^2\mathfrak{p}^3\left(\sum_{i=1}^{\infty} \frac{1}{i!}\left(\frac{\mathfrak{t}^2}{\mathfrak{s}^2\mathfrak{p}^2}\right)^i\right)^{\frac{3}{2}}}$$

Multiplying both the numerator and the denominator by $\frac{\mathfrak{t}^3}{\mathfrak{s}^3\mathfrak{p}^3}$ and observing that $\left(\frac{\mathfrak{t}^2}{\mathfrak{s}^2\mathfrak{p}^2}\right)^{\frac{3}{2}} = \frac{\mathfrak{t}^3}{\mathfrak{s}^3\mathfrak{p}^3}$ yields

$$= \frac{\mathfrak{s}\sum_{i=0}^{\infty}\frac{1}{2^i}\cdot\left(\frac{\mathfrak{t}^2}{\mathfrak{s}^2\mathfrak{p}^2}\right)^i\cdot\frac{1}{i!}}{\mathfrak{r}\mathfrak{t}\left(\sum_{i=1}^{\infty}\frac{1}{i!}\left(\frac{\mathfrak{t}^2}{\mathfrak{s}^2\mathfrak{p}^2}\right)^{(i-1)}\right)^{\frac{3}{2}}}$$

Renumbering i to $i-1$ in the sum in the denominator

$$= \frac{\mathfrak{s}\sum_{i=0}^{\infty}\frac{1}{2^i}\cdot\left(\frac{\mathfrak{t}^2}{\mathfrak{s}^2\mathfrak{p}^2}\right)^i\cdot\frac{1}{i!}}{\mathfrak{r}\mathfrak{t}\left(\sum_{i=0}^{\infty}\frac{1}{(i+1)!}\left(\frac{\mathfrak{t}^2}{\mathfrak{s}^2\mathfrak{p}^2}\right)^i\right)^{\frac{3}{2}}}$$

We know that $2^i \geq (i+1)$ for all $i \in \mathbb{N}$

$$< \frac{\mathfrak{s}}{\mathfrak{r}\mathfrak{t}}.$$ □

Equipped with Lemma 4.2.7 the contraction property of T follows as shown in the next result.

Theorem 4.2.8. *The mapping T as defined in Eq. (4.27) is a contraction mapping.*

Proof. For T to be a contraction mapping we have to show that $|T'(x)|$ is less than one for all $x \in \mathbb{R}$. The first derivative of T is given at $y \in \mathbb{R}$ by

$$\begin{aligned} T'(y) &= \frac{d}{dy}\left(\frac{1}{\sqrt{1-\exp\left(-\frac{\pi^2}{4y^2}\right)}}\right) \\ &= \frac{\pi^2\exp\left(-\frac{\pi^2}{4y^2}\right)}{4y^3\left(1-\exp\left(-\frac{\pi^2}{4y^2}\right)\right)^{\frac{3}{2}}}. \end{aligned}$$

Using Lemma 4.2.7 with $\mathfrak{s}=2, \mathfrak{p}=y, \mathfrak{r}=1$ and $\mathfrak{t}=\pi$ yields that the first derivative is less than $\frac{2}{\pi}$ for all $y \in \mathbb{R}$. Mathematically,

$$T'(y) < \frac{2}{\pi} < 1 \text{ for all } y \in \mathbb{R} \Rightarrow \sup_{y\in\mathbb{R}}|T'(y)| \leq \frac{2}{\pi} < 1.$$

Hence, $T(y)$ is a contraction mapping. □

Theorem 4.2.6 implies that rT is also a contraction mapping for any $r \in (0,1]$. Next we show that the first factor in Eq. (4.26) is less than one.

Lemma 4.2.9. *For every $a, b \in \mathbb{R}$ with $a \geq b > 0$ and $k \in \mathbb{Z}^+$ with $k > 1$ the following holds*

$$\frac{(a+b)^k - (a-b)^k}{2kb\,(a+b)^{k-1}} < 1. \tag{4.28}$$

And if $k = 1$ we have

$$\frac{(a+b)^k - (a-b)^k}{2kb\,(a+b)^{k-1}} = 1$$

for all $a \geq b > 0$.

Proof. In the case of $a > b$ we use a telescopic sum

$$\frac{(a+b)^k - (a-b)^k}{2kb\,(a+b)^{k-1}} = \frac{((a+b)-(a-b))\sum_{i=0}^{k-1}(a+b)^{k-1-i}(a-b)^i}{2kb\,(a+b)^{k-1}} \tag{4.29a}$$

Simplification and factoring gives

$$= \frac{2b(a+b)^{k-1}\sum_{i=0}^{k-1}(a+b)^{-i}(a-b)^i}{2kb\,(a+b)^{k-1}} \tag{4.29b}$$

$$= \frac{\sum_{i=0}^{k-1}(a+b)^{-i}(a-b)^i}{k}$$

$$= \frac{1}{k}\sum_{i=0}^{k-1}\left(\frac{a-b}{a+b}\right)^i$$

$$a > b \Rightarrow < \frac{1}{k}\sum_{i=0}^{k-1} 1 \tag{4.29c}$$

$$< 1.$$

In case $a = b$ we get

$$\frac{(a+b)^k - (a-b)^k}{2kb\,(a+b)^{k-1}} = \frac{1}{k} < 1. \qquad \square$$

In Lemma 4.2.9 we had an assumption that k is a positive integer. However, as k is the slope in the S-N curve it can be any real number greater than one. In the next theorem we extend Lemma 4.2.9 for all $k \in \mathbb{R}$ and $k > 1$.

Theorem 4.2.10. *For every $a, b \in \mathbb{R}$ with $a \geq b > 0$ and $k \in \mathbb{R}^+$ with $k > 1$ inequality in Eq* (4.28) *holds.*

Proof. Let us define

$$\mathcal{T} : [1, \infty) \to \mathbb{R}, k \mapsto \frac{(a+b)^k - (a-b)^k}{2kb\,(a+b)^{k-1}}, \tag{4.30}$$

where a and b are constants. If $a = b$ and $k > 1$ then $\mathcal{T}(k) = \frac{1}{k} < 1$ and when $k = 1$ we have $\mathcal{T}(1) = 1$. In Section A.2.1 we prove that $\mathcal{T}$ is strictly convex. Strict convexity of $\mathcal{T}$ implies

$$\mathcal{T}(k) < t\mathcal{T}(k_1) + (1-t)\mathcal{T}(k_1 + 1)$$

with $k_1 = \lfloor k \rfloor$ and $t = k_1 - k + 1$. From Lemma 4.2.9 we know that $\mathcal{T}(k_1) \leq 1$ and $\mathcal{T}(k_1 + 1) < 1$. Hence, $\mathcal{T}(k) < 1$. $\square$

The following is true for the fixed point equation in Eq. (4.25).

Theorem 4.2.11. *Equation* (4.25) *has a unique fixed point.*

Proof. Combining Theorem 4.2.8 and Theorem 4.2.10 we have shown that Eq. (4.26) is a contraction mapping. We can now use Theorem 4.2.6 (Contraction Mapping Theorem) to conclude that Eq. (4.25) has a unique fixed point. □

From Theorem 4.2.11 we get that there exists one unique solution to the fixed point equation in Eq. (4.25). Additionally, we can now compute all the parameters of the approximation function g. Now that we have a way to compute $\check{c}(\boldsymbol{\sigma})$ we give some of its properties.

As a consequence of Theorem 4.2.10 the first factor in Eq. (4.26) lies in the interval $\left[\frac{1}{\sqrt{k}}, 1\right)$ for different values of $a(\boldsymbol{\sigma})$ and $b(\boldsymbol{\sigma})$ with fixed k. For each point in this interval Eq. (4.25) has a unique fixed point.

In Algorithm 4.2.1 we describe a method to compute the fixed points of equations of the form $y = \varphi(y)$.

Algorithm 4.2.1: Computing fixed point y for equations of the form $y = \varphi(y)$

Data: $\varphi(y)$ and $\epsilon > 0$
Result: y such that $y = \varphi(y)$
begin
  $y \longleftarrow 0.5$
  $n \longleftarrow 0$
  while $|y_n - y_{n-1}| > \epsilon$ *and* $n \leq max\_iter$ **do**
    $y_{n+1} \longleftarrow \varphi(y_n)$
    $n \longleftarrow n + 1$
  end
  return y_n
end

We can prove that, if φ is a contraction mapping, then Algorithm 4.2.1 converges to the unique fixed point of the equation $y = \varphi(y)$. We use the definition of Cauchy sequences for the proof.

Definition 4.2.12 (Cauchy sequence)**.** Given a metric space (X, d), a sequence $\{y_n\}$ is Cauchy, if for every positive real number $\epsilon > 0$, there is a positive integer N such that for all positive integers $m, n > N$, the distance $d(y_m, y_n) < \epsilon$.

Theorem 4.2.13. *If φ is a contraction mapping then the iterates y_n in Algorithm 4.2.1 with $\varphi(y)$ and $\epsilon > 0$ always converges to the unique fixed point.*

Proof. Since $\varphi(y)$ is a contraction mapping with $q = \sup_{y' \in \mathbb{R}} |\varphi'(y')| < 1$, then for the sequence of iterates $\{y_n, n = 0, 1, 2, \ldots\}$ generated in Algorithm 4.2.1, we have:

$$|y_2 - y_1| = |\varphi(y_1) - \varphi(y_0)| \leq q|y_1 - y_0|,$$

$$|y_3 - y_2| = |\varphi(y_2) - \varphi(y_1)| \leq q|y_2 - y_1|,$$

$$\ldots,$$

and

$$|y_n - y_{n-1}| = |\varphi(y_{n-1}) - \varphi(y_{n-2})| \leq q|y_{n-1} - y_{n-2}|.$$

Combining the above inequalities yields:

$$|y_n - y_{n-1}| \leq q^{n-1}|y_1 - y_0|.$$

Since $q < 1, q^{n-1} \to 0$ as $n \to \infty$. Therefore, we can show $\{y_n\}$ is a Cauchy sequence and thus it converges to a point y^*.

We let n go to infinity on both sides of $y_n = \varphi(y_{n-1})$ to obtain $y^* = \varphi(y^*)$. Hence, y^* is a fixed point of φ. So we proved that the iterates in Algorithm 4.2.1 converges to the unique fixed point. □

Equation (4.26) is a fixed point equation and we can apply Algorithm 4.2.1 with the right hand side of Eq. (4.26) as φ and y as $\breve{c}(\boldsymbol{\sigma})$. Since Eq. (4.26) is a contraction mapping, from Theorem 4.2.13 convergence to the unique fixed point is guaranteed.

From Eq. (4.25) we can also obtain the lower and upper bound for $\breve{c}(\boldsymbol{\sigma})$. We can rewrite Eq. (4.25) as

$$\breve{c}(\boldsymbol{\sigma}) = \sqrt{\frac{(a(\boldsymbol{\sigma}) + b(\boldsymbol{\sigma}))^k - (a(\boldsymbol{\sigma}) - b(\boldsymbol{\sigma}))^k}{2kb(\boldsymbol{\sigma})(a(\boldsymbol{\sigma}) + b(\boldsymbol{\sigma}))^{k-1}\left(1 - \exp\left(-\frac{\pi^2}{4\breve{c}^2(\boldsymbol{\sigma})}\right)\right)}}, \tag{4.31a}$$

$$\text{Eq. (4.29)} \Rightarrow = \sqrt{\frac{1}{k}\sum_{i=0}^{k-1}\left(\frac{a(\boldsymbol{\sigma}) - b(\boldsymbol{\sigma})}{a(\boldsymbol{\sigma}) + b(\boldsymbol{\sigma})}\right)^i \frac{1}{\left(1 - \exp\left(-\frac{\pi^2}{4\breve{c}^2(\boldsymbol{\sigma})}\right)\right)}}. \tag{4.31b}$$

In Eq. (4.31) we see that increasing $b(\boldsymbol{\sigma})$ decreases the right hand side of the equation. The maximum value of the right hand side of Eq. (4.31) is obtained in the limiting case when $\breve{b}(\boldsymbol{\sigma}) \to 0^+$. Similarly, the minimum value of the right hand side of Eq. (4.31) is obtained in the limiting case when $\breve{b}(\boldsymbol{\sigma}) \to a(\boldsymbol{\sigma})^-$. Hence, the equation for the upper and the lower bound for the parameter $\breve{c}(\boldsymbol{\sigma})$ for the different values of k can be obtained from Eq. (4.31) in the limiting cases when $b(\boldsymbol{\sigma}) \to 0^+$ and $b(\boldsymbol{\sigma}) \to a(\boldsymbol{\sigma})^-$ respectively. In (4.31b) taking the limit $b(\boldsymbol{\sigma}) \to 0^+$ gives

$$\breve{c}(\boldsymbol{\sigma}) = \frac{1}{\sqrt{1 - \exp\left(-\frac{\pi^2}{4\breve{c}^2(\boldsymbol{\sigma})}\right)}}. \tag{4.32}$$

Equation (4.32) is independent of k and the unique fixed point can be computed using Algorithm 4.2.1. A similar analysis for the lower bound for the limiting case $b(\boldsymbol{\sigma}) \to a(\boldsymbol{\sigma})^-$ in (4.31a) gives us

$$\breve{c}(\boldsymbol{\sigma}) = \frac{1}{\sqrt{k\left(1 - \exp\left(-\frac{\pi^2}{4\breve{c}^2(\boldsymbol{\sigma})}\right)\right)}}. \tag{4.33}$$

Again we can compute the fixed point of Eq. 4.33 using Algorithm 4.2.1.

In Figure 4.4 we see the lower and upper bound for $\breve{c}(\boldsymbol{\sigma})$ for the different values of k. We observe that as k approaches one, the difference between the upper and the lower bound decreases. From

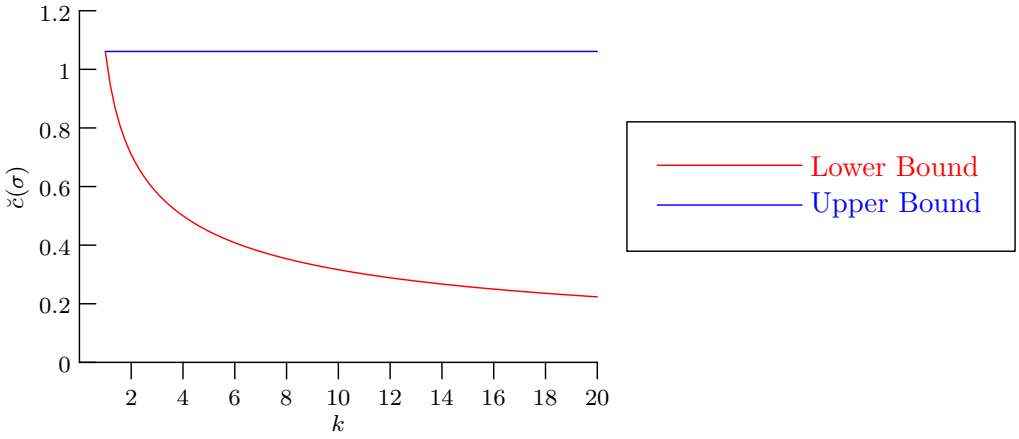

Figure 4.4.: Upper and lower bounds of $\breve{c}(\boldsymbol{\sigma})$ for different values of k.

Eq. (4.33) we see that $\frac{1}{\sqrt{k}}$ is a strict lower bound for $\breve{c}(\boldsymbol{\sigma})$.

In this section, we gave an approximation to the damage function in the case of one slope with $a(\boldsymbol{\sigma}) \geq b(\boldsymbol{\sigma})$. We derived the parameters $\breve{a}$, $\breve{b}$, $\breve{c}$ and $\breve{d}$ for the approximation. In the next section we give the approximation of the damage $\hat{d}$ for the case $a(\boldsymbol{\sigma}) < b(\boldsymbol{\sigma})$.

4.2.2. Case $a(\boldsymbol{\sigma}) < b(\boldsymbol{\sigma})$

In this case the damage profile has two peaks as seen in Figure 4.2(b). If $\hat{a}(\boldsymbol{\sigma}) = 0$, then both the peaks have a value of $\frac{b(\boldsymbol{\sigma})^k}{\sigma_e^k N_e}$ as from Theorem 2.3.13 we get $s^-_{max,1}(\boldsymbol{\sigma}) = b(\boldsymbol{\sigma})$ and $s^-_{max,2}(\boldsymbol{\sigma}) = b(\boldsymbol{\sigma})$. Without loss of generality we can assume that $\alpha^-_{max,1}(\boldsymbol{\sigma})$ and $\alpha^-_{max,2}(\boldsymbol{\sigma})$ are in the interval $[0, \pi)$. We have $|\alpha^-_{max,1}(\boldsymbol{\sigma}) - \alpha^-_{max,2}(\boldsymbol{\sigma})| = \frac{\pi}{2}$. At $\alpha^-_{max,1}(\boldsymbol{\sigma})$ we have the peak with the larger value of damage and at $\alpha^-_{max,2}(\boldsymbol{\sigma})$ we have the peak with the smaller value of damage.

From Theorem 2.3.12 the interval in which the peak with larger damage value lie is

$$I_1 = \left[\alpha_{max}(\boldsymbol{\sigma}) - \frac{\pi}{4} - \frac{\theta}{2}, \alpha_{max}(\boldsymbol{\sigma}) + \frac{\pi}{4} + \frac{\theta}{2}\right) \tag{4.34}$$

and the interval in which the peak with the smaller damage value lie is

$$I_2 = \left[\alpha_{min}(\boldsymbol{\sigma}) - \frac{\pi}{4} + \frac{\theta}{2}, \alpha_{min}(\boldsymbol{\sigma}) + \frac{\pi}{4} - \frac{\theta}{2}\right). \tag{4.35}$$

Now that we have the two intervals we can give the approximation. Let $\tilde{g}$ denote the function approximating the damage around the peaks:

$$\tilde{g}(\boldsymbol{\sigma}, \alpha) = \begin{cases} f_{\breve{a}_1(\boldsymbol{\sigma}),\breve{b}_1(\boldsymbol{\sigma}),\breve{c}_1(\boldsymbol{\sigma})}(\alpha) + \breve{d}_1(\boldsymbol{\sigma}), & \text{if } \alpha \in I_1 \\ f_{\breve{a}_2(\boldsymbol{\sigma}),\breve{b}_2(\boldsymbol{\sigma}),\breve{c}_2(\boldsymbol{\sigma})}(\alpha) + \breve{d}_2(\boldsymbol{\sigma}), & \text{if } \alpha \in I_2 \end{cases}, \tag{4.36}$$

where $\breve{b}_1(\boldsymbol{\sigma}) = \alpha^-_{max,1}(\boldsymbol{\sigma})$, $\breve{b}_2(\boldsymbol{\sigma}) = \alpha^-_{max,2}(\boldsymbol{\sigma})$ and $f_{\breve{a}_1(\boldsymbol{\sigma}),\breve{b}_1(\boldsymbol{\sigma}),\breve{c}_1(\boldsymbol{\sigma})}$ and $f_{\breve{a}_2(\boldsymbol{\sigma}),\breve{b}_2(\boldsymbol{\sigma}),\breve{c}_2(\boldsymbol{\sigma})}$ are Gaussian functions from Definition 4.0.1.

The function in Eq. (4.36) has 8 parameters $\breve{a}_1$, $\breve{a}_2$, $\breve{b}_1$, $\breve{b}_2$, $\breve{c}_1$, $\breve{c}_2$, $\breve{d}_1$ and $\breve{d}_2$ which have to be determined before we can use the approximation in any optimization problem.

From Theorem 2.3.13, the maximum value of the absolute scalar stress on the interval I_1 is $s^-_{max,1} = a(\boldsymbol{\sigma}) + b(\boldsymbol{\sigma})$ at $\alpha = \breve{b}_1(\boldsymbol{\sigma}) = \alpha^-_{max,1}(\boldsymbol{\sigma})$. Therefore, when the damage and its approximation are evaluated at $\alpha = \breve{b}_1(\boldsymbol{\sigma})$ we get

$$\breve{a}_1(\boldsymbol{\sigma}) + \breve{d}_1(\boldsymbol{\sigma}) = \frac{(a(\boldsymbol{\sigma}) + b(\boldsymbol{\sigma}))^k}{\sigma_e^k N_e}. \tag{4.37}$$

Similarly, from Theorem 2.3.13, the maximum value of the absolute scalar stress on the interval I_2 is $s^-_{max,2} = b(\boldsymbol{\sigma}) - a(\boldsymbol{\sigma})$ at $\alpha = \breve{b}_2(\boldsymbol{\sigma}) = \alpha^-_{max,2}(\boldsymbol{\sigma})$ which gives

$$\breve{a}_2(\boldsymbol{\sigma}) + \breve{d}_2(\boldsymbol{\sigma}) = \frac{(b(\boldsymbol{\sigma}) - a(\boldsymbol{\sigma}))^k}{\sigma_e^k N_e}. \tag{4.38}$$

Finally, from Lemma 2.3.11 and Theorem 2.3.13, the scalar stress at the end points of the two intervals I_1 and I_2 is zero. Inserting the end points of the intervals in the approximation function $\tilde{g}$ and equating it to the damage $\hat{d}$ gives us two additional equations that have to be satisfied

$$\breve{a}_1(\boldsymbol{\sigma}) \exp\left(-\frac{(\pi + 2\theta)^2}{16\breve{c}_1^2(\boldsymbol{\sigma})}\right) + \breve{d}_1(\boldsymbol{\sigma}) = 0, \tag{4.39}$$

$$\breve{a}_2(\boldsymbol{\sigma}) \exp\left(-\frac{(\pi - 2\theta)^2}{16\breve{c}_2^2(\boldsymbol{\sigma})}\right) + \breve{d}_2(\boldsymbol{\sigma}) = 0. \tag{4.40}$$

The conditions in Eq. 4.39 and Eq. 4.40 make the approximation function $\tilde{g}$ continuous and differentiable at the point of minimum in the interval $I_1 \cup I_2$. Figure 4.5 gives a visual representation of the intervals I_1 and I_2 and equations Eq. (4.37), Eq. (4.38) and Eq. (4.39).

We can rewrite $\phi(\boldsymbol{\sigma})$ from Theorem 2.3.13 in terms of $\breve{b}_1(\boldsymbol{\sigma})$ for interval I_1 as

$$\phi(\boldsymbol{\sigma}) = \begin{cases} \frac{\pi}{2} - 2\breve{b}_1(\boldsymbol{\sigma}) + 2n_5\pi, & \text{if } \hat{a} \geq 0 \\ -\frac{\pi}{2} - 2\breve{b}_1(\boldsymbol{\sigma}) + 2n_5\pi, & \text{if } \hat{a} < 0 \end{cases}, \tag{4.41}$$

and in terms of $\breve{b}_2(\boldsymbol{\sigma})$ for interval I_2 as:

$$\phi(\boldsymbol{\sigma}) = \begin{cases} -\frac{\pi}{2} - 2\breve{b}_2(\boldsymbol{\sigma}) + 2n_6\pi, & \text{if } \hat{a} \geq 0 \\ \frac{\pi}{2} - 2\breve{b}_2(\boldsymbol{\sigma}) + 2n_6\pi, & \text{if } \hat{a} < 0 \end{cases}, \tag{4.42}$$

where $n_5, n_6 \in \mathbb{Z}$. We use the above equations in the next theorem where we give a result on the quality of our approximation.

Theorem 4.2.14. *Given the stress $\boldsymbol{\sigma} = (\sigma_{xx}, \sigma_{yy}, \sigma_{xy})^T$ with $a(\boldsymbol{\sigma}) < b(\boldsymbol{\sigma})$. If the approximation function $\tilde{g}$ is defined as in Eq. (4.36) where $\breve{b}_1(\boldsymbol{\sigma}) = \alpha^-_{max,1}(\boldsymbol{\sigma})$, $\breve{b}_2(\boldsymbol{\sigma}) = \alpha^-_{max,2}(\boldsymbol{\sigma})$ and parameters $\breve{a}_1(\boldsymbol{\sigma})$, $\breve{a}_2(\boldsymbol{\sigma})$, $\breve{d}_1(\boldsymbol{\sigma})$ and $\breve{d}_2(\boldsymbol{\sigma})$ satisfy Eq. (4.37), Eq. (4.38), Eq. (4.39), and Eq. (4.40) and additionally, if*

$$\breve{c}_1(\boldsymbol{\sigma}) = \sqrt{\frac{\breve{a}_1(\boldsymbol{\sigma})\sigma_e^k N_e}{2kb(\boldsymbol{\sigma})(a(\boldsymbol{\sigma}) + b(\boldsymbol{\sigma}))^{k-1}}}, \tag{4.43}$$

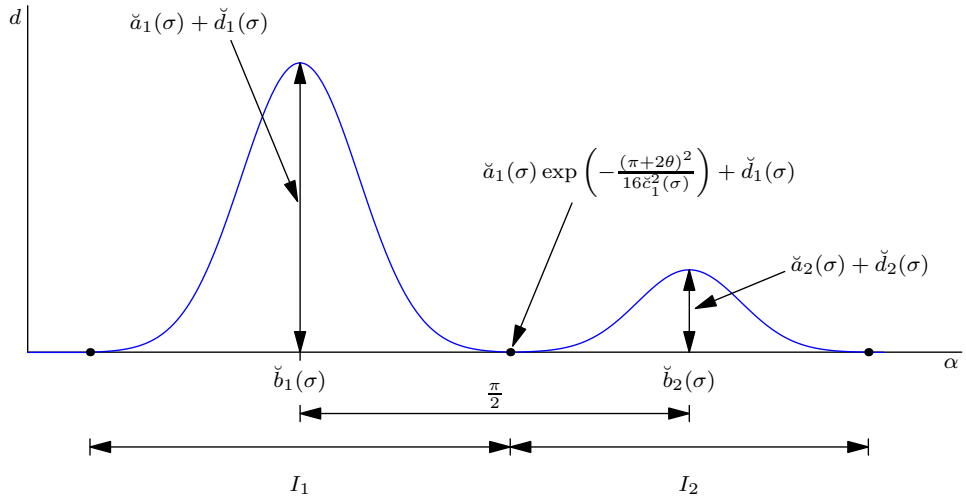

Figure 4.5.: Explanation of approximation around maximum for one slope and $a(\boldsymbol{\sigma}) < b(\boldsymbol{\sigma})$.

and

$$\breve{c}_2(\boldsymbol{\sigma}) = \sqrt{\frac{\breve{a}_2(\boldsymbol{\sigma})\sigma_e^k N_e}{2kb(\boldsymbol{\sigma})(b(\boldsymbol{\sigma}) - a(\boldsymbol{\sigma}))^{k-1}}}, \tag{4.44}$$

then for $\alpha \in I_1 \cup I_2$, the function $\tilde{g}(\boldsymbol{\sigma}, \alpha)$ is an approximation to the damage function $\hat{d}$ from Eq. (4.4) of order 4, i.e.,

$$|\hat{d}(\boldsymbol{\sigma}, \alpha) - \tilde{g}(\boldsymbol{\sigma}, \alpha)| = \begin{cases} O((\alpha - \breve{b}_1(\boldsymbol{\sigma}))^4), & \alpha \in I_1 \\ O((\alpha - \breve{b}_2(\boldsymbol{\sigma}))^4), & \alpha \in I_2 \end{cases}$$

Proof. Similar to the proof of Theorem 4.2.1, we use the Taylor's expansion of both damage function $\hat{d}$ and its approximation function $\tilde{g}$ around the points of maxima.

Depending on the sign of $\hat{a}(\boldsymbol{\sigma})$ the intervals I_1 and I_2 can be further divided into two sub intervals. If $\hat{a}(\boldsymbol{\sigma}) \geq 0$ and $\alpha \in I_1$, then for the peak with the larger damage value to lie in this interval we have $b(\boldsymbol{\sigma}) \sin(2\alpha + \phi(\boldsymbol{\sigma})) > 0$ and similarly for $\alpha \in I_2$ to have the peak with the smaller damage value we have $b(\boldsymbol{\sigma}) \sin(2\alpha + \phi(\boldsymbol{\sigma})) \leq 0$. If $\hat{a}(\boldsymbol{\sigma}) < 0$ and $\alpha \in I_1$, then for the peak with the larger damage value to lie in this interval we have $b(\boldsymbol{\sigma}) \sin(2\alpha + \phi(\boldsymbol{\sigma})) \leq 0$ and for $\alpha \in I_2$ to have the peak with the smaller damage value we have $b(\boldsymbol{\sigma}) \sin(2\alpha + \phi(\boldsymbol{\sigma})) > 0$. Using this to simplify the absolute value of the scalar stress s in equation for the damage $\hat{d}$ we get

$$\hat{d}(\boldsymbol{\sigma}, \alpha) = \frac{1}{\sigma_e^k N_e} \begin{cases} (a(\boldsymbol{\sigma}) + b(\boldsymbol{\sigma}) \sin(2\alpha + \phi(\boldsymbol{\sigma})))^k, & \text{if } \alpha \in I_1, \hat{a}(\boldsymbol{\sigma}) \geq 0, \\ (a(\boldsymbol{\sigma}) - b(\boldsymbol{\sigma}) \sin(2\alpha + \phi(\boldsymbol{\sigma})))^k, & \text{if } \alpha \in I_1, \hat{a}(\boldsymbol{\sigma}) < 0, \\ (-b(\boldsymbol{\sigma}) \sin(2\alpha + \phi(\boldsymbol{\sigma})) - a(\boldsymbol{\sigma}))^k, & \text{if } \alpha \in I_2, \hat{a}(\boldsymbol{\sigma}) \geq 0, \\ (b(\boldsymbol{\sigma}) \sin(2\alpha + \phi(\boldsymbol{\sigma})) - a(\boldsymbol{\sigma}))^k, & \text{if } \alpha \in I_2, \hat{a}(\boldsymbol{\sigma}) < 0. \end{cases} \tag{4.45}$$

We insert $\phi(\boldsymbol{\sigma})$ from Eq. (4.41) and Eq. (4.42) in Eq. (4.45). We know from trigonometry that

$\sin(-\frac{\pi}{2} + 2\alpha - 2\breve{b}_1(\boldsymbol{\sigma}) + 2n_5\pi) = \cos(2\alpha - 2\breve{b}_1(\boldsymbol{\sigma}))$ which simplifies Eq. (4.45) to

$$\hat{d}(\boldsymbol{\sigma}, \alpha) = \frac{1}{\sigma_e^k N_e} \begin{cases} \Big(a(\boldsymbol{\sigma}) + b(\boldsymbol{\sigma}) \cos(2\alpha - 2\breve{b}_1(\boldsymbol{\sigma}))\Big)^k, & \alpha \in I_1 \\ \Big(b(\boldsymbol{\sigma}) \cos(2\alpha - 2\breve{b}_2(\boldsymbol{\sigma})) - a(\boldsymbol{\sigma})\Big)^k, & \alpha \in I_2. \end{cases} \tag{4.46}$$

Next, we look at the two intervals separately. For the interval I_1 the steps are exactly the same as that in Theorem 4.2.1. We get the series representation of damage $\hat{d}(\boldsymbol{\sigma}, \alpha)$ at the point of maximum $\breve{b}_1(\boldsymbol{\sigma})$ in the interval I_1 as

$$\hat{d}(\boldsymbol{\sigma}, \alpha) = \frac{(a(\boldsymbol{\sigma}) + b(\boldsymbol{\sigma}))^k}{\sigma_e^k N_e} - \frac{2kb(\boldsymbol{\sigma})(a(\boldsymbol{\sigma}) + b(\boldsymbol{\sigma}))^{k-1}}{\sigma_e^k N_e}(\alpha - \breve{b}_1(\boldsymbol{\sigma}))^2 + O((\alpha - \breve{b}_1(\boldsymbol{\sigma}))^4), \forall \alpha \in I_1 \tag{4.47}$$

and the series representation of the approximation $\tilde{g}(\boldsymbol{\sigma}, \alpha) = f_{\breve{a}_1(\boldsymbol{\sigma}), \breve{b}_1(\boldsymbol{\sigma}), \breve{c}_1(\boldsymbol{\sigma})}(\alpha) + \breve{d}_1(\boldsymbol{\sigma})$ at $\breve{b}_1(\boldsymbol{\sigma})$ on the interval I_1 as

$$\begin{aligned} f_{\breve{a}_1(\boldsymbol{\sigma}), \breve{b}_1(\boldsymbol{\sigma}), \breve{c}_1(\boldsymbol{\sigma})}(\alpha) + \breve{d}_1(\boldsymbol{\sigma}) &= (\breve{a}_1(\boldsymbol{\sigma}) + \breve{d}_1(\boldsymbol{\sigma})) - \frac{\breve{a}_1(\boldsymbol{\sigma})}{\breve{c}_1(\boldsymbol{\sigma})^2}(\alpha - \breve{b}_1(\boldsymbol{\sigma}))^2 + O((\alpha - \breve{b}_1(\boldsymbol{\sigma}))^4) \\ &= \frac{(a(\boldsymbol{\sigma}) + b(\boldsymbol{\sigma}))^k}{\sigma_e^k N_e} - \frac{\breve{a}_1(\boldsymbol{\sigma})}{\breve{c}_1(\boldsymbol{\sigma})^2}(\alpha - \breve{b}_1(\boldsymbol{\sigma}))^2 + O((\alpha - \breve{b}_1(\boldsymbol{\sigma}))^4), \forall \alpha \in I_1 \end{aligned} \tag{4.48}$$

Subtracting approximation function $\tilde{g}$ in Eq (4.48) from damage d in Eq (4.47) yields for $\alpha \in I_1$

$$\left|\hat{d}(\boldsymbol{\sigma}, \alpha) - \tilde{g}(\boldsymbol{\sigma}, \alpha)\right| = \left(\frac{\breve{a}_1(\boldsymbol{\sigma})}{\breve{c}_1(\boldsymbol{\sigma})^2} - \frac{2kb(\boldsymbol{\sigma})(a(\boldsymbol{\sigma}) + b(\boldsymbol{\sigma}))^{k-1}}{\sigma_e^k N_e}\right)(\alpha - \breve{b}_1(\boldsymbol{\sigma}))^2 + O((\alpha - \breve{b}_1(\boldsymbol{\sigma}))^4)$$

Choosing $\breve{c}_1(\boldsymbol{\sigma})$ such that the term $(\alpha - \breve{b}_1(\boldsymbol{\sigma}))^2$ vanishes gives us Eq. (4.43).

On the interval I_2 the damage $\hat{d}$ is given as

$$\begin{aligned} \hat{d}(\boldsymbol{\sigma}, \alpha) &= \frac{\Big(b(\boldsymbol{\sigma}) \cos(2\alpha - 2\breve{b}_2(\boldsymbol{\sigma})) - a(\boldsymbol{\sigma})\Big)^k}{\sigma_e^k N_e}, \forall \alpha \in I_2 \\ &= \frac{1}{\sigma_e^k N_e} \sum_{t=0}^{k} \binom{k}{t} (-a(\boldsymbol{\sigma}))^{k-t} b(\boldsymbol{\sigma})^t \cos^t(2\alpha - 2\breve{b}_2(\boldsymbol{\sigma})), \forall \alpha \in I_2 \end{aligned}$$

Inserting the series expansion of $\cos(2\alpha - 2\breve{b}_2(\boldsymbol{\sigma}))$ and further simplifications gives us

$$\hat{d}(\boldsymbol{\sigma}, \alpha) = \frac{(b(\boldsymbol{\sigma}) - a(\boldsymbol{\sigma}))^k}{\sigma_e^k N_e} - \frac{2kb(\boldsymbol{\sigma})(b(\boldsymbol{\sigma}) - a(\boldsymbol{\sigma}))^{k-1}}{\sigma_e^k N_e}(\alpha - \breve{b}_2(\boldsymbol{\sigma}))^2 + O(\alpha - \breve{b}_2(\boldsymbol{\sigma}))^4, \forall \alpha \in I_2 \tag{4.49}$$

and the series representation of approximation $\tilde{g}(\boldsymbol{\sigma}, \alpha) = f_{\breve{a}_2(\boldsymbol{\sigma}), \breve{b}_2(\boldsymbol{\sigma}), \breve{c}_2(\boldsymbol{\sigma})}(\alpha) + \breve{d}_2(\boldsymbol{\sigma})$ at $\breve{b}_2(\boldsymbol{\sigma})$ on the interval I_2 as

$$\begin{aligned} f_{\breve{a}_2(\boldsymbol{\sigma}), \breve{b}_2(\boldsymbol{\sigma}), \breve{c}_2(\boldsymbol{\sigma})}(\alpha) + \breve{d}_2(\boldsymbol{\sigma}) &= (\breve{a}_2(\boldsymbol{\sigma}) + \breve{d}_2(\boldsymbol{\sigma})) - \frac{\breve{a}_2(\boldsymbol{\sigma})}{\breve{c}_2(\boldsymbol{\sigma})^2}(\alpha - \breve{b}_2(\boldsymbol{\sigma}))^2 + O(\alpha - \breve{b}_2(\boldsymbol{\sigma}))^4 \\ &= \frac{(b(\boldsymbol{\sigma}) - a(\boldsymbol{\sigma}))^k}{\sigma_e^k N_e} - \frac{\breve{a}_2(\boldsymbol{\sigma})}{\breve{c}_2(\boldsymbol{\sigma})^2}(\alpha - \breve{b}_2(\boldsymbol{\sigma}))^2 + O(\alpha - \breve{b}_2(\boldsymbol{\sigma}))^4 \end{aligned} \tag{4.50}$$

Subtracting approximation function $\tilde{g}$ in Eq (4.50) from damage d in Eq (4.49) yields for $\alpha \in I_2$

$$\left|\hat{d}(\boldsymbol{\sigma},\alpha) - \tilde{g}(\boldsymbol{\sigma},\alpha)\right| = \left(\frac{\breve{a}_2(\boldsymbol{\sigma})}{\breve{c}_2(\boldsymbol{\sigma})^2} - \frac{2kb(\boldsymbol{\sigma})(a(\boldsymbol{\sigma})+b(\boldsymbol{\sigma}))^{k-1}}{\sigma_e^k N_e}\right)(\alpha - \breve{b}_2(\boldsymbol{\sigma}))^2 + O((\alpha - \breve{b}_2(\boldsymbol{\sigma}))^4)$$

Choosing $\breve{c}_2(\boldsymbol{\sigma})$ such that the term $(\alpha - \breve{b}_2(\boldsymbol{\sigma}))^2$ vanishes gives us Eq. (4.44). □

In the next lemma we give the equations to compute the parameters $\breve{a}_1(\boldsymbol{\sigma})$ and $\breve{d}_1(\boldsymbol{\sigma})$ in the definition of the approximation function $\tilde{g}$ from Eq. (4.36).

Lemma 4.2.15. *The parameters $\breve{a}_1(\boldsymbol{\sigma})$ and $\breve{d}_1(\boldsymbol{\sigma})$ in Eq. (4.36) are given as*

$$\breve{a}_1(\boldsymbol{\sigma}) = \frac{(a(\boldsymbol{\sigma})+b(\boldsymbol{\sigma}))^k}{\sigma_e^k N_e \left(1 - \exp\left(-\frac{(\pi+2\theta)^2}{16\breve{c}_1^2(\boldsymbol{\sigma})}\right)\right)}, \tag{4.51}$$

$$\breve{d}_1(\boldsymbol{\sigma}) = \frac{(a(\boldsymbol{\sigma})+b(\boldsymbol{\sigma}))^k \exp\left(-\frac{(\pi+2\theta)^2}{16\breve{c}_1^2(\boldsymbol{\sigma})}\right)}{\sigma_e^k N_e \left(1 - \exp\left(-\frac{(\pi+2\theta)^2}{16\breve{c}_1^2(\boldsymbol{\sigma})}\right)\right)}, \tag{4.52}$$

where $\theta = \frac{a(\boldsymbol{\sigma})}{b(\boldsymbol{\sigma})}$.

Proof. The two equations, Eq. (4.37) and Eq. (4.39) have three unknowns. We use these two equations to give $\breve{a}_1(\boldsymbol{\sigma})$ and $\breve{d}_1(\boldsymbol{\sigma})$ in terms of $\breve{c}_1(\boldsymbol{\sigma})$. Subtracting Eq. (4.39) from Eq. (4.37) we get a equation in $\breve{a}_1(\boldsymbol{\sigma})$ and $\breve{c}_1(\boldsymbol{\sigma})$:

$$\breve{a}_1(\boldsymbol{\sigma})\left(1 - \exp\left(-\frac{(\pi+2\theta)^2}{16\breve{c}_1^2(\boldsymbol{\sigma})}\right)\right) = \frac{(a(\boldsymbol{\sigma})+b(\boldsymbol{\sigma}))^k}{\sigma_e^k N_e} \tag{4.53}$$

Rearranging Eq. (4.53) gives us Eq. (4.51) for computing $\breve{a}_1(\boldsymbol{\sigma})$. Inserting the value of $\breve{a}_1(\boldsymbol{\sigma})$ into Eq. (4.39) and further simplifications gives us Eq. (4.52) for computing $\breve{d}_1(\boldsymbol{\sigma})$. □

In the next lemma we give the equations to compute the parameters $\breve{a}_2(\boldsymbol{\sigma})$ and $\breve{d}_2(\boldsymbol{\sigma})$ in the definition of the approximation function $\tilde{g}$ from Eq. (4.36).

Lemma 4.2.16. *The parameters $\breve{a}_2(\boldsymbol{\sigma})$ and $\breve{d}_2(\boldsymbol{\sigma})$ in Eq. (4.36) are given as*

$$\breve{a}_2(\boldsymbol{\sigma}) = \frac{(b(\boldsymbol{\sigma})-a(\boldsymbol{\sigma}))^k}{\sigma_e^k N_e \left(1 - \exp\left(-\frac{(\pi-2\theta)^2}{16\breve{c}_2^2(\boldsymbol{\sigma})}\right)\right)}, \tag{4.54}$$

$$\breve{d}_2(\boldsymbol{\sigma}) = \frac{(b(\boldsymbol{\sigma})-a(\boldsymbol{\sigma}))^k \exp\left(-\frac{(\pi-2\theta)^2}{16\breve{c}_2^2(\boldsymbol{\sigma})}\right)}{\sigma_e^k N_e \left(1 - \exp\left(-\frac{(\pi-2\theta)^2}{16\breve{c}_2^2(\boldsymbol{\sigma})}\right)\right)}. \tag{4.55}$$

where $\theta = \frac{a(\boldsymbol{\sigma})}{b(\boldsymbol{\sigma})}$.

Proof. The two equations, Eq. (4.38) and Eq. (4.40) have three unknowns. We use these two equations to give $\breve{a}_2(\boldsymbol{\sigma})$ and $\breve{d}_2(\boldsymbol{\sigma})$ in terms of $\breve{c}_2(\boldsymbol{\sigma})$. Subtracting Eq. (4.40) from Eq. (4.38) we

get a equation in $\breve{a}_2(\boldsymbol{\sigma})$ and $\breve{c}_2(\boldsymbol{\sigma})$:

$$\breve{a}_2(\boldsymbol{\sigma})\left(1-\exp\left(-\frac{(\pi-2\theta)^2}{16\breve{c}_2^2(\boldsymbol{\sigma})}\right)\right)=\frac{(b(\boldsymbol{\sigma})-a(\boldsymbol{\sigma}))^k}{\sigma_e^k N_e} \tag{4.56}$$

Rearranging Eq. (4.56) gives us Eq. (4.54) for computing $\breve{a}_2(\boldsymbol{\sigma})$. Inserting the value of $\breve{a}_1(\boldsymbol{\sigma})$ into Eq. (4.40) and further simplifications gives us Eq. (4.55) for computing $\breve{d}_2(\boldsymbol{\sigma})$. □

The next corollary gives us equation for computing $\breve{c}_1(\boldsymbol{\sigma})$ and $\breve{c}_2(\boldsymbol{\sigma})$.

Corollary 4.2.17. *The parameters $\breve{c}_1(\boldsymbol{\sigma})$ and $\breve{c}_2(\boldsymbol{\sigma})$ in the definition of the approximation function $\tilde{g}$ in Eq. (4.36) are given as*

$$\breve{c}_1(\boldsymbol{\sigma})=\sqrt{\frac{a(\boldsymbol{\sigma})+b(\boldsymbol{\sigma})}{2kb(\boldsymbol{\sigma})\left(1-\exp\left(-\frac{(\pi+2\theta)^2}{16\breve{c}_1^2(\boldsymbol{\sigma})}\right)\right)}}, \tag{4.57}$$

$$\breve{c}_2(\boldsymbol{\sigma})=\sqrt{\frac{b(\boldsymbol{\sigma})-a(\boldsymbol{\sigma})}{2kb(\boldsymbol{\sigma})\left(1-\exp\left(-\frac{(\pi-2\theta)^2}{16\breve{c}_2^2(\boldsymbol{\sigma})}\right)\right)}}. \tag{4.58}$$

Proof. Inserting $\breve{a}_1(\boldsymbol{\sigma})$ from Eq. (4.51) into Eq. (4.43) gives $\breve{c}_1(\boldsymbol{\sigma})$ and inserting $\breve{a}_2(\boldsymbol{\sigma})$ from Eq. (4.54) into Eq. (4.44) gives $\breve{c}_2(\boldsymbol{\sigma})$. □

Eq. (4.57) and Eq. (4.58) are fixed point equations similar to one in Eq. (4.25). In order to use the approximate function $\tilde{g}$ we have to first compute $\breve{c}_1(\boldsymbol{\sigma})$ and $\breve{c}_2(\boldsymbol{\sigma})$. Since, these two parameters are given by a fixed point equation we next prove that Eq. (4.57) and Eq. (4.58) have a unique fixed point. We make use of the following result in the proof.

Lemma 4.2.18. *We have*

$$\frac{\sqrt{1-y}}{\pi-2\sin^{-1}y}<\frac{1}{2\sqrt{2}}$$

for all $y\in[0,1)$.

Proof. From [28] we know that $\sin^{-1}y+\cos^{-1}y=\frac{\pi}{2}$, which simplifies

$$\frac{\sqrt{1-y}}{\pi-2\sin^{-1}y}=\frac{\sqrt{1-y}}{2\cos^{-1}y}$$

for $y\in[0,1)$. The term $\frac{\sqrt{1-y}}{2\cos^{-1}y}$ is increasing in the interval $[0,1)$. The Taylor series for the term at $y=1$ is

$$\begin{aligned}\frac{\sqrt{1-y}}{2\cos^{-1}y}&=\frac{1}{2\sqrt{2}}-\frac{1-y}{24\sqrt{2}}-\frac{17\sqrt{2}(1-y)^2}{5760}+O\left((1-y)^3\right)\\&<\frac{1}{2\sqrt{2}}.\end{aligned}$$

□

Theorem 4.2.19. *Both Eq. (4.57) and Eq. (4.58) have a unique fixed point.*

Proof. The proof is similar to the proof of Theorem 4.2.11. Let us define

$$T_1 : \mathbb{R} \to \mathbb{R}, y \mapsto \sqrt{\frac{a(\boldsymbol{\sigma}) + b(\boldsymbol{\sigma})}{2kb(\boldsymbol{\sigma})}} \frac{1}{\sqrt{1 - \exp\left(-\left(\frac{\pi+2\theta}{4y}\right)^2\right)}}. \tag{4.59}$$

with a real constant $k > 1$. Next, we show that T_1 is a contraction mapping which implies that the fixed point equation in (4.57) is also a contraction mapping. Then due to the Contraction mapping theorem (4.57) has a unique fixed point. The first derivative of T_1 is

$$\begin{aligned} T_1'(y) &= \sqrt{\frac{a(\boldsymbol{\sigma}) + b(\boldsymbol{\sigma})}{2kb(\boldsymbol{\sigma})}} \frac{d}{dy} \left(\frac{1}{\sqrt{1 - \exp\left(-\frac{(\pi+2\theta)^2}{16y^2}\right)}} \right) \\ &= \sqrt{\frac{a(\boldsymbol{\sigma}) + b(\boldsymbol{\sigma})}{2kb(\boldsymbol{\sigma})}} \frac{(\pi + 2\theta)^2 \sqrt{\exp\left(\frac{(\pi+2\theta)^2}{16y^2}\right)}}{16y^3 \left(\exp\left(\frac{(\pi+2\theta)^2}{16y^2}\right) - 1\right)^{\frac{3}{2}}} \end{aligned}$$

We apply Lemma 4.2.7 for $\mathfrak{s} = 4$, $\mathfrak{p} = y$, $\mathfrak{r} = \sqrt{\frac{2kb(\boldsymbol{\sigma})}{a(\boldsymbol{\sigma})+b(\boldsymbol{\sigma})}}$ and $\mathfrak{t} = \pi + 2\theta$ and obtain that

$$T_1'(x) < \sqrt{\frac{a(\boldsymbol{\sigma}) + b(\boldsymbol{\sigma})}{2kb(\boldsymbol{\sigma})}} \frac{4}{\pi + 2\theta} \text{ for all } x \in \mathbb{R}.$$

We know that $\theta = \sin^{-1}\left(\frac{a(\boldsymbol{\sigma})}{b(\boldsymbol{\sigma})}\right)$. Therefore, the term $\sqrt{\frac{a(\boldsymbol{\sigma})+b(\boldsymbol{\sigma})}{2b(\boldsymbol{\sigma})}} \frac{4}{\pi+2\theta}$ can also be written as $\sqrt{\frac{1+\sin\theta}{2}} \frac{4}{\pi+2\theta}$. It is shown in Theorem A.3.1 that the term $\sqrt{\frac{1+\sin\theta}{2}} \frac{4}{\pi+2\theta}$ is decreasing for $\theta \in \left[0, \frac{\pi}{2}\right]$. The evaluation of the term at $\theta = 0$ yields the value $\frac{4}{\sqrt{2}\pi} < 1$. Figure 4.6 illustrates the term $\sqrt{\frac{1+\sin\theta}{2}} \frac{4}{\pi+2\theta}$ on the interval $\left[0, \frac{\pi}{2}\right]$. Since, $\sqrt{\frac{1+\sin\theta}{2}} \frac{4}{\pi+2\theta}$ for all $\theta \in \left[0, \frac{\pi}{2}\right]$ is less than one we get that $\sqrt{\frac{a(\boldsymbol{\sigma})+b(\boldsymbol{\sigma})}{2kb(\boldsymbol{\sigma})}} \frac{4}{\pi+2\theta}$ is also less than one. We conclude:

$$T_1'(y) < \sqrt{\frac{a(\boldsymbol{\sigma}) + b(\boldsymbol{\sigma})}{2kb(\boldsymbol{\sigma})}} \frac{4}{\pi + 2\theta} < 1 \text{ for all } y \in \mathbb{R} \Rightarrow \sup_{y' \in \mathbb{R}} |T_1'(y')| \leq \sqrt{\frac{a(\boldsymbol{\sigma}) + b(\boldsymbol{\sigma})}{2kb(\boldsymbol{\sigma})}} \frac{4}{\pi + 2\theta} < 1.$$

This proves that the fixed point equation in (4.57) is a contraction mapping.

Next we prove the contraction property for the fixed point equation (4.58). Let us define

$$T_2 : \mathbb{R} \to \mathbb{R}, y \mapsto \sqrt{\frac{1-t}{2k}} \sqrt{\frac{1}{1 - \exp\left(-\frac{(\pi - 2\sin^{-1} t)^2}{16y^2}\right)}} \tag{4.60}$$

where $0 \leq t < 1$ and $k > 1$ are fixed. The first derivative of T_2 at y is given by

$$T_2'(x) = \sqrt{\frac{1-t}{2k}} \frac{(\pi - 2\sin^{-1} t)^2 \sqrt{\exp\left(\frac{(\pi-2\sin^{-1} t)^2}{16y^2}\right)}}{16y^3 \left(\exp\left(\frac{(\pi-2\sin^{-1} t)^2}{16y^2}\right) - 1\right)^{\frac{3}{2}}}$$

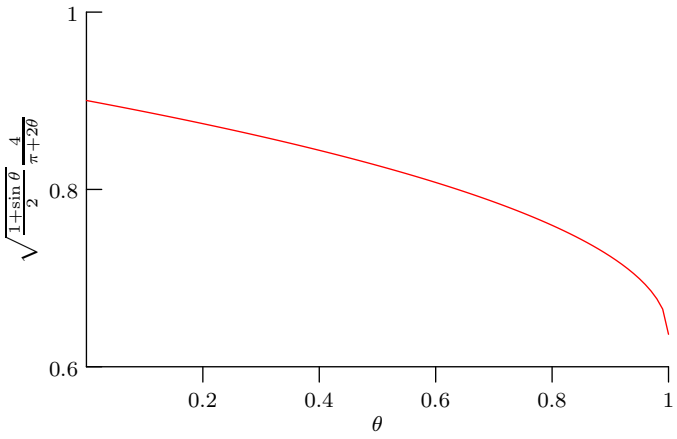

Figure 4.6.: Value of $\sqrt{\frac{1+\sin\theta}{2}}\frac{4}{\pi+2\theta}$.

We apply Lemma 4.2.7 for $\mathfrak{s} = 4$, $\mathfrak{p} = y$, $\mathfrak{r} = \sqrt{\frac{2k}{1-t}}$ and $\mathfrak{t} = \pi - 2\sin^{-1} t$ and obtain that

$$< \sqrt{\frac{1-t}{2k}} \frac{4}{(\pi - 2\sin^{-1} t)} \tag{4.61}$$

$$= \frac{4}{\sqrt{2k}} \frac{\sqrt{1-t}}{(\pi - 2\sin^{-1} t)}. \tag{4.62}$$

To the inequality in (4.62) we may apply Lemma 4.2.18 to get

$$T_2'(y) < \frac{1}{2\sqrt{2}} \frac{4}{\sqrt{2k}} < \frac{1}{\sqrt{k}} \text{ for all } x \in \mathbb{R} \Rightarrow \sup_{x\in\mathbb{R}} |T_2'(y)| \leq \frac{1}{\sqrt{k}} < 1.$$

This proves that $T_2(y)$ is a contraction mapping and has a unique fixed point. $T_2(y)$ is the right hand side of the fixed point equation in (4.58) for $t = \frac{a(s)}{b(s)}$ and $\theta = \sin^{-1} t$. Hence, we have shown that both fixed point operators are contraction mappings and have unique fixed points. □

The Theorem 4.2.19 says that we can compute both $\breve{c}_1(\boldsymbol{\sigma})$ and $\breve{c}_2(\boldsymbol{\sigma})$ from their respective fixed point equations. Once we have these two parameters we can proceed the computation of other parameters.

Next we give equations solving which we get the upper and lower bound for $\breve{c}_1(\boldsymbol{\sigma})$ and $\breve{c}_2(\boldsymbol{\sigma})$. After squaring and rearranging Eq. (4.57) and Eq. (4.58) we get

$$\breve{c}_1^2(\boldsymbol{\sigma}) \left(1 - \exp\left(-\frac{(\pi+2\theta)^2}{16\breve{c}_1^2(\boldsymbol{\sigma})}\right)\right) = \frac{a(\boldsymbol{\sigma}) + b(\boldsymbol{\sigma})}{2kb(\boldsymbol{\sigma})} \tag{4.63}$$

and

$$\breve{c}_2^2(\boldsymbol{\sigma}) \left(1 - \exp\left(-\frac{(\pi+2\theta)^2}{16\breve{c}_2^2(\boldsymbol{\sigma})}\right)\right) = \frac{b(\boldsymbol{\sigma}) - a(\boldsymbol{\sigma})}{2kb(\boldsymbol{\sigma})} \tag{4.64}$$

In Eq. (4.63) we see that increasing $a(\boldsymbol{\sigma})$ increases the right hand side of the equation. The

maximum value of $\breve{c}_1(\boldsymbol{\sigma})$, for different values of k, is obtained from Eq. (4.63) in the limiting case $a(\boldsymbol{\sigma}) \to b(\boldsymbol{\sigma})^-$ as

$$\breve{c}_1^2(\boldsymbol{\sigma}) \left(1 - \exp\left(-\frac{\pi^2}{4\breve{c}_1^2(\boldsymbol{\sigma})}\right)\right) = \frac{1}{k}$$

which is similar to Eq. (4.33) for the lower bound of $\breve{c}(\boldsymbol{\sigma})$ in the case $a(\boldsymbol{\sigma}) \geq b(\boldsymbol{\sigma})$. In the limiting case $a(\boldsymbol{\sigma}) \to b(\boldsymbol{\sigma})^-$ the value of θ is $\frac{\pi}{2}$. Similarly, the lower bound for $\breve{c}_1(\boldsymbol{\sigma})$ for different values of k is obtained in the limiting case $a(\boldsymbol{\sigma}) \to 0^+$ from the following equation

$$\breve{c}_1^2(\boldsymbol{\sigma}) \left(1 - \exp\left(-\frac{\pi^2}{16\breve{c}_1^2(\boldsymbol{\sigma})}\right)\right) = \frac{1}{2k}. \tag{4.65}$$

Similarly, in Eq. (4.64) we see that increasing $a(\boldsymbol{\sigma})$ decreases the right hand side of the equation. The maximum value of $\breve{c}_2(\boldsymbol{\sigma})$, for different values of k, is obtained from Eq. (4.64) in the limiting case $a(\boldsymbol{\sigma}) \to 0^+$ as

$$\breve{c}_2^2(\boldsymbol{\sigma}) \left(1 - \exp\left(-\frac{\pi^2}{16\breve{c}_1^2(\boldsymbol{\sigma})}\right)\right) = \frac{1}{2k}. \tag{4.66}$$

It is interesting to note that Eq. (4.65) for the lower bound of $\breve{c}_1(\boldsymbol{\sigma})$ has the same form as the equation for the upper bound of $\breve{c}_2(\boldsymbol{\sigma})$. The lower bound for $\breve{c}_2(\boldsymbol{\sigma})$ coincides with the assumption that $\breve{c}_2(\boldsymbol{\sigma})$ has to be greater than zero. Figure 4.7 gives the lower and upper bound for $\breve{c}_1(\boldsymbol{\sigma})$ and $\breve{c}_2(\boldsymbol{\sigma})$ for different values of k.

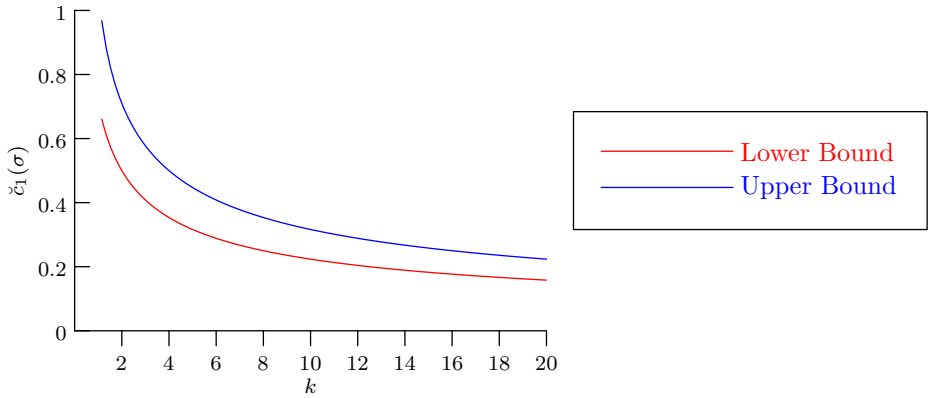

(a) Lower and upper bounds for $\breve{c}_1(\boldsymbol{\sigma})$.

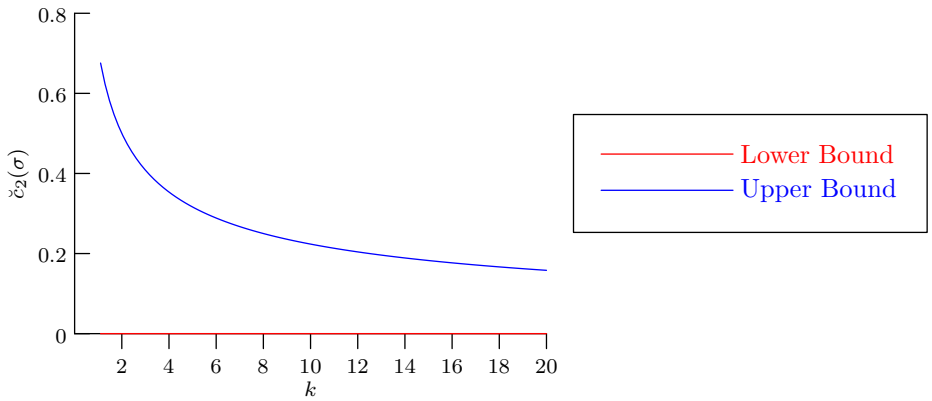

(b) Lower and upper bounds for $\breve{c}_2(\boldsymbol{\sigma})$.

Figure 4.7.: Lower and upper bounds for $\breve{c}_1(\boldsymbol{\sigma})$ and $\breve{c}_2(\boldsymbol{\sigma})$ for different values of k.

In this section, we gave an approximation to the damage function in the case of one slope with $a(\boldsymbol{\sigma}) < b(\boldsymbol{\sigma})$. We derived the parameters $\breve{a}_1(\boldsymbol{\sigma})$, $\breve{a}_2(\boldsymbol{\sigma})$, $\breve{b}_1(\boldsymbol{\sigma})$, $\breve{b}_2(\boldsymbol{\sigma})$, $\breve{c}_1(\boldsymbol{\sigma})$, $\breve{c}_2(\boldsymbol{\sigma})$, $\breve{d}_1(\boldsymbol{\sigma})$ and $\breve{d}_2(\boldsymbol{\sigma})$ for the approximation function $\tilde{g}$ and discussed properties of these parameters. This concludes the section on approximation of damage around the point of maximum damage. In the next section, we use our ideas on the approximation of the damage around the point of maximum to approximate the damage on $\mathbb{R}$.

4.3. Approximation of the damage function on $\mathbb{R}$

In Section 4.2, an approximation to the damage function in the neighbourhood of the maxima was derived. In this section, we give an approximation of damage on $\mathbb{R}$. The parameters for the approximation function are derived and their properties are discussed. Similar to the discussion in Section 4.2 we consider two sub-cases, i.e., $a(\boldsymbol{\sigma}) \geq b(\boldsymbol{\sigma})$ and $a(\boldsymbol{\sigma}) < b(\boldsymbol{\sigma})$. Figure 4.8 gives example plots for four periods of damage in the case of one slope.

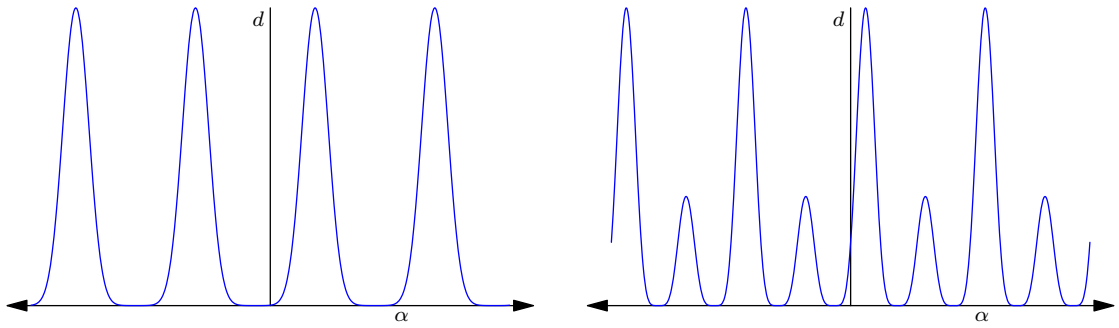

(a) An example plot of damage $\hat{d}$ for the case $a(\boldsymbol{\sigma}) \geq b(\boldsymbol{\sigma})$.

(b) An example plot of damage $\hat{d}$ for the case $a(\boldsymbol{\sigma}) < b(\boldsymbol{\sigma})$.

Figure 4.8.: The damage profiles for one slope and one block extended to the real line $\mathbb{R}$.

4.3.1. Case $a(\boldsymbol{\sigma}) \geq b(\boldsymbol{\sigma})$

Without loss of generality, we assume that the point of maximum damage $\breve{b}(\boldsymbol{\sigma}) \in [0, \pi)$ because the damage function $\hat{d}$ is a periodic function with period π. The other points of maximum damage are $\breve{b}(\boldsymbol{\sigma}) + i\pi$ where $i \in \mathbb{Z}$. To approximate the damage function $\hat{d}$ on $\mathbb{R}$ we place the Gaussian functions one after another at $\breve{b}(\boldsymbol{\sigma}) + i\pi$, for all $i \in \mathbb{Z}$. We define the approximation of the damage function $\hat{d}$ on $\mathbb{R}$ as

$$g_{\mathbb{R}} : \mathbb{R}^3 \times \mathbb{R} \to \mathbb{R}, (\boldsymbol{\sigma}, \alpha) \mapsto \sum_{i=-\infty}^{\infty} f_{\breve{a}(\boldsymbol{\sigma}),\breve{b}(\boldsymbol{\sigma}),\breve{c}(\boldsymbol{\sigma})}(\alpha - i\pi) + \breve{d}(\boldsymbol{\sigma}), \alpha \in \mathbb{R} \tag{4.67}$$

where $f_{\breve{a}(\boldsymbol{\sigma}),\breve{b}(\boldsymbol{\sigma}),\breve{c}(\boldsymbol{\sigma})}$ is a Gaussian function from Eq. (4.1) with parameters $\breve{a}(\boldsymbol{\sigma})$, $\breve{b}(\boldsymbol{\sigma})$ and $\breve{c}(\boldsymbol{\sigma})$. The parameters $\breve{a}(\boldsymbol{\sigma})$ and $\breve{c}(\boldsymbol{\sigma})$ are same for all the Gaussian functions. However, the point of maximum for the i-th Gaussian function in the sum in Eq. (4.67) is given as $\breve{b}(\boldsymbol{\sigma}) + i\pi$.

We want the approximation $g_{\mathbb{R}}$ to be exact at the maxima. Consequently, the approximation in Eq. (4.67) evaluated at $\alpha = \breve{b}(\boldsymbol{\sigma}) + i\pi$ should yield the maximum damage for any $i \in \mathbb{Z}$. We obtain the following equation

$$\breve{a}(\boldsymbol{\sigma}) \sum_{i=-\infty}^{\infty} \exp\left(-\frac{i^2\pi^2}{\breve{c}^2(\boldsymbol{\sigma})}\right) + \breve{d}(\boldsymbol{\sigma}) = \frac{(a(\boldsymbol{\sigma}) + b(\boldsymbol{\sigma}))^k}{\sigma_e^k N_e}. \tag{4.68}$$

The right hand side of Eq. (4.68) is the maximum damage and the left hand side of Eq. (4.68) is obtained by evaluating the approximation function $g_{\mathbb{R}}$ at $\alpha = \breve{b}(\boldsymbol{\sigma}) + i\pi$ for all $i \in \mathbb{Z}$. Equation (4.68) has to be satisfied for the approximation $g_{\mathbb{R}}$ to be exact at the maxima. Similarly, when we evaluate $g_{\mathbb{R}}$ at $\alpha = \breve{b}(\boldsymbol{\sigma}) + (2i+1)\frac{\pi}{2}$ for any $i \in \mathbb{Z}$ we should get the minimum damage.

$$\breve{a}(\boldsymbol{\sigma}) \sum_{i=-\infty}^{\infty} \exp\left(-\frac{(2i+1)^2\pi^2}{4\breve{c}^2(\boldsymbol{\sigma})}\right) + \breve{d}(\boldsymbol{\sigma}) = \frac{(a(\boldsymbol{\sigma}) - b(\boldsymbol{\sigma}))^k}{\sigma_e^k N_e}. \tag{4.69}$$

Again, Eq. (4.69) has to be satisfied for the approximation $g_{\mathbb{R}}$ to be exact at the minima. The condition in Eq. (4.69) implies that the approximation function is continuous and differentiable at the points of minima.

In the next theorem, we establish an approximation of $\hat{d}$ of order 4.

Theorem 4.3.1. *Given the stress $\boldsymbol{\sigma} = (\sigma_{xx}, \sigma_{yy}, \sigma_{xy})^T$ with $a(\boldsymbol{\sigma}) \geq b(\boldsymbol{\sigma})$. If $g_{\mathbb{R}}$ is as defined in Eq. (4.67) and parameters $\breve{a}(\boldsymbol{\sigma})$, $\breve{b}(\boldsymbol{\sigma})$ and $\breve{d}(\boldsymbol{\sigma})$ satisfying Eq. (4.7), Eq. (4.68) and Eq. (4.69), and additionally, if*

$$\frac{2kb(\boldsymbol{\sigma})(a(\boldsymbol{\sigma}) + b(\boldsymbol{\sigma}))^{k-1}}{\sigma_e^k N_e} + \frac{\breve{a}(\boldsymbol{\sigma})}{\breve{c}^2(\boldsymbol{\sigma})} \sum_{i=-\infty}^{\infty} \left(\frac{2i^2\pi^2}{\breve{c}^2(\boldsymbol{\sigma})} - 1\right) \exp\left(-\frac{i^2\pi^2}{\breve{c}^2(\boldsymbol{\sigma})}\right) = 0, \tag{4.70}$$

then $g_{\mathbb{R}}$ is an approximation of damage function $\hat{d}$ defined in Eq. (4.4) on $\mathbb{R}$ of order 4, i.e.

$$\left|\hat{d}(\boldsymbol{\sigma}, \alpha) - g_{\mathbb{R}}(\boldsymbol{\sigma}, \alpha)\right| = O((\alpha - \breve{b}(\boldsymbol{\sigma}))^4).$$

Proof. The proof is similar to the Theorem 4.2.1. The condition (4.70) is chosen such that the term $(\alpha - \breve{b}(\boldsymbol{\sigma}))^2$ in the difference of the Taylor series expansion, around $\breve{b}(\boldsymbol{\sigma})$, of $\hat{d}$ and $g_{\mathbb{R}}$ can be neglected. The Taylor series expansion of $g_{\mathbb{R}}(\boldsymbol{\sigma}, \alpha)$ around $\breve{b}(\boldsymbol{\sigma})$ is derived in Corollary A.1.3 and given in Eq. (A.17) as

$$g_{\mathbb{R}}(\boldsymbol{\sigma}, \alpha) = \breve{a}(\boldsymbol{\sigma}) \sum_{i=-\infty}^{\infty} \exp\left(-\frac{i^2\pi^2}{\breve{c}^2(\boldsymbol{\sigma})}\right) + \frac{\breve{a}(\boldsymbol{\sigma})}{\breve{c}^2(\boldsymbol{\sigma})} \sum_{i=-\infty}^{\infty} \left(\frac{2i^2\pi^2}{\breve{c}^2(\boldsymbol{\sigma})} - 1\right) \exp\left(-\frac{i^2\pi^2}{\breve{c}^2(\boldsymbol{\sigma})}\right) (\alpha - \breve{b}(\boldsymbol{\sigma}))^2 + \breve{d}(\boldsymbol{\sigma}) + O((\alpha - \breve{b}(\boldsymbol{\sigma}))^4). \tag{4.71}$$

Using equation (4.68) we rewrite $g_{\mathbb{R}}(\boldsymbol{\sigma}, \alpha)$ as

$$g_{\mathbb{R}}(\boldsymbol{\sigma}, \alpha) = \frac{(a(\boldsymbol{\sigma}) + b(\boldsymbol{\sigma}))^k}{\sigma_e^k N_e} + \frac{\breve{a}(\boldsymbol{\sigma})}{\breve{c}^2(\boldsymbol{\sigma})} \sum_{i=-\infty}^{\infty} \left(\frac{2i^2\pi^2}{\breve{c}^2(\boldsymbol{\sigma})} - 1\right) \exp\left(-\frac{i^2\pi^2}{\breve{c}^2(\boldsymbol{\sigma})}\right) (\alpha - \breve{b}(\boldsymbol{\sigma}))^2 + O((\alpha - \breve{b}(\boldsymbol{\sigma}))^4). \tag{4.72}$$

From (4.18) we get the Taylor series of damage function $\hat{d}$ as

$$\hat{d}(\boldsymbol{\sigma},\alpha) = \frac{(a(\boldsymbol{\sigma})+b(\boldsymbol{\sigma}))^k}{\sigma_e^k N_e} - \frac{2kb(\boldsymbol{\sigma})(a(\boldsymbol{\sigma})+b(\boldsymbol{\sigma}))^{k-1}}{\sigma_e^k N_e}(\alpha-\breve{b}(\boldsymbol{\sigma}))^2 + O((\alpha-\breve{b}(\boldsymbol{\sigma}))^4) \tag{4.73}$$

Subtracting the Taylor series of $g_{\mathbb{R}}(\boldsymbol{\sigma},\alpha)$ from the Taylor series of $\hat{d}(\boldsymbol{\sigma},\alpha)$ and proceeding as in Theorem 4.2.1 leads to the result.

$$\begin{aligned}\left|\hat{d}(\boldsymbol{\sigma},\alpha) - g_{\mathbb{R}}(\boldsymbol{\sigma},\alpha)\right| = -\frac{\breve{a}(\boldsymbol{\sigma})}{\breve{c}^2(\boldsymbol{\sigma})}\sum_{i=-\infty}^{\infty}\left(\frac{2i^2\pi^2}{\breve{c}^2(\boldsymbol{\sigma})}-1\right)\exp\left(-\frac{i^2\pi^2}{\breve{c}^2(\boldsymbol{\sigma})}\right)(\alpha-\breve{b}(\boldsymbol{\sigma}))^2 \\ - \frac{2kb(\boldsymbol{\sigma})(a(\boldsymbol{\sigma})+b(\boldsymbol{\sigma}))^{k-1}}{\sigma_e^k N_e}(\alpha-\breve{b}(\boldsymbol{\sigma}))^2 + O\left((\alpha-\breve{b}(\boldsymbol{\sigma}))^4\right)\end{aligned} \tag{4.74}$$

For the term $(\alpha-\breve{b}(\boldsymbol{\sigma}))^2$ to vanish we choose the multiplier associated with it to be zero which yields Eq. (4.70). □

For the approximation function $g_{\mathbb{R}}$ to be valid the series in Eq. (4.69) and Eq. (4.70) must converge. We use the Comparison Test of the First Kind for proving that the series $\sum_{i=-\infty}^{\infty}\exp\left(-\frac{(2i+1)^2\pi^2}{4\breve{c}^2(\boldsymbol{\sigma})}\right)$ in Eq. (4.69) and series $\sum_{i=-\infty}^{\infty}\exp\left(-\frac{i^2\pi^2}{\breve{c}^2(\boldsymbol{\sigma})}\right)$ and series $\sum_{i=0}^{\infty} i^2\exp\left(-\frac{i^2\pi^2}{\breve{c}^2(\boldsymbol{\sigma})}\right)$ in Eq. (4.70) converge.

Theorem 4.3.2 (Comparison Test of First Kind)**.** *Given two series $\sum a_i$ and $\sum c_i$ with $a_i, c_i \geq 0$ for all i and $a_i \leq c_i$ for all i. Then, if $\sum c_i$ is convergent then so is $\sum a_i$.*

Proof. For details about the proof please refer [19]. □

Lemma 4.3.3. *The series $\sum_{i=-\infty}^{\infty}\exp\left(-\left(\frac{(2i+1)\pi}{2\breve{c}(\boldsymbol{\sigma})}\right)^2\right)$ in Eq. (4.69) and series $\sum_{i=-\infty}^{\infty}\exp\left(-\frac{i^2\pi^2}{\breve{c}^2(\boldsymbol{\sigma})}\right)$ and series $\sum_{i=0}^{\infty} i^2\exp\left(-\frac{i^2\pi^2}{\breve{c}^2(\boldsymbol{\sigma})}\right)$ in Eq. (4.70) are finite for all $0<\breve{c}(\boldsymbol{\sigma})<\infty$.*

Proof. The proof for each series is shown separately.

Case I. Consider the series with elements $c_i = \exp\left(-\frac{(8i+1)\pi^2}{4\breve{c}^2(\boldsymbol{\sigma})}\right), i \in \mathbb{N}_0$. The series $\sum_{i=0}^{\infty} c_i$ is a geometric series where the first element of the series is $\exp\left(-\frac{\pi^2}{4\breve{c}^2(\boldsymbol{\sigma})}\right)$ and the common ratio is $\exp\left(-\frac{2\pi^2}{\breve{c}^2(\boldsymbol{\sigma})}\right) < 1$. Hence, using the series sum formula for infinite geometric series we get

$$\sum_{i=0}^{\infty} c_i = \frac{\exp\left(-\frac{\pi^2}{4\breve{c}^2(\boldsymbol{\sigma})}\right)}{1-\exp\left(-\frac{2\pi^2}{\breve{c}^2(\boldsymbol{\sigma})}\right)}$$

We can rewrite the series in Eq. (4.69) as

$$\sum_{i=-\infty}^{\infty}\exp\left(-\frac{(2i+1)^2\pi^2}{4\breve{c}^2(\boldsymbol{\sigma})}\right) = 2\sum_{i=0}^{\infty}\exp\left(-\frac{(2i+1)^2\pi^2}{4\breve{c}^2(\boldsymbol{\sigma})}\right) =: 2\sum_{i=0}^{\infty} a_i$$

where $a_i = \exp\left(-\frac{(2i+1)^2\pi^2}{4\breve{c}^2(\boldsymbol{\sigma})}\right)$ for all $i \in \mathbb{N}_0$. We know that $(2i+1)^2 \geq (8i+1)$ for all $i \in \mathbb{N}_0$ which implies that $a_i \leq c_i$. Hence, $2\sum_{i=0}^{\infty} a_i$ is absolutely convergent according to the Comparison Test of First Kind.

Case II. We can rewrite the series $\sum_{i=-\infty}^{\infty} \exp\left(-\frac{i^2\pi^2}{\breve{c}^2(\boldsymbol{\sigma})}\right)$ in Eq. (4.70) as

$$\sum_{i=-\infty}^{\infty} \exp\left(-\frac{i^2\pi^2}{\breve{c}^2(\boldsymbol{\sigma})}\right) = 1 + 2\sum_{i=1}^{\infty} \exp\left(-\frac{i^2\pi^2}{\breve{c}^2(\boldsymbol{\sigma})}\right) =: 1 + 2\sum_{i=1}^{\infty} a_i$$

where $a_i = \exp\left(-\frac{i^2\pi^2}{\breve{c}^2(\boldsymbol{\sigma})}\right), i \in \mathbb{N}$. Similar to the proof in Case I we consider the series with elements $c_i = \exp\left(-\frac{(3i-2)\pi^2}{\breve{c}^2(\boldsymbol{\sigma})}\right)$. The series $\sum_{i=1}^{\infty} c_i$ is a geometric series where the first element of the series is $\exp\left(-\frac{\pi^2}{\breve{c}^2(\boldsymbol{\sigma})}\right)$ and the common ratio is $\exp\left(-\frac{3\pi^2}{\breve{c}^2(\boldsymbol{\sigma})}\right) < 1$. Hence, using the series sum formula for infinite geometric series we get

$$\sum_{i=1}^{\infty} c_i = \frac{\exp\left(-\frac{\pi^2}{\breve{c}^2(\boldsymbol{\sigma})}\right)}{1 - \exp\left(-\frac{3\pi^2}{\breve{c}^2(\boldsymbol{\sigma})}\right)}$$

We see that $i^2 \geq 3i - 2$ for all $i \in \mathbb{N}$, which implies $a_i \leq c_i$ for all $i \in \mathbb{N}$. Hence, $1 + 2\sum_{i=1}^{\infty} a_i$ is absolutely convergent according to the Comparison Test of First Kind.

Case III. We can rewrite the series $\sum_{i=-\infty}^{\infty} i^2 \exp\left(-\frac{i^2\pi^2}{\breve{c}^2(\boldsymbol{\sigma})}\right)$ in Eq. (4.70) as

$$\sum_{i=-\infty}^{\infty} i^2 \exp\left(-\frac{i^2\pi^2}{\breve{c}^2(\boldsymbol{\sigma})}\right) = 2\sum_{i=1}^{\infty} i^2 \exp\left(-\frac{i^2\pi^2}{\breve{c}^2(\boldsymbol{\sigma})}\right) =: 2\sum_{i=1}^{\infty} a_i$$

where $a_i = i^2 \exp\left(-\frac{i^2\pi^2}{\breve{c}^2(\boldsymbol{\sigma})}\right)$ for all $i \in \mathbb{N}$. We consider the series with elements $c_i = \exp\left(-\frac{(3i-2)\pi^2}{4\breve{c}^2(\boldsymbol{\sigma})}\right)$. The series $\sum_{i=1}^{\infty} c_i$ is a geometric series where the first element of the series is $\exp\left(-\frac{\pi^2}{4\breve{c}^2(\boldsymbol{\sigma})}\right)$ and the common ratio is $\exp\left(-\frac{3\pi^2}{4\breve{c}^2(\boldsymbol{\sigma})}\right) < 1$. Hence, using the series sum formula for infinite geometric series we get

$$\sum_{i=1}^{\infty} c_i = \frac{\exp\left(-\frac{\pi^2}{4\breve{c}^2(\boldsymbol{\sigma})}\right)}{1 - \exp\left(-\frac{3\pi^2}{4\breve{c}^2(\boldsymbol{\sigma})}\right)}$$

Using induction it is easy to see that $a_i \leq c_i$ for all $i \in \mathbb{N}$. Hence, $2\sum_{i=1}^{\infty} a_i$ is absolutely convergent according to the Comparison Test of First Kind. □

From Lemma 4.3.3 we know that the series $\sum_{i=-\infty}^{\infty} \exp\left(-\left(\frac{(2i+1)\pi}{2\breve{c}(\boldsymbol{\sigma})}\right)^2\right)$ in Eq. (4.69) and series $\sum_{i=-\infty}^{\infty} \exp\left(-\frac{i^2\pi^2}{\breve{c}^2(\boldsymbol{\sigma})}\right)$ and series $\sum_{i=0}^{\infty} i^2 \exp\left(-\frac{i^2\pi^2}{\breve{c}^2(\boldsymbol{\sigma})}\right)$ in Eq. (4.70) are finite for all $0 < \breve{c}(\boldsymbol{\sigma}) < \infty$. In the next lemma we give the equations to compute the parameters $\breve{a}(\boldsymbol{\sigma})$ and $\breve{d}(\boldsymbol{\sigma})$ in the definition of the approximation function $g_{\mathbb{R}}$ from Eq. (4.67).

Lemma 4.3.4. *The parameters $\breve{a}(\boldsymbol{\sigma})$ and $\breve{d}(\boldsymbol{\sigma})$ in the definition of the approximation function $g_{\mathbb{R}}$*

in Eq. (4.67) *are given as*

$$\breve{a}(\boldsymbol{\sigma}) = \frac{(a(\boldsymbol{\sigma}) + b(\boldsymbol{\sigma}))^k - (a(\boldsymbol{\sigma}) - b(\boldsymbol{\sigma}))^k}{\sigma_e^k N_e \sum_{i=-\infty}^{\infty} \left(\exp\left(-\frac{i^2\pi^2}{\breve{c}^2(\boldsymbol{\sigma})}\right) - \exp\left(-\frac{(2i+1)^2\pi^2}{4\breve{c}^2(\boldsymbol{\sigma})}\right)\right)} \tag{4.75}$$

and

$$\breve{d}(\boldsymbol{\sigma}) = \frac{(a(\boldsymbol{\sigma}) - b(\boldsymbol{\sigma}))^k \sum_{i=-\infty}^{\infty} \exp\left(-\frac{i^2\pi^2}{\breve{c}^2(\boldsymbol{\sigma})}\right) - (a(\boldsymbol{\sigma}) + b(\boldsymbol{\sigma}))^k \sum_{i=-\infty}^{\infty} \exp\left(-\frac{(2i+1)^2\pi^2}{4\breve{c}^2(\boldsymbol{\sigma})}\right)}{\sigma_e^k N_e \sum_{i=-\infty}^{\infty} \left(\exp\left(-\frac{i^2\pi^2}{\breve{c}^2(\boldsymbol{\sigma})}\right) - \exp\left(-\frac{(2i+1)^2\pi^2}{4\breve{c}^2(\boldsymbol{\sigma})}\right)\right)}. \tag{4.76}$$

Proof. The two equations, Eq. (4.68) and Eq. (4.69) have three unknowns. We can use these two equations to give $\breve{a}(\boldsymbol{\sigma})$ and $\breve{d}(\boldsymbol{\sigma})$ in terms of $\breve{c}(\boldsymbol{\sigma})$. Subtracting Eq. (4.69) from Eq. (4.68) we get a equation in $\breve{a}(\boldsymbol{\sigma})$ and $\breve{c}(\boldsymbol{\sigma})$:

$$\breve{a}(\boldsymbol{\sigma}) \left(\sum_{i=-\infty}^{\infty} \left(\exp\left(-\frac{i^2\pi^2}{\breve{c}^2(\boldsymbol{\sigma})}\right) - \exp\left(-\frac{(2i+1)^2\pi^2}{4\breve{c}^2(\boldsymbol{\sigma})}\right)\right)\right) = \frac{(a(\boldsymbol{\sigma}) + b(\boldsymbol{\sigma}))^k - (a(\boldsymbol{\sigma}) - b(\boldsymbol{\sigma}))^k}{\sigma_e^k N_e}. \tag{4.77}$$

Rearranging Eq. (4.77) gives us Eq. (4.75) for computing $\breve{a}(\boldsymbol{\sigma})$. Inserting the value of $\breve{a}(\boldsymbol{\sigma})$ into Eq. (4.68) and further simplification gives us Eq. (4.76) for computing $\breve{d}(\boldsymbol{\sigma})$. □

The next corollary gives us an equation for computing $\breve{c}(\boldsymbol{\sigma})$ in Eq. (4.67).

Corollary 4.3.5. *The parameter* $\breve{c}(\boldsymbol{\sigma})$ *in the definition of the approximation function* $g_{\mathbb{R}}$ *in Eq.* (4.67) *is given as*

$$\breve{c}(\boldsymbol{\sigma}) = \left(\frac{\left((a(\boldsymbol{\sigma}) + b(\boldsymbol{\sigma}))^k - (a(\boldsymbol{\sigma}) - b(\boldsymbol{\sigma}))^k\right) \sum_{i=-\infty}^{\infty} \left(\breve{c}^2(\boldsymbol{\sigma}) - 2\pi^2 i^2\right) \exp\left(-\frac{i^2\pi^2}{\breve{c}^2(\boldsymbol{\sigma})}\right)}{2kb(\boldsymbol{\sigma})(a(\boldsymbol{\sigma}) + b(\boldsymbol{\sigma}))^{k-1} \sum_{i=-\infty}^{\infty} \left(\exp\left(-\frac{i^2\pi^2}{\breve{c}^2(\boldsymbol{\sigma})}\right) - \exp\left(-\frac{(2i+1)^2\pi^2}{4\breve{c}^2(\boldsymbol{\sigma})}\right)\right)} \right)^{\frac{1}{4}} \tag{4.78}$$

Proof. Inserting $\breve{a}(\boldsymbol{\sigma})$ from Eq. (4.75) into Eq. (4.70) gives

$$\frac{\left((a(\boldsymbol{\sigma}) + b(\boldsymbol{\sigma}))^k - (a(\boldsymbol{\sigma}) - b(\boldsymbol{\sigma}))^k\right) \sum_{i=-\infty}^{\infty} \left(\frac{2i^2\pi^2}{\breve{c}^2(\boldsymbol{\sigma})} - 1\right) \exp\left(-\frac{i^2\pi^2}{\breve{c}^2(\boldsymbol{\sigma})}\right)}{\breve{c}^2(\boldsymbol{\sigma}) \sum_{i=-\infty}^{\infty} \left(\exp\left(-\frac{i^2\pi^2}{\breve{c}^2(\boldsymbol{\sigma})}\right) - \exp\left(-\frac{(2i+1)^2\pi^2}{4\breve{c}^2(\boldsymbol{\sigma})}\right)\right)} + 2kb(\boldsymbol{\sigma})(a(\boldsymbol{\sigma}) + b(\boldsymbol{\sigma}))^{k-1} = 0 \tag{4.79}$$

Rearranging and further simplification gives Eq. (4.78), a fixed point equation in $\breve{c}(\boldsymbol{\sigma})$. □

Figure 4.9 illustrates the solutions for the Eq. (4.78) for possible values of $b(\boldsymbol{\sigma}) \leq a(\boldsymbol{\sigma}) < \sigma_{max}$, with $a(\boldsymbol{\sigma}) + b(\boldsymbol{\sigma}) < \sigma_{max}$ and $\sigma_{max} = 180$, for two different values of k. Since, with increasing index i of the sum the elements are getting exponentially smaller we only take the first 1000 terms on both sides of zero in the summation in Eq. (4.78) without introducing large error.

In this subsection, we gave an approximation of the damage function $\hat{d}$ on the real line $\mathbb{R}$ for the case $a(\boldsymbol{\sigma}) \geq b(\boldsymbol{\sigma})$. In the next section we give an approximation of the damage function on the real line $\mathbb{R}$ when $a(\boldsymbol{\sigma}) < b(\boldsymbol{\sigma})$.

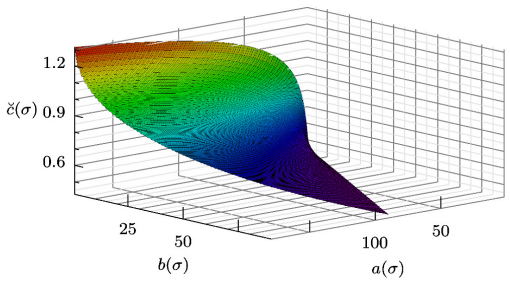

(a) $k = 5$.

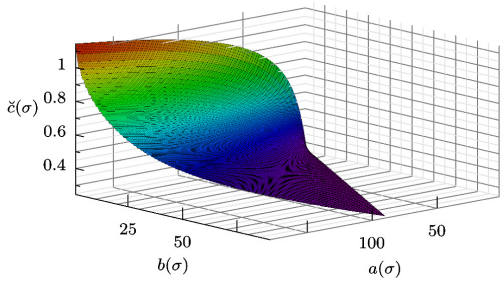

(b) $k = 15$.

Figure 4.9.: Fixed points of equation (4.78) for $k = 5$ and $k = 15$ for $b(\boldsymbol{\sigma}) \leq a(\boldsymbol{\sigma}) < \sigma_{max}$ with $a(\boldsymbol{\sigma}) + b(\boldsymbol{\sigma}) < \sigma_{max}$ and $\sigma_{max} = 180$.

4.3.2. Case $a(\boldsymbol{\sigma}) < b(\boldsymbol{\sigma})$

Without loss of generality we assume that $\breve{b}_1(\boldsymbol{\sigma}) \in [0, \pi)$ and $\breve{b}_2(\boldsymbol{\sigma}) \in [0, \pi)$ because the damage function $\hat{d}$ from Eq. (4.4) is periodic with period π. The other peaks occur at $\breve{b}_1(\boldsymbol{\sigma}) + i\pi$ and $\breve{b}_2(\boldsymbol{\sigma}) + i\pi$, $i \in \mathbb{Z}$. We proceed in the same way as in Subsection 4.3.1 for the case of $a(\boldsymbol{\sigma}) \geq b(\boldsymbol{\sigma})$ to approximate damage function $\hat{d}$ from Eq. (4.4) on $\mathbb{R}$. The approximation of the damage function on $\mathbb{R}$ is then given as

$$\tilde{g}_{\mathbb{R}}(\boldsymbol{\sigma}, \alpha) = \begin{cases} \sum_{i=-\infty}^{\infty} f_{\breve{a}_1(\boldsymbol{\sigma}),\breve{b}_1(\boldsymbol{\sigma}),\breve{c}_1(\boldsymbol{\sigma})}(\alpha - i\pi) + \breve{d}_1(\boldsymbol{\sigma}), & \text{if } \alpha \in \hat{I}_1 \\ \sum_{i=-\infty}^{\infty} f_{\breve{a}_2(\boldsymbol{\sigma}),\breve{b}_2(\boldsymbol{\sigma}),\breve{c}_2(\boldsymbol{\sigma})}(\alpha - i\pi) + \breve{d}_2(\boldsymbol{\sigma}), & \text{if } \alpha \in \hat{I}_2 \end{cases}, \tag{4.80}$$

where $\breve{b}_1(\boldsymbol{\sigma}) = \alpha^-_{max,1}(\boldsymbol{\sigma})$, $\breve{b}_2(\boldsymbol{\sigma}) = \alpha^-_{max,2}(\boldsymbol{\sigma})$ and $f_{\breve{a}_1(\boldsymbol{\sigma}),\breve{b}_1(\boldsymbol{\sigma}),\breve{c}_1(\boldsymbol{\sigma})}$ and $f_{\breve{a}_2(\boldsymbol{\sigma}),\breve{b}_2(\boldsymbol{\sigma}),\breve{c}_2(\boldsymbol{\sigma})}$ are Gaussian functions from Definition 4.0.1 and the interval $\hat{I}_1$ is the extension of the interval I_1 in Eq (2.33) from Theorem 2.3.12 as

$$\hat{I}_1 = \bigcup_{i=-\infty}^{\infty} \left[\alpha^-_{max,1}(\boldsymbol{\sigma}) - \frac{\pi}{4} - \frac{\theta}{2} + i\pi,\, \alpha^-_{max,1}(\boldsymbol{\sigma}) + \frac{\pi}{4} + \frac{\theta}{2} + i\pi \right), \tag{4.81}$$

and the interval $\hat{I}_2$ is the extension of the interval I_2 in Eq (2.34) from Theorem 2.3.12 as

$$\hat{I}_2 = \bigcup_{i=-\infty}^{\infty} \left[\breve{b}_2(\boldsymbol{\sigma}) - \frac{\pi}{4} + \frac{\theta}{2} + i\pi,\, \breve{b}_2(\boldsymbol{\sigma}) + \frac{\pi}{4} - \frac{\theta}{2} + i\pi \right). \tag{4.82}$$

The approximation function $\tilde{g}_{\mathbb{R}}$ in Eq. (4.80) has 8 parameters $\breve{a}_1$, $\breve{a}_2$, $\breve{b}_1$, $\breve{b}_2$, $\breve{c}_1$, $\breve{c}_2$, $\breve{d}_1$ and $\breve{d}_2$ which have to be determined before we can use the approximation in any optimization problem.

The peaks with larger damage value occurs at $\alpha = \breve{b}_1(\boldsymbol{\sigma}) + i\pi$ where $i \in \mathbb{Z}$. In Theorem 2.3.13 we showed that the maximum value of the absolute scalar stress on the interval $\hat{I}_1$ is given by $s^-_{max,1} = a(\boldsymbol{\sigma}) + b(\boldsymbol{\sigma})$. The approximation in Eq. (4.80) when evaluated at $\alpha = \breve{b}_1(\boldsymbol{\sigma}) + i\pi$ for any $i \in \mathbb{Z}$ should give the peak with larger damage value. Evaluating the damage function $\hat{d}$ and its

approximation $\tilde{g}_{\mathbb{R}}$ at $\alpha = \breve{b}_1(\boldsymbol{\sigma}) + i\pi$ yields

$$\breve{a}_1(\boldsymbol{\sigma}) \sum_{i=-\infty}^{\infty} \exp\left(-\frac{i^2\pi^2}{\breve{c}_1^2(\boldsymbol{\sigma})}\right) + \breve{d}_1(\boldsymbol{\sigma}) = \frac{(a(\boldsymbol{\sigma}) + b(\boldsymbol{\sigma}))^k}{\sigma_e^k N_e}. \tag{4.83}$$

Again, from Theorem 2.3.13, the maximum value of the absolute scalar stress on the interval $\hat{I}_2$ is $s^-_{max,2} = b(\boldsymbol{\sigma}) - a(\boldsymbol{\sigma})$ at $\alpha = \breve{b}_2(\boldsymbol{\sigma}) = \alpha^-_{max,2}$. Evaluating the damage function $\hat{d}$ and its approximation $\tilde{g}_{\mathbb{R}}$ at $\alpha = \breve{b}_2(\boldsymbol{\sigma}) + i\pi$ yields

$$\breve{a}_2(\boldsymbol{\sigma}) \sum_{i=-\infty}^{\infty} \exp\left(-\frac{i^2\pi^2}{\breve{c}_2^2(\boldsymbol{\sigma})}\right) + \breve{d}_2(\boldsymbol{\sigma}) = \frac{(b(\boldsymbol{\sigma}) - a(\boldsymbol{\sigma}))^k}{\sigma_e^k N_e}. \tag{4.84}$$

Finally, from Lemma 2.3.11 and Theorem 2.3.13, the scalar stress at the limits of the the subintervals in $\hat{I}_1$ and $\hat{I}_2$ is zero. Evaluating the damage function $\hat{d}$ and its approximation $\tilde{g}_{\mathbb{R}}$ at the end points results in the following equations:

$$\breve{a}_1(\boldsymbol{\sigma}) \sum_{i=-\infty}^{\infty} \exp\left(-\frac{(\frac{\pi}{4} + \frac{\theta}{2} + i\pi)^2}{\breve{c}_1^2(\boldsymbol{\sigma})}\right) + \breve{d}_1(\boldsymbol{\sigma}) = 0, \tag{4.85}$$

$$\breve{a}_2(\boldsymbol{\sigma}) \sum_{i=-\infty}^{\infty} \exp\left(-\frac{(\frac{\pi}{4} - \frac{\theta}{2} - i\pi)^2}{\breve{c}_2^2(\boldsymbol{\sigma})}\right) + \breve{d}_2(\boldsymbol{\sigma}) = 0. \tag{4.86}$$

The conditions in Eq. (4.85) and Eq. (4.86) implies that the approximation function $\tilde{g}_{\mathbb{R}}$ is continuous and differentiable at the points of minima.

In the next Theorem we establish the quality of the approximation function $\tilde{g}_{\mathbb{R}}$ from Eq. (4.80).

Theorem 4.3.6. *Given stress $\boldsymbol{\sigma} = (\sigma_{xx}, \sigma_{yy}, \sigma_{xy})^T$ with $a(\boldsymbol{\sigma}) < b(\boldsymbol{\sigma})$. If the approximation function $\tilde{g}_{\mathbb{R}}$ as defined in Eq. (4.80) where $\breve{b}_1(\boldsymbol{\sigma}) = \alpha^-_{max,1}$, $\breve{b}_2(\boldsymbol{\sigma}) = \alpha^-_{max,2}$ and parameters $\breve{a}_1(\boldsymbol{\sigma})$, $\breve{a}_2(\boldsymbol{\sigma})$, $\breve{d}_1(\boldsymbol{\sigma})$ and $\breve{d}_2(\boldsymbol{\sigma})$ satisfy Eq. (4.83), Eq. (4.84), Eq. (4.85) and Eq. (4.86), and additionally if $\breve{c}_1(\boldsymbol{\sigma})$ and $\breve{c}_2(\boldsymbol{\sigma})$ satisfy equations*

$$\frac{2b(\boldsymbol{\sigma})k(a(\boldsymbol{\sigma}) + b(\boldsymbol{\sigma}))^{k-1}}{\sigma_e^k N_e} + \frac{\breve{a}_1(\boldsymbol{\sigma})}{\breve{c}_1^2(\boldsymbol{\sigma})} \sum_{i=-\infty}^{\infty} \left(\frac{2i^2\pi^2}{\breve{c}_1^2(\boldsymbol{\sigma})} - 1\right) \exp\left(-\frac{i^2\pi^2}{\breve{c}_1^2(\boldsymbol{\sigma})}\right) = 0 \tag{4.87}$$

and

$$\frac{2b(\boldsymbol{\sigma})k(b(\boldsymbol{\sigma}) - a(\boldsymbol{\sigma}))^{k-1}}{\sigma_e^k N_e} + \frac{\breve{a}_2(\boldsymbol{\sigma})}{\breve{c}_2^2(\boldsymbol{\sigma})} \sum_{i=-\infty}^{\infty} \left(\frac{2i^2\pi^2}{\breve{c}_2^2(\boldsymbol{\sigma})} - 1\right) \exp\left(-\frac{i^2\pi^2}{\breve{c}_2^2(\boldsymbol{\sigma})}\right) = 0, \tag{4.88}$$

then for $\alpha \in \hat{I}_1 \cup \hat{I}_2$, the function $\tilde{g}_{\mathbb{R}}(\boldsymbol{\sigma}, \alpha)$ is an approximation to the damage function $\hat{d}(\boldsymbol{\sigma}, \alpha)$ from Eq. (4.4) of order 4, i.e.,

$$\left|\hat{d}(\boldsymbol{\sigma}, \alpha) - \tilde{g}_{\mathbb{R}}(\boldsymbol{\sigma}, \alpha)\right| = \begin{cases} O((\alpha - \breve{b}_1(\boldsymbol{\sigma}))^4), & \text{if } \alpha \in \hat{I}_1 \\ O((\alpha - \breve{b}_2(\boldsymbol{\sigma}))^4), & \text{if } \alpha \in \hat{I}_2 \end{cases}$$

Proof. Similar to proof of Theorem 4.2.1, we use the Taylor's expansion of both the damage function $\hat{d}$ and its approximation $\tilde{g}_{\mathbb{R}}$ around the points of maxima. The condition (4.87) is chosen such that the term $(\alpha - \breve{b}_1(\boldsymbol{\sigma}))^2$ in the difference of the Taylor series expansion, around $\breve{b}_1(\boldsymbol{\sigma})$,

of $\hat{d}$ and $\tilde{g}_{\mathbb{R}}$ when $\alpha \in \hat{I}_1$ can be neglected. Similarly, the condition (4.88) is chosen such that the term $(\alpha - \breve{b}_2(\boldsymbol{\sigma}))^2$ in the difference of the Taylor series expansion, around $\breve{b}_2(\boldsymbol{\sigma})$, of $\hat{d}(\boldsymbol{\sigma}, \alpha)$ and $\tilde{g}(\boldsymbol{\sigma}, \alpha)_{\mathbb{R}}$ when $\alpha \in I_2$ can be neglected. The Taylor series expansion of $\tilde{g}_{\mathbb{R}}(\boldsymbol{\sigma}, \alpha)$ at $\breve{b}_1(\boldsymbol{\sigma})$ is derived in Corollary A.1.4 and given in Eq. (A.18) as

$$\tilde{g}_{\mathbb{R}}(\boldsymbol{\sigma}, \alpha) = \breve{a}_1(\boldsymbol{\sigma}) \sum_{i=-\infty}^{\infty} \exp\left(-\frac{i^2\pi^2}{\breve{c}_1^2(\boldsymbol{\sigma})}\right) + \frac{\breve{a}_1(\boldsymbol{\sigma})}{\breve{c}_1^2(\boldsymbol{\sigma})} \sum_{i=-\infty}^{\infty} \left(\frac{2i^2\pi^2}{\breve{c}_1^2(\boldsymbol{\sigma})} - 1\right) \exp\left(-\frac{i^2\pi^2}{\breve{c}_1^2(\boldsymbol{\sigma})}\right) (\alpha - \breve{b}_1(\boldsymbol{\sigma}))^2 + \breve{d}_1(\boldsymbol{\sigma}) + O((\alpha - \breve{b}_1(\boldsymbol{\sigma}))^4), \alpha \in \hat{I}_1, \quad (4.89)$$

and the Taylor series expansion of $\tilde{g}_{\mathbb{R}}(\boldsymbol{\sigma}, \alpha)$ at $\breve{b}_2(\boldsymbol{\sigma})$ is derived in Corollary A.1.5 and given in Eq. (A.19) as

$$\tilde{g}_{\mathbb{R}}(\boldsymbol{\sigma}, \alpha) = \breve{a}_2(\boldsymbol{\sigma}) \sum_{i=-\infty}^{\infty} \exp\left(-\frac{i^2\pi^2}{\breve{c}_2^2(\boldsymbol{\sigma})}\right) + \frac{\breve{a}_2(\boldsymbol{\sigma})}{\breve{c}_2^2(\boldsymbol{\sigma})} \sum_{i=-\infty}^{\infty} \left(\frac{2i^2\pi^2}{\breve{c}_2^2(\boldsymbol{\sigma})} - 1\right) \exp\left(-\frac{i^2\pi^2}{\breve{c}_2^2(\boldsymbol{\sigma})}\right) (\alpha - \breve{b}_2(\boldsymbol{\sigma}))^2 + \breve{d}_2(\boldsymbol{\sigma}) + O((\alpha - \breve{b}_2(\boldsymbol{\sigma}))^4), \alpha \in \hat{I}_2. \quad (4.90)$$

The Taylor series of damage function $\hat{d}$ at $\breve{b}_1(\boldsymbol{\sigma})$ for the case $a(\boldsymbol{\sigma}) < b(\boldsymbol{\sigma})$ is given in Eq. (4.47) as

$$\hat{d}(\boldsymbol{\sigma}, \alpha) = \frac{(a(\boldsymbol{\sigma}) + b(\boldsymbol{\sigma}))^k}{\sigma_e^k N_e} - \frac{2kb(\boldsymbol{\sigma})(a(\boldsymbol{\sigma}) + b(\boldsymbol{\sigma}))^{k-1}}{\sigma_e^k N_e} (\alpha - \breve{b}_1(\boldsymbol{\sigma}))^2 + O((\alpha - \breve{b}_1(\boldsymbol{\sigma}))^4), \forall \alpha \in I_1 \quad (4.91)$$

and the Taylor series of damage function $\hat{d}$ at $\breve{b}_2(\boldsymbol{\sigma})$ for the case $a(\boldsymbol{\sigma}) < b(\boldsymbol{\sigma})$ is given in Eq. (4.49) as

$$\hat{d}(\boldsymbol{\sigma}, \alpha) = \frac{(b(\boldsymbol{\sigma}) - a(\boldsymbol{\sigma}))^k}{\sigma_e^k N_e} - \frac{2kb(\boldsymbol{\sigma})(b(\boldsymbol{\sigma}) - a(\boldsymbol{\sigma}))^{k-1}}{\sigma_e^k N_e} (\alpha - \breve{b}_2(\boldsymbol{\sigma}))^2 + O(\alpha - \breve{b}_2(\boldsymbol{\sigma}))^4, \forall \alpha \in I_2 \quad (4.92)$$

Next, we subtract approximation function $\tilde{g}_{\mathbb{R}}$ from damage $\hat{d}$ for the two intervals. We then choose the multipliers in front of the terms $(\alpha - \breve{b}_1(\boldsymbol{\sigma}))^2$ and $(\alpha - \breve{b}_2(\boldsymbol{\sigma}))^2$ such that these terms vanish leading us to the conditions Eq. (4.87) and Eq. (4.88). □

For simplicity reasons, let us rename the following series:

$$\mathcal{T}_1 := \sum_{i=-\infty}^{\infty} \exp\left(-\frac{i^2\pi^2}{\breve{c}_1^2(\boldsymbol{\sigma})}\right) \qquad \mathcal{T}_2 := \sum_{i=-\infty}^{\infty} \exp\left(-\frac{i^2\pi^2}{\breve{c}_2^2(\boldsymbol{\sigma})}\right) \quad (4.93)$$

$$\mathcal{T}_3 := \sum_{i=-\infty}^{\infty} \exp\left(-\frac{(\frac{\pi}{4} + \frac{\theta}{2} + i\pi)^2}{\breve{c}_1^2(\boldsymbol{\sigma})}\right), \qquad \mathcal{T}_4 := \sum_{i=-\infty}^{\infty} \exp\left(-\frac{(\frac{\pi}{4} - \frac{\theta}{2} - i\pi)^2}{\breve{c}_2^2(\boldsymbol{\sigma})}\right). \quad (4.94)$$

To be able to satisfy conditions in Eq. (4.85) and Eq. (4.86) the series $\mathcal{T}_3$ and $\mathcal{T}_4$ should all be finite. We have already proven the absolute convergence of $\mathcal{T}_1$ and $\mathcal{T}_2$ in Lemma 4.3.3. It remains to investigate that $\mathcal{T}_3$ and $\mathcal{T}_4$ are also finite.

Lemma 4.3.7. *$\mathcal{T}_3$ and $\mathcal{T}_4$ are absolutely convergent.*

Proof. We consider two series with elements given as $c_i = \exp\left(-\frac{(24i+1)\pi^2 + (16i+4)\theta\pi + 4\theta^2}{16\breve{c}_1^2(\boldsymbol{\sigma})}\right)$ and $d_i = \exp\left(-\frac{-(40i+31)\pi^2 + (16i+4)\theta\pi + 4\theta^2}{16\breve{c}_1^2(\boldsymbol{\sigma})}\right)$. The series $\sum_{i=0}^{\infty} c_i$ is a geometric series where the first

element of the series is $\exp\left(-\frac{\pi^2+4\theta\pi+4\theta^2}{16\breve{c}_1^2(\boldsymbol{\sigma})}\right)$ and the common ratio is $\exp\left(-\frac{24\pi^2+16\theta\pi}{16\breve{c}_1^2(\boldsymbol{\sigma})}\right) < 1$. Hence, using the series sum formula for infinite geometric series we get

$$\sum_{i=0}^{\infty} c_i = \frac{\exp\left(-\frac{\pi^2+4\theta\pi+4\theta^2}{16\breve{c}_1^2(\boldsymbol{\sigma})}\right)}{1-\exp\left(-\frac{24\pi^2+16\theta\pi}{16\breve{c}_1^2(\boldsymbol{\sigma})}\right)}$$

Similarly, the series $\sum_{i=-\infty}^{-1} d_i$ is a geometric series where the first element of the series is $\exp\left(-\frac{9\pi^2-12\theta\pi+4\theta^2}{16\breve{c}_1^2(\boldsymbol{\sigma})}\right)$ and the common ratio is $\exp\left(-\frac{40\pi^2-16\theta\pi}{16\breve{c}_1^2(\boldsymbol{\sigma})}\right) < 1$. Hence, using the series sum formula for infinite geometric series we get

$$\sum_{i=-\infty}^{-1} d_i = \frac{\exp\left(-\frac{9\pi^2-12\theta\pi+4\theta^2}{16\breve{c}_1^2(\boldsymbol{\sigma})}\right)}{1-\exp\left(-\frac{40\pi^2-16\theta\pi}{16\breve{c}_1^2(\boldsymbol{\sigma})}\right)}$$

We can rewrite the series $\mathcal{T}_3$ as

$$\mathcal{T}_3 =: \sum_{i=-\infty}^{\infty} a_i = \sum_{i=0}^{\infty} a_i + \sum_{i=-\infty}^{-1} a_i$$

where $a_i = \exp\left(-\frac{(\frac{\pi}{4}+\frac{\theta}{2}+i\pi)^2}{\breve{c}_1^2(\boldsymbol{\sigma})}\right)$, $i \in \mathbb{Z}$. We see that $((24i+1)\pi^2+(16i+4)\theta\pi+4\theta^2) \leq (\pi+2\theta+4i\pi)^2$ for $i \in \mathbb{N}_0$ which implies $a_i \leq c_i$ for $i \in \mathbb{N}_0$ and similarly, $a_i \leq d_i$ for $i = -1, -2, -3, \ldots$. Hence, $\sum_{i=0}^{\infty} a_i$ and $\sum_{i=-\infty}^{-1} a_i$ is absolutely convergent according to the Comparison Test of First Kind. The sum of two converging sequence is converging so $\mathcal{T}_3$ also converges absolutely.

Similarly, $\mathcal{T}_4$ also converges with $c_i = \exp\left(-\frac{(40i-31)\pi^2+(16i-4)\theta\pi+4\theta^2}{16\breve{c}_1^2(\boldsymbol{\sigma})}\right)$ for $i = 1, 2, 3, \ldots$ and $d_i = \exp\left(-\frac{-(24i-1)\pi^2+(16i-4)\theta\pi+4\theta^2}{16\breve{c}_1^2(\boldsymbol{\sigma})}\right)$ for $i = 0, -1, -2, \ldots$. □

In the next lemma we give the equations to compute the parameters $\breve{a}_1(\boldsymbol{\sigma})$ and $\breve{d}_1(\boldsymbol{\sigma})$ in the definition of the approximation function $\tilde{g}_{\mathbb{R}}$ from Eq. (4.80).

Lemma 4.3.8. *The parameters $\breve{a}_1(\boldsymbol{\sigma})$ and $\breve{d}_1(\boldsymbol{\sigma})$ in the definition of the approximation function $\tilde{g}_{\mathbb{R}}$ from Eq.* (4.80) *are given as*

$$\breve{a}_1(\boldsymbol{\sigma}) = \frac{(a(\boldsymbol{\sigma})+b(\boldsymbol{\sigma}))^k}{\sigma_e^k N_e(\mathcal{T}_1-\mathcal{T}_3)} \tag{4.95}$$

and

$$\breve{d}_1(\boldsymbol{\sigma}) = \frac{(a(\boldsymbol{\sigma})+b(\boldsymbol{\sigma}))^k}{\sigma_e^k N_e} - \breve{a}_1(\boldsymbol{\sigma})\mathcal{T}_1 \tag{4.96}$$

where $\mathcal{T}_1$ and $\mathcal{T}_3$ are from Eq. (4.93) *and Eq.* (4.94)*, respectively.*

Proof. The two equations, Eq. (4.83) and Eq. (4.85) have three unknowns. Subtracting Eq. (4.85) from Eq. (4.83) we get an equation in $\breve{a}_1(\boldsymbol{\sigma})$ and $\breve{c}_1(\boldsymbol{\sigma})$:

$$\breve{a}_1(\boldsymbol{\sigma})\left(\sum_{i=-\infty}^{\infty}\exp\left(-\frac{i^2\pi^2}{\breve{c}_1^2(\boldsymbol{\sigma})}\right) - \sum_{i=-\infty}^{\infty}\exp\left(-\frac{(\frac{\pi}{4}+\frac{\theta}{2}+i\pi)^2}{\breve{c}_1^2(\boldsymbol{\sigma})}\right)\right) = \frac{(a(\boldsymbol{\sigma})+b(\boldsymbol{\sigma}))^k}{\sigma_e^k N_e}$$

$$\Rightarrow \breve{a}_1(\boldsymbol{\sigma})\left(\mathcal{T}_1-\mathcal{T}_3\right) = \frac{(a(\boldsymbol{\sigma})+b(\boldsymbol{\sigma}))^k}{\sigma_e^k N_e}. \tag{4.97}$$

Rearranging Eq. (4.97) gives us Eq. (4.95) for computing $\breve{a}_1(\boldsymbol{\sigma})$. We get Eq. (4.96) from Eq. (4.83). □

Next, we give the equations to compute the parameters $\breve{a}_2(\boldsymbol{\sigma})$ and $\breve{d}_2(\boldsymbol{\sigma})$ in the definition of the approximation function $\tilde{g}_{\mathbb{R}}$ from Eq. (4.80).

Lemma 4.3.9. *The parameters $\breve{a}_2(\boldsymbol{\sigma})$ and $\breve{d}_2(\boldsymbol{\sigma})$ in the definition of the approximation function $\tilde{g}_{\mathbb{R}}$ from Eq. (4.80) are given as*

$$\breve{a}_2(\boldsymbol{\sigma}) = \frac{(b(\boldsymbol{\sigma}) - a(\boldsymbol{\sigma}))^k}{\sigma_e^k N_e(\mathcal{T}_2 - \mathcal{T}_4)} \tag{4.98}$$

and

$$\breve{d}_2(\boldsymbol{\sigma}) = \frac{(b(\boldsymbol{\sigma}) - a(\boldsymbol{\sigma}))^k}{\sigma_e^k N_e} - \breve{a}_2(\boldsymbol{\sigma})\mathcal{T}_2 \tag{4.99}$$

where $\mathcal{T}_2$ and $\mathcal{T}_4$ are from Eq. (4.93) and Eq. (4.94), respectively.

Proof. The two equations, Eq. (4.84) and Eq. (4.86) have three unknowns. Subtracting Eq. (4.86) from Eq. (4.84) we get an equation in $\breve{a}_2(\boldsymbol{\sigma})$ and $\breve{c}_2(\boldsymbol{\sigma})$:

$$\begin{aligned}\breve{a}_2(\boldsymbol{\sigma}) \left(\sum_{i=-\infty}^{\infty} \exp\left(-\frac{i^2\pi^2}{\breve{c}_2^2(\boldsymbol{\sigma})}\right) - \sum_{i=-\infty}^{\infty} \exp\left(-\frac{(\frac{\pi}{4} - \frac{\theta}{2} - i\pi)^2}{\breve{c}_2^2(\boldsymbol{\sigma})}\right)\right) &= \frac{(b(\boldsymbol{\sigma}) - a(\boldsymbol{\sigma}))^k}{\sigma_e^k N_e} \\ \Rightarrow \breve{a}_2(\boldsymbol{\sigma})\left(\mathcal{T}_2 - \mathcal{T}_4\right) &= \frac{(b(\boldsymbol{\sigma}) - a(\boldsymbol{\sigma}))^k}{\sigma_e^k N_e}. \end{aligned} \tag{4.100}$$

Rearranging Eq. (4.100) gives us Eq. (4.98) for computing $\breve{a}_1(\boldsymbol{\sigma})$. We get Eq. (4.99) from Eq. (4.84). □

The next corollary gives us equation for computing $\breve{c}_1(\boldsymbol{\sigma})$ and $\breve{c}_2(\boldsymbol{\sigma})$.

Corollary 4.3.10. *The parameters $\breve{c}_1(\boldsymbol{\sigma})$ and $\breve{c}_2(\boldsymbol{\sigma})$ in the definition of the approximation function $\tilde{g}_{\mathbb{R}}$ in Eq. (4.80) are given as*

$$\breve{c}_1(\boldsymbol{\sigma}) = \left(\frac{(a(\boldsymbol{\sigma}) + b(\boldsymbol{\sigma})) \sum_{i=-\infty}^{\infty} \left(\breve{c}_1^2(\boldsymbol{\sigma}) - 2i^2\pi^2\right) \exp\left(-\frac{i^2\pi^2}{\breve{c}_1^2(\boldsymbol{\sigma})}\right)}{2kb(\boldsymbol{\sigma})(\mathcal{T}_1 - \mathcal{T}_3)} \right)^{\frac{1}{4}} \tag{4.101}$$

and

$$\breve{c}_2(\boldsymbol{\sigma}) = \left(\frac{(b(\boldsymbol{\sigma}) - a(\boldsymbol{\sigma})) \sum_{i=-\infty}^{\infty} \left(\breve{c}_2^2(\boldsymbol{\sigma}) - 2i^2\pi^2\right) \exp\left(-\frac{i^2\pi^2}{\breve{c}_2^2(\boldsymbol{\sigma})}\right)}{2kb(\boldsymbol{\sigma})(\mathcal{T}_2 - \mathcal{T}_4)} \right)^{\frac{1}{4}} \tag{4.102}$$

where $\mathcal{T}_1$, $\mathcal{T}_2$, $\mathcal{T}_3$ and $\mathcal{T}_4$ are from Eq. (4.93) and Eq. (4.94).

Proof. Inserting $\breve{a}_1(\boldsymbol{\sigma})$ from Eq. (4.95) into Eq. (4.87) gives

$$\frac{2b(\boldsymbol{\sigma})k(a(\boldsymbol{\sigma}) + b(\boldsymbol{\sigma}))^{k-1}}{\sigma_e^k N_e} + \frac{(a(\boldsymbol{\sigma}) + b(\boldsymbol{\sigma}))^k}{\sigma_e^k N_e(\mathcal{T}_1 - \mathcal{T}_3)\breve{c}_1^2(\boldsymbol{\sigma})} \sum_{i=-\infty}^{\infty} \left(\frac{2i^2\pi^2}{\breve{c}_1^2(\boldsymbol{\sigma})} - 1\right) \exp\left(-\frac{i^2\pi^2}{\breve{c}_1^2(\boldsymbol{\sigma})}\right) = 0$$

$$\Rightarrow 2b(\boldsymbol{\sigma})k + \frac{a(\boldsymbol{\sigma}) + b(\boldsymbol{\sigma})}{(\mathcal{T}_1 - \mathcal{T}_3)\breve{c}_1^2(\boldsymbol{\sigma})} \sum_{i=-\infty}^{\infty} \left(\frac{2i^2\pi^2}{\breve{c}_1^2(\boldsymbol{\sigma})} - 1 \right) \exp\left(-\frac{i^2\pi^2}{\breve{c}_1^2(\boldsymbol{\sigma})} \right) = 0 \quad (4.103)$$

Rearranging and further simplification gives Eq. (4.101), a fixed point equation in $\breve{c}_1(\boldsymbol{\sigma})$.

Similarly, inserting $\breve{a}_2(\boldsymbol{\sigma})$ from Eq. (4.98) into Eq. (4.88) gives

$$\frac{2b(\boldsymbol{\sigma})k(b(\boldsymbol{\sigma}) - a(\boldsymbol{\sigma}))^{k-1}}{\sigma_e^k N_e} + \frac{(b(\boldsymbol{\sigma}) - a(\boldsymbol{\sigma}))^k}{\sigma_e^k N_e(\mathcal{T}_2 - \mathcal{T}_4)\breve{c}_2^2(\boldsymbol{\sigma})} \sum_{i=-\infty}^{\infty} \left(\frac{2i^2\pi^2}{\breve{c}_2^2(\boldsymbol{\sigma})} - 1 \right) \exp\left(-\frac{i^2\pi^2}{\breve{c}_2^2(\boldsymbol{\sigma})} \right) = 0$$

$$\Rightarrow 2b(\boldsymbol{\sigma})k + \frac{b(\boldsymbol{\sigma}) - a(\boldsymbol{\sigma})}{(\mathcal{T}_2 - \mathcal{T}_4)\breve{c}_2^2(\boldsymbol{\sigma})} \sum_{i=-\infty}^{\infty} \left(\frac{2i^2\pi^2}{\breve{c}_2^2(\boldsymbol{\sigma})} - 1 \right) \exp\left(-\frac{i^2\pi^2}{\breve{c}_2^2(\boldsymbol{\sigma})} \right) = 0 \quad (4.104)$$

Rearranging and further simplification gives Eq. (4.102), a fixed point equation in $\breve{c}_2(\boldsymbol{\sigma})$. □

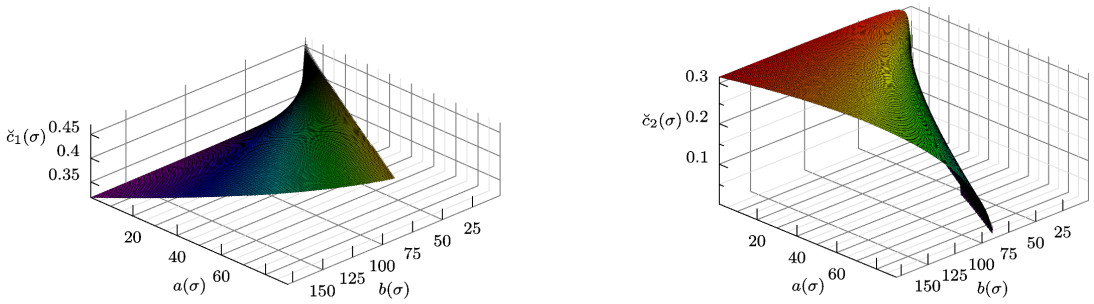

(a) Fixed points for $\breve{c}_1(\boldsymbol{\sigma})$.

(b) Fixed points for $\breve{c}_2(\boldsymbol{\sigma})$.

Figure 4.10.: Fixed points of Eq. (4.101) and Eq. (4.102) for $k = 5$, $a(\boldsymbol{\sigma}) < b(\boldsymbol{\sigma}) < \sigma_{max}$ with $a(\boldsymbol{\sigma}) + b(\boldsymbol{\sigma}) < \sigma_{max}$ and $\sigma_{max} = 180$.

Figure 4.10 illustrates the solutions for the Eq. (4.101) and Eq. (4.102) for possible values of $a(\boldsymbol{\sigma}) < b(\boldsymbol{\sigma}) < \sigma_{max}$, with $a(\boldsymbol{\sigma}) + b(\boldsymbol{\sigma}) < \sigma_{max}$ and $\sigma_{max} = 180$, for two different values of k. Since, with increasing index i of the sum, the summands are getting exponentially smaller we only take the first 1000 terms on both sides of zero in the summation in Eq. (4.101) and Eq. (4.102) without introducing large error.

This subsection gave an approximation to the damage function for $\alpha \in \mathbb{R}$ in one slope case with $a(\boldsymbol{\sigma}) < b(\boldsymbol{\sigma})$. We derived the parameters for the approximation function $\tilde{g}_{\mathbb{R}}$ and discussed their properties. In the next section we give an approximation to the damage function on the interval $[0, \pi)$.

4.4. Approximation of the damage on the interval $[0, \pi)$

When we have more than one block load in the load time series it is not necessary that the damage from these block loads is centered at the same point. Therefore, it is important that we can approximate the damage function from each block load on any interval of period π. In this section, we give approximation of damage function $\hat{d}$ on the interval $[0, \pi)$. The damage from the

block load could be shifted more towards either half of the interval $[0, \pi)$ as shown in Figure 4.11 for the case $a(\boldsymbol{\sigma}) \geq b(\boldsymbol{\sigma})$ and Figure 4.12 for the case $a(\boldsymbol{\sigma}) < b(\boldsymbol{\sigma})$.

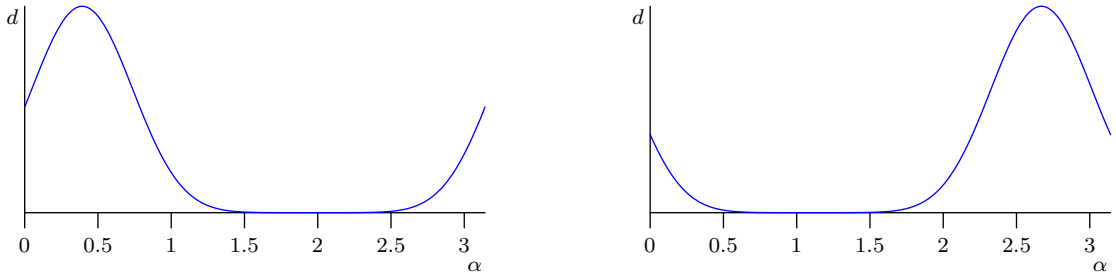

(a) Damage shifted towards left. (b) Damage shifted towards right.

Figure 4.11.: Possible shift of damage for $a(\boldsymbol{\sigma}) \geq b(\boldsymbol{\sigma})$.

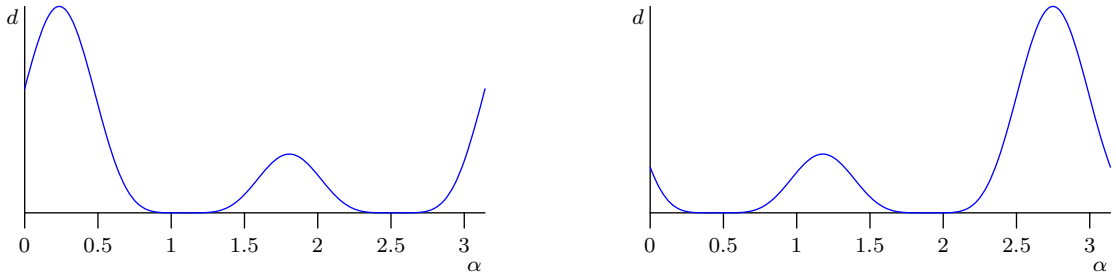

(a) Damage shifted towards left. (b) Damage shifted towards right.

Figure 4.12.: Possible shift of damage for $a(\boldsymbol{\sigma}) < b(\boldsymbol{\sigma})$.

From Figure 4.12 we see that by adding one Gaussian function on each side of the Gaussian function with centre in the interval $[0, \pi)$ we can approximate the damage function $\hat{d}$. It would mean in this case that the summation index i in Eq. (4.67) and Eq. (4.80) is restricted to -1, 0 and 1 in place of $-\infty$ to ∞.

4.4.1. Case $a(\boldsymbol{\sigma}) \geq b(\boldsymbol{\sigma})$

We give an approximation of the damage function $\hat{d}$ in Eq. (4.4) on the interval $[0, \pi)$ by restricting the summation index in Eq. (4.67) to -1, 0 and 1 as

$$g_{[0,\pi)} : \mathbb{R}^3 \times [0, \pi) \to \mathbb{R}, (\boldsymbol{\sigma}, \alpha) \mapsto \sum_{i=-1}^{1} f_{\breve{a}(\boldsymbol{\sigma}),\breve{b}(\boldsymbol{\sigma}),\breve{c}(\boldsymbol{\sigma})}(\alpha - i\pi) + \breve{d}(\boldsymbol{\sigma}), \alpha \in [0, \pi) \tag{4.105}$$

where $f_{\breve{a}(\boldsymbol{\sigma}),\breve{b}(\boldsymbol{\sigma}),\breve{c}(\boldsymbol{\sigma})}$ is a Gaussian function from Eq. (4.1) with parameters $\breve{a}(\boldsymbol{\sigma})$, $\breve{b}(\boldsymbol{\sigma})$ and $\breve{c}(\boldsymbol{\sigma})$. We want the approximation $g_{[0,\pi)}$ to be exact at the maxima. Consequently, the approximation in Eq. (4.105) evaluated at $\alpha = \breve{b}(\boldsymbol{\sigma})$ should yield the maximum damage. We obtain the following

equation when damage function $\hat{d}$ and approximation function $g_{[0,\pi)}$ are evaluated at $\breve{b}(\boldsymbol{\sigma})$

$$\breve{a}(\boldsymbol{\sigma})\sum_{i=-1}^{1}\exp\left(-\frac{i^2\pi^2}{\breve{c}^2(\boldsymbol{\sigma})}\right)+\breve{d}(\boldsymbol{\sigma})=\frac{(a(\boldsymbol{\sigma})+b(\boldsymbol{\sigma}))^k}{\sigma_e^k N_e}, \tag{4.106}$$

Equation (4.106) has to be satisfied for the approximation function $g_{[0,\pi)}$ to be exact at $\breve{b}(\boldsymbol{\sigma})$. Similarly, when we evaluate the approximation function $g_{[0,\pi)}$ at $\alpha=\breve{b}(\boldsymbol{\sigma})+\frac{\pi}{2}$ we should get the minimum damage:

$$\breve{a}(\boldsymbol{\sigma})\sum_{i=-1}^{1}\exp\left(-\frac{(2i+1)^2\pi^2}{4\breve{c}^2(\boldsymbol{\sigma})}\right)+\breve{d}(\boldsymbol{\sigma})=\frac{(a(\boldsymbol{\sigma})-b(\boldsymbol{\sigma}))^k}{\sigma_e^k N_e}. \tag{4.107}$$

Again, Eq. (4.107) has to be satisfied for the approximation $g_{[0,\pi)}$ to be exact at the minima. The condition in Eq. (4.107) implies that the approximation function is continuous and differentiable at the point of minimum in the interval $[0,\pi)$.

In the next theorem, we establish that the function $g_{[0,\pi)}$ is an approximation of damage function $\hat{d}$ of order 4.

Corollary 4.4.1. *Given the stress $\boldsymbol{\sigma}=(\sigma_{xx},\sigma_{yy},\sigma_{xy})^T$ with $a(\boldsymbol{\sigma})\geq b(\boldsymbol{\sigma})$. If $g_{[0,\pi)}$ is as defined in Eq. (4.105) and parameters $\breve{a}(\boldsymbol{\sigma})$, $\breve{b}(\boldsymbol{\sigma})$ and $\breve{d}(\boldsymbol{\sigma})$ satisfying Eq. (4.7), Eq. (4.106) and Eq. (4.107) and additionally, if*

$$\frac{2kb(\boldsymbol{\sigma})(a(\boldsymbol{\sigma})+b(\boldsymbol{\sigma}))^{k-1}}{\sigma_e^k N_e}+\frac{\breve{a}(\boldsymbol{\sigma})}{\breve{c}^2(\boldsymbol{\sigma})}\sum_{i=-1}^{1}\left(\frac{2i^2\pi^2}{\breve{c}^2(\boldsymbol{\sigma})}-1\right)\exp\left(-\frac{i^2\pi^2}{\breve{c}^2(\boldsymbol{\sigma})}\right)=0, \tag{4.108}$$

then $g_{[0,\pi)}$ is an approximation of damage function $\hat{d}$ defined in Eq. (4.4) on $[0,\pi)$ of order 4, i.e.,

$$\left|\hat{d}(\boldsymbol{\sigma},\alpha)-g_{[0,\pi)}(\boldsymbol{\sigma},\alpha)\right|=O((\alpha-\breve{b}(\boldsymbol{\sigma}))^4).$$

Proof. The proof follows directly from Theorem 4.3.1 by restricting the summation index i to -1, 0 and 1. □

In the next lemma we give the equations to compute the parameters $\breve{a}(\boldsymbol{\sigma})$ and $\breve{d}(\boldsymbol{\sigma})$ in the definition of the approximation function $g_{[0,\pi)}$ from Eq. (4.105).

Corollary 4.4.2. *The parameters $\breve{a}(\boldsymbol{\sigma})$ and $\breve{d}(\boldsymbol{\sigma})$ in the definition of the approximation function $g_{[0,\pi)}$ in Eq. (4.67) are given as*

$$\breve{a}(\boldsymbol{\sigma})=\frac{(a(\boldsymbol{\sigma})+b(\boldsymbol{\sigma}))^k-(a(\boldsymbol{\sigma})-b(\boldsymbol{\sigma}))^k}{\sigma_e^k N_e\sum_{i=-1}^{1}\left(\exp\left(-\frac{i^2\pi^2}{\breve{c}^2(\boldsymbol{\sigma})}\right)-\exp\left(-\frac{(2i+1)^2\pi^2}{4\breve{c}^2(\boldsymbol{\sigma})}\right)\right)} \tag{4.109}$$

and

$$\breve{d}(\boldsymbol{\sigma})=\frac{(a(\boldsymbol{\sigma})-b(\boldsymbol{\sigma}))^k\sum_{i=-1}^{1}\exp\left(-\frac{i^2\pi^2}{\breve{c}^2(\boldsymbol{\sigma})}\right)-(a(\boldsymbol{\sigma})+b(\boldsymbol{\sigma}))^k\sum_{i=-1}^{1}\exp\left(-\frac{(2i+1)^2\pi^2}{4\breve{c}^2(\boldsymbol{\sigma})}\right)}{\sigma_e^k N_e\sum_{i=-1}^{1}\left(\exp\left(-\frac{i^2\pi^2}{\breve{c}^2(\boldsymbol{\sigma})}\right)-\exp\left(-\frac{(2i+1)^2\pi^2}{4\breve{c}^2(\boldsymbol{\sigma})}\right)\right)}. \tag{4.110}$$

Proof. The proof follows from Lemma 4.3.4 by restricting the summation index i to -1, 0 and 1. □

The next corollary gives us an equation for computing $\breve{c}(\boldsymbol{\sigma})$ in Eq. (4.105).

Corollary 4.4.3. *The parameter $\breve{c}(\boldsymbol{\sigma})$ in the definition of the approximation function $g_{[0,\pi)}$ in Eq. (4.105) is given as*

$$\breve{c}(\boldsymbol{\sigma}) = \left(\frac{\tilde{t} \sum_{i=-1}^{1} \left(\breve{c}^2(\boldsymbol{\sigma}) - 2\pi^2 i^2 \right) \exp\left(-\frac{i^2\pi^2}{\breve{c}^2(\boldsymbol{\sigma})} \right)}{\sum_{i=-1}^{1} \left(\exp\left(-\frac{i^2\pi^2}{\breve{c}^2(\boldsymbol{\sigma})} \right) - \exp\left(-\frac{(2i+1)^2\pi^2}{4\breve{c}^2(\boldsymbol{\sigma})} \right) \right)} \right)^{\frac{1}{4}}. \tag{4.111}$$

where $\tilde{t} := \frac{(a(\boldsymbol{\sigma})+b(\boldsymbol{\sigma}))^k - (a(\boldsymbol{\sigma})-b(\boldsymbol{\sigma}))^k}{2kb(\boldsymbol{\sigma})(a(\boldsymbol{\sigma})+b(\boldsymbol{\sigma}))^{k-1}}$.

Proof. The proof follows from Corollary 4.3.5 by restricting the summation index i to -1, 0 and 1. □

From the proof of Lemma 4.2.9 we know that $\tilde{t}$ is an element of the interval $\left[\frac{1}{k}, 1\right]$. Equation (4.111) is a fixed point equation for $\breve{c}(\boldsymbol{\sigma})$. We can prove the existence of a fixed point of Eq. (4.111) in terms of the Intermediate Value Theorem.

Theorem 4.4.4 (Intermediate Value Theorem)**.** *Let $f \in C([a,b])$ be a continuous function, and assume that $u \in [\min(f(a), f(b)), \max(f(a), f(b))]$. Then there exists a value $c \in [a,b]$ such that $f(c) = u$.*

Theorem 4.4.5. *Equation (4.111) has a fixed point in $\left[\frac{1}{k}, 2\right]$ for $k \in \mathbb{R}$, $k > 1$ and $\tilde{t} \in \left[\frac{1}{k}, 1\right]$.*

Proof. Let us define the function:

$$\mathcal{T} : \left[\frac{1}{k}, 2\right] \mapsto \mathbb{R}, y \mapsto \left(\frac{\tilde{t} \sum_{i=-1}^{1} \left(y^2 - 2\pi^2 i^2 \right) \exp\left(-\frac{i^2\pi^2}{y^2} \right)}{\sum_{i=-1}^{1} \left(\exp\left(-\frac{i^2\pi^2}{y^2} \right) - \exp\left(-\frac{(2i+1)^2\pi^2}{4y^2} \right) \right)} \right)^{\frac{1}{4}} - y. \tag{4.112}$$

First, we observe that the denominator of $\mathcal{T}(y)$ is never zero which implies that $\mathcal{T}(y)$ has no points of discontinuity. Next, we evaluate the function $\mathcal{T}$ at the interval limits:

$$\begin{aligned} \mathcal{T}(2) &= \left(\frac{\tilde{t} \sum_{i=-1}^{1} \left(2^2 - 2\pi^2 i^2 \right) \exp\left(-\frac{i^2\pi^2}{2^2} \right)}{\sum_{i=-1}^{1} \left(\exp\left(-\frac{i^2\pi^2}{2^2} \right) - \exp\left(-\frac{(2i+1)^2\pi^2}{4\cdot 2^2} \right) \right)} \right)^{\frac{1}{4}} - 2 \\ &= -2 + \left(1.98069\tilde{t} \right)^{\frac{1}{4}} \\ &< 0, \text{ for all } \tilde{t} \in \left[\frac{1}{k}, 1\right]. \end{aligned}$$

$$\mathcal{T}\left(\frac{1}{k}\right) = \left(\frac{\tilde{t} \sum_{i=-1}^{1} \left(\frac{1}{k^2} - 2\pi^2 i^2 \right) \exp\left(-i^2\pi^2 k^2 \right)}{\sum_{i=-1}^{1} \left(\exp\left(-i^2\pi^2 k^2 \right) - \exp\left(-\frac{(2i+1)^2\pi^2 k^2}{4} \right) \right)} \right)^{\frac{1}{4}} - \frac{1}{k}, \tag{4.113}$$

In Corollary A.3.5 in Section A.3.1 we prove that

$$\mathcal{T}\left(\frac{1}{k}\right) > 0.$$

Since $\mathcal{T}\left(\frac{1}{k}\right) > 0$ and $\mathcal{T}(2) < 0$, the Intermediate Value Theorem tells us that $\mathcal{T}(c) = 0$ for some c in the interval $\left[\frac{1}{k}, 2\right]$. This is true for all values of $k > 1$ and $\breve{t}$ in interval $[\frac{1}{k}, 1]$. This gives us

$$\mathcal{T}(c) = 0 \Rightarrow c = \left(\frac{\tilde{t} \sum_{i=-1}^{1} \left(c^2 - 2\pi^2 i^2\right) \exp\left(-\frac{i^2\pi^2}{c^2}\right)}{\sum_{i=-1}^{1} \left(\exp\left(-\frac{i^2\pi^2}{c^2}\right) - \exp\left(-\frac{(2i+1)^2\pi^2}{4c^2}\right)\right)} \right)^{\frac{1}{4}}. \tag{4.114}$$

Equation (4.114) gives us Eq. (4.111) when replacing c by $\breve{c}(\boldsymbol{\sigma})$. Hence, we have proven that Eq. (4.111) has a fixed point in the interval $\left[\frac{1}{k}, 2\right]$. □

Now we can compute $\breve{c}(\boldsymbol{\sigma})$ and other parameters for the approximation. We see from Eq. (4.111) that $\breve{c}(\boldsymbol{\sigma})$ is an increasing function with respect to the $\tilde{t}$. Therefore, the equation for the upper and lower bound for the parameter $\breve{c}(\boldsymbol{\sigma})$ for different values of k can be obtained from Eq. (4.111) when $\tilde{t} = 1$ and $\tilde{t} = \frac{1}{k}$, respectively. In Figure 4.13, we see the lower and upper bound for $\breve{c}(\boldsymbol{\sigma})$ for different values of k. Similar to the observation made in the previous sections we can see that the upper bound is constant with respect to k.

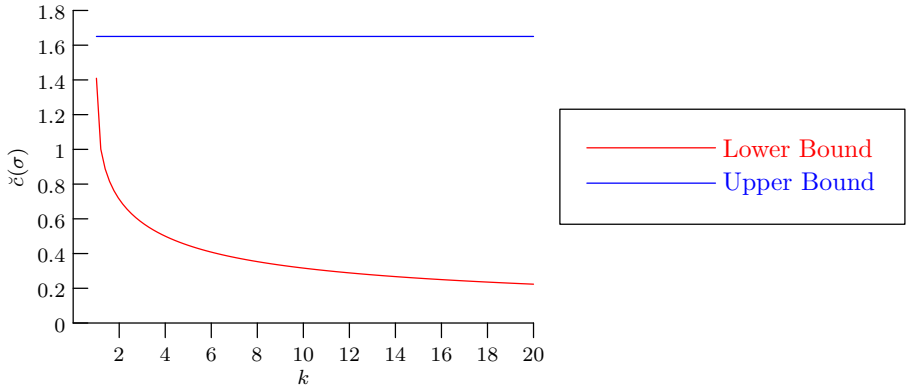

Figure 4.13.: Upper and lower bounds of $\breve{c}(\boldsymbol{\sigma})$ for different values of k.

In this subsection, we have developed approximation to the damage function, for the interval $[0, \pi)$, in the case of one slope, with $a(\boldsymbol{\sigma}) \geq b(\boldsymbol{\sigma})$, by restricting the summation index i of the approximation function developed for the case when $\alpha \in \mathbb{R}$. We derived the parameters $\breve{a}(\boldsymbol{\sigma})$, $\breve{b}(\boldsymbol{\sigma})$, $\breve{c}(\boldsymbol{\sigma})$ and $\breve{d}(\boldsymbol{\sigma})$ for the approximation and discussed properties of the parameters. In the next subsection we give the approximation for the case $a(\boldsymbol{\sigma}) < b(\boldsymbol{\sigma})$.

4.4.2. Case $a(\boldsymbol{\sigma}) < b(\boldsymbol{\sigma})$

For approximating damage on the interval $[0, \pi)$ when stress $\boldsymbol{\sigma}$ is such that $a(\boldsymbol{\sigma}) < b(\boldsymbol{\sigma})$, we take the same approach as in the Section 4.4.1. The summation index i in Eq. (4.80), Eq. (4.83) and

Eq. (4.84) is restricted to -1, 0 and 1. Approximation function $\tilde{g}_{[0,\pi)}$ is defined as

$$\tilde{g}_{[0,\pi)}(\boldsymbol{\sigma},\alpha) = \begin{cases} \sum_{i=-1}^{1} f_{\breve{a}_1(\boldsymbol{\sigma}),\breve{b}_1(\boldsymbol{\sigma}),\breve{c}_1(\boldsymbol{\sigma})}(\alpha - i\pi) + \breve{d}_1(\boldsymbol{\sigma}), & \text{if } \alpha \in \tilde{I}_1 \\ \sum_{i=-1}^{1} f_{\breve{a}_2(\boldsymbol{\sigma}),\breve{b}_2(\boldsymbol{\sigma}),\breve{c}_2(\boldsymbol{\sigma})}(\alpha - i\pi) + \breve{d}_2(\boldsymbol{\sigma}), & \text{if } \alpha \in \tilde{I}_2 \end{cases}, \tag{4.115}$$

where $\breve{b}_1(\boldsymbol{\sigma}) = \alpha^{-}_{max,1}$, $\breve{b}_2(\boldsymbol{\sigma}) = \alpha^{-}_{max,2}$ and $f_{\breve{a}_1(\boldsymbol{\sigma}),\breve{b}_1(\boldsymbol{\sigma}),\breve{c}_1(\boldsymbol{\sigma})}$ and $f_{\breve{a}_2(\boldsymbol{\sigma}),\breve{b}_2(\boldsymbol{\sigma}),\breve{c}_2(\boldsymbol{\sigma})}$ are Gaussian functions from Definition 4.0.1 and the interval $\tilde{I}_1$ is the restriction of the interval $\hat{I}_1$ in Eq. (4.81) as

$$\tilde{I}_1 = \hat{I}_1 \cap [0,\pi), \tag{4.116}$$

and the interval $\tilde{I}_2$ is the restriction of the interval $\hat{I}_2$ in Eq. (4.82) as

$$\tilde{I}_2 = \hat{I}_2 \cap [0,\pi), \tag{4.117}$$

The approximation function $\tilde{g}_{[0,\pi)}$ has 8 parameters $\breve{a}_1$, $\breve{a}_2$, $\breve{b}_1$, $\breve{b}_2$, $\breve{c}_1$, $\breve{c}_2$, $\breve{d}_1$ and $\breve{d}_2$ which have to be determined before we can use the approximation in any optimization problem.

The approximation function $\tilde{g}_{[0,\pi)}$ in Eq. (4.115) when evaluated at $\alpha = \breve{b}_1(\boldsymbol{\sigma})$ should give the peak with maximal damage. Additionally, we have from Theorem 2.3.13 that the maximum magnitude of the scalar stress on the interval $\tilde{I}_1$ is given by $s^{-}_{max,1} = a(\boldsymbol{\sigma}) + b(\boldsymbol{\sigma})$. This gives us the following equation at $\alpha = \breve{b}_1(\boldsymbol{\sigma})$:

$$\breve{a}_1(\boldsymbol{\sigma}) \sum_{i=-1}^{1} \exp\left(-\frac{i^2\pi^2}{\breve{c}_1^2(\boldsymbol{\sigma})}\right) + \breve{d}_1(\boldsymbol{\sigma}) = \frac{(a(\boldsymbol{\sigma}) + b(\boldsymbol{\sigma}))^k}{\sigma_e^k N_e}. \tag{4.118}$$

Similarly, when we evaluate $\tilde{g}_{[0,\pi)}$ at $\alpha = \breve{b}_2(\boldsymbol{\sigma})$ we get the peak with the smaller value of damage

$$\breve{a}_2(\boldsymbol{\sigma}) \sum_{i=-1}^{1} \exp\left(-\frac{i^2\pi^2}{\breve{c}_2^2(\boldsymbol{\sigma})}\right) + \breve{d}_2(\boldsymbol{\sigma}) = \frac{(b(\boldsymbol{\sigma}) - a(\boldsymbol{\sigma}))^k}{\sigma_e^k N_e}. \tag{4.119}$$

At the limits of the interval $\tilde{I}_1$ and $\tilde{I}_2$ the damage is zero. Evaluating function $\tilde{g}_{[0,\pi)}$ at these limits results in the following equations

$$\breve{a}_1(\boldsymbol{\sigma}) \sum_{i=-1}^{1} \exp\left(-\frac{(\frac{\pi}{4} + \frac{\theta}{2} + i\pi)^2}{\breve{c}_1^2(\boldsymbol{\sigma})}\right) + \breve{d}_1(\boldsymbol{\sigma}) = 0, \tag{4.120}$$

$$\breve{a}_2(\boldsymbol{\sigma}) \sum_{i=-1}^{1} \exp\left(-\frac{(\frac{\pi}{4} - \frac{\theta}{2} - i\pi)^2}{\breve{c}_2^2(\boldsymbol{\sigma})}\right) + \breve{d}_2(\boldsymbol{\sigma}) = 0. \tag{4.121}$$

The conditions in Eq. (4.120) and Eq. (4.121) implies that the approximation function $\tilde{g}_{[0,\pi)}$ is continuous and differentiable at the point of minima.

In the next corollary, we establish the quality of the approximation function $\tilde{g}_{[0,\pi)}$.

Corollary 4.4.6. *Given stress $\boldsymbol{\sigma} = (\sigma_{xx}, \sigma_{yy}, \sigma_{xy})^T$ with $a(\boldsymbol{\sigma}) < b(\boldsymbol{\sigma})$. If the approximation function $\tilde{g}_{[0,\pi)}$ as defined in Eq. (4.115) where $\breve{b}_1(\boldsymbol{\sigma}) = \alpha^{-}_{max,1}(\boldsymbol{\sigma})$, $\breve{b}_2(\boldsymbol{\sigma}) = \alpha^{-}_{max,2}$ and parameters $\breve{a}_1(\boldsymbol{\sigma})$, $\breve{a}_2(\boldsymbol{\sigma})$, $\breve{d}_1(\boldsymbol{\sigma})$ and $\breve{d}_2(\boldsymbol{\sigma})$ satisfy Eq. (4.118), Eq. (4.119), Eq. (4.120) and Eq. (4.121), and*

additionally, if $\breve{c}_1(\boldsymbol{\sigma})$ *and* $\breve{c}_2(\boldsymbol{\sigma})$ *satisfy equations*

$$\frac{2b(\boldsymbol{\sigma})k(a(\boldsymbol{\sigma})+b(\boldsymbol{\sigma}))^{k-1}}{\sigma_e^k N_e}+\frac{\breve{a}_1(\boldsymbol{\sigma})}{\breve{c}_1^2(\boldsymbol{\sigma})}\sum_{i=-1}^{1}\left(\frac{2i^2\pi^2}{\breve{c}_1^2(\boldsymbol{\sigma})}-1\right)\exp\left(-\frac{i^2\pi^2}{\breve{c}_1^2(\boldsymbol{\sigma})}\right)=0 \tag{4.122}$$

and

$$\frac{2b(\boldsymbol{\sigma})k(b(\boldsymbol{\sigma})-a(\boldsymbol{\sigma}))^{k-1}}{\sigma_e^k N_e}+\frac{\breve{a}_2(\boldsymbol{\sigma})}{\breve{c}_2^2(\boldsymbol{\sigma})}\sum_{i=-1}^{1}\left(\frac{2i^2\pi^2}{\breve{c}_2^2(\boldsymbol{\sigma})}-1\right)\exp\left(-\frac{i^2\pi^2}{\breve{c}_2^2(\boldsymbol{\sigma})}\right)=0, \tag{4.123}$$

then for $\alpha\in\tilde{I}_1\cup\tilde{I}_2$*, the function* $\tilde{g}_{[0,\pi)}(\boldsymbol{\sigma},\alpha)$ *is an approximation to the damage function* $\hat{d}(\boldsymbol{\sigma},\alpha)$ *from Eq.* (4.4) *of order 4, i.e.,*

$$\left|\hat{d}(\boldsymbol{\sigma},\alpha)-\tilde{g}_{[0,\pi)}(\boldsymbol{\sigma},\alpha)\right|=\begin{cases}O((\alpha-\breve{b}_1(\boldsymbol{\sigma}))^4), & \text{if } \alpha\in\tilde{I}_1\\ O((\alpha-\breve{b}_2(\boldsymbol{\sigma}))^4), & \text{if } \alpha\in\tilde{I}_2\end{cases}$$

Proof. The proof follows directly from Theorem 4.3.6 by restricting the summation index i to -1, 0 and 1. □

In the next lemma we give the equations to compute the parameters $\breve{a}_1(\boldsymbol{\sigma})$ and $\breve{d}_1(\boldsymbol{\sigma})$ in the definition of the approximation function $\tilde{g}_{[0,\pi)}$ from Eq. (4.115).

Lemma 4.4.7. *The parameters* $\breve{a}_1(\boldsymbol{\sigma})$ *and* $\breve{d}_1(\boldsymbol{\sigma})$ *in the definition of the approximation function* $\tilde{g}_{[0,\pi)}$ *from Eq.* (4.115) *are given as*

$$\breve{a}_1(\boldsymbol{\sigma})=\frac{(a(\boldsymbol{\sigma})+b(\boldsymbol{\sigma}))^k}{\sigma_e^k N_e\left(\sum_{i=-1}^{1}\exp\left(-\frac{i^2\pi^2}{\breve{c}_1^2(\boldsymbol{\sigma})}\right)-\sum_{i=-1}^{1}\exp\left(-\frac{\left(\frac{\pi}{4}+\frac{\theta}{2}+i\pi\right)^2}{\breve{c}_1^2(\boldsymbol{\sigma})}\right)\right)} \tag{4.124}$$

and

$$\breve{d}_1(\boldsymbol{\sigma})=\frac{(a(\boldsymbol{\sigma})+b(\boldsymbol{\sigma}))^k}{\sigma_e^k N_e}-\breve{a}_1(\boldsymbol{\sigma})\sum_{i=-1}^{1}\exp\left(-\frac{i^2\pi^2}{\breve{c}_1^2(\boldsymbol{\sigma})}\right). \tag{4.125}$$

Proof. The two equations, Eq. (4.118) and Eq. (4.120) have three unknowns. Subtracting Eq. (4.120) from Eq. (4.118) we get an equation in $\breve{a}_1(\boldsymbol{\sigma})$ and $\breve{c}_1(\boldsymbol{\sigma})$:

$$\breve{a}_1(\boldsymbol{\sigma})\left(\sum_{i=-1}^{1}\exp\left(-\frac{i^2\pi^2}{\breve{c}_1^2(\boldsymbol{\sigma})}\right)-\sum_{i=-1}^{1}\exp\left(-\frac{(\frac{\pi}{4}+\frac{\theta}{2}+i\pi)^2}{\breve{c}_1^2(\boldsymbol{\sigma})}\right)\right)=\frac{(a(\boldsymbol{\sigma})+b(\boldsymbol{\sigma}))^k}{\sigma_e^k N_e} \tag{4.126}$$

Rearranging Eq. (4.126) gives us Eq. (4.124) for computing $\breve{a}_1(\boldsymbol{\sigma})$. We get Eq. (4.125) from Eq. (4.118). □

Next, we give the equations to compute the parameters $\breve{a}_2(\boldsymbol{\sigma})$ and $\breve{d}_2(\boldsymbol{\sigma})$ in the definition of the approximation function $\tilde{g}_{[0,\pi)}$ from Eq. (4.115).

Lemma 4.4.8. *The parameters* $\breve{a}_2(\boldsymbol{\sigma})$ *and* $\breve{d}_2(\boldsymbol{\sigma})$ *in the definition of the approximation function*

$\tilde{g}_{[0,\pi)}$ *from Eq.* (4.115) *are given as*

$$\breve{a}_2(\boldsymbol{\sigma}) = \frac{(b(\boldsymbol{\sigma}) - a(\boldsymbol{\sigma}))^k}{\sigma_e^k N_e \left(\sum_{i=-1}^{1} \exp\left(-\frac{i^2\pi^2}{\breve{c}_2^2(\boldsymbol{\sigma})} \right) - \sum_{i=-1}^{1} \exp\left(-\frac{\left(\frac{\pi}{4} - \frac{\theta}{2} - i\pi\right)^2}{\breve{c}_2^2(\boldsymbol{\sigma})} \right) \right)} \tag{4.127}$$

and

$$\breve{d}_2(\boldsymbol{\sigma}) = \frac{(b(\boldsymbol{\sigma}) - a(\boldsymbol{\sigma}))^k}{\sigma_e^k N_e} - \breve{a}_2(\boldsymbol{\sigma}) \sum_{i=-1}^{1} \exp\left(-\frac{i^2\pi^2}{\breve{c}_2^2(\boldsymbol{\sigma})} \right). \tag{4.128}$$

Proof. The two equations, Eq. (4.119) and Eq. (4.121) have three unknowns. Subtracting Eq. (4.121) from Eq. (4.119) we get an equation in $\breve{a}_2(\boldsymbol{\sigma})$ and $\breve{c}_2(\boldsymbol{\sigma})$:

$$\breve{a}_2(\boldsymbol{\sigma}) \left(\sum_{i=-1}^{1} \exp\left(-\frac{i^2\pi^2}{\breve{c}_2^2(\boldsymbol{\sigma})} \right) - \sum_{i=-1}^{1} \exp\left(-\frac{(\frac{\pi}{4} - \frac{\theta}{2} - i\pi)^2}{\breve{c}_2^2(\boldsymbol{\sigma})} \right) \right) = \frac{(b(\boldsymbol{\sigma}) - a(\boldsymbol{\sigma}))^k}{\sigma_e^k N_e} \tag{4.129}$$

Rearranging Eq. (4.129) gives us Eq. (4.127) for computing $\breve{a}_1(\boldsymbol{\sigma})$. We get Eq. (4.128) from Eq. (4.119). □

The next corollary gives us equation for computing $\breve{c}_1(\boldsymbol{\sigma})$ and $\breve{c}_2(\boldsymbol{\sigma})$ in the definition of the approximation function $\tilde{g}_{[0,\pi)}$ from Eq. (4.115).

Corollary 4.4.9. *The parameters* $\breve{c}_1(\boldsymbol{\sigma})$ *and* $\breve{c}_2(\boldsymbol{\sigma})$ *in the definition of the approximation function* $\tilde{g}_{[0,\pi)}$ *in Eq.* (4.115) *are given as*

$$\breve{c}_1(\boldsymbol{\sigma}) = \left(\frac{\tilde{t}_1 \sum_{i=-\infty}^{\infty} \left(\breve{c}_1^2(\boldsymbol{\sigma}) - 2i^2\pi^2 \right) \exp\left(-\frac{i^2\pi^2}{\breve{c}_1^2(\boldsymbol{\sigma})} \right)}{\sum_{i=-1}^{1} \exp\left(-\frac{i^2\pi^2}{\breve{c}_2^2(\boldsymbol{\sigma})} \right) - \sum_{i=-1}^{1} \exp\left(-\frac{\left(\frac{\pi}{4} + \frac{\theta}{2} + i\pi\right)^2}{\breve{c}_2^2(\boldsymbol{\sigma})} \right)} \right)^{\frac{1}{4}} \tag{4.130}$$

where $\tilde{t}_1 = \frac{a(\boldsymbol{\sigma}) + b(\boldsymbol{\sigma})}{2kb(\boldsymbol{\sigma})}$ *and*

$$\breve{c}_2(\boldsymbol{\sigma}) = \left(\frac{\tilde{t}_2 \sum_{i=-\infty}^{\infty} \left(\breve{c}_2^2(\boldsymbol{\sigma}) - 2i^2\pi^2 \right) \exp\left(-\frac{i^2\pi^2}{\breve{c}_2^2(\boldsymbol{\sigma})} \right)}{2k \left(\sum_{i=-1}^{1} \exp\left(-\frac{i^2\pi^2}{\breve{c}_2^2(\boldsymbol{\sigma})} \right) - \sum_{i=-1}^{1} \exp\left(-\frac{\left(\frac{\pi}{4} - \frac{\theta}{2} - i\pi\right)^2}{\breve{c}_2^2(\boldsymbol{\sigma})} \right) \right)} \right)^{\frac{1}{4}} \tag{4.131}$$

where $\tilde{t}_2 = \frac{b(\boldsymbol{\sigma}) - a(\boldsymbol{\sigma})}{b(\boldsymbol{\sigma})}$.

Proof. Inserting $\breve{a}_1(\boldsymbol{\sigma})$ from Eq. (4.124) into Eq. (4.122) after rearranging and simplification gives Eq. (4.130), a fixed point equation in $\breve{c}_1(\boldsymbol{\sigma})$.

Similarly, inserting $\breve{a}_2(\boldsymbol{\sigma})$ from Eq. (4.127) into Eq. (4.123) after rearranging and simplification gives Eq. (4.131), a fixed point equation in $\breve{c}_2(\boldsymbol{\sigma})$. □

Since $a(\boldsymbol{\sigma}) < b(\boldsymbol{\sigma})$, the value of $\tilde{t}_1$ lies in the interval $\left[\frac{1}{2k}, \frac{1}{k}\right)$. Equation (4.130) is a fixed point equation for $\breve{c}_1(\boldsymbol{\sigma})$. We can prove the existence of fixed points of Eq. (4.130) in terms of the

Intermediate Value Theorem.

Theorem 4.4.10. *For $k \in \mathbb{R}$, $k > 1$ and $\tilde{t}_1 \in \left[\frac{1}{2k}, \frac{1}{k}\right)$. The Eq. (4.130) has a fixed point in $\left[\frac{1}{2k}, 2\right]$.*

Proof. Let us consider a function

$$\mathcal{T}_1 : \left[\frac{1}{2k}, 2\right] \mapsto \mathbb{R}, y \mapsto \left(\frac{\tilde{t}_1 \sum_{i=-1}^{1} \left(y^2 - 2i^2\pi^2\right) \exp\left(-\frac{i^2\pi^2}{y^2}\right)}{k \sum_{i=-1}^{1} \left(\exp\left(-\frac{i^2\pi^2}{y^2}\right) - \exp\left(-\frac{\left(\frac{\pi}{4}+\frac{\theta}{2}+i\pi\right)^2}{y^2}\right)\right)} \right)^{\frac{1}{4}} - y. \tag{4.132}$$

First, we observe that the denominator of $\mathcal{T}_1(y)$ is never zero which implies that $\mathcal{T}_1(y)$ has no points of discontinuity. Next, we evaluate the function $\mathcal{T}_1$ at the interval limits:

$$\mathcal{T}_1(2) = \left(\frac{\tilde{t}_1 \sum_{i=-1}^{1} \left(2^2 - 2i^2\pi^2\right) \exp\left(-\frac{i^2\pi^2}{2^2}\right)}{\sum_{i=-1}^{1} \left(\exp\left(-\frac{i^2\pi^2}{2^2}\right) - \exp\left(-\frac{\left(\frac{\pi}{4}+\frac{\theta}{2}+i\pi\right)^2}{2^2}\right)\right)} \right)^{\frac{1}{4}} - 2 \tag{4.133}$$

In Section A.3.2, we prove that $\mathcal{T}_1(2) < 0$ for all $k > 1$ and $\tilde{t}_1 \in \left[\frac{1}{2k}, \frac{1}{k}\right)$. Now we evaluate

$$\mathcal{T}_1\left(\frac{1}{2k}\right) = \left(\frac{\tilde{t}_1 \sum_{i=-1}^{1} \left(1 - 8k^2i^2\pi^2\right) \exp\left(-2^2k^2i^2\pi^2\right)}{4k^2 \sum_{i=-1}^{1} \left(\exp\left(-2^2k^2i^2\pi^2\right) - \exp\left(-2^2k^2\left(\frac{\pi}{4}+\frac{\theta}{2}+i\pi\right)^2\right)\right)} \right)^{\frac{1}{4}} - \frac{1}{2k} \tag{4.134}$$

In Corollary A.3.6, we show that $\mathcal{T}_1\left(\frac{1}{2k}\right) > 0$ for all $k > 1$ and $\tilde{t}_1 \in \left[\frac{1}{2k}, \frac{1}{k}\right)$. Since $\mathcal{T}_1\left(\frac{1}{2k}\right) > 0$ and $\mathcal{T}_1(2) < 0$, the Intermediate Value Theorem tells us that $\mathcal{T}(c) = 0$ for some c in the interval $\left[\frac{1}{2k}, 2\right]$. This is true for all values of $k > 1$ and $\tilde{t}_1 \in \left[\frac{1}{2k}, \frac{1}{k}\right)$. This gives us

$$\mathcal{T}_1(c) = 0 \Rightarrow c = \left(\frac{\tilde{t}_1 \sum_{i=-1}^{1} \left(c^2 - 2i^2\pi^2\right) \exp\left(-\frac{i^2\pi^2}{c^2}\right)}{k \sum_{i=-1}^{1} \left(\exp\left(-\frac{i^2\pi^2}{c^2}\right) - \exp\left(-\frac{\left(\frac{\pi}{4}+\frac{\theta}{2}+i\pi\right)^2}{c^2}\right)\right)} \right)^{\frac{1}{4}}. \tag{4.135}$$

Equation (4.135) gives us Eq. (4.130) when replacing c by $\breve{c}_1(\boldsymbol{\sigma})$. Hence, we have proven that Eq. (4.122) has a fixed point in the interval $\left[\frac{1}{2k}, 2\right]$. □

Now we can compute $\breve{c}_1(\boldsymbol{\sigma})$ and parameters $\breve{a}_1(\boldsymbol{\sigma})$ and $\breve{d}_1(\boldsymbol{\sigma})$ for the approximation. The parameter is increasing with respect to the $\tilde{t}_1$. Therefore, the the upper and lower bound for the parameter $\breve{c}_1(\boldsymbol{\sigma})$ for different values of k can be obtained from Eq. (4.130) when $\tilde{t}_1 = \frac{1}{k}$ and $\tilde{t}_1 = \frac{1}{2k}$ respectively. In Figure 4.14 we see the lower and upper bound for $\breve{c}_1(\boldsymbol{\sigma})$ for different values of k.

Equation (4.123) is a fixed point equation for the parameter $\breve{c}_2(\boldsymbol{\sigma})$. We can prove the existence of fixed points using Intermediate Value Theorem similar to the proof for $\breve{c}_1(\boldsymbol{\sigma})$. Now we can compute the parameter $\breve{c}_2(\boldsymbol{\sigma})$, $\breve{a}_2(\boldsymbol{\sigma})$ and $\breve{d}_1(\boldsymbol{\sigma})$ for the approximation function $\tilde{g}_{[0,\pi)}$. Again, the parameter $\breve{c}_2(\boldsymbol{\sigma})$ is increasing with respect to the $\tilde{t}_2$. Therefore, the equation for the upper bound for the parameter $\breve{c}_2(\boldsymbol{\sigma})$ for different values of k can be obtained from Eq. (4.131) when $\tilde{t}_2 = 0.5$.

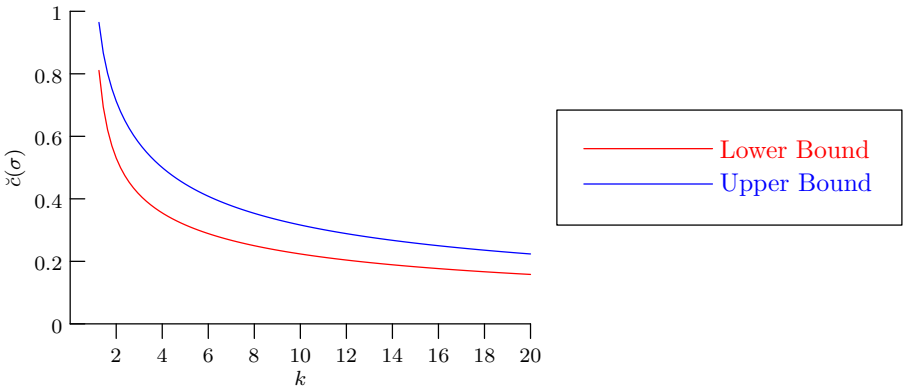

Figure 4.14.: Upper and lower bounds of $\check{c}_1(\boldsymbol{\sigma})$ for different values of k.

The lower bound is given by the requirement that $\check{c}_2(\boldsymbol{\sigma}) > 0$. In Figure 4.15 we see the lower and upper bound for the parameter $\check{c}_2(\boldsymbol{\sigma})$ for different values of k.

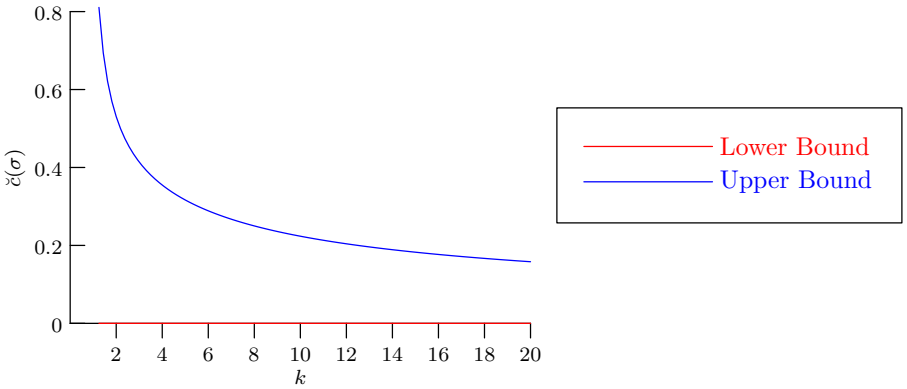

Figure 4.15.: Upper and lower bounds of $\check{c}_2(\boldsymbol{\sigma})$ for different values of k.

4.4.3. Simplification of model for the case $a(\boldsymbol{\sigma}) < b(\boldsymbol{\sigma})$

In Section 4.4.2, we gave an approximation function for damage when a load time series with one block load was applied on the component under testing for the case $a(\boldsymbol{\sigma}) < b(\boldsymbol{\sigma})$. For the approximation function $\tilde{g}_{[0,\pi)}$ we have to keep track of intervals $\tilde{I}_1$ and $\tilde{I}_2$ where the two peaks are centered. When there are more than one block in the load time series the tracking of different intervals becomes more complicated. As the number of blocks increase the number of overlap between intervals from different blocks also increases. This increases the complexity during the optimization. In this section, we simplify the approximation function $\tilde{g}_{[0,\pi)}$ such that the need for tracking of the intervals $\tilde{I}_1$ and $\tilde{I}_2$ for each block is not required.

Even after the simplification of the model there is no change in how fast the damage should fall towards its minimum value, therefore, we keep $\check{c}_1(\boldsymbol{\sigma})$ and $\check{c}_2(\boldsymbol{\sigma})$ from Section 4.4.2. We redefine our approximation function for the damage $\hat{d}$ in the case $a(\boldsymbol{\sigma}) < b(\boldsymbol{\sigma})$ on the interval $[0, \pi)$ as

below

$$\hat{g}(\boldsymbol{\sigma},\alpha) = \sum_{i=-1}^{1} \left(f_{\breve{a}_1(\boldsymbol{\sigma}),\breve{b}_1(\boldsymbol{\sigma}),\breve{c}_1(\boldsymbol{\sigma})}(\alpha - i\pi) + f_{\breve{a}_2(\boldsymbol{\sigma}),\breve{b}_2(\boldsymbol{\sigma}),\breve{c}_2(\boldsymbol{\sigma})}(\alpha - i\pi) \right) + \breve{d}_1(\boldsymbol{\sigma}) \tag{4.136}$$

The peak with the maximal damage value occurs at $\alpha = \breve{b}_1(\boldsymbol{\sigma})$. Evaluating the approximation function $\hat{g}$ and the damage function $\hat{d}$ at $\breve{b}_1(\boldsymbol{\sigma})$ yields

$$\sum_{i=-1}^{1} \left(\breve{a}_1(\boldsymbol{\sigma}) \exp\left(-\frac{i^2\pi^2}{\breve{c}_1^2(\boldsymbol{\sigma})} \right) + \breve{a}_2(\boldsymbol{\sigma}) \exp\left(-\frac{(2i+1)^2\pi^2}{4\breve{c}_2^2(\boldsymbol{\sigma})} \right) \right) + \breve{d}_1(\boldsymbol{\sigma}) = \frac{(a(\boldsymbol{\sigma}) + b(\boldsymbol{\sigma}))^k}{\sigma_e^k N_e} \tag{4.137}$$

The peak with the smaller damage value is at $\alpha = \breve{b}_2(\boldsymbol{\sigma})$. Again, evaluating the approximation function $\hat{g}$ and the damage function $\hat{d}$ at $\breve{b}_2(\boldsymbol{\sigma})$ yields

$$\sum_{i=-1}^{1} \left(\breve{a}_1(\boldsymbol{\sigma}) \exp\left(-\frac{(2i+1)^2\pi^2}{4\breve{c}_1^2(\boldsymbol{\sigma})} \right) + \breve{a}_2(\boldsymbol{\sigma}) \exp\left(-\frac{i^2\pi^2}{\breve{c}_2^2(\boldsymbol{\sigma})} \right) \right) + \breve{d}_1(\boldsymbol{\sigma}) = \frac{(b(\boldsymbol{\sigma}) - a(\boldsymbol{\sigma}))^k}{\sigma_e^k N_e} \tag{4.138}$$

Finally, the damage function $\hat{d}$ is zero at the end point of interval $\tilde{I}_1$ and $\tilde{I}_2$. So, we want for the consistency that the approximation function $\hat{g}$ should also be zero at the limits of the interval. This gives us an additional equation:

$$\sum_{i=-1}^{1} \left(\breve{a}_1(\boldsymbol{\sigma}) \exp\left(-\frac{(\frac{\pi}{4} + \frac{\theta}{2} + i\pi)^2}{\breve{c}_1^2(\boldsymbol{\sigma})} \right) + \breve{a}_2(\boldsymbol{\sigma}) \exp\left(-\frac{(\frac{\pi}{4} - \frac{\theta}{2} + i\pi)^2}{\breve{c}_2^2(\boldsymbol{\sigma})} \right) \right) + \breve{d}_1(\boldsymbol{\sigma}) = 0 \tag{4.139}$$

So we have three equations for three unknowns. Therefore, we can solve for $\breve{a}_1(\boldsymbol{\sigma})$, $\breve{a}_2(\boldsymbol{\sigma})$ and $\breve{d}_1(\boldsymbol{\sigma})$. In Figure 4.16 we compare the approximations given in this section and Section 4.4.2.

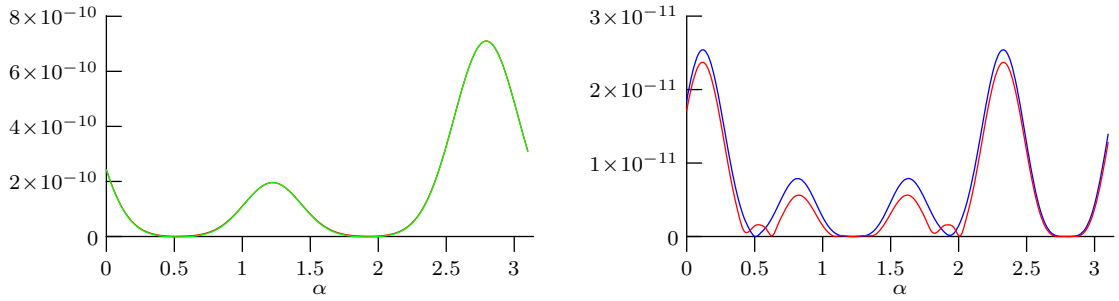

(a) Approximated damage in red and simplified damage in green.

(b) Error $|\hat{d}(\boldsymbol{\sigma},\alpha) - \tilde{g}_{[0,\pi)}(\boldsymbol{\sigma},\alpha)|$ in blue and error $|\hat{d}(\boldsymbol{\sigma},\alpha) - \hat{g}(\boldsymbol{\sigma},\alpha)|$ in red.

Figure 4.16.: Comparison of $\tilde{g}_{[0,\pi)}$ and $\hat{g}$.

We see in Figure 4.16 (b) that error in the case of simplified approximation function $\hat{g}$ as defined in Eq. (4.136) on the interval $[0,\pi)$ has smaller magnitude almost everywhere except in the neighbourhood of the end points of intervals $\tilde{I}_1$ and $\tilde{I}_2$ when compared with the approximation function $\tilde{g}_{[0,\pi)}$ from Eq. (4.115). We use $\hat{g}$ as an approximation for the damage function $\hat{d}$ when $a(\boldsymbol{\sigma}) < b(\boldsymbol{\sigma})$.

4.5. Numerical results and comparisons

In the previous sections we gave approximations for damage function $\hat{d}$ from Eq. (4.4) for three different intervals. The first approximation was for the interval centered around the point of maximum damage extending $\frac{\pi}{2}$ on both sides. The second model was derived for the complete real line $\mathbb{R}$ and finally we gave an approximation for the interval $[0, \pi)$.

In this section, we compare the approximation function and the damage function for the interval $[0, \pi)$ for the two cases $a(\boldsymbol{\sigma}) \geq b(\boldsymbol{\sigma})$ and $a(\boldsymbol{\sigma}) < b(\boldsymbol{\sigma})$ as it is the most interesting interval for us. For comparison of the approximation function and the damage function around point of maximum see Section B.1.

4.5.1. Case $a(\boldsymbol{\sigma}) \geq b(\boldsymbol{\sigma})$

We compare the actual damage $\hat{d}$ and the approximation function $g_{[0,\pi)}$ for three values of the ratio $\frac{b(\boldsymbol{\sigma})}{a(\boldsymbol{\sigma})}$. In Figure 4.17 we see the actual damage function$\hat{d}$, approximation function $g_{[0,\pi)}$ and the error for $\frac{b(\boldsymbol{\sigma})}{a(\boldsymbol{\sigma})} \approx 0$. In Figure 4.18 we see the actual damage function$\hat{d}$, approximation function $g_{[0,\pi)}$ and error for $\frac{b(\boldsymbol{\sigma})}{a(\boldsymbol{\sigma})} = 0.5$. In Figure 4.19 we see the actual damage function$\hat{d}$, approximation function $g_{[0,\pi)}$ and error for $\frac{b(\boldsymbol{\sigma})}{a(\boldsymbol{\sigma})} = 1$.

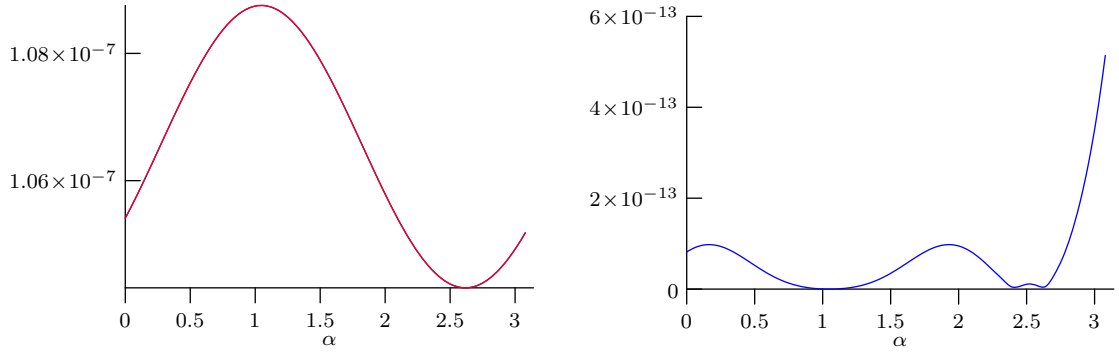

(a) Approximation (red) and actual (blue) damage.

(b) Error $|\hat{d}(\boldsymbol{\sigma}, \alpha) - g_{[0,\pi)}(\boldsymbol{\sigma}, \alpha)|$.

Figure 4.17.: Approximation in $[0, \pi)$ when $\frac{b(\boldsymbol{\sigma})}{a(\boldsymbol{\sigma})} \approx 0$.

We observe in Figure 4.17 (a), Figure 4.18 (a) and Figure 4.19 (a) that the function $g_{[0,\pi)}$ is a good approximation of the actual damage function $\hat{d}$. Furthermore, the error around the point of maximum is small which was a requirement we had put forth on the approximation. In Table 4.1 we see the ratio of maximum damage to the maximum error for different values of the ratio $\frac{b(\boldsymbol{\sigma})}{a(\boldsymbol{\sigma})}$. As can be seen from the Table 4.1 the ratio of maximum damage to the maximum error is always less than 0.02. Therefore, the maximum error is small compared to the maximum damage.

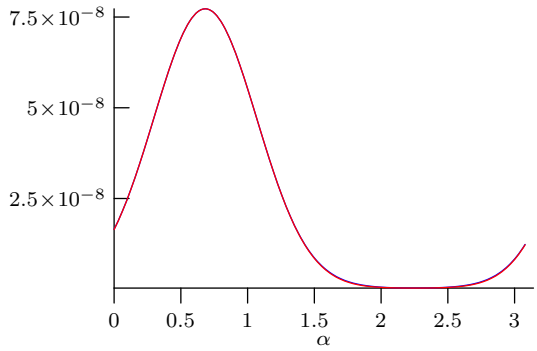

(a) Approximation (red) and actual (blue) damage.

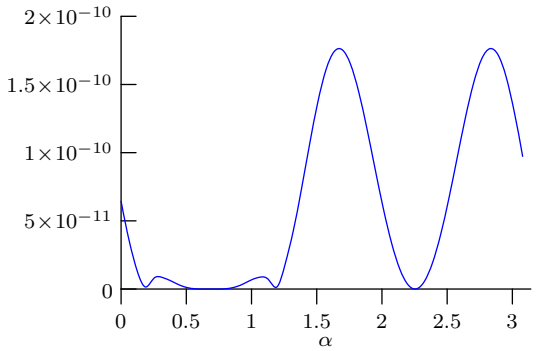

(b) Error $|\hat{d}(\boldsymbol{\sigma}, \alpha) - g_{[0,\pi)}(\boldsymbol{\sigma}, \alpha)|$.

Figure 4.18.: Approximation in $[0, \pi)$ when $\frac{b(\boldsymbol{\sigma})}{a(\boldsymbol{\sigma})} = 0.5$.

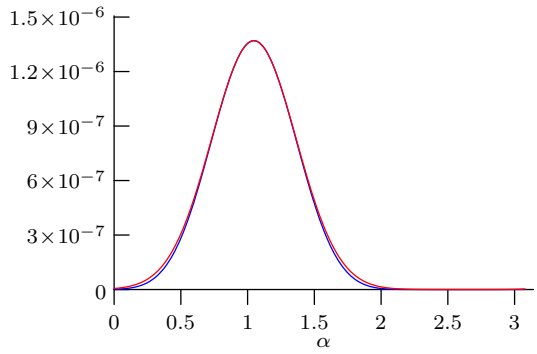

(a) Approximation (red) and actual (blue) damage.

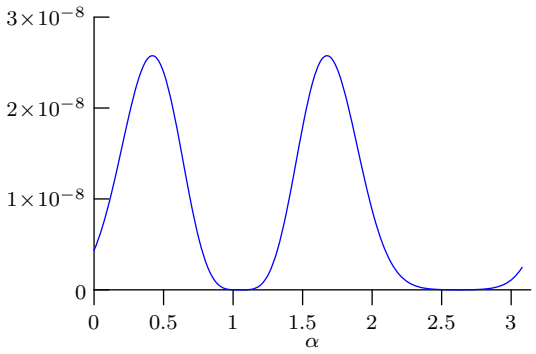

(b) Error $|\hat{d}(\boldsymbol{\sigma}, \alpha) - g_{[0,\pi)}(\boldsymbol{\sigma}, \alpha)|$.

Figure 4.19.: Approximation in $[0, \pi)$ when $\frac{b(\boldsymbol{\sigma})}{a(\boldsymbol{\sigma})} = 1$.

4.5.2. Case $a(\boldsymbol{\sigma}) < b(\boldsymbol{\sigma})$

When $a(\boldsymbol{\sigma}) < b(\boldsymbol{\sigma})$ we observe two peaks. If $a(\boldsymbol{\sigma}) = 0$, then both these peaks are of the same height. We compare actual damage $\hat{d}$ and approximation function $\hat{g}$ from Eq. (4.136) for two values of the ratio $\frac{b(\boldsymbol{\sigma})}{a(\boldsymbol{\sigma})}$. In Figure 4.20, we see the actual damage $\hat{d}$, approximation function $\hat{d}$ and the error function for $\frac{b(\boldsymbol{\sigma})}{a(\boldsymbol{\sigma})} \approx 0$. In Figure 4.21, we see the actual damage $\hat{d}$, approximation function $\hat{d}$ and error function for $\frac{b(\boldsymbol{\sigma})}{a(\boldsymbol{\sigma})} = 0.128$. The smaller the ratio $\frac{b(\boldsymbol{\sigma})}{a(\boldsymbol{\sigma})}$ is, the smaller is the difference between the heights of the two peaks. However, if the ratio is closer to one, then the contribution of the smaller peak becomes negligible in comparison to the higher peak. This can be observed from Figure 4.21(a), where by changing the ratio to 0.128 the peak with the smaller height has less than half the height of the other peak which is higher.

In Table 4.2, we see the ratio of maximum damage to the maximum error for different values of the ratio $\frac{a(\boldsymbol{\sigma})}{b(\boldsymbol{\sigma})}$. As can be seen from the Table 4.2, the ratio of maximum damage to the maximum error is always less than 0.04. Therefore, the maximum error is comparatively small.

Ratio $\frac{b(\boldsymbol{\sigma})}{a(\boldsymbol{\sigma})}$	$\frac{\lvert\hat{d}(\boldsymbol{\sigma},\alpha)-g_{[0,\pi)}(\boldsymbol{\sigma},\alpha)\rvert}{\max_{\alpha\in[0,\pi)}\, g_{[0,\pi)}(\boldsymbol{\sigma},\alpha)}$
0	0.0004
0.1	0.0040
0.2	0.0111
0.3	0.0121
0.4	0.0079
0.5	0.0023
0.6	0.0047
0.7	0.0095
0.8	0.0134
0.9	0.0164
1.0	0.0188

Table 4.1.: The ratio of maximum damage to the maximum error for different values of ratio $\frac{b(\boldsymbol{\sigma})}{a(\boldsymbol{\sigma})}$ in the case of $a(\boldsymbol{\sigma}) \geq b(\boldsymbol{\sigma})$.

Ratio $\frac{a(\boldsymbol{\sigma})}{b(\boldsymbol{\sigma})}$	$\frac{\lvert\hat{d}(\boldsymbol{\sigma},\alpha)-\hat{g}(\boldsymbol{\sigma},\alpha)\rvert}{\max_{\alpha\in[0,\pi)}\, \hat{g}(\boldsymbol{\sigma},\alpha)}$
0	0.0360
0.1	0.0337
0.2	0.0320
0.3	0.0306
0.4	0.0293
0.5	0.0279
0.6	0.0263
0.7	0.0245
0.8	0.0225
0.9	0.0205
1.0	0.0188

Table 4.2.: The ratio of maximum damage to the maximum error for different values of ratio $\frac{a(\boldsymbol{\sigma})}{b(\boldsymbol{\sigma})}$ in the case of $a(\boldsymbol{\sigma}) < b(\boldsymbol{\sigma})$.

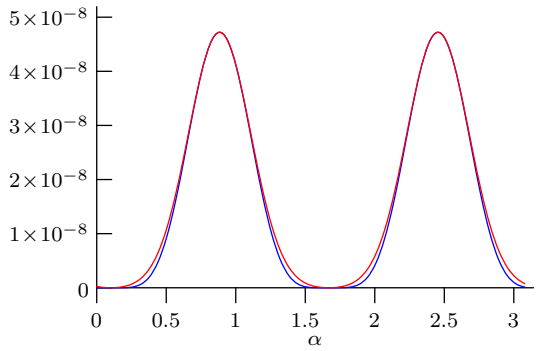

(a) Approximation (red) and actual (blue) damage.

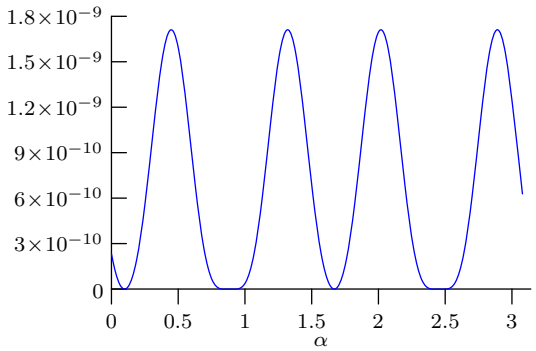

(b) Error $|\hat{d}(\boldsymbol{\sigma}, \alpha) - \hat{g}(\boldsymbol{\sigma}, \alpha)|$.

Figure 4.20.: Approximation around maximum when $\frac{a(\boldsymbol{\sigma})}{b(\boldsymbol{\sigma})} = 0$.

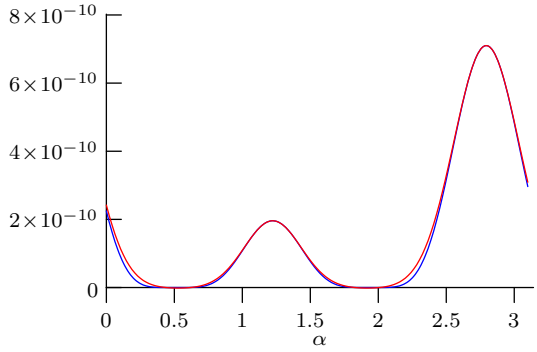

(a) Actual damage in blue and Simplified damage in red.

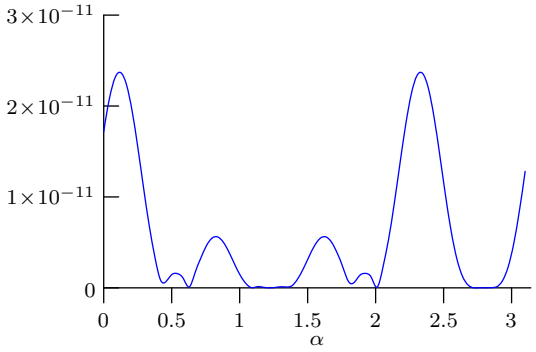

(b) Error $|\hat{d}(\boldsymbol{\sigma}, \alpha) - \hat{g}(\boldsymbol{\sigma}, \alpha)|$

Figure 4.21.: Approximation in $[0, \pi)$ when $\frac{a(\boldsymbol{\sigma})}{b(\boldsymbol{\sigma})} = 0.128$.

We have established an approximation of the damage function $\hat{d}$ that depends only on the plane angle α. The approximation functions in this chapter are for a load time series with one block load. In general if we have more than one block, then for each block load we have corresponding Gaussian functions which approximate the damage. We see in Chapter 6, that computing total damage in case of a load time series with more than one block, we have to add all the Gaussian approximation functions for each block load. In the next chapter we develop a clustering algorithm based on the idea of the sum of Gaussian functions. The clustering algorithm is used to find the maximum damage considering all plane angles α. Using the Gaussian approximation functions developed in this chapter and Clustering algorithm developed in the next chapter we do not need to discretize the interval of plane angle α to find the maximum damage in each iteration of optimization.

5. Clustering of Gaussian functions

In Chapter 4 we developed a model for approximating damage for a given stress $\boldsymbol{\sigma}$ such that the plane angle α is the only independent variable. In Section 2.4.3 of Chapter 2 we studied the case when a load time series with block loads $\mathbf{L}_b$ is acting on the component. We also computed the total damage as the sum of damages from each of the individual block loads in the load time series. For the approximate damage model developed in Chapter 4, the total damage computation is given as the sum of the Gaussian functions which approximate the damage from the individual block loads (Section 6.1). We know that the component fails along the plane with the maximum damage. The goal of the remodeling of damage was to find the plane α where the total damage is maximum. The plane with the maximum damage is also referred to as the critical plane.

In this chapter we introduce the idea of clustering of Gaussian functions. This forms the basis for finding the plane of maximum damage at different points on a component when being acted upon by a load time series with block loads $\mathbf{L}_b$ in Chapter 6.

The sum of Gaussian functions is similar to the Gaussian Mixture Model (GMM). A GMM is a parametric probability density function represented as a weighted sum of Gaussian component densities [31]. GMM is applied in image segmentation, speaker identification and many other fields (for applications of GMM see [15, 32, 33]). In GMM parameters are estimated from the training data. Parameter estimation is not a concern in the case of damage approximation. We have already given derivations and bounds for the parameters of the damage approximation in Chapter 4.

The difference between the Gaussian approximation of damage and GMM is that the Gaussian functions used in GMM are probability density functions which is not the case in the damage approximation. However, the critical planes in the damage approximation corresponds to the modes of the GMM. Therefore, the mode finding algorithms in [7] for GMM or methods for merging the Gaussian mixture components in [16] can be modified to be used for the damage approximation. In Section 5.1 we derive conditions for a single maxima, similar to the ones given for the unimodality by Aprausheva et al. in [3]. In [3] Aprausheva et al. studied the GMM for the case when the variance of all the Gaussian density functions were the same. In this chapter we consider general Gaussian functions with each Gaussian function having a different parameter $\check{c}$.

In Section 5.2 we describe a clustering algorithm to compute the critical plane (the plane with the global maximum) for the sum of Gaussian functions. In general there does not exist any method that can directly find the global maximum even in the one-dimensional case with only two Gaussian functions. Therefore, the clustering algorithm we develop is iterative. In Section 5.3 we give an approximate point of maximum for the sum of Gaussian functions in a cluster obtained by

applying the clustering algorithm developed in Section 5.2. The numerical results are presented in Section 5.4.

5.1. Sum of Gaussian functions and number of maxima

In this section we give sufficient conditions for the sum of two or more Gaussian functions to have only one global maximum. However, it may not always be possible to have one global maximum and therefore, at the end of this section we give bounds on the number of maxima (n_m) a sum of Gaussian functions can have when certain conditions are fulfilled. Using these conditions we develop a clustering algorithm in Section 5.2 that groups together Gaussian functions into clusters with each cluster being a potential local maximum.

Let us denote by $\mathcal{G} : \mathbb{R} \to \mathbb{R}$ the sum of Gaussian functions given as

$$\mathcal{G}(\alpha) = \sum_{i=1}^{n_g} \breve{a}_i \exp\left(-\left(\frac{\alpha - \breve{b}_i}{\breve{c}_i}\right)^2\right) \tag{5.1}$$

where n_g is the number of Gaussian functions. The i^{th} Gaussian function has parameters $\breve{a}_i$, $\breve{b}_i$ and $\breve{c}_i$. Without loss of generality we can assume that $\breve{b}_i \leq \breve{b}_{i+1}$ for all $i < n_g$, otherwise we can renumber the Gaussian functions to satisfy this ordering. We want to find α^* for which the value of the sum $\mathcal{G}$ is maximum. For α^* to be a point of maximum it has to be a root of the following equation

$$\mathcal{G}'(\alpha) = 0. \tag{5.2}$$

Next we prove that all the roots of Eq. (5.2) always lie in-between $\breve{b}_1$ and $\breve{b}_{n_g}$. In other words all the maxima and minima of a sum of Gaussian functions $\mathcal{G}$ always lie in between the point of maximum of the first Gaussian function and the point of maximum of the last Gaussian function present in $\mathcal{G}$.

Theorem 5.1.1. *All roots of Eq.* (5.2) *are in the interval* $\left[\breve{b}_1, \breve{b}_{n_g}\right]$.

Proof. The first derivative of $\mathcal{G}$ is given as

$$\mathcal{G}'(\alpha) = \frac{d}{d\alpha}\left(\sum_{i=1}^{n_g} \breve{a}_i \exp\left(-\left(\frac{\alpha - \breve{b}_i}{\breve{c}_i}\right)^2\right)\right) \tag{5.3a}$$

$$= -2\sum_{i=1}^{n_g} \frac{\alpha - \breve{b}_i}{\breve{c}_i^2} \breve{a}_i \exp\left(-\left(\frac{\alpha - \breve{b}_i}{\breve{c}_i}\right)^2\right). \tag{5.3b}$$

The first derivative is always positive for all $\alpha \leq \breve{b}_1$ and it is always negative for all $\alpha \geq \breve{b}_{n_g}$. Hence, from Intermediate Value Theorem we know that all points which are root of Eq. (5.2) is in the interval $\left[\breve{b}_1, \breve{b}_{n_g}\right]$. □

From Theorem 5.1.1 we know the interval in which all the roots of Eq. (5.2) lie. In the next step we prove that the number of maxima in the sum of Gaussian functions $\mathcal{G}$ is always more than the

number of minima. This is equivalent to proving that the number of times the graph of the first derivative of $\mathcal{G}$ crosses the horizontal axis is odd.

Lemma 5.1.2. *Given $\mathcal{G}$ as defined in Eq. (5.1), the graph of $\mathcal{G}'$ crosses the horizontal axis an odd number of times.*

Proof. From Eq. (5.3b) in the proof of Theorem 5.1.1 we know that the graph of $\mathcal{G}'$ is positive for all $\alpha \leq \breve{b}_1$ and it is negative for all $\alpha \geq \breve{b}_{n_g}$. Let us suppose that $\mathcal{G}'$ crosses the α-axis an even number of times. Then starting from being positive for $\alpha \leq \breve{b}_1$ the changes in sign gives $\mathcal{G}'$ as positive for all $\alpha \geq \breve{b}_{n_g}$. This is a contradiction to the fact that $\mathcal{G}'$ is negative for all $\alpha \geq \breve{b}_{n_g}$. Hence, the graph of $\mathcal{G}'$ crosses the horizontal axis an odd number of times. □

In order to find the points of maximum we need to find the roots of the Eq. (5.2). In the next Theorem we derive a fixed point equation for the roots of the Eq. (5.2).

Theorem 5.1.3. *Equation (5.2) is equivalent to the fixed point equation*

$$\alpha = \varphi(\alpha) \tag{5.4}$$

where

$$\varphi(\alpha) = \left(\sum_{i=1}^{n_g} \frac{\breve{b}_i}{\breve{c}_i^2} \breve{a}_i \exp\left(-\left(\frac{\alpha - \breve{b}_i}{\breve{c}_i} \right)^2 \right) \right) \left(\sum_{j=1}^{n_g} \frac{\breve{a}_j \exp\left(-\left(\frac{\alpha - \breve{b}_j}{\breve{c}_j} \right)^2 \right)}{\breve{c}_j^2} \right)^{-1}. \tag{5.5}$$

Proof. The first derivative of $\mathcal{G}$ is given in Eq. (5.3b). Equating the first derivative of $\mathcal{G}$ to zero gives

$$-2 \sum_{i=1}^{n_g} \frac{\alpha - \breve{b}_i}{\breve{c}_i^2} \breve{a}_i \exp\left(-\left(\frac{\alpha - \breve{b}_i}{\breve{c}_i} \right)^2 \right) = 0.$$

Collecting like terms together and rearranging gives us

$$\Rightarrow \alpha \sum_{j=1}^{n_g} \frac{\breve{a}_j \exp\left(-\left(\frac{\alpha - \breve{b}_j}{\breve{c}_j} \right)^2 \right)}{\breve{c}_j^2} = \sum_{i=1}^{n_g} \frac{\breve{b}_i}{\breve{c}_i^2} \breve{a}_i \exp\left(-\left(\frac{\alpha - \breve{b}_i}{\breve{c}_i} \right)^2 \right).$$

Dividing both sides of the equation by the term after α on the left hand side of the equation leads to $\alpha = \varphi(\alpha)$

$$\Rightarrow \alpha = \left(\sum_{i=1}^{n_g} \frac{\breve{b}_i}{\breve{c}_i^2} \breve{a}_i \exp\left(-\left(\frac{\alpha - \breve{b}_i}{\breve{c}_i} \right)^2 \right) \right) \left(\sum_{j=1}^{n_g} \frac{\breve{a}_j \exp\left(-\left(\frac{\alpha - \breve{b}_j}{\breve{c}_j} \right)^2 \right)}{\breve{c}_j^2} \right)^{-1}. \tag{5.6}$$

□

All the fixed points of Eq. (5.4) are roots of the Eq. (5.2). We can further simplify our fixed point

equation by defining $\Psi_i(\alpha) := \frac{\breve{a}_i}{\breve{c}_i^2} \exp\left(-\left(\frac{\alpha-\breve{b}_i}{\breve{c}_i}\right)^2\right)$ which reduces φ to

$$\varphi(\alpha) = \left(\sum_{i=1}^{n_g} \breve{b}_i \Psi_i(\alpha)\right) \left(\sum_{j=1}^{n_g} \Psi_j(\alpha)\right)^{-1}. \tag{5.7}$$

For φ to have only one fixed point it must be a contraction mapping. For φ to be a contraction mapping the first derivative of φ must be less than one:

$$\varphi'(\alpha) < 1.$$

Theorem 5.1.4. *We have $\varphi'(\alpha) < 1$ if and only if*

$$\sum_{j>i}(p_{ij}(\alpha) - 2)\Psi_i(\alpha)\Psi_j(\alpha) - \sum_{i=1}^{n_g} \Psi_i^2(\alpha) < 0,\ \alpha \in \left[\breve{b}_1, \breve{b}_{n_g}\right] \tag{5.8}$$

where

$$p_{ij}(\alpha) = 2\left(\breve{b}_j - \breve{b}_i\right)\left(\frac{\breve{b}_j - \alpha}{\breve{c}_j^2} + \frac{\alpha - \breve{b}_i}{\breve{c}_i^2}\right). \tag{5.9}$$

Proof. We compute the first derivative of φ as a starting point for the proof. The first derivative of φ can be computed as:

$$\frac{d}{d\alpha}(\varphi(\alpha)) = \frac{d}{d\alpha}\left(\left(\sum_{i=1}^{n_g} \breve{b}_i \Psi_i(\alpha)\right)\left(\sum_{j=1}^{n_g} \Psi_j(\alpha)\right)^{-1}\right)$$

We use the quotient rule of differentiation, $\frac{d}{d\alpha}\left(\frac{g(\alpha)}{h(\alpha)}\right) = \frac{g'(\alpha)h(\alpha) - h'(\alpha)g(\alpha)}{h^2(\alpha)}$, to get

$$\begin{aligned}\frac{d}{d\alpha}(\varphi(\alpha)) = \Bigg(&\sum_{i=1}^{n_g} -\frac{2\breve{b}_i(\alpha - \breve{b}_i)}{\breve{c}_i^2}\Psi_i(\alpha)\sum_{j=1}^{n_g}\Psi_j(\alpha) \\ &+ \sum_{j=1}^{n_g}\frac{2(\alpha - \breve{b}_j)}{\breve{c}_j^2}\Psi_j(\alpha)\sum_{i=1}^{n_g}\breve{b}_i\Psi_i(\alpha)\Bigg)\left(\sum_{j=1}^{n_g}\Psi_j(\alpha)\right)^{-2}\end{aligned} \tag{5.10}$$

For $n_g \geq j > i$ collecting the ij^{th} term from the numerator of the derivative gives us

$$2\left(-\frac{\breve{b}_i(\alpha - \breve{b}_i)}{\breve{c}_i^2} - \frac{\breve{b}_j(\alpha - \breve{b}_j)}{\breve{c}_j^2} + \frac{\breve{b}_i(\alpha - \breve{b}_j)}{\breve{c}_j^2} + \frac{\breve{b}_j(\alpha - \breve{b}_i)}{\breve{c}_i^2}\right)\Psi_i(\alpha)\Psi_j(\alpha). \tag{5.11}$$

In other cases when $j = i$ we get that the ii^{th} terms are all zero. After rearranging and simplification of the terms in Eq. (5.11) we get the ij^{th} term as

$$2\left(\breve{b}_j - \breve{b}_i\right)\left(\frac{\breve{b}_j - \alpha}{\breve{c}_j^2} + \frac{\alpha - \breve{b}_i}{\breve{c}_i^2}\right)\Psi_i(\alpha)\Psi_j(\alpha) = p_{ij}(\alpha)\Psi_i(\alpha)\Psi_j(\alpha). \tag{5.12}$$

Inserting Eq. (5.12) for the numerator of the term in the right hand side of Eq. (5.10) reduces the first derivative to the form

$$\frac{d}{d\alpha}(\varphi(\alpha)) = \left(\sum_{j>i} p_{ij}(\alpha)\Psi_i(\alpha)\Psi_j(\alpha)\right)\left(\sum_{j=1}^{n_g}\Psi_j(\alpha)\right)^{-2} \tag{5.13}$$

For φ to be a contraction mapping the first derivative in Eq. (5.13) has to be less than one on the interval $\left[\breve{b}_1, \breve{b}_{n_g}\right]$. From Eq. (5.13) this leads to the following inequality:

$$\left(\sum_{j>i} p_{ij}(\alpha)\Psi_i(\alpha)\Psi_j(\alpha)\right)\left(\sum_{j=1}^{n_g}\Psi_j(\alpha)\right)^{-2} < 1$$

Multiplying both sides by $\left(\sum_{j=1}^{n_g}\Psi_j(\alpha)\right)^2$ leads to

$$\sum_{j>i} p_{ij}(\alpha)\Psi_i(\alpha)\Psi_j(\alpha) < \left(\sum_{j=1}^{n_g}\Psi_j(\alpha)\right)^2$$

Collecting terms on left hand side gives us the result:

$$\sum_{j>i}(p_{ij}(\alpha)-2)\Psi_i(\alpha)\Psi_j(\alpha) - \sum_{j=1}^{n_g}\Psi_j^2(\alpha) < 0$$

This completes the proof. □

We see later that the value of $p_{ij}(\alpha)$ is very important for the number of maxima in $\mathcal{G}$. In the next Lemma we look at some of the properties of $p_{ij}(\alpha)$. We show that p_{ij} is a linear function in α and further show that it is increasing or decreasing depending on which of the parameters $\breve{c}_i$ or $\breve{c}_j$ is larger.

Lemma 5.1.5. *Following statements are true for $p_{ij}(\alpha)$ with $j > i$*

(i) $p_{ij}(\alpha)$ is a linear function in α,

(ii) when $\breve{c}_i > \breve{c}_j$ then $p_{ij}(\breve{b}_i) > p_{ij}(\breve{b}_j)$ and

(iii) when $\breve{c}_j > \breve{c}_i$ then $p_{ij}(\breve{b}_j) > p_{ij}(\breve{b}_i)$.

(iv) For $\alpha \in \left[\breve{b}_i, \breve{b}_j\right]$ we have

$$p_{ij}(\alpha) \in \left[2\left(\breve{b}_j - \breve{b}_i\right)^2 \min\left(\frac{1}{\breve{c}_i^2}, \frac{1}{\breve{c}_j^2}\right), 2\left(\breve{b}_j - \breve{b}_i\right)^2 \max\left(\frac{1}{\breve{c}_i^2}, \frac{1}{\breve{c}_j^2}\right)\right]$$

Proof. (i) We can rewrite $p_{ij}(\alpha)$ in Eq. (5.9) as below

$$p_{ij}(\alpha) = \frac{2\left(\breve{b}_j - \breve{b}_i\right)}{\breve{c}_i^2 \breve{c}_j^2}\left(\breve{c}_j^2 - \breve{c}_i^2\right)\alpha + \frac{2\left(\breve{b}_j - \breve{b}_i\right)}{\breve{c}_i^2 \breve{c}_j^2}\left(\breve{c}_i^2 \breve{b}_j - \breve{c}_j^2 \breve{b}_i\right). \tag{5.14}$$

We see that Eq. (5.14) is linear in α.

(ii) From Eq. (5.14) we see that when $\breve{c}_i > \breve{c}_j$ the slope $\frac{dp_{ij}(\alpha)}{d\alpha} < 0$ for all α and therefore $p_{ij}(\alpha)$ is a decreasing function. Hence, $p_{ij}(\breve{b}_i) > p_{ij}(\breve{b}_j)$ because $\breve{b}_j > \breve{b}_i$.

(iii) Similarly, when $\breve{c}_j > \breve{c}_i$ then the slope in Eq. (5.14) is positive and therefore $p_{ij}(\alpha)$ is an increasing function. Hence, $p_{ij}(\breve{b}_j) > p_{ij}(\breve{b}_i)$ because $\breve{b}_j > \breve{b}_i$.

(iv) Since $p_{ij}(\alpha)$ is linear in α from (i), inserting the end points of the interval $\left[\breve{b}_i, \breve{b}_j\right]$ in the Eq. (5.9) leads to:

$$p_{ij}\left(\breve{b}_i\right) = \frac{2\left(\breve{b}_j - \breve{b}_i\right)^2}{\breve{c}_j^2} \text{ and } p_{ij}\left(\breve{b}_j\right) = \frac{2\left(\breve{b}_j - \breve{b}_i\right)^2}{\breve{c}_i^2}.$$

Which gives us the interval. □

In the next Corollary we give the first sufficient condition for a single maximum for the sum of Gaussian functions $\mathcal{G}$.

Corollary 5.1.6. *If $p_{ij}(\alpha) \leq 2$ on the interval $\left[\breve{b}_1, \breve{b}_{n_g}\right]$ for all $j > i$ then the sum of Gaussian functions $\mathcal{G}$ as given in Eq. (5.1) has a single maximum.*

Proof. When $p_{ij}(\alpha) \leq 2$ on the interval $\left[\breve{b}_1, \breve{b}_{n_g}\right]$ for all $j > i$ then from Eq. (5.8) in Theorem 5.1.4 we know that the first derivative of φ is less than one which implies that φ is a contraction mapping. From the Contraction mapping theorem we know that φ has a unique fixed point which implies that there is only one root of Eq. (5.2). Therefore, from Lemma 5.1.2 we know that $\mathcal{G}$ has only one maximum. □

When $\breve{c}_i = \breve{c}_j$ then $p_{ij}(\alpha)$ corresponds to the square of *Mahalanobis distance* in the case of GMM. Condition in Corollary 5.1.6 is very restrictive and may not be usually possible to satisfy even if there is a unique fixed point for Eq. (5.4). Additionally, computing $p_{ij}(\alpha)$ for all $n_g \geq j > i$ and $\alpha \in \left[\breve{b}_1, \breve{b}_{n_g}\right]$ is time consuming and not very efficient. In the next results we give conditions for single maximum when $n_g = 2$ for different cases.

Corollary 5.1.7. *For $n_g = 2$ it is sufficient to have $p_{12}(\alpha) \leq 2$ on the interval $\left[\breve{b}_1, \breve{b}_2\right]$ for $\mathcal{G}$ to have a single maximum.*

Proof. Follows directly from Corollary 5.1.6. □

From Remark iv we can check p_{12} at the end points and if the value at the end points is less then two we have $p_{12}(\alpha) \leq 2$ on the interval $\left[\breve{b}_1, \breve{b}_2\right]$. In the next result we see that we do not need to compute p_{ij} at all if we want p_{ij} to be less than some value t on the interval $\left[\breve{b}_i, \breve{b}_j\right]$.

Lemma 5.1.8. *Any two Gaussian functions have $p_{ij}(\alpha) \leq t$ on the interval $\left[\breve{b}_i, \breve{b}_j\right]$ iff*

$$\breve{b}_j - \breve{b}_i \leq \sqrt{\frac{t}{2}} \min\left(\breve{c}_i, \breve{c}_j\right) \tag{5.15}$$

Proof. We first prove the '$\Rightarrow$' direction. We know $p_{ij}(\alpha) \leq t$ on the interval $\left[\breve{b}_i, \breve{b}_j\right]$. So, the maximum value of p_{ij} on this interval is also less than t. Using (iv) from Lemma 5.1.5 we get

$$2\left(\breve{b}_j - \breve{b}_i\right)^2 \max\left(\frac{1}{\breve{c}_i^2}, \frac{1}{\breve{c}_j^2}\right) \leq t$$

We know that for every $z, y > 0$ we have $\max(z^2, y^2) = (\max(z, y))^2$ which gives

$$\Leftrightarrow \left(\breve{b}_j - \breve{b}_i\right)^2 \left(\max\left(\frac{1}{\breve{c}_i}, \frac{1}{\breve{c}_j}\right)\right)^2 \leq \frac{t}{2} \tag{5.16}$$

Since both sides of the inequality in (5.16) are positive we take the square root and observe that $\breve{b}_j > \breve{b}_i$ to get

$$\Leftrightarrow \left(\breve{b}_j - \breve{b}_i\right) \max\left(\frac{1}{\breve{c}_i}, \frac{1}{\breve{c}_j}\right) \leq \sqrt{\frac{t}{2}}$$

We know that $\max\left(\frac{1}{\breve{c}_i}, \frac{1}{\breve{c}_i}\right) = \frac{1}{\min(\breve{c}_i, \breve{c}_j)}$, which gives us

$$\Leftrightarrow \left(\breve{b}_j - \breve{b}_i\right) \frac{1}{\min\left(\breve{c}_i, \breve{c}_j\right)} \leq \sqrt{\frac{t}{2}}$$
$$\Leftrightarrow \left(\breve{b}_j - \breve{b}_i\right) \leq \sqrt{\frac{t}{2}} \min\left(\breve{c}_i, \breve{c}_j\right)$$

We have so far shown the '$\Rightarrow$' direction. The '$\Leftarrow$' direction follows as all the steps in the proof of the '$\Rightarrow$' direction are if and only if relations. This completes the proof. □

Corollary 5.1.9. *Any two Gaussian functions have $p_{ij}(\alpha) \leq 2$ on the interval $\left[\breve{b}_i, \breve{b}_j\right]$ iff*

$$\breve{b}_j - \breve{b}_i \leq \min\left(\breve{c}_i, \breve{c}_j\right) \tag{5.17}$$

Proof. Follows directly from Lemma 5.1.8 by taking $t = 2$. □

As a consequence of Corollary 5.1.9 we know that for any two Gaussian functions, $p_{ij}(\alpha) \leq 2$ on $\alpha \in \left[\breve{b}_i, \breve{b}_j\right]$ is true if and only if the difference $\breve{b}_j - \breve{b}_i$ is not more than the minimum of the parameters $\breve{c}_i$ and $\breve{c}_j$. From this result we do not need to check if $p_{ij}(\alpha) \leq 2$ is true over the entire interval we just check if the condition in Corollary 5.1.9 is true.

In Corollary 5.1.7 we showed that if $p_{12}(\alpha) \leq 2$ on the interval $\left[\breve{b}_1, \breve{b}_2\right]$ then $\mathcal{G}$ has a single maximum. In the next result we show that for $n_g = 2$ we have a single maximum even when $p_{12}(\alpha) \leq 4$ on the interval $\left[\breve{b}_1, \breve{b}_2\right]$.

Theorem 5.1.10. *In case of $n_g = 2$, $\mathcal{G}$ as in Eq. (5.1) have a single maximum if*

$$p_{12}(\alpha) \leq 4$$

for $\alpha \in \left[\breve{b}_1, \breve{b}_2\right]$.

Proof. From Theorem 5.1.4 the condition for the first derivative of $\varphi(\alpha)$ to be less than one, when $n_g = 2$, is

$$\left(p_{12}(\alpha) - 2\right) \Psi_1(\alpha)\Psi_2(\alpha) - \Psi_1^2(\alpha) - \Psi_2^2(\alpha) < 0.$$

Taking all terms independent of p_{12} on one side and using $a^2 + b^2 + 2ab = (a+b)^2$ to get

$$p_{12}(\alpha)\Psi_1(\alpha)\Psi_2(\alpha) < \left(\Psi_1(\alpha) + \Psi_2(\alpha)\right)^2$$

Dividing both sides by $\Psi_1(\alpha)\Psi_2(\alpha)$ and simplifying finally gives

$$p_{12}(\alpha) < \left(\sqrt{\frac{\Psi_1(\alpha)}{\Psi_2(\alpha)}} + \sqrt{\frac{\Psi_2(\alpha)}{\Psi_1(\alpha)}}\right)^2. \tag{5.18}$$

The minimum value of the right hand side of the inequality in (5.18) is 4 as it is of the form $(z + \frac{1}{z})^2$ and the term $z + \frac{1}{z}$ for $z > 0$ is always greater than 2. Hence, when $p_{12}(\alpha) \leq 4$ the first derivative of φ is less than one and therefore Eq. (5.4) has a unique fixed point and $\mathcal{G}$ has a single maximum. □

In some cases even when $p_{12}(\alpha) > 4$ for some subinterval $S \subset \left[\breve{b}_1, \breve{b}_2\right]$ we can still have a single maximum for the sum. In Figure 5.1 we see cases when $p_{12}(\alpha) < 2$ for all $\alpha \in \left[\breve{b}_1, \breve{b}_2\right]$, $p_{12}(\alpha) < 4$ for all $\alpha \in \left[\breve{b}_1, \breve{b}_2\right]$ and $p_{12}(\alpha) > 4$ for some subinterval $S \subset \left[\breve{b}_1, \breve{b}_2\right]$ with two and one maximum respectively. In (d) we see an example where the sum of two Gaussian function has a single maximum even when $p_{12}(\alpha) > 4$ on some subinterval $S \subset \left[\breve{b}_1, \breve{b}_2\right]$.

In Theorem 5.1.10 we stopped at Eq. (5.18). Continuing from there we give in Theorem 5.1.12 another property which when satisfied gives us a single maximum even when $p_{12}(\alpha) > 4$ on a subset S of the interval $\left[\breve{b}_1, \breve{b}_2\right]$. Next we prove a result which is used in proving Theorem 5.1.12.

Lemma 5.1.11. *For $t > 4$ and $z > 0$ the interval on which the inequality $t < \left(z + \frac{1}{z}\right)^2$ is satisfied by z is given as*

$$\mathcal{I} = \left(0, \frac{1}{2}\left(\sqrt{t} - \sqrt{t-4}\right)\right) \bigcup \left(\frac{1}{2}\left(\sqrt{t} + \sqrt{t-4}\right), \infty\right).$$

Proof. The inequality can be written as a quadratic inequality as shown in the steps below:

$$t < \left(z + \frac{1}{z}\right)^2$$

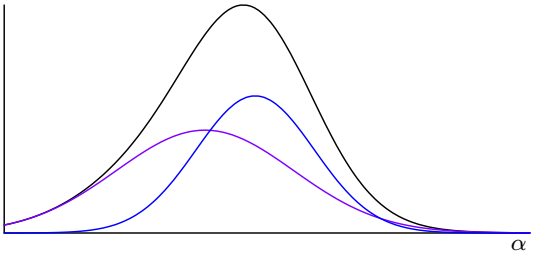

(a) Example for $p_{12}(\alpha) < 2$ for all $\alpha \in \left[\breve{b}_1, \breve{b}_2\right]$

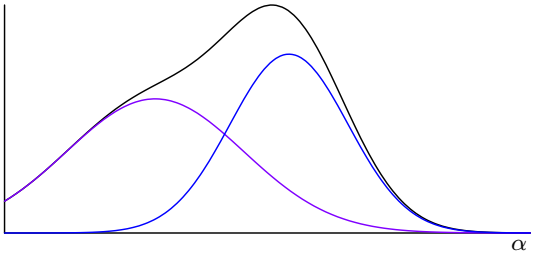

(b) Example for $p_{12}(\alpha) < 4$ for all $\alpha \in \left[\breve{b}_1, \breve{b}_2\right]$.

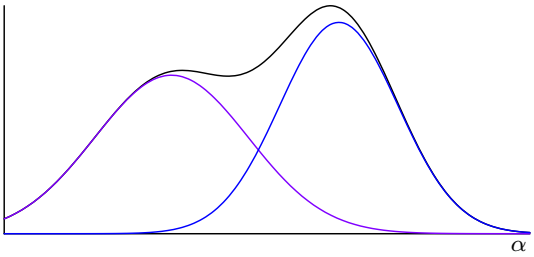

(c) Example for $p_{12}(\alpha) > 4$ for some subinterval $S \subset \left[\breve{b}_1, \breve{b}_2\right]$ with two maxima

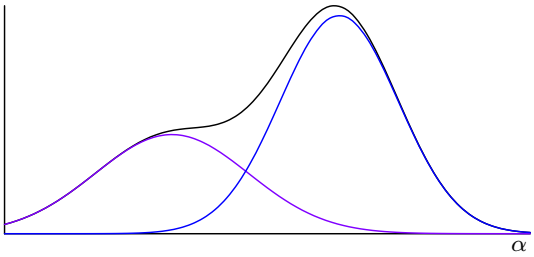

(d) Example for $p_{12}(\alpha) > 4$ for some subinterval $S \subset \left[\breve{b}_1, \breve{b}_2\right]$ with one maximum.

Figure 5.1.: Sum of two Gaussian functions with different values of p_{12}. The sum of the Gaussian functions is given in black and the individual Gaussian functions are in blue and purple.

Both the sides of the inequality are positive. We take the square root to get

$$\Rightarrow \sqrt{t} < \frac{z^2+1}{z}$$

Multiplying both sides of the inequality by z and collecting terms on one side we get a quadratic inequality

$$\Rightarrow z^2 - \sqrt{t}z + 1 > 0.$$

Now we look at the associated two-variable equation, $y = z^2 - \sqrt{t}z + 1$, and consider where its graph is above the horizontal axis. To do so we have to find when the graph crosses the horizontal axis. In other words we have to find where $z^2 - \sqrt{t}z + 1$ is zero:

$$z^2 - \sqrt{t}z + 1 = 0$$

$$\text{Quadratic Formula} \Rightarrow \left(z - \frac{1}{2}\left(\sqrt{t} - \sqrt{t-4}\right)\right)\left(z - \frac{1}{2}\left(\sqrt{t} + \sqrt{t-4}\right)\right) = 0$$

Which gives us

$$z = \frac{1}{2}\left(\sqrt{t} - \sqrt{t-4}\right) \text{ or } z = \frac{1}{2}\left(\sqrt{t} + \sqrt{t-4}\right).$$

These zeros divide the interval $(0, \infty)$ into three subintervals and using the sign test we get the interval $\mathcal{I}$. □

In the next Theorem we give a sufficient condition which when satisfied, the sum of two Gaussian functions has a single maximum even when $p_{12}(\alpha) > 4$ on a subset of interval $\left[\breve{b}_1, \breve{b}_2\right]$.

Theorem 5.1.12. *If $n_g = 2$ and $p_{12}(\alpha) > 4$ on $\alpha \in S \subset \left[\breve{b}_1, \breve{b}_2\right]$, then the sum of two Gaussian functions has a single maximum if the following condition is satisfied on S*

$$\left|\ln\left(\frac{\Psi_2(\alpha)}{\Psi_1(\alpha)}\right)\right| > 2\ln\left(\frac{\sqrt{p_{12}(\alpha)} + \sqrt{p_{12}(\alpha) - 4}}{2}\right). \tag{5.19}$$

Proof. Substituting $t = p_{12}(\alpha)$ and $z = \sqrt{\frac{\Psi_2(\alpha)}{\Psi_1(\alpha)}}$ in Lemma 5.1.11 the inequalities that must be satisfied at all points of S are given by the interval $\mathcal{I}$ as

$$\sqrt{\frac{\Psi_2(\alpha)}{\Psi_1(\alpha)}} > \frac{\sqrt{p_{12}(\alpha)} + \sqrt{p_{12}(\alpha) - 4}}{2} \text{ or } \sqrt{\frac{\Psi_2(\alpha)}{\Psi_1(\alpha)}} < \frac{\sqrt{p_{12}(\alpha)} - \sqrt{p_{12}(\alpha) - 4}}{2}$$

All terms in the inequalities are positive and taking natural logarithm of the inequalities gives us

$$\ln\left(\frac{\Psi_2(\alpha)}{\Psi_1(\alpha)}\right) > 2\ln\left(\frac{\sqrt{p_{12}(\alpha)} + \sqrt{p_{12}(\alpha) - 4}}{2}\right) \text{ or } \ln\left(\frac{\Psi_2(\alpha)}{\Psi_1(\alpha)}\right) < 2\ln\left(\frac{\sqrt{p_{12}(\alpha)} - \sqrt{p_{12}(\alpha) - 4}}{2}\right)$$

Observing that $\frac{\sqrt{p_{12}(\alpha)} - \sqrt{p_{12}(\alpha)-4}}{2} = \frac{2}{\sqrt{p_{12}(\alpha)} + \sqrt{p_{12}(\alpha)-4}}$ we get

$$\ln\left(\frac{\Psi_2(\alpha)}{\Psi_1(\alpha)}\right) > 2\ln\left(\frac{\sqrt{p_{12}(\alpha)} + \sqrt{p_{12}(\alpha) - 4}}{2}\right) \text{ or}$$
$$\ln\left(\frac{\Psi_2(\alpha)}{\Psi_1(\alpha)}\right) < -2\ln\left(\frac{\sqrt{p_{12}(\alpha)} + \sqrt{p_{12}(\alpha) - 4}}{2}\right) \tag{5.20}$$

Combining both inequalities into one we get the result. □

So far we have relaxed the assumptions for the case $n_g = 2$ such that the first derivative of $\varphi(\alpha)$ is less than one on the interval $\left[\breve{b}_1, \breve{b}_2\right]$ which implies that $\mathcal{G}$ has one maximum. In the next results we give relaxed conditions for the general case of $n_g > 2$. We begin by showing that $p_{ij}(\alpha)$ with $i \neq 1$ and $j \neq n_g$ have to be less than two on the interval $\left[\breve{b}_i, \breve{b}_j\right]$ instead of interval $\left[\breve{b}_1, \breve{b}_{n_g}\right]$ as proven in Corollary 5.1.6.

Theorem 5.1.13. *For $n_g > 2$ if we have $p_{ij}(\alpha) \leq 2$ for all $j > i$ on the interval $\left[\breve{b}_i, \breve{b}_j\right]$ then $p_{ij}(\alpha) < 2$ on the interval $\left[\breve{b}_1, \breve{b}_{n_g}\right]$ for all $j > i$ with $i \neq 1$ and $j \neq n_g$.*

Proof. We consider the case $\breve{c}_i > \breve{c}_j$ first. In this case we know from Lemma 5.1.5(ii) that $p_{ij}(\alpha)$ is a decreasing function. Hence, the maximum value of p_{ij} is obtained by evaluating at $\breve{b}_1$. If we can show that $p_{ij}\left(\breve{b}_1\right) \leq 2$ we are done. Evaluating p_{ij} at $\alpha = \breve{b}_1$ gives

$$p_{ij}\left(\breve{b}_1\right) = 2\left(\breve{b}_j - \breve{b}_i\right)\left(\frac{\breve{b}_j - \breve{b}_1}{\breve{c}_j^2} + \frac{\breve{b}_1 - \breve{b}_i}{\breve{c}_i^2}\right)$$

$$= 2\left(\breve{b}_j - \breve{b}_i\right)\left(\frac{\breve{b}_j - \breve{b}_1}{\breve{c}_j^2} - \frac{\breve{b}_i - \breve{b}_1}{\breve{c}_i^2}\right)$$

Adding and subtracting $\breve{b}_i$ from the numerator of the first term in the parenthesis results in

$$= 2\left(\breve{b}_j - \breve{b}_i\right)\left(\frac{\breve{b}_j - \breve{b}_i + \breve{b}_i - \breve{b}_1}{\breve{c}_j^2} - \frac{\breve{b}_i - \breve{b}_1}{\breve{c}_i^2}\right).$$

Collecting similar terms together and expanding the product we get

$$= 2\frac{\left(\breve{b}_j - \breve{b}_i\right)^2}{\breve{c}_j^2} + 2\left(\breve{b}_j - \breve{b}_i\right)\left(\breve{b}_i - \breve{b}_1\right)\left(\frac{1}{\breve{c}_j^2} - \frac{1}{\breve{c}_i^2}\right).$$

Taking $2\frac{\left(\breve{b}_j - \breve{b}_i\right)^2}{\breve{c}_j^2}$ common from both the terms gives

$$= 2\frac{\left(\breve{b}_j - \breve{b}_i\right)^2}{\breve{c}_j^2}\left(1 + \frac{\breve{b}_i - \breve{b}_1}{\breve{b}_j - \breve{b}_i}\left(1 - \frac{\breve{c}_j^2}{\breve{c}_i^2}\right)\right).$$

Let us now assume that the claim is false. This would mean that $p_{ij}\left(\breve{b}_1\right) > 2$. Hence, we should have

$$p_{ij}\left(\breve{b}_1\right) = 2\frac{\left(\breve{b}_j - \breve{b}_i\right)^2}{\breve{c}_j^2}\left(1 + \frac{\breve{b}_i - \breve{b}_1}{\breve{b}_j - \breve{b}_i}\left(1 - \frac{\breve{c}_j^2}{\breve{c}_i^2}\right)\right) > 2.$$

We know that $\left(1 - \frac{\breve{c}_j^2}{\breve{c}_i^2}\right) < 1$ as $\breve{c}_i > \breve{c}_j$,

$$\frac{\left(\breve{b}_j - \breve{b}_i\right)^2}{\breve{c}_j^2}\left(1 + \frac{\breve{b}_i - \breve{b}_1}{\breve{b}_j - \breve{b}_i}\right) > 1,$$
$$\Rightarrow \frac{\left(\breve{b}_j - \breve{b}_i\right)\left(\breve{b}_j - \breve{b}_1\right)}{\breve{c}_j^2} > 1.$$

We have $p_{1j}(\alpha) \leq 2$ on $\left[\breve{b}_1, \breve{b}_j\right]$ and $p_{ij}(\alpha) \leq 2$ on $\left[\breve{b}_i, \breve{b}_j\right]$ and as a result of Corollary 5.1.9 we get $\breve{b}_j - \breve{b}_i \leq \breve{c}_j$ and $\breve{b}_j - \breve{b}_1 \leq \breve{c}_j$ which leads to a contradiction. Hence the assumption that $p_{ij}(\breve{b}_1) > 2$ is false.

Next we consider the case $\breve{c}_j > \breve{c}_i$. In this case we know from Lemma 5.1.5(iii) that $p_{ij}(\alpha)$ is an increasing function. Hence, the maximum value of p_{ij} is obtained by evaluating at $\breve{b}_{n_g}$. If we can show that $p_{ij}(\breve{b}_{n_g}) \leq 2$ we are done. Evaluating p_{ij} at $\alpha = \breve{b}_{n_g}$ gives

$$p_{ij}\left(\breve{b}_{n_g}\right) = 2\left(\breve{b}_j - \breve{b}_i\right)\left(\frac{\breve{b}_j - \breve{b}_{n_g}}{\breve{c}_j^2} + \frac{\breve{b}_{n_g} - \breve{b}_i}{\breve{c}_i^2}\right)$$

$$= 2\left(\breve{b}_j - \breve{b}_i\right)\left(\frac{\breve{b}_{n_g} - \breve{b}_i}{\breve{c}_i^2} - \frac{\breve{b}_{n_g} - \breve{b}_j}{\breve{c}_j^2}\right)$$

Similar to the case of $\breve{c}_i > \breve{c}_j$ we simplify to

$$= 2\frac{\left(\breve{b}_j - \breve{b}_i\right)^2}{\breve{c}_i^2}\left(1 + \frac{\breve{b}_{n_g} - \breve{b}_i}{\breve{b}_j - \breve{b}_i}\left(1 - \frac{\breve{c}_i^2}{\breve{c}_j^2}\right)\right).$$

Let us now assume that the claim is false. This would mean that $p_{ij}(\breve{b}_{n_g}) > 2$. Hence, we should have

$$p_{ij}\left(\breve{b}_{n_g}\right) = 2\frac{\left(\breve{b}_j - \breve{b}_i\right)^2}{\breve{c}_i^2}\left(1 + \frac{\breve{b}_{n_g} - \breve{b}_i}{\breve{b}_j - \breve{b}_i}\left(1 - \frac{\breve{c}_i^2}{\breve{c}_j^2}\right)\right) > 2$$

$$\left(1 - \frac{\breve{c}_i^2}{\breve{c}_j^2}\right) < 1 \Rightarrow \frac{(\breve{b}_j - \breve{b}_i)^2}{\breve{c}_i^2}\left(1 + \frac{\breve{b}_{n_g} - \breve{b}_j}{\breve{b}_j - \breve{b}_i}\right) > 1$$

$$\Rightarrow \frac{\left(\breve{b}_j - \breve{b}_i\right)(\breve{b}_{n_g} - \breve{b}_i)}{\breve{c}_i^2} > 1.$$

We have $p_{in_g}(\alpha) \leq 2$ on $\left[\breve{b}_i, \breve{b}_{n_g}\right]$ and $p_{ij}(\alpha) \leq 2$ on $\left[\breve{b}_i, \breve{b}_j\right]$ which implies from Corollary 5.1.9 that $\breve{b}_{n_g} - \breve{b}_i \leq \breve{c}_i$ and $\breve{b}_j - \breve{b}_i \leq \breve{c}_i$ and leads to a contradiction. Hence the assumption that $p_{ij}(\breve{b}_{n_g}) > 2$ is false.

Hence, we have shown that $p_{ij}(\alpha) < 2$ on the interval $\left[\breve{b}_1, \breve{b}_{n_g}\right]$ for all $j > i$ with $i \neq 1$ and $j \neq n_g$. □

In Theorem 5.1.13 we have given conditions for the single maximum when $n_g = 2$ that are not as strict as the conditions of Corollary 5.1.6. We have shown that it is sufficient to have the value of $p_{ij}(\alpha) \leq 2$ for the i^{th} and the j^{th} interior Gaussian functions on interval $\left[\breve{b}_i, \breve{b}_j\right]$ which implies that it is also less than two on the full interval $\left[\breve{b}_1, \breve{b}_{n_g}\right]$. In the next result we give a similar condition if either $i = 1$ or $j = n_g$.

Theorem 5.1.14. *For $n_g > 2$ if we have $p_{ij}(\alpha) \leq 2$ for all $j > i$ on the interval $\left[\breve{b}_i, \breve{b}_j\right]$ then both $p_{1j}(\alpha)$ and $p_{in_g}(\alpha)$ are less than two on the interval $\left[\breve{b}_1, \breve{b}_{n_g}\right]$ for all $j > 1$ and $i < n_g$.*

Proof. In case $\breve{c}_j \leq \min\left(\breve{c}_1, \breve{c}_{n_g}\right)$ then from Lemma 5.1.5(ii) we have p_{1j} is a decreasing function of α and from Lemma 5.1.5(iii) we have p_{jn_g} is an increasing function of α. Therefore, the maximum value of p_{1j} and p_{jn_g} is less than two on the complete interval $\left[\breve{b}_1, \breve{b}_{n_g}\right]$.

When $\breve{c}_j > \min\left(\breve{c}_1, \breve{c}_{n_g}\right)$ we prove similar to the proof for Theorem 5.1.13 that $p_{1j}\left(\breve{b}_{n_g}\right)$ and $p_{jn_g}\left(\breve{b}_1\right)$ are less than two and therefore, $p_{1j}(\alpha)$ and $p_{jn_g}(\alpha)$ are less than two on the interval $\left[\breve{b}_1, \breve{b}_{n_g}\right]$. □

Theorem 5.1.15. *Given the sum of Gaussian functions $\mathcal{G}$ as defined in Eq. (5.1), if $p_{ij}(\alpha) \leq 2$ on the interval $\left[\breve{b}_i, \breve{b}_j\right]$ for all $j > i$ then the sum $\mathcal{G}$ has a single maximum.*

Proof. It follows from Theorem 5.1.13 and Theorem 5.1.14 that for all $p_{ij}(\alpha) < 2$ on the interval $\left[\breve{b}_i, \breve{b}_j\right]$ implies $p_{ij}(\alpha) < 2$ on the interval $\left[\breve{b}_1, \breve{b}_{n_g}\right]$. From Corollary 5.1.6 we know that the sum of Gaussian functions $\mathcal{G}$ has a single maximum if $p_{ij}(\alpha) \leq 2$ on the interval $\left[\breve{b}_1, \breve{b}_{n_g}\right]$ and the result follows. □

From Theorem 5.1.15 we now have a necessary condition which p_{ij} has to satisfy for the sum of Gaussian functions $\mathcal{G}$ to have a single maximum. Next we prove some results for parameters $\breve{c}_i$ and $p_{ij}(\alpha)$ when conditions of Theorem 5.1.15 are satisfied.

Lemma 5.1.16. *For $n_g > 2$ if we have $p_{ij}(\alpha) \leq 2$ for all $j > i$ on the interval $\left[\breve{b}_i, \breve{b}_j\right]$ then $\breve{c}_i \geq \frac{\breve{b}_{n_g} - \breve{b}_1}{2}$.*

Proof. Suppose that for some i we have $\breve{c}_i < \frac{\breve{b}_{n_g} - \breve{b}_1}{2}$ with $p_{1i}(\alpha) \leq 2$ on the interval $\left[\breve{b}_1, \breve{b}_i\right]$ and $p_{in_g}(\alpha) \leq 2$ on the interval $\left[\breve{b}_i, \breve{b}_{n_g}\right]$. However, $\breve{c}_i < \frac{\breve{b}_{n_g} - \breve{b}_1}{2}$ means that even if the i^{th} Gaussian function is located in the middle of the first and the last Gaussian function we still have $p_{1i}(\alpha) \geq 2$ on some subinterval $S_1 \subset \left[\breve{b}_1, \breve{b}_i\right]$ and similarly we have $p_{in_g}(\alpha) \geq 2$ in some subinterval $S_2 \subset \left[\breve{b}_i, \breve{b}_{n_g}\right]$. This is a contradiction to the fact that $p_{1i} \leq 2$ on the interval $\left[\breve{b}_1, \breve{b}_i\right]$ and $p_{in_g}(\alpha) \leq 2$ on the interval $\left[\breve{b}_i, \breve{b}_{n_g}\right]$. In other words we were wrong to assume that $\breve{c}_i < \frac{\breve{b}_{n_g} - \breve{b}_1}{2}$. □

In Figure 5.2 we see in red the intervals in which $\breve{b}_i$ should lie for different values of $t \in [0, 1]$ where $\breve{c}_i = t\left(\breve{b}_{n_g} - \breve{b}_1\right)$ such that $p_{1i}(\alpha) \leq 2$ on the interval $\left[\breve{b}_1, \breve{b}_i\right]$. Similarly, we see in blue the interval in which $\breve{b}_i$ should lie for different values of t where $\breve{c}_i = t\left(\breve{b}_{n_g} - \breve{b}_1\right)$ such that $p_{in_g}(\alpha) \leq 2$ on the interval $\left[\breve{b}_i, \breve{b}_{n_g}\right]$. In order for both $p_{1i}(\alpha) < 2$ as well as $p_{in_g}(\alpha) < 2$ we must have an overlap between the red and blue intervals. We observe that when $t = 0.5$ the overlap of the two intervals reduces to a point and for all values of $t < 0.5$ there is no overlapping interval. However, when $t \geq 1$ then $\breve{b}_i$ can be anywhere in the interval $\left[\breve{b}_1, \breve{b}_{n_g}\right]$.

Lemma 5.1.17. *Let $n_g > 2$ with $p_{ij}(\alpha) \leq 2$ for all $j > i$. If for some $\hat{j} \leq n_g$*

$$\breve{b}_{\hat{j}} \neq \frac{\breve{b}_1 + \breve{b}_{n_g}}{2}$$

then $p_{1\hat{j}}(\alpha)$ and $p_{\hat{j}n_g}(\alpha)$ both cannot be equal to two on one end point of the interval $\left[\breve{b}_1, \breve{b}_{\hat{j}}\right]$ and $\left[\breve{b}_{\hat{j}}, \breve{b}_{n_g}\right]$ respectively.

Proof. At the end points of the interval $\left[\breve{b}_1, \breve{b}_{\hat{j}}\right]$, $p_{1\hat{j}}$ is either $\frac{2(\breve{b}_{\hat{j}} - \breve{b}_1)^2}{\breve{c}_1^2}$ or $\frac{2(\breve{b}_{\hat{j}} - \breve{b}_1)^2}{\breve{c}_{\hat{j}}^2}$. We have $\frac{2(\breve{b}_{\hat{j}} - \breve{b}_1)^2}{\breve{c}_1^2} < \frac{2(\breve{b}_{n_g} - \breve{b}_1)^2}{\breve{c}_1^2} < 2$. Hence, the only possibility for $p_{1\hat{j}}$ to be two at the end points of

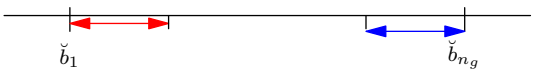

(a) For $t = 0.25$ we have no overlap.

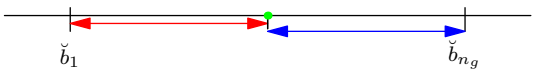

(b) For $t = 0.5$ the overlap is a point.

(c) For $t = 0.75$ the overlap is an interval.

(d) For $t = 1$ the overlap is the entire interval $[\breve{b}_1, \breve{b}_{n_g}]$.

Figure 5.2.: Interval where $\breve{b}_i$ can lie such that $p_{1i}(\alpha) \leq 2$ on the interval $\left[\breve{b}_1, \breve{b}_i\right]$ in red and $p_{in_g}(\alpha) \leq 2$ on the interval $\left[\breve{b}_i, \breve{b}_{n_g}\right]$ in blue. The overlapping interval in green.

the interval is when $\breve{c}_{\hat{j}} = \breve{b}_{\hat{j}} - \breve{b}_1$. This leads us to the conclusion that $\frac{2(\breve{b}_{n_g} - \breve{b}_{\hat{j}})^2}{\breve{c}_1^2} \neq 2$ since, $\breve{b}_{\hat{j}} - \breve{b}_1 \neq \breve{b}_{n_g} - \breve{b}_{\hat{j}}$. For $p_{\hat{j}n_g}$ it follows similarly. □

Theorem 5.1.18. *Let $n_g > 2$. If we have $p_{ij}(\alpha) \leq 2$ on the interval $\left[\breve{b}_i, \breve{b}_j\right]$ for all $n_g \geq j > i$ then the number of pairs (i, j) such that $p_{ij}(\alpha) = 2$ is bounded from above by n_g.*

Proof. We have $p_{1n_g}(\alpha) \leq 2$, which implies from Corollary 5.1.9 that $\breve{b}_{n_g} - \breve{b}_1 \leq \min\left(\breve{c}_1, \breve{c}_{n_g}\right)$. Additionally, we have from Lemma 5.1.16 that $\breve{c}_i \geq \frac{\breve{b}_{n_g} - \breve{b}_1}{2}$ for $1 < i < n_g$. From Lemma 5.1.17 we know for $\breve{b}_i \neq \frac{\breve{b}_1 + \breve{b}_{n_g}}{2}$ it is not possible to have both $p_{1i}(\alpha) = 2$ and $p_{in_g}(\alpha) = 2$. So, it is only possible for one of $p_{1i}(\alpha)$ or $p_{in_g}(\alpha)$ to be equal to two. This gives us an upper bound of $n_g - 1$. However, if there exists a j such that $\breve{b}_j = \frac{\breve{b}_1 + \breve{b}_{n_g}}{2}$ and $\breve{c}_j = \frac{\breve{b}_{n_g} - \breve{b}_1}{2}$ then both $p_{1j}(\alpha) = 2$ and $p_{jn_g}(\alpha) = 2$ on one end point of $\left[\breve{b}_1, \breve{b}_j\right]$ and $\left[\breve{b}_j, \breve{b}_{n_g}\right]$ respectively. This makes the upper bound n_g. □

In the next result we further generalize Theorem 5.1.15.

Theorem 5.1.19. *In case of $n_g \geq 2$, there is only one maximum for the sum of Gaussian functions $\mathcal{G}$ if*

$$p_{1i}(\alpha) \leq 2 \text{ for all } \alpha \in \left[\breve{b}_1, \breve{b}_i\right], i = 2, \ldots, n_g \text{ and}$$

$$p_{in_g}(\alpha) \leq 2 \text{ for all } \alpha \in \left[\breve{b}_i, \breve{b}_{n_g}\right], i = 1, \ldots, n_g - 1.$$

Proof. We have $p_{1i}(\alpha) \leq 2$ for all $\alpha \in \left[\breve{b}_1, \breve{b}_i\right]$ that implies $\breve{c}_i^2 \geq \left(\breve{b}_i - \breve{b}_1\right)^2$ from Corollary 5.1.9. Also, $p_{in_g}(\alpha) \leq 2$ which implies $\breve{c}_i^2 \geq \left(\breve{b}_{n_g} - \breve{b}_i\right)^2$ from Corollary 5.1.9. The result follows by observing that $\max_{\alpha \in \left[\breve{b}_i, \breve{b}_j\right]} p_{ij}(\alpha) < 2$ for all $n_g \geq j > i$:

$$\max_{\alpha \in \left[\breve{b}_i, \breve{b}_j\right]} p_{ij}(\alpha) = 2\left(\breve{b}_j - \breve{b}_i\right)^2 \max\left(\frac{1}{\breve{c}_i^2}, \frac{1}{\breve{c}_j^2}\right)$$

$$\text{Corollary 5.1.9} \Rightarrow \leq \max\left(\frac{2\left(\breve{b}_j-\breve{b}_i\right)^2}{\max\left(\left(\breve{b}_{n_g}-\breve{b}_i\right)^2,\left(\breve{b}_i-\breve{b}_1\right)^2\right)},\frac{2\left(\breve{b}_j-\breve{b}_i\right)^2}{\max\left(\left(\breve{b}_{n_g}-\breve{b}_j\right)^2,\left(\breve{b}_j-\breve{b}_1\right)^2\right)}\right)$$
$$< 2,$$

The final inequality is true because we have $\left(\breve{b}_j-\breve{b}_i\right)^2 < \max\left(\left(\breve{b}_{n_g}-\breve{b}_i\right)^2,\left(\breve{b}_i-\breve{b}_1\right)^2\right)$ and also $\left(\breve{b}_j-\breve{b}_i\right)^2 < \max\left(\left(\breve{b}_{n_g}-\breve{b}_j\right)^2,\left(\breve{b}_j-\breve{b}_1\right)^2\right)$. The result follows from Theorem 5.1.15. □

So far we have considered conditions for having a single maximum for sum of n_g Gaussian functions. However, we did not discuss yet what happens in situations where these conditions are not satisfied. In what follows the theorems for single maximum are used as the basis for estimating the upper bound for the number of maxima (n_m) in a sum of Gaussian function with $n_g \geq 3$. The following results are similar to the results obtained in [3].

Corollary 5.1.20. *For $n_g \geq 3$, if there exists a value of $s \geq 1$ and $t \geq 1$ with $s+t \leq n_g$ such that*

$$p_{s,s+k}(\alpha) \leq 2 \text{ for } \alpha \in \left[\breve{b}_s, \breve{b}_{s+k}\right], 1 \leq k \leq t, \text{ and} \tag{5.21}$$

$$p_{s+k,s+t}(\alpha) \leq 2 \text{ for } \alpha \in \left[\breve{b}_{s+k}, \breve{b}_{s+t}\right], 0 \leq k < t, \tag{5.22}$$

the number of maxima n_m in the sum of n_g Gaussian functions satisfies the inequality

$$n_m \leq n_g - t$$

Proof. The proof follows from Corollary 2.1 in [3]. □

Corollary 5.1.20 in some sense defines a cluster of $t+1$ Gaussian functions and this idea is used for the clustering algorithm that is developed in the next section. In general we can have more than one such clusters of Gaussian function that in the absence of other Gaussian functions would give a single maximum.

Corollary 5.1.21. *For $n_g > 2$, if there exists at least one value*

$$p_{t,t+1}(\alpha) \leq 4,\ t \in \{1,2,\ldots,n_g-1\}, \alpha \in \left[\breve{b}_t, \breve{b}_{t+1}\right]$$

then the number of maxima satisfies the inequality

$$n_m \leq n_g - 1.$$

Proof. The proof follows from Corollary 3.1 in [3]. □

In this section we gave several results on the sufficient condition for a single maximum for sum of n_g Gaussian functions with parameters $\breve{a}_i$, $\breve{b}_i$ and $\breve{c}_i$. We ended the section with results on the bounds for n_m. In the next section we show how we use our theory to derive an algorithm that

clusters the Gaussian functions such that each cluster is a potential local maximum. The obtained clusters are then used to find the point of a global maximum.

5.2. Clustering algorithm for Gaussian functions in sum $\mathcal{G}$

When $p_{n_g 1}(\alpha) > 2$ on some subinterval of $\left[\breve{b}_1, \breve{b}_{n_g}\right]$, there is no information about the number of maxima the sum of the Gaussian functions $\mathcal{G}$ have. From Theorem 5.1.1 we know that all the maxima and minima of $\mathcal{G}$ lies in the interval $\left[\breve{b}_1, \breve{b}_{n_g}\right]$. Thus, one obvious procedure to find all the points of maximum of $\mathcal{G}$ is to use a hill-climbing algorithm starting from individual points of maximum of the Gaussian functions in $\mathcal{G}$ (see [7]). However this approach is highly inefficient when there are hundreds of Gaussian functions in the sum. If individual Gaussian functions in the sum interact with each other, then the number of maxima n_m of $\mathcal{G}$ is less than the number of Gaussian functions n_g in the sum.

Keeping this in mind we group together Gaussian functions into clusters with each cluster being a potential maximum. Then we can run a hill-climbing algorithm or fixed point iterations for each cluster's point of maximum (which is computed empirically). In [16] Henning describes the ridge-line unimodal method to find modes for Gaussian mixtures, which is based on the idea of a ridge-line developed by Ray and Lindsay in [30]. We use a modified version of the ridge-line unimodal method, given by Henning, to cluster the Gaussian functions in the sum $\mathcal{G}$. Unlike Henning we want to find clusters by which we can approximate the regions in which the global maximum could lie. We can then use a fixed point iterations or hill-climbing algorithms to get to the global maximum.

Before we proceed any further we give a precise definition of what we mean by a "cluster" in general in Definition 5.2.1. We modify this definition of a "cluster" in Definition 5.2.4 to the context of Gaussian functions by the help of *cluster distance* defined in Definition 5.2.2.

Definition 5.2.1 (Clustering)**.** Given n_g Gaussian functions with parameters $\breve{b}_i$ and $\breve{c}_i$, $i = 1, 2, \ldots, n_g$. Let for $i = 1, 2, \ldots, m^*$ with $m^* \leq n_g$ the collection of indices

$$\mathfrak{C}_i \subset \{1, 2, \ldots, n_g\}$$

form a partition of the indices $\{1, 2, \ldots, n_g\}$, i.e.,

$$\bigcup_{i=1}^{m^*} \mathfrak{C}_i = \{1, 2, \ldots, n_g\}$$

and

$$\mathfrak{C}_i \cap \mathfrak{C}_j = \emptyset, \text{ for all } i \neq j$$

then $\hat{\mathscr{C}} = \{\mathfrak{C}_1, \mathfrak{C}_2, \ldots, \mathfrak{C}_{m^*}\}$ is called a Clustering of the n_g Gaussian function.

We denote by $\mathfrak{C}_i$ a *cluster* that has indices of Gaussian functions in the sum that are part of this cluster. In Definition 5.2.2 we introduce the idea of a *within-cluster distance* $\mathfrak{D}$ for every cluster $\mathfrak{C} \in \hat{\mathscr{C}}$. For any cluster $\mathfrak{C}$, the within-cluster distance $\mathfrak{D}_{\mathfrak{C}}$ gives information about how much do the

Gaussian functions in the cluster interact with each other. The smaller the value of within-cluster distance for any cluster is, the higher is the interaction between the Gaussian functions whose indices are present in the cluster.

Definition 5.2.2 (Within-Cluster Distance)**.** Given a clustering $\hat{\mathscr{C}}$, then we define for each cluster $\mathfrak{C} \in \hat{\mathscr{C}}$ with $|\mathfrak{C}| \geq 2$ a within-cluster distance $\mathfrak{D}_{\mathfrak{C}}$ as

$$\mathfrak{D}_{\mathfrak{C}} = \max_{\alpha \in \left[\breve{b}_i, \breve{b}_j\right]} p_{ij}(\alpha), \forall i < j \text{ and } i, j \in \mathfrak{C} \tag{5.23}$$

where p_{ij} is as defined in Eq. (5.9). When $|\mathfrak{C}| = 1$ then $\mathfrak{D}_{\mathfrak{C}} = 0$.

In Theorem 5.2.3 we prove that for a cluster, if the within-cluster distance is less than two, then the sum of Gaussian functions whose indices are in the cluster, have a single maximum in the absence of all other clusters.

Theorem 5.2.3. *If a cluster $\mathfrak{C}$ has a within-cluster distance $\mathfrak{D}_{\mathfrak{C}} \leq 2$, then the sum of Gaussian functions whose indices are in the cluster $\mathfrak{C}$, have a single maximum in the absence of all other clusters.*

Proof. In the absence of all other clusters, the within-cluster distance $\mathfrak{D}_{\mathfrak{C}} \leq 2$ implies that the sum of Gaussian functions whose indices are in the cluster $\mathfrak{C}$ satisfy the assumption of Theorem 5.1.15. Therefore, from the result of Theorem 5.1.15 we get a single maximum for the sum of Gaussian functions whose indices are in the cluster $\mathfrak{C}$. □

In the context of Gaussian functions we want every cluster in our clustering to give a single maximum in the absence of all other clusters. We define a *Gaussian Clustering* as a clustering where individual clusters in the clustering have a within-cluster distance of less than two.

Definition 5.2.4 (Gaussian Clustering)**.** Given n_g Gaussian functions with parameters $\breve{b}_i$ and $\breve{c}_i$, $i = 1, 2, \ldots, n_g$ and clustering $\mathscr{C}$ as in Definition 5.2.1. If additionally for all $i \leq m^*$ we have a within-cluster distance $\mathfrak{D}_{\mathfrak{C}_i} \leq 2$ then $\mathscr{C}$ is called a Gaussian Clustering.

In case of a Gaussian clustering we denote $\mathfrak{C}$ as *Gaussian cluster*. In the next result we prove that each individual Gaussian cluster in the absence of all other clusters have a single maximum.

Corollary 5.2.5. *Given a Gaussian Clustering $\mathscr{C}$ as in Definition 5.2.4, then for each Gaussian cluster $\mathfrak{C} \in \mathscr{C}$, the sum of all Gaussian functions in the cluster have a single maximum in the absence of all other clusters.*

Proof. From the definition of a Gaussian cluster we have that the within-cluster distance is less than two. This fulfills the assumptions of Theorem 5.2.3 for each Gaussian cluster $\mathfrak{C} \in \mathscr{C}$ and proves the result. □

Sometimes for a Gaussian clustering it is possible that when we merge two Gaussian clusters together we still get a single maximum in the absence of all other clusters. Before we give conditions for this specific case we introduce the idea of *between-cluster distance* in Definition 5.2.6. This is the idea we build a clustering algorithm upon.

Definition 5.2.6 (Between-Cluster Distance)**.** For a clustering $\hat{\mathscr{C}}$ we define between-cluster distance $\mathfrak{D}_{\mathfrak{C}_i,\mathfrak{C}_j}$ for any two clusters $\mathfrak{C}_i, \mathfrak{C}_j \in \hat{\mathscr{C}}$ as

$$\mathfrak{D}_{\mathfrak{C}_i,\mathfrak{C}_j} = \max_{\hat{i}\in\mathfrak{C}_i} \max_{\hat{j}\in\mathfrak{C}_j} \max_{\alpha\in I_{\hat{i},\hat{j}}} p_{\hat{i}\hat{j}}(\alpha) \tag{5.24}$$

where p_{ij} is as defined in Eq. (5.9) and $I_{\hat{i},\hat{j}}$ is the interval enclosed in between the points $\breve{b}_{\hat{i}}$ and $\breve{b}_{\hat{j}}$.

Similar to the within-cluster distance, the between-cluster distance gives us information about how two clusters interact with each other. If the value of between-cluster distance is small it means that there is high interaction between the components of the two clusters. Additionally for two clusters with between-cluster distance less than two we can prove that the two clusters have a single maximum even when merged together.

Theorem 5.2.7. *If two Gaussian clusters $\mathfrak{C}_i$ and $\mathfrak{C}_j$ have a between-cluster distance $\mathfrak{D}_{\mathfrak{C}_i,\mathfrak{C}_j} \leq 2$, then the sum of all Gaussian functions in Gaussian clusters $\mathfrak{C}_i$ and $\mathfrak{C}_j$ have a single maximum in the absence of all other clusters .*

Proof. From the definition of Gaussian clusters the within-cluster distance for $\mathfrak{C}_i$ and $\mathfrak{C}_j$ is less than two, i.e., $p_{\hat{i}\hat{j}}(\alpha) \leq 2$ on $\alpha \in \left[\breve{b}_{\hat{i}}, \breve{b}_{\hat{j}}\right]$ for all $\hat{i} < \hat{j}$ and $\hat{i}, \hat{j} \in \mathfrak{C}_i$ and similarly, $p_{\hat{i}\hat{j}}(\alpha) \leq 2$ on $\alpha \in \left[\breve{b}_{\hat{i}}, \breve{b}_{\hat{j}}\right]$ for all $\hat{i} < \hat{j}$ and $\hat{i}, \hat{j} \in \mathfrak{C}_j$. Combining this with the fact that when $\mathfrak{D}_{\mathfrak{C}_i,\mathfrak{C}_j} \leq 2$, from definition of between-cluster distance, we also have that $p_{\hat{i}\hat{j}}(\alpha) \leq 2$, for $\alpha \in I_{\hat{i},\hat{j}}$, and all $\hat{i} \in \mathfrak{C}_i$ and $\hat{j} \in \mathfrak{C}_j$. Therefore, the assumptions of Theorem 5.1.15 are satisfied and from the result of Theorem 5.1.15 we get a single maximum for the sum of Gaussian functions whose indices are in the clusters $\mathfrak{C}_i$ and $\mathfrak{C}_j$. □

Theorem 5.2.7 implies that two Gaussian clusters with between-cluster distance less than two give a single Gaussian cluster when merged. The between-cluster distance and within-cluster distance are important as they enable us to reduce the number of clusters in a clustering by merging two clusters with between-cluster distance and within-cluster distances less than two. We use this idea to get a Gaussian clustering for a sum $\mathcal{G}$ of n_g Gaussian functions such that each Gaussian cluster in the absence of other clusters have a single maximum. The basic idea of the clustering algorithm is that we begin with assigning each Gaussian function in $\mathcal{G}$ to a separate cluster and at every iteration merge clusters until no more clusters can be merged together.

The Clustering algorithm described in Algorithm 5.2.1 is iterative and at each iteration in line 8 it tries to find two clusters that can be merged together. The search for the cluster pair can be done in may ways, for example, we can start from the leftmost clusters and move towards the rightmost clusters or start from the rightmost cluster and move towards the leftmost cluster or choose clusters randomly. In Section 5.4 we look at the effects of different selection criteria on the resulting Gaussian clustering. At each iteration the number of clusters is reduced by one. The algorithm ends when the number of clusters at an iteration do not decrease. In the next result we prove that at each iteration the clustering obtained in Algorithm 5.2.1 is a Gaussian clustering.

Theorem 5.2.8. *At every iteration in Algorithm 5.2.1 the clustering $\mathscr{C}_{it}$ is a Gaussian clustering.*

Algorithm 5.2.1: Clustering Algorithm for Gaussian functions

Data: Parameters $\breve{b}_i$, $\breve{c}_i$ with $i = 1, 2, \ldots, n_g$
Result: $\mathscr{C}_{it}$

begin
  $\mathscr{C}_0 \longleftarrow \{\mathfrak{C}_1, \mathfrak{C}_2, \ldots, \mathfrak{C}_{n_g}\}$ ▷ Start with all Gaussian functions as current clusters.
  $m^* \longleftarrow |\mathscr{C}_0| + 1$ ▷ Initialize number of clusters.
  $it \longleftarrow 0$ ▷ Initialize number of iteration.
  while $m^* > |\mathscr{C}_{it}|$ **do**
    $m^* \longleftarrow |\mathscr{C}_{it}|$
    $it \longleftarrow it + 1$
    if *exists* $i, j \leq m^*, i \neq j$ *with between-cluster distance* $\mathfrak{D}_{\mathfrak{C}_i, \mathfrak{C}_j} \leq 2$ **then**
      $\mathfrak{C}_{ij} \longleftarrow \mathfrak{C}_i \cup \mathfrak{C}_j$ ▷ Merged cluster.
      $\mathscr{C}_{it} \longleftarrow (\mathscr{C}_{it-1} - \{\mathfrak{C}_i, \mathfrak{C}_j\}) \cup \{\mathfrak{C}_{ij}\}$ ▷ Add merged clusters.
    end
  end
  return $\mathscr{C}_{it}$
end

Proof. We first prove that $\mathscr{C}_0$ is a Gaussian clustering. The clusters in $\mathscr{C}_0$ are individual Gaussian functions and therefore, the within-cluster distance for each of these clusters is zero. This implies that $\mathscr{C}_0$ is a Gaussian clustering. At following iteration steps we merge two Gaussian clusters when between-cluster distance between them is less than two. Therefore, from Theorem 5.2.7 we know that the merged cluster is also a Gaussian cluster which implies that $\mathscr{C}_{it}$ is a Gaussian clustering at each iteration. □

In Figure 5.3 we see the iterations of the clustering algorithm applied for an example where we have $n_g = 5$ Gaussian functions in the sum $\mathcal{G}$ and we find pairs from left end.

Algorithm 5.2.1 described above does not always find the optimal number of clusters. This is because in developing the clustering algorithm we did not consider the parameter $\breve{a}$, the height of the Gaussian function, at all. When $p_{ij}(\alpha) > 4$, the parameters $\breve{a}_i$ and $\breve{a}_j$ can still make the two Gaussian function to have a single maximum. Therefore, as a result of Algorithm 5.2.1 we only get clusters that divide the interval $\left[\breve{b}_1, \breve{b}_{n_g}\right]$ into subintervals with a possible presence of a local maximum of $\mathcal{G}$ in each subinterval. By the application of Algorithm 5.2.1 we have therefore reduced the number of times we have to run the hill-climbing algorithm or the fixed point iterations to find the global point of maximum to m^* instead of n_g. Next we prove that the number of Gaussian clusters m^* obtained from Algorithm 5.2.1 are always more than or equal to the number of maxima of $\mathcal{G}$, $\hat{m}^*$.

Theorem 5.2.9. *Application of Algorithm 5.2.1 on the Gaussian functions in $\mathcal{G}$ gives us the following relationship between the number of Gaussian clusters m^* and number of maxima of $\mathcal{G}$, $\hat{m}^*$:*

$$\hat{m}^* \leq m^*. \tag{5.25}$$

Proof. (Proof by contradiction.) We assume that $\hat{m}^* > m^*$. This means that the number of clusters are less than the number of maxima of $\mathcal{G}$. This in turn implies that there exists at least one Gaussian cluster $\mathfrak{C}$ in the Gaussian clustering $\mathscr{C}$ obtained from Algorithm 5.2.1 that has at

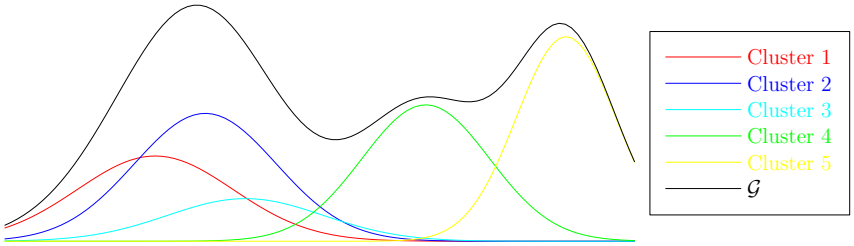

(a) Initialization of all the Gaussian functions as clusters.

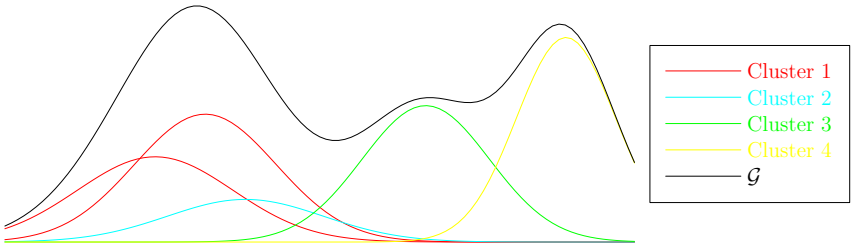

(b) Iteration 1: Cluster 1 and Cluster 2 in (a) satisfy the assumptions of Corollary 5.1.20 and are merged into one cluster.

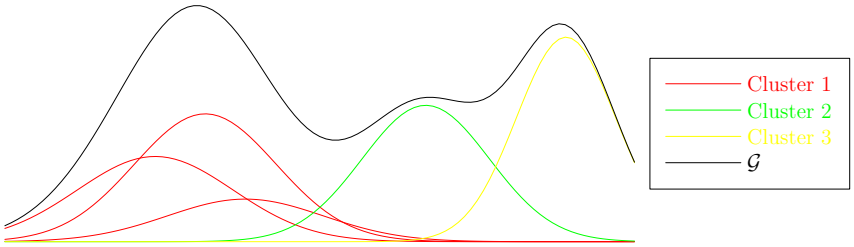

(c) Iteration 2: Cluster 1 and Cluster 2 in (b) are merged into one cluster.

Figure 5.3.: Iterations of Clustering Algorithm on an example case with $n_g = 5$ Gaussian functions in the sum $\mathcal{G}$. In the third iteration the algorithm finds no new pairs that satisfy the assumptions of Corollary 5.1.20. The algorithm ends after three iterations giving three clusters.

least two maxima in the absence of all other clusters. However, this contradicts the definition of Gaussian clusters as being clusters that have only one maximum for the sum of Gaussian functions whose indices are in the cluster. So our assumption that $\hat{m}^* > m^*$ is false. This completes the proof. □

In this section we developed an algorithm for clustering Gaussian functions in the sum $\mathcal{G}$. The next section gives an empirical approximation of the point of maximum of each cluster from where we can start hill-climbing or fixed point iterations to get the point of global maximum and the maximum value of the sum of Gaussian functions in each cluster.

5.3. Points of maximum of sum of Gaussian functions $\mathcal{G}$

In the previous section we considered an algorithm for partitioning the Gaussian functions in the sum $\mathcal{G}$ into a Gaussian clustering $\mathscr{C}$. In this section we show how to compute an approximation of the point of maximum for each Gaussian cluster $\mathfrak{C} \in \mathscr{C}$ which then serves as a starting point for the hill-climbing algorithm or fixed point iteration for computing the points of maximum of $\mathcal{G}$. Therefore, the number of starting points is equal to the number of clusters m^*.

The approximate point of maximum of a Gaussian cluster $\mathfrak{C} \in \mathscr{C}$ can be computed from the empirical formula

$$\alpha_{\mathfrak{C}} = \frac{\sum_{i \in \mathfrak{C}} \breve{a}_i \breve{b}_i}{\sum_{i \in \mathfrak{C}} \breve{a}_i} \tag{5.26}$$

where $\breve{a}_i$ is the height and $\breve{b}_i$ is the point of maximum of the Gaussian function corresponding to the i-th index in the Gaussian cluster $\mathfrak{C}$. It is intuitive to see that the point of maximum of a cluster is in the vicinity of the Gaussian function with the maximum height or in the vicinity of a point where more than one Gaussian functions are present. The empirical formula in Eq. (5.26) is based on this idea. In Figure 5.4 we see the approximate point of maximum computed from Eq. (5.26) for the Example in Figure 5.3.

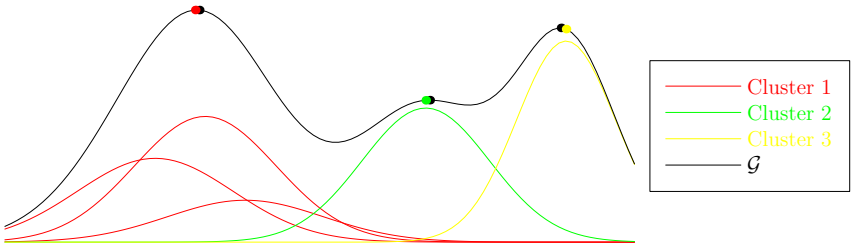

Figure 5.4.: Approximate point of maximum of Gaussian clusters computed by Eq. (5.26) for the example in Figure 5.3. The black dots are the exact points of maximum of $\mathcal{G}$ and the dots in the color corresponding to the color of the clusters are the approximate point of maxima computed by Eq. (5.26).

From Figure 5.4 we see that the approximate point of maximum of a Gaussian cluster is in the neighbourhood of the the point of maximum of the sum of Gaussian functions $\mathcal{G}$. We can now use a hill-climbing algorithm or a fixed point iterations to converge to the point of maximum starting at the approximate points of maximum of clusters. Algorithm 5.3.1 describes the process of finding the points of maximum of the sum of Gaussian functions $\mathcal{G}$.

In Algorithm 5.3.1 we provide the parameters $\breve{b}_i$ and $\breve{c}_i$ for all the Gaussian functions in the sum $\mathcal{G}$. An important information provided to the algorithm is the fixed point operator φ. If we give the fixed point operator from Eq. (5.5) we get the exact points of maximum for the Gaussian approximation. In Chapter 6 we use the fixed point operator for the total damage function that gives us the exact points of maximum for the total damage. Additionally, ϵ and $maxIter$ are also provided which decide the quality of the points of maximum computed and maximum number of iterations allowed, respectively. The Gaussian clustering is computed first and then an

Algorithm 5.3.1: Points of maximum of $\mathcal{G}$

Data: $\mathcal{G}$ with n_g Gaussian functions with parameters $\breve{a}_i$, $\breve{b}_i$ and $\breve{c}_i$, $i = 1, 2, \ldots, n_g$, ϵ, φ and $maxIter$
Result: α^*

```
1  begin
2      𝒞 ⟵ Get Gaussian clustering by Algorithm 5.2.1   ▷ Get Gaussian clustering for 𝒢.
3      m* ⟵ |𝒞|                                          ▷ Initialize number of clusters.
4      α* ⟵ 0_{m*}                                       ▷ Initialize points of maximum
5      for it ⟵ 1 to m* do
6          α_0 ⟵ α_{𝔠_it}                    ▷ Approximate cluster maximum from Eq. (5.26)
7          temp ⟵ 0
8          counter ⟵ 0
9          while |α_counter − temp| > ϵ and counter < maxIter do
10             temp ⟵ α_counter
11             counter ⟵ counter + 1
12             α_counter ⟵ φ(α_{counter−1})
13         end
14         α*_it ⟵ α_counter
15     end
16     Remove point of maxima in α* that are repeated more than once.
17     return α*
18 end
```

approximate point of maximum for each Gaussian cluster is computed. The approximate point of maximum is then used as the starting point for the fixed point equation (5.4) to get the point of maximum of $\mathcal{G}$. It is possible that even after starting at different points the fixed point iterations could still converge to the same point of maximum. This is evident from Theorem 5.2.9 which states that the number of clusters m^* is more than or equal to the number of maxima $\hat{m}^*$ of $\mathcal{G}$. Therefore, we remove those points of maxima that are repeated more than once in α^*. In the example in Figure 5.4 we have $m^* = \hat{m}^*$.

In this section we saw how to compute the points of maximum of the sum of Gaussian functions by using the Gaussian clustering computed by Algorithm 5.2.1. In the next section we use the Algorithms on more complex examples and discuss the results obtained.

5.4. Numerical results and discussion

In this section we apply Algorithm 5.2.1 and Algorithm 5.3.1 to some examples. In line 8 of Algorithm 5.2.1 we did not specify in detail how to choose pair of clusters that are merged. However, in Figure 5.3 we showed an example where we chose the cluster pairs moving from the leftmost clusters towards the rightmost clusters.

Next we see three possible ways to select pair of clusters that are merged:

1. The search for the pair of clusters that can be merged is started from the two leftmost clusters and we move towards the rightmost clusters. The steps are shown in Algorithm

5.4.1:

Algorithm 5.4.1: Choosing pair of clusters starting from left

Data: $\mathcal{G}$ with n_g Gaussian functions with parameters $\breve{b}_i$ and $\breve{c}_i$, $i = 1, 2, \ldots, n_g$ and Gaussian Clustering $\mathscr{C} = \{\mathfrak{C}_1, \mathfrak{C}_2, \ldots, \mathfrak{C}_{m^*}\}$.

Result: The index i and j of the clusters that can be merged or FALSE if no such clusters exist.

```
1  begin
2      m* ⟵ |𝒞|
3      for i ⟵ 1 to (m* − 1) do
4          for j ⟵ (i + 1) to m* do
5              if between-cluster distance, 𝔇_{𝔠_i,𝔠_j} ≤ 2 then
6                  return i, j
7              end
8          end
9      end
10     return FALSE
11 end
```

Algorithm 5.4.1 starts with the leftmost cluster and returns the indices if it has a between-cluster distance less than two with any other cluster, otherwise it moves one cluster to the right and repeats the process. The algorithm returns $FALSE$ if there does not exist any cluster pair with between-cluster distance less than two. Algorithm 5.4.1 in the worst case makes $\frac{1}{2}m^*(m^* - 1)$ calls to the between-cluster distance function.

2. The second method looks for a pair of clusters that can be merged starting from the two rightmost clusters and moving towards the leftmost clusters. The steps are identical to the steps of Algorithm 5.4.1 however we start from the rightmost cluster and move towards the leftmost cluster in this case:

Algorithm 5.4.2: Choosing pair of clusters starting from right

Data: $\mathcal{G}$ with n_g Gaussian functions with parameters $\breve{b}_i$ and $\breve{c}_i$, $i = 1, 2, \ldots, n_g$ and Gaussian Clustering $\mathscr{C} = \{\mathfrak{C}_1, \mathfrak{C}_2, \ldots, \mathfrak{C}_{m^*}\}$.

Result: The index i and j of the clusters that can be merged or FALSE if no such clusters exist.

```
1  begin
2      m* ⟵ |𝒞|
3      for i ⟵ m* to 2 do
4          for j ⟵ (i − 1) to 1 do
5              if between-cluster distance, 𝔇_{𝔠_i,𝔠_j} ≤ 2 then
6                  return i, j
7              end
8          end
9      end
10     return FALSE
11 end
```

Algorithm 5.4.2 makes in the worst case $\frac{1}{2}m^*(m^* - 1)$ calls to the between-cluster distance function.

3. In the previous two cases we looked for a possible cluster pair which had between-cluster distance less than two starting from the leftmost cluster or the rightmost cluster. However, this may not be the most efficient way to get clusters in the context of clustering Gaussian functions. In clustering Gaussian functions we want the largest clusters to have the maximum number of components (Gaussian functions). If we can find such clusters the probability of the maximum of the $\mathcal{G}$ to be suitably represented by the clusters is higher than any general cluster. Keeping this in mind we give a new algorithm where we find the largest cluster from within the Gaussian functions and repeat the process on the remaining functions until no more Gaussian functions are left to be clustered:

Algorithm 5.4.3: Choosing cluster with maximum number of Gaussian functions

Data: n_g Gaussian functions with parameters $\breve{b}_i$ and $\breve{c}_i$, $i = 1, 2, \ldots, n_g$.
Result: Gaussian cluster $\mathfrak{C}$ with maximum number of components and set of Gaussian functions not in $\mathfrak{C}$.

begin
  $m \longleftarrow n_g$
  $m^* \longleftarrow 0$ ▷ Initialize the size of largest cluster.
  $\mathfrak{C}_0 = \{1, 2, \ldots, n_g\}$ ▷ Basic cluster.
  $\mathfrak{C} \longleftarrow \emptyset$ ▷ Initialize the largest cluster.
  for $i \longleftarrow 1$ **to** m **do**
    $\mathfrak{C}_i \longleftarrow \{i\}$ ▷ Start with i-th Gaussian function as the Cluster
    $isSwap \longleftarrow TRUE$
    $\mathfrak{C}_{temp} \longleftarrow \mathfrak{C}_0 - \mathfrak{C}_i$ ▷ $\mathfrak{C}_{temp}$ has elements not in $\mathfrak{C}_i$
    while *isSwap* **do**
      $isSwap \longleftarrow FALSE$
      Assignment Step:
      for $j \longleftarrow 1$ **to** $|\mathfrak{C}_{temp}|$ **do**
        if *within-cluster distance after adding* $\mathfrak{C}_{temp,j}$ *to* $\mathfrak{C}_i$ *is less than two* **then**
          $\mathfrak{C}_i \longleftarrow \mathfrak{C}_i \cup \mathfrak{C}_{temp,j}$
        end
      end
      $\mathfrak{C}_{temp} \longleftarrow \mathfrak{C}_{temp} - \mathfrak{C}_i$
      Swapping Step:
      Find $q \in \mathfrak{C}_i$ with maximum decrease in within-cluster distance when removed from $\mathfrak{C}_i$.
      $\mathfrak{d}_{max} \longleftarrow$ the maximum decrease
      if *exists* $r \in \mathfrak{C}_{temp}$ *with minimum increase in within-cluster distance when added to* $\mathfrak{C}_i$ *and the increase in within-cluster distance is less than* $\mathfrak{d}_{max}$ **then**
        $\mathfrak{C}_i \longleftarrow (\mathfrak{C}_i - q) \cup r$
        $\mathfrak{C}_{temp} \longleftarrow (\mathfrak{C}_{temp} - r) \cup q$
        $isSwap \longleftarrow TRUE$
      end
    end
    if $m^* < |\mathfrak{C}_i|$ **then**
      $m^* \longleftarrow |\mathfrak{C}_i|$
      $\mathfrak{C} \longleftarrow \mathfrak{C}_i$
    end
  end
  return $\mathfrak{C}$, $\mathfrak{C}_0 - \mathfrak{C}$
end

Algorithm 5.4.3 finds the largest Gaussian cluster by building clusters starting at each given Gaussian function and selecting the largest cluster from them. For the i-th Gaussian function it consists of an assignment step (lines 13-17) and a swapping step (lines 19-25) which are repeated until there is no more swapping possible. In the assignment step it adds to the current cluster $\mathfrak{C}_i$ all Gaussian functions such that the within-cluster distance is less than two. In the swapping step it tries to find if there exist any Gaussian functions which are not in $\mathfrak{C}_i$ and can be swapped by a Gaussian function in $\mathfrak{C}_i$ such that the within-cluster distance is reduced. To give a Gaussian clustering, Algorithm 5.4.3 is repeatedly applied on the remaining Gaussian functions returned from previous run of the algorithm until all Gaussian functions are clustered. In worst case this algorithm makes $O(n_g^4)$ function calls to the within-cluster distance function. However, this algorithm has a potential for parallelization as computing of the largest cluster starting from each Gaussian function can be done on more than one threads simultaneously.

It is intuitive that the Gaussian clustering as a result of application of Algorithm 5.4.3 should in general result in larger clusters. The three algorithms can be made faster by a preprocessing step where we compute the maximum value of p_{ij} on the interval $\left[\breve{b}_i, \breve{b}_j\right]$ by using Lemma 5.1.5 $\forall i, j \in \{1, 2, \ldots, n_g\}$ and storing it as a matrix. Before we can compare the three methods we define the idea of a *strong clustering*.

Definition 5.4.1 (Strong Clustering)**.** Given n Gaussian clusterings $\mathscr{C}_i, i = 1, 2, \ldots, n$ each consisting of n_g Gaussian functions, then a strong clustering is one whose largest cluster has more elements than the largest cluster of other clusterings. If there are more than one clusterings with same number of elements in the largest cluster, we look at the second largest cluster and so on until there is just one clustering left or we have reached the last cluster. If more than one clusterings have same number of clusters and same number of Gaussian functions in each cluster, all of them are strong clusterings.

To compare how the three methods perform with the strong clustering as the main criterion, tests were performed where the three algorithms ran 20 times on 1000 different random tests for each $n_g \in \{1, 2, \ldots, 50\}$. One was added to the score for each method for every instance for which the method resulted in a strong clustering in comparison to the two other methods. If more than one method lead to the same Gaussian clustering all of their scores are increased by one. In Figure 5.5 we see the average scores for 20 runs of the three methods for different values of n_g.

As the number of Gaussian function n_g to be clustered increases we observe from Figure 5.5 that Algorithm 5.4.1 and Algorithm 5.4.2 result on an average, lesser number of strong clusterings. The scores for these two algorithms eventually goes to zero. Therefore, when $n_g \geq 10$ we use Algorithm 5.4.3.

So far we did not compare the three algorithms on the basis of time required for clustering. After running the three algorithms on 10000 test cases for many different values of n_g we see that Algorithm 5.4.3 takes approximately seven times the time taken by Algorithm 5.4.1 and Algorithm 5.4.2. Algorithms 5.4.1 and 5.4.2 as expected took approximately the same amount of time. In Figure 5.6 we see the average time for clustering taken by the three algorithms for different values of n_g.

Next we apply Algorithm 5.2.1 on a specific example.

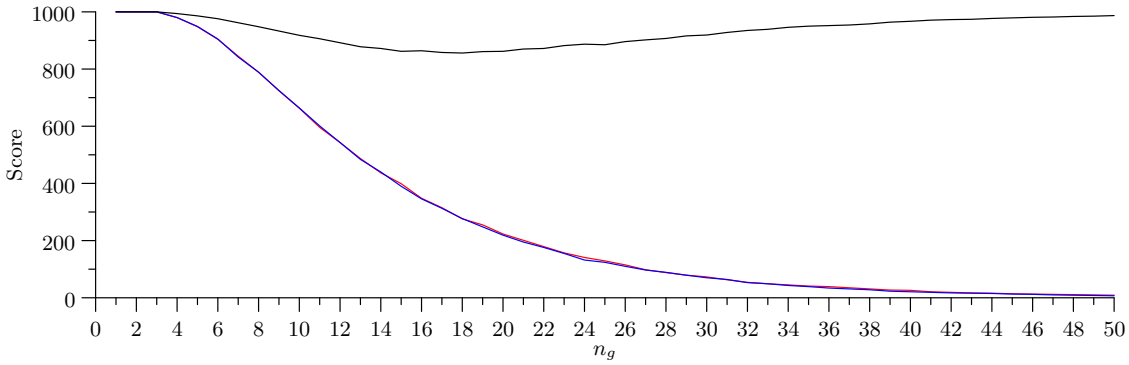

Figure 5.5.: Average scores for 20 runs of the Algorithm 5.4.1 (red), Algorithm 5.4.2 (blue) and Algorithm 5.4.3 (black) on 1000 random tests with respect to the strong clustering in Definition 5.4.1. The maximum possible score is 1000.

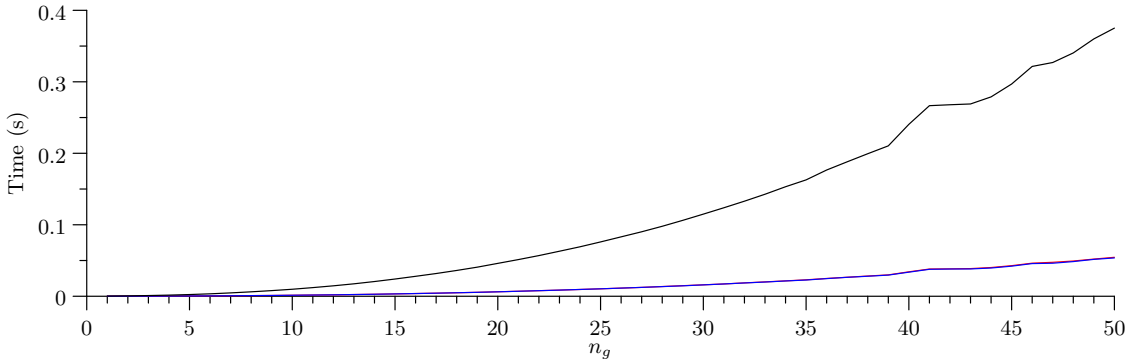

Figure 5.6.: Average runtime of the Algorithm 5.4.1 (red), Algorithm 5.4.2 (blue) and Algorithm 5.4.3 (black) for 10000 random tests for different values of n_g. Tests were performed on a 32-bit Ubuntu 13.10 system with 3.8 GB RAM and Core$^{\text{TM}}$ i3 CPU M 380 from Intel®.

Example 5.4.2. We randomly generate 12 Gaussian functions with parameters $\breve{a}_i$, $\breve{b}_i$ and $\breve{c}_i$ for $i = 1, 2, \ldots, 12$ as below:

The Gaussian functions and the sum of these Gaussian functions is shown in the Figure 5.7. We see that the sum of the Gaussian functions have two peaks.

Algorithm 5.2.1 is run on this example. We first use Algorithm 5.4.1 to identify clusters that can be merged to get the Gaussian clustering also seen in Figure 5.8:

$$\mathscr{C}_{Left2Right} = \{\{1, 2, 3, 4\}, \{5, 6, 7\}, \{8, 9, 10, 11, 12\}\}.$$

Then we use Algorithm 5.4.2 in Algorithm 5.2.1 to identify clusters that can be merged to get the Gaussian clustering also seen in Figure 5.9:

$$\mathscr{C}_{Right2Left} = \{\{1, 2, 3, 4\}, \{5, 6\}, \{7, 8, 9, 10, 11, 12\}\}.$$

Table 5.1.: Values of parameter $\breve{a}_i$, $\breve{b}_i$ and $\breve{c}_i$ of Gaussian functions used in the example.

i	$\breve{a}_i$	$\breve{b}_i$	$\breve{c}_i$
1	0.2305	0.2549	0.6786
2	0.5870	0.5765	0.8108
3	0.5502	0.5936	0.6063
4	0.8000	0.9309	0.7359
5	0.2077	1.1576	1.0000
6	0.3507	1.7185	0.7868
7	0.3012	1.9654	1.0000
8	0.6225	2.1576	0.8085
9	0.8000	2.3395	0.7468
10	0.1948	2.4370	0.8328
11	0.4709	2.4512	0.9443
12	0.8000	2.9198	1.0000

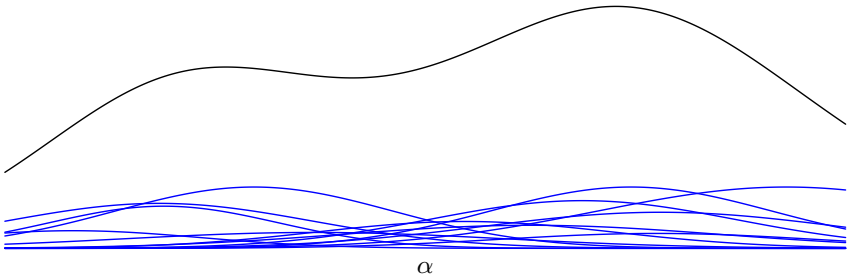

Figure 5.7.: Gaussian functions and their sum $\mathcal{G}$ from Example 5.4.2.

Finally, we use Algorithm 5.2.1 with Algorithm 5.4.3 for finding largest cluster at each iteration from the unclustered Gaussian functions to get the Gaussian clustering also seen in Figure 5.10:

$$\mathscr{C}_{LargestCluster} = \{\{1,2\},\{3,4,5,6,7,9\},\{10,8\},\{11,12\}\}.$$

We see that the three Gaussian clusterings obtained have different Gaussian clusters. The Gaussian clustering from Algorithm 5.4.1 $\mathscr{C}_{Left2Right}$ and the Gaussian clustering from Algorithm 5.4.2 $\mathscr{C}_{Right2Left}$ has three Gaussian clusters and the Gaussian clustering from Algorithm 5.4.3 $\mathscr{C}_{LargestCluster}$ has four Gaussian clusters. However, the largest Gaussian cluster in $\mathscr{C}_{LargestCluster}$ and $\mathscr{C}_{Right2Left}$ has six elements.

In Figure 5.7 we see that the example sum of Gaussian function $\mathcal{G}$ has two peaks. In Figure 5.11 we see the approximate point of maximum of the Gaussian clusters in the Gaussian clusterings obtained in Example 5.4.2. We see that the approximate point of maximum of Gaussian clusters obtained in the case of Algorithm 5.4.3 is closer to the actual points of maximum when compared with the approximate points of maximum of the Gaussian clusters obtained in the other two algorithms. In what follows, we use Algorithm 5.4.3 for clustering of the Gaussian functions in a sum $\mathcal{G}$.

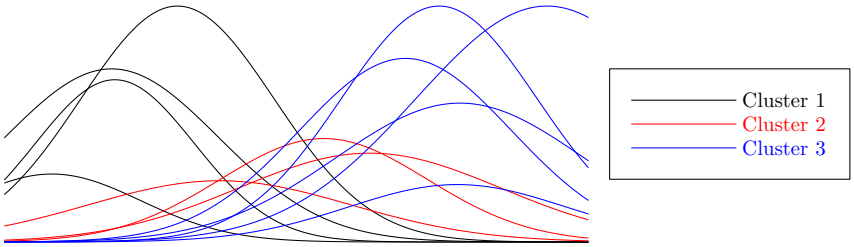

Figure 5.8.: Gaussian clustering $\mathscr{C}_{Left2Right}$ obtained by applying Algorithm 5.2.1 using Algorithm 5.4.1 to identify clusters that can be merged together.

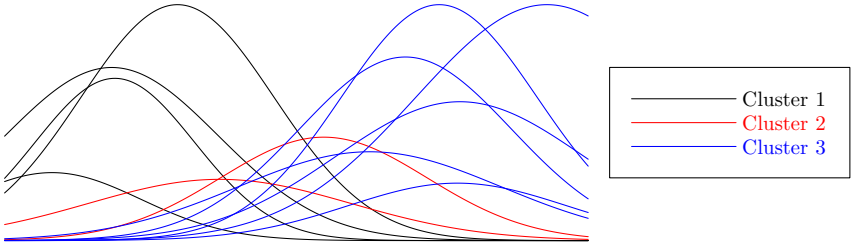

Figure 5.9.: Gaussian clustering $\mathscr{C}_{Right2Left}$ obtained by applying Algorithm 5.2.1 using Algorithm 5.4.2 to identify clusters that can be merged together.

In this chapter we proved conditions for the sum of Gaussian functions $\mathcal{G}$ to have a single maximum. We also gave bounds on the number of maxima when the conditions for single maximum are not satisfied by the Gaussian functions in the sum $\mathcal{G}$. Using these conditions we gave a clustering algorithm. Finally, we described three methods by which the clustering part of the algorithm could be done and compared the three methods with respect to the strong clustering and average runtime. In the next chapter, we use the clustering algorithm for finding the plane of maximum damage for each hotspot at each iteration in the optimization.

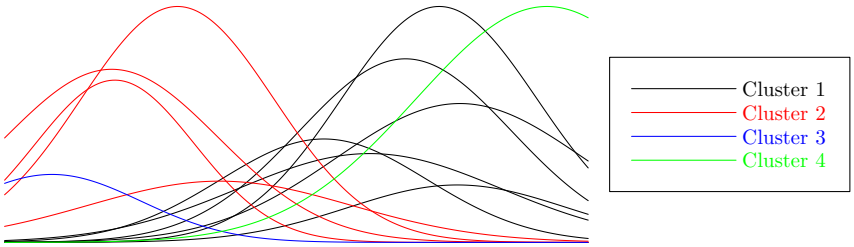

Figure 5.10.: Gaussian clustering $\mathscr{C}_{Right2Left}$ obtained by applying Algorithm 5.2.1 using Algorithm 5.4.2 to identify clusters that can be merged together.

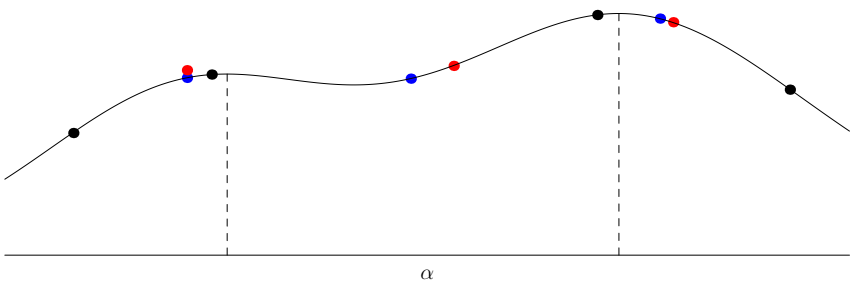

Figure 5.11.: Approximate point of maximum obtained for each Gaussian cluster of the Gaussian clusterings obtained in Example 5.4.2 for the three algorithms. The red dots, the blue dots and the black dots represent the approximate point of maximum for each Gaussian cluster obtained by Algorithm 5.4.1 ($\mathscr{C}_{Left2Right}$), Algorithm 5.4.2 ($\mathscr{C}_{Right2Left}$) and Algorithm 5.4.3 ($\mathscr{C}_{LargestCluster}$), respectively. Since, Algorithm 5.4.2 and Algorithm 5.4.1 have a common Gaussian cluster there is an overlap as seen by two dots one above another. By dashed lines we see the location of the two peaks.

6. Testrig optimization with clustering

In Chapter 4, we remodeled damage from a block load as Gaussian functions when the S-N curve has one slope. In Section 6.1, we see how the total damage is computed from the Gaussian functions which approximate the damage from a block load. In Chapter 5, we gave a clustering algorithm to cluster the Gaussian functions in the sum of Gaussian functions $\mathcal{G}$. We use Algorithm 5.3.1 on the clusters obtained from the Clustering algorithm to get the exact point of maxima for the total damage at each hotspot in Section 6.2. In Section 6.3, we compare the results obtained for the damage optimization with discretization and clustering on two examples. Finally, we describe a new application of the Gaussian functions and clustering algorithm to shift the plane of maximum total damage to a desired plane α. This shifting of the plane of maximum total damage at a hotspot to a desired plane angle α was not achievable from the previous approaches.

6.1. Total damage from approximation

In Section 4.4, damage was remodelled as Gaussian functions for the load time series with one block for the interval $[0, \pi)$. We have so far not discussed the general case when the load time series with block loads $\mathbf{L}_b$ has m block loads. In this case the load time series with block loads $\mathbf{L}_b$ can be represented as amplitude matrix $\mathbf{L}_{b,a}$. The stress matrix is then given from Eq. (2.49) as

$$\mathbf{\Sigma}_{\mathbf{x}}(\mathbf{L}_{b,a}) = \tilde{\boldsymbol{\sigma}}_{\mathbf{x}}\mathbf{L}_{b,a} = (\boldsymbol{\sigma}_{\mathbf{x}}(\mathbf{l}_{b,1}), \boldsymbol{\sigma}_{\mathbf{x}}(\mathbf{l}_{b,2}), \cdots, \boldsymbol{\sigma}_{\mathbf{x}}(\mathbf{l}_{b,m})) = (\boldsymbol{\sigma}_1, \boldsymbol{\sigma}_2, \ldots, \boldsymbol{\sigma}_m)$$

at hotspot $\mathbf{x}$. The i-th column of the stress matrix $\mathbf{\Sigma}_{\mathbf{x}}$ represents the stress at hotspot $\mathbf{x}$ induced by the amplitudes of the i-th block load for each force/moment acting through the actuators $\mathbf{l}_{b,i}$. We can partition $\mathbf{\Sigma}_{\mathbf{x}}$ into two sets depending on if $a(\boldsymbol{\sigma}_i) \geq b(\boldsymbol{\sigma}_i)$. We include all the block loads for which $a(\boldsymbol{\sigma}_i) \geq b(\boldsymbol{\sigma}_i)$ in the set $\mathcal{I}_g$ and the remaining block loads in the set $\mathcal{I}_l$.

$$\mathcal{I}_g := \{i | a(\boldsymbol{\sigma}_i) \geq b(\boldsymbol{\sigma}_i) \geq 0, i = 1, 2, \ldots, m\}.$$

$$\mathcal{I}_l := \{1, 2, \ldots, m\} - \mathcal{I}_l.$$

The total damage at any point $\alpha \in [0, \pi)$ is then given as

$$G(\mathbf{\Sigma}_{\mathbf{x}}(\mathbf{L}_{b,a}), \alpha) = \sum_{i \in \mathcal{I}_g} g_{[0,\pi)}(\boldsymbol{\sigma}_i, \alpha) + \sum_{j \in \mathcal{I}_l} \hat{g}(\boldsymbol{\sigma}_j, \alpha). \tag{6.1}$$

where the approximation function $g_{[0,\pi)}$ is from Eq. (4.105) and the approximation function $\hat{g}$ is from Eq. (4.136).

We simplify Eq. (6.1) by renaming and renumbering each Gaussian function. In Eq. (6.1) we have

altogether $3|\mathcal{I}_g| + 6|\mathcal{I}_l|$ Gaussian functions. Three each for every block i in $\mathcal{I}_g$ and six altogether from the two peaks for every block j in $\mathcal{I}_l$. Let us denote by $\mathcal{B}$ the list of points of maximum of all the Gaussian functions in the approximation of the damage due to the individual block loads of the load time series $\mathbf{L}$, i.e., all elements of list $\mathcal{B}$ are from one of $\breve{b}(\boldsymbol{\sigma}_i)+t\pi$, $\breve{b}_1(\boldsymbol{\sigma}_j)+t\pi$ or $\breve{b}_2(\boldsymbol{\sigma}_j)+t\pi$, where $t \in \{-1, 0, 1\}$, $i \in \mathcal{I}_g$ and $j \in \mathcal{I}_l$. The elements in $\mathcal{B}$ are arranged in an ascending order, i.e., $\mathcal{B}_1 = \min \mathcal{B}$ and $\mathcal{B}_{3|\mathcal{I}_g|+6|\mathcal{I}_l|} = \max \mathcal{B}$.

For every element in $\mathcal{B}$ we have corresponding elements in lists $\mathcal{A}$ and $\mathcal{C}$. $\mathcal{A}$ consists of the parameters $\breve{a}(\boldsymbol{\sigma}_i)$, $\breve{a}_1(\boldsymbol{\sigma}_j)$ and $\breve{a}_2(\boldsymbol{\sigma}_j)$, $\mathcal{C}$ has elements consisting of $\breve{c}(\boldsymbol{\sigma}_i)$, $\breve{c}_1(\boldsymbol{\sigma}_j)$ and $\breve{c}_2(\boldsymbol{\sigma}_j)$ where $i \in \mathcal{I}_g$ and $j \in \mathcal{I}_l$. However, each of these parameters occur thrice in the list corresponding to each t in $\{-1, 0, 1\}$. Finally we give a list $\mathcal{D}$ which consists of $\breve{d}(\boldsymbol{\sigma}_i)$ for $i \in \mathcal{I}_g$ and $\breve{d}_1(\boldsymbol{\sigma}_j)$ for $j \in \mathcal{S}_l$ and the order here is not important. The total damage G in Eq. (6.1) at hotspot $\mathbf{x}$ can now be rewritten as

$$G(\boldsymbol{\Sigma}_{\mathbf{x}}(\mathbf{L}_{b,a}), \alpha) = \sum_{i=1}^{3|\mathcal{I}_g|+6|\mathcal{I}_l|} \mathcal{A}_i \exp\left(-\left(\frac{\alpha - \mathcal{B}_i}{\mathcal{C}_i}\right)^2\right) + \sum_{i=1}^{m} \mathcal{D}_i \tag{6.2}$$

The total damage G from Eq. (6.2) is similar to the sum of Gaussian functions $\mathcal{G}$ in Chapter 5. So, all the results obtained in that chapter are also applicable to the total damage G. In the next section, we explain the steps involved in using the Gaussian approximation from Chapter 4 and clustering algorithm from Chapter 5 in the testrig damage optimization (WSDP).

6.2. Optimization with clustering

In this section, we use the approximate point of maxima of the clusters obtained by the clustering algorithm to get the exact point of maximum of the total damage at every hotspot $\mathbf{x}_i \in \mathfrak{X}$ during each iteration in the optimization. Before we can give the algorithm for finding the point of maximum at hotspot $\mathbf{x}_i$ we look at the roots of the first derivative of the total damage $\hat{D}_{\mathbf{x}_i}$ with respect to α assuming all other parameters are fixed as given in Theorem 2.4.11. The roots of the first derivative are given by the equation

$$\frac{d\hat{D}_{\mathbf{x}_i}(\hat{\mathbf{L}}, \mathcal{V}, \alpha)}{d\alpha} = \frac{k}{N_e \sigma_e^k} \sum_{j=1}^{m} \nu_j |\mathbf{n}(\alpha) \cdot \boldsymbol{\sigma}_{\mathbf{x}_i,j}|^{k-2} \left(\mathbf{n}(\alpha) \cdot \boldsymbol{\sigma}_{\mathbf{x}_i,j}\right) \left(\mathbf{n}'(\alpha) \cdot \boldsymbol{\sigma}_{\mathbf{x}_i,j}\right) = 0 \tag{6.3}$$

The above equation can be written in the form of a fixed point equation that is used as the fixed point operator in Algorithm 6.2.1 for finding the point of maximum and the total maximum damage.

Theorem 6.2.1. *Equation* (6.3) *is equivalent to the fixed point equation*

$$\alpha = \varphi_d(\alpha)$$

where

$$\varphi_d(\alpha) = \frac{1}{2} \tan^{-1}\left(\frac{\sum_{j=1}^{m} \nu_j |\mathbf{n}(\alpha) \cdot \boldsymbol{\sigma}_{\mathbf{x},j}|^{k-2} \left(\mathbf{n}(\alpha) \cdot \boldsymbol{\sigma}_{\mathbf{x}_i,j}\right) \left(\boldsymbol{\sigma}_{\mathbf{x}_i,j,xx} - \boldsymbol{\sigma}_{\mathbf{x}_i,j,yy}\right)}{2 \sum_{j=1}^{m} \nu_j |\mathbf{n}(\alpha) \cdot \boldsymbol{\sigma}_{\mathbf{x}_i,j}|^{k-2} \left(\mathbf{n}(\alpha) \cdot \boldsymbol{\sigma}_{\mathbf{x},j}\right) \boldsymbol{\sigma}_{\mathbf{x}_i,j,xy}}\right) \tag{6.4}$$

with $\boldsymbol{\sigma}_{\mathbf{x}_i,j} = (\boldsymbol{\sigma}_{\mathbf{x}_i,j,xx}, \boldsymbol{\sigma}_{\mathbf{x}_i,j,yy}, \boldsymbol{\sigma}_{\mathbf{x}_i,j,xy})^T$.

Proof. We can rewrite Eq. (6.3) as

$$\frac{k}{N_e\sigma_e^k}\sum_{j=1}^{m}\nu_j|\mathbf{n}(\alpha)\cdot\boldsymbol{\sigma}_{\mathbf{x}_i,j}|^{k-2}\left(\mathbf{n}(\alpha)\cdot\boldsymbol{\sigma}_{\mathbf{x}_i,j}\right)\times \\ \left((-\cos(2\alpha),\cos(2\alpha),2\sin(2\alpha))\cdot(\boldsymbol{\sigma}_{\mathbf{x}_i,j,xx},\boldsymbol{\sigma}_{\mathbf{x}_i,j,yy},\boldsymbol{\sigma}_{\mathbf{x}_i,j,xy})^T\right)=0$$

$$\frac{k}{N_e\sigma_e^k}\sum_{j=1}^{m}\nu_j|\mathbf{n}(\alpha)\cdot\boldsymbol{\sigma}_{\mathbf{x}_i,j}|^{k-2}\left(\mathbf{n}(\alpha)\cdot\boldsymbol{\sigma}_{\mathbf{x}_i,j}\right)\times \\ \left(-\cos(2\alpha)\boldsymbol{\sigma}_{\mathbf{x}_i,j,xx}+\cos(2\alpha)\boldsymbol{\sigma}_{\mathbf{x}_i,j,yy}+2\sin(2\alpha)\boldsymbol{\sigma}_{\mathbf{x}_i,j,xy}\right))=0$$

After collecting terms with $\cos(2\alpha)$ and $\sin(2\alpha)$ together and rearranging we get

$$\left(\frac{2k}{N_e\sigma_e^k}\sum_{j=1}^{m}\nu_j|\mathbf{n}(\alpha)\cdot\boldsymbol{\sigma}_{\mathbf{x}_i,j}|^{k-2}\left(\mathbf{n}(\alpha)\cdot\boldsymbol{\sigma}_{\mathbf{x}_i,j}\right)\boldsymbol{\sigma}_{\mathbf{x}_i,j,xy}\right)\sin(2\alpha) \\ =\left(\frac{k}{N_e\sigma_e^k}\sum_{j=1}^{m}\nu_j|\mathbf{n}(\alpha)\cdot\boldsymbol{\sigma}_{\mathbf{x}_i,j}|^{k-2}\left(\mathbf{n}(\alpha)\cdot\boldsymbol{\sigma}_{\mathbf{x}_i,j}\right)\left(\boldsymbol{\sigma}_{\mathbf{x}_i,j,xx}-\boldsymbol{\sigma}_{\mathbf{x}_i,j,yy}\right)\right)\cos(2\alpha)$$

Further simplification gives us the result. □

We use φ_d from Eq. (6.4) in Algorithm 6.2.1 to find the point of maximum total damage. We can now find the point of maximum total damage at each iteration of the optimization. In the next section, we use Algorithm 6.2.1 in the optimization and compare the results obtained with the results from the discretization for two examples.

6.3. Numerical results and comparisons

In this section, we compare the results obtained from the testrig damage optimization problem with and without clustering. We do not discuss here the testrig stress optimization problem as in Section 3.2 we had already seen that testrig damage optimization is better. From the results presented in Section 3.2, it was seen that the maximum total damage from discretization of the interval of plane angle α introduces discretization errors which could be as high as 10% at more than one hotspot. This would lead to overestimation of the fatigue lifetime of a component. Therefore, the remodeling of damage and the corresponding clustering algorithm was developed to be able to remove the discretization errors so that the results of the optimization are more reliable and give the actual picture of what is to be expected.

We compare the two methods for one testrig configuration on two test example. The first example being that of the knuckle from the previous considerations in Section 3.2 where we now assume that the material has one slope and the second example is an artificial component created for testing of the algorithms that are developed. At the end of this section, we give a new application of the clustering algorithm to restrict the plane of maximum total damage resulting at a hotspot

Algorithm 6.2.1: The plane of maximum total damage $\alpha^*_{\mathbf{x}_i}$ and the total maximum damage for hotspot $\mathbf{x}_i$ using the Gaussian approximation and clustering during the optimization

Data: The amplitude vector at p-th iteration $\hat{\mathbf{L}}_p$, stress tensor $\tilde{\boldsymbol{\sigma}}_{\mathbf{x}_i}$ at hotspot $\mathbf{x}_i$ and number of blocks m.
Result: The plane of maximum total damage $\alpha^*_{\mathbf{x}_i}$ and the maximum damage.

begin
  $\widehat{\boldsymbol{\Sigma}} \longleftarrow \hat{\boldsymbol{\Sigma}}_{\mathbf{x}_i}\hat{\mathbf{L}} = (\boldsymbol{\sigma}_1, \boldsymbol{\sigma}_2, \ldots, \boldsymbol{\sigma}_m)$ ▷ Compute stress σ_i for all blocks.
  for $j \longleftarrow 1$ **to** m **do**
    Compute $a(\boldsymbol{\sigma}_j)$ from Eq. (2.12) and $b(\boldsymbol{\sigma}_j)$ from Eq. (2.9)
    if $a(\boldsymbol{\sigma}_j) \geq b(\boldsymbol{\sigma}_j)$ **then**
      Compute $\breve{c}(\boldsymbol{\sigma}_j)$ from fixed point equation in Eq. (4.111).
      Compute $\breve{b}(\boldsymbol{\sigma}_j) = \alpha^+_{max}(\boldsymbol{\sigma}_j)$ from Eq. (2.18), $\breve{a}(\boldsymbol{\sigma}_j)$ from Eq. (4.109) and $\breve{d}(\boldsymbol{\sigma}_j)$ from Eq. (4.110)
      Assign to the ordered lists $\mathcal{A}$, $\mathcal{B}$, $\mathcal{C}$ and $\mathcal{D}$ for Eq. (6.2) to hold.
    else
      Compute $\breve{c}_1(\boldsymbol{\sigma}_j)$ from fixed point equation in Eq. (4.130) and $\breve{c}_2(\boldsymbol{\sigma}_j)$ from fixed point equation in Eq. (4.131).
      Compute $\breve{b}_1(\boldsymbol{\sigma}_j) = \alpha^-_{max,1}(\boldsymbol{\sigma}_j)$ from Eq. (2.36), $\breve{b}_2(\boldsymbol{\sigma}_j) = \alpha^-_{max,2}(\boldsymbol{\sigma}_j)$ from Eq. (2.36) and $\breve{a}_1(\boldsymbol{\sigma}_j)$, $\breve{a}_2(\boldsymbol{\sigma}_j)$ and $\breve{d}_1(\boldsymbol{\sigma}_j)$ satisfying Eq. (4.137), Eq. (4.138) and Eq. (4.139).
      Assign to the ordered lists $\mathcal{A}$, $\mathcal{B}$, $\mathcal{C}$ and $\mathcal{D}$ for Eq. (6.2) to hold.
    end
  end
  $\alpha^*_{\mathbf{x}_i} \longleftarrow$ Algorithm 5.3.1 with lists $\mathcal{B}$ and $\mathcal{C}$, fixed point operator φ_d from Eq. (6.4), ϵ and $maxIter$.
  Evaluate $\hat{D}_{\mathbf{x}_i}$ at each point in $\alpha^*_{\mathbf{x}_i}$ and return the point of maximum and the maximum total damage value.
end

from the optimized load time series in the neighborhood of some point.

6.3.1. First Example: Knuckle

We described the purpose of a knuckle in a vehicle in Section 3.2.1. The knuckle we are using for our algorithms is shown in Figure 3.2. The knuckle has seven possible attachment points. We use one of these attachment point as the fixation point A_f to fix the component in the testrig. We do not want the number of force/moment n acting through the actuators to be more than three so in all the results presented we have $n = 3$. The number of hotspots n_h is given to be ten. The location of the ten hotspots is given by $\mathfrak{X} = \{\mathbf{x}_1, \mathbf{x}_2, \ldots, \mathbf{x}_{10}\}$. We have been given the reference stress time series and the the reference damage values for each hotspot. The reference damage values $D^{(ref)}$ for the hotspots are given in Table 3.1.

The material of the knuckle is assumed to have one slope in the S-N curve. The value of the alternating stress where the slope changes is $\sigma_e = 55.01kPa$ and the corresponding value of the number of cycles is $N_e = 1 \times 10^8$. The ultimate tensile stress and the maximum allowed stress value is given as $\sigma_u = 190.5kPa$ and $\sigma_{max} = 190.5kPa$, respectively. The slope is $k = 5$. We use the inbuilt function *fmincon* of MATLAB with the *interior-point* algorithm for the damage

optimization.

We will again use the testrig configuration $\mathcal{TC}_2$ from Eq. (3.20) to compare the results obtained from optimization with and without clustering.

$$\mathcal{TC}_2 = (3, \{5, 4, 2\}, \{(5, \{f_x\}), (4, \{f_y\}), (2, \{f_z\})\}) \tag{6.5}$$

The index of the fixation point is $A_f = 3$. We apply load time series at $\mathfrak{F} = (5_{f_x}, 4_{f_y}, 2_{f_z})$, i.e., at the attachment point with index 5 we apply forces along the x-axis, at the attachment point with index 4 we apply forces along the y-axis and at the attachment point with index 2 we apply forces along the z-axis. For the damage optimization problem we additionally fix the number of block loads m to 15, the number of cycles for each block load $\nu_i = 5, i = 1, 2, \ldots, m$ and the weights w_i to be all equal. The constraints on the maximum and minimum loads that can be applied through the actuators is given as $l_l = -10000$ Newtons and $l_u = 10000$ Newtons. We are also given the stress tensor $\tilde{\boldsymbol{\sigma}}_{\mathbf{x}_i}$ for the ten hotspots.

For both the damage optimization with and without clustering we used as the starting point the same random vector with maximum magnitude half the maximum allowed load l_u in the testrig. This is a feasible point. All calculations are done on an Intel Core i3 CPU with 2.53 GHz and 4 GB RAM. Calculating a solution using damage optimization without clustering takes 102.31 seconds for 614 iterations. This corresponds to an average of 0.166 seconds for each iteration. On the other hand calculating a solution using damage optimization with clustering takes 424, 87 seconds for 582 iterations. This corresponds to an average of 0.723 seconds for each iteration. We see that the clustering is 4 times slower but the objective function value for damage optimization without clustering is 3.4769 while that for damage optimization with clustering is 3.4495. One thing to note here is that the objective function value ideally should be as close as possible to two but since we have restricted the maximum load that can be applied to 10000 Newtons and reduced the number of blocks to 15 this is expected. The runtime for damage optimization with clustering depends on the number of blocks chosen as the clustering algorithm is expensive. One way to reduce the time would be by parallelization of the clustering algorithm.

In Figure 6.1, we see the maximum total damage at the ten hotspots resulting from the load time series obtained through damage optimization without clustering and with clustering. We see in Figure 6.1 that the maximum total damage from the damage optimization with clustering is at least as close or closer to the reference damage when compared with the maximum total damage from the damage optimization without clustering at nine hotspots. Therefore, we get slightly better results in terms of the total maximum damage.

In Table 6.1, we see the magnitude of relative error for the two cases. As expected, we observe that the damage optimization with clustering has slightly better results:

In Figure 6.2, we see the points of maximum total damage returned by the clustering algorithm. All the points of the maximum total damage returned coincide with the actual points of maximum. Therefore, the maximum total damage used at each iteration of the optimization is the actual maximum total damage. The solution of the optimization problem are more reliable when clustering is used.

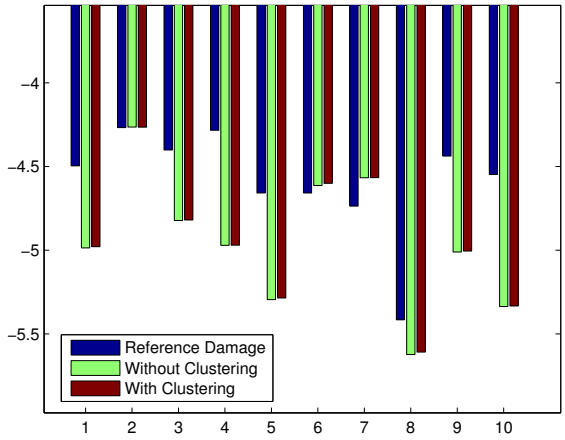

Figure 6.1.: The maximum total damage at the ten hotspots resulting from the load time series obtained through damage optimization without clustering (green) and with clustering (brown). The horizontal axis is the index of the hotspots and the vertical axis is the damage values on the logarithmic scale.

i	$\frac{\lvert D^{(ref)}_{\mathbf{x}_i} - \tilde{D}_{\mathbf{x}_i} \rvert}{\tilde{D}_{\mathbf{x}_i}}$ w/o	$\frac{\lvert D^{(ref)}_{\mathbf{x}_i} - \tilde{D}_{\mathbf{x}_i} \rvert}{\tilde{D}_{\mathbf{x}_i}}$ w/
1	2.0875	2.0361
2	0.0084	0.0059
3	1.6379	1.6207
4	3.8652	3.8582
5	3.3339	3.2378
6	0.0970	0.1226
7	0.3239	0.3246
8	0.6136	0.5582
9	2.7382	2.6902
10	5.1373	5.0910

Table 6.1.: The relative error in damage for maximum total damage computed from the load time series obtained as a result of the two optimization.

6.3.2. Second Example: Artificial Component

The component in Figure 6.3 has four possible attachment points. We use one of these attachment point as the fixation point A_f to fix the component in the testrig. We do not want the number of force/moment n acting through the actuators to be more than three so in all the results presented we have $n = 3$. The number of hotspots n_h is given to be ten. The location of the ten hotspots is given by $\mathfrak{X} = \{\mathbf{x}_1, \mathbf{x}_2, \ldots, \mathbf{x}_{10}\}$. We have been given the reference stress time series and the the reference damage values for each hotspot. The reference damage values $D^{(ref)}$ for the hotspots are given in Table 3.1:

The material of the component has one slope in the S-N curve. The value of the alternating stress on the S-N curve is $\sigma_e = 80kPa$ and the corresponding value of the number of cycles is $N_e = 1 \times 10^6$. The ultimate tensile stress and the maximum allowed stress value is given as

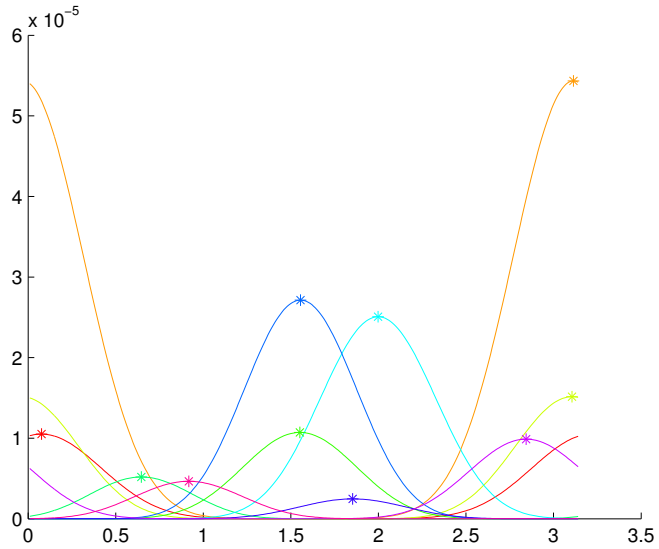

Figure 6.2.: The total damage function for the ten hotspots for the plane angle $\alpha \in [0, \pi)$. With * are shown the points of total maximum damage returned by the clustering algorithm. The horizontal axis gives the plane α and the vertical axis gives the total damage.

i	$D_{\mathbf{x}_i}^{(ref)}$
1	3.7225×10^{-3}
2	2.5521×10^{-3}
3	1.4389×10^{-3}
4	5.9046×10^{-4}
5	5.0265×10^{-4}
6	4.9796×10^{-4}
7	5.0265×10^{-4}
8	4.9796×10^{-4}
9	4.5812×10^{-4}
10	3.8482×10^{-4}

Table 6.2.: The reference damage values for the ten hotspots on the component.

$\sigma_u = 450$ kPa and $\sigma_{max} = 450$ kPa, respectively. The slope is $k = 5$.

The testrig configuration we consider is given as:

$$\mathcal{TC} = (1, \{2, 3, 4\}, \{(2, \{f_z\}), (3, \{f_x\}), (4, \{f_y\})\}). \tag{6.6}$$

The index of the fixation point is $A_f = 1$. We apply load time series at $\mathfrak{F} = (2_{f_z}, 3_{f_x}, 4_{f_y})$, i.e., at the attachment point with index 2 we apply forces along the z-axis, at the attachment points with index 3 we apply forces along the x-axis and at the attachment point with index 4 we apply forces along the y-axis. For the damage optimization problem we additionally fix the number of block loads m to 10, the number of cycles for each block load $\nu_i = 1000, i = 1, 2, \ldots, m$ and the weights w_i to be all equal. The constraints on the maximum and minimum loads that can be applied through the actuators is given as $l_l = -20000$ Newtons and $l_u = 20000$ Newtons, respectively. We are also given the stress tensor $\tilde{\boldsymbol{\sigma}}_{\mathbf{x}_i}$ for the ten hotspots.

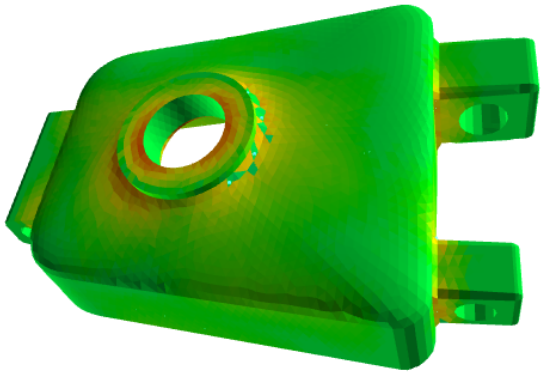

Figure 6.3.: An artificial test example.

For the damage optimization we used a random vector with maximum magnitude half the maximum allowed load l_u in the testrig. All calculations are done on an Intel Core i3 CPU with 2.53 GHz and 4 GB RAM. Calculating a solution using damage optimization with clusters takes 60.40 seconds for 158 iterations. This corresponds to an average of 0.38 seconds for each iteration. Calculating a solution using damage optimization without clusters takes 16.58 seconds for 167 iterations. This corresponds to an average of 0.099 seconds for each iteration. Again, damage optimization without clusters is faster but takes more number of iterations.

The objective function value for the damage optimization with clustering and without clustering are almost the same at 2.0302 and 2.0304, respectively. As discussed earlier the minimum value of the objective function is two and both these values are close to two. So, both these approach work equally well for the artificial example.

6.3.3. Example: Shifting plane of maximum total damage in the neighborhood of a given point.

In this section we show that using the conditions developed in Chapter 5 we can add additional constraint to the optimization problem which restricts the plane of maximum damage for a hotspot to lie in the neighborhood of a selected point. We take the same testrig configuration as in Section 6.3.2. The additional constraint was added to the hotspot with index 1 and the selected point was $\hat{\alpha} = 1.0$. The constraint is

$$\left\| \frac{2(\hat{\alpha} - \breve{b}_{\mathbf{x}_1,j})^2}{\breve{c}^2_{\mathbf{x}_1,j}} \right\|_\infty \leq 2 \tag{6.7}$$

where $\breve{b}_{\mathbf{x}_1,j}$ and $\breve{c}_{\mathbf{x}_1,j}$ are the parameters of the Gaussian function approximating j-th block load. This is a naive approach and more sophisticated approaches could be use to get even better results than presented here.

In Figure 6.4, we see the plot of the total damage with (red) and without (blue) the additional constraint from Eq. (6.7).

In this section, we looked at three examples where we applied the clustering algorithm to compute

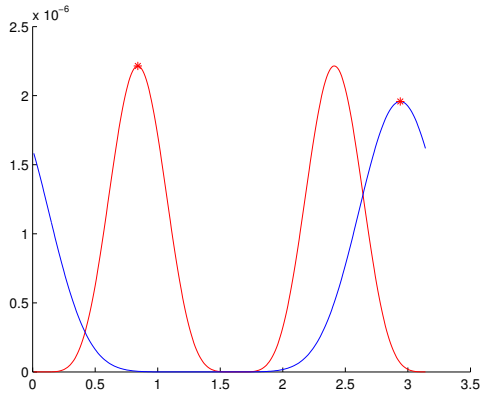

Figure 6.4.: The plot of the total damage with (red) and without (blue) the additional constraint from Eq. (6.7)

the maximum total damage for each iteration in the damage optimization. In the first example in Section 6.3.1, the component to be tested was a knuckle for which we saw that the clustering algorithm was slightly better in objective function value and at the same time the points of maximum total damage used in clustering were the actual points of maximum total damage thereby making the solution obtained from clustering more reliable than the solution obtained in the case of damage optimization without clustering. The number of iterations to converge to the optimal solution was also less in the case of optimization with clustering.

In the second example in Section 6.3.2 we looked at an artificial example. In this case as well the objective function values for the damage optimization with clustering algorithm are slightly better than that obtained in damage optimization with clustering. The number of iterations to converge to a solution in this example taken by optimization with clustering is again less than the number of iterations taken by optimization without clustering.

In the third example we saw how we can use the conditions developed in Chapter 5 to add an additional constraint to the damage optimization problem in order to shift the point of maximum total damage of a hotspot to the neighborhood of a selected plane.

Thus, we see that in general testrig damage optimization with clustering is better than the testrig damage optimization without clustering. However, the reliability of the solutions obtained is much higher in the case of damage optimization with clusters as the actual points of maximum are used for computing the maximum total damage at each iteration of the optimization. Additionally, the idea of clustering can also be used to shift the point of maximum total damage to the neighborhood of a new point. This can find applications in case we want to test the component at a point along a particular plane angle α.

7. Conclusions and future research topics

Estimating fatigue life of components is an important aspect of vehicle design. No vehicle manufacturing company want their vehicles to fail due to the fatigue failure of a component before the expected lifetime of the vehicle. The fatigue lifetime of the components is estimated by application of load time series in testrigs. Mathematical optimization in testrig is a relatively new field of research. There are many challenges that needs to be answered in this discipline. The most important aspect that has to be considered during mathematical optimization in testrig is the validity of the theoretical results obtained to be applicable in practice. Keeping this in mind we gave a testrig damage optimization problem (WSDP) which used block loads as building blocks for the load time series. The optimized load time series with block loads obtained by the testrig damage optimization (WSDP) have considerably less number of points compared to the load time series obtained in the testrig stress optimization problem (TSOP) that is the current state of the art. Due to the simplicity and smaller number of points in the load time series from (WSDP) they would lead to reduction in total time and costs involved in performing tests on a testrig. The (WSDP) is shown to be an improvement on the (TSOP).

As our main result, we remodelled damage from block loads as Gaussian functions on three intervals of interest when the S-N curve has one slope. We derived conditions which when satisfied by the Gaussian functions, they give a single maximum. These conditions can be easily extended to be used in the Gaussian Mixture Models (GMM) for finding modes which has application in image segmentation, speaker identification and many other fields. Remodelling of damage function enabled us to be able to select the plane of maximum total damage at a hotspot. This was not possible by any of the previous approaches. Extension of the Gaussian approximation to the case when S-N curve has two slopes is a promising field of future research.

Although testrig damage optimization problem was presented as a multi-objective problem and was solved by weighted-sum-of-objective-functions approach, we did not consider in detail the multi-objective nature of the problem. It would be interesting to investigate the effects of changing the weights of objective functions associated with different hotspot on the results of the multi-objective problem and to be able to give a representative set of the efficient solutions. This could then be used as an interactive decision support tool that can be used by the decision makers to decide between solutions of the different instances of the problem.

We investigated the effects of increasing the number of times a unit of block load is repeated for a single block on results of the optimization. Number of blocks and number of times a unit of block load is repeated was not optimized and were fixed for every problem instance. However, from the results obtained one can safely state that the number of blocks and also the number of times a unit of the block is repeated need not be very large. This could be included as optimization parameters in any future research in this field. However, this would considerably increase the complexity of

the optimization problem as both these parameters are integers.

So far, the focus of the implementation was on the quality of the solutions and the stability of the program. To improve the performance of the methods, the implementation can be improved for speed. Clustering of Gaussian functions is a significant driver of the running time. Parallelization of Algorithm 5.4.3 that is used for clustering of the Gaussian functions and clever computation of between-cluster and within-cluster distances can result in speed improvements.

A. Proofs

A.1. Taylor Series

In this section, we derive the Taylor series for functions from the previous chapters.

Theorem A.1.1. *The Taylor series of the damage function $\hat{d}$ from Eq. (4.16) at $\breve{b}(\boldsymbol{\sigma})$ is given as*

$$\hat{d}(\boldsymbol{\sigma},\alpha) = \hat{d}(\boldsymbol{\sigma},\breve{b}(\boldsymbol{\sigma})) + \frac{2kb(\boldsymbol{\sigma})}{\sigma_e^k N_e}\left(a(\boldsymbol{\sigma})+b(\boldsymbol{\sigma})\right)^{k-1}(\alpha-\breve{b}(\boldsymbol{\sigma}))^2 + O\left((\alpha-\breve{b}(\boldsymbol{\sigma}))^4\right) \tag{A.1}$$

Proof. From Eq. (4.16), the damage function $\hat{d}$ is given as:

$$\hat{d}(\boldsymbol{\sigma},\alpha) = \frac{1}{\sigma_e^k N_e}\left(a(\boldsymbol{\sigma})+b(\boldsymbol{\sigma})\cos\left(2\alpha-2\breve{b}(\boldsymbol{\sigma})\right)\right)^k, \alpha\in I.$$

The Taylor series of $\hat{d}(\boldsymbol{\sigma},\alpha)$ at $\breve{b}(\boldsymbol{\sigma})$ is the power series (by using the big O notation)

$$\hat{d}(\boldsymbol{\sigma},\alpha) = \hat{d}(\boldsymbol{\sigma},\breve{b}(\boldsymbol{\sigma})) + \frac{d'(\boldsymbol{\sigma},\breve{b}(\boldsymbol{\sigma}))}{1!}(\alpha-\breve{b}(\boldsymbol{\sigma})) + \frac{d''(\boldsymbol{\sigma},\breve{b}(\boldsymbol{\sigma}))}{2!}(\alpha-\breve{b}(\boldsymbol{\sigma}))^2 + \frac{d^{(3)}(\boldsymbol{\sigma},\breve{b}(\boldsymbol{\sigma}))}{3!}(\alpha-\breve{b}(\boldsymbol{\sigma}))^3 + O\left((\alpha-\breve{b}(\boldsymbol{\sigma}))^4\right) \tag{A.2}$$

Next, we take the derivatives of the damage function $\hat{d}$ and evaluate them at $\alpha=\breve{b}(\boldsymbol{\sigma})$. The first derivative of the damage function $\hat{d}$ is

$$d'(\boldsymbol{\sigma},\alpha) = \frac{2kb(\boldsymbol{\sigma})}{\sigma_e^k N_e}\left(a(\boldsymbol{\sigma})+b(\boldsymbol{\sigma})\cos\left(2\alpha-2\breve{b}(\boldsymbol{\sigma})\right)\right)^{k-1}\sin\left(2\alpha-2\breve{b}(\boldsymbol{\sigma})\right). \tag{A.3}$$

Evaluating the first derivative $\hat{d}'$ at $\alpha=\breve{b}(\boldsymbol{\sigma})$ leads to $d'(\boldsymbol{\sigma},\breve{b}(\boldsymbol{\sigma}))=0$ since $\sin(0)=0$. Intuitively, all the odd derivatives of the damage function $\hat{d}$ are zero when evaluated at $\alpha=\breve{b}(\boldsymbol{\sigma})$ as all the terms in every odd derivative are a multiple of $\sin(2\alpha-\breve{b}(\boldsymbol{\sigma}))$ which evaluates to zero at $\alpha=\breve{b}(\boldsymbol{\sigma})$. However, this is not true for the case of even derivatives of the damage function $\hat{d}$.

The second derivative of the damge function $\hat{d}$ can be computed by observing that $d''=(d')'$ and using the product rule of differentiation, $\frac{d}{dx}(uv)=v\frac{du}{dx}+u\frac{dv}{dx}$, to get

$$d''(\boldsymbol{\sigma},\alpha) = \frac{4k(k-1)b^2(\boldsymbol{\sigma})}{\sigma_e^k N_e}\left(a(\boldsymbol{\sigma})+b(\boldsymbol{\sigma})\cos\left(2\alpha-2\breve{b}(\boldsymbol{\sigma})\right)\right)^{k-2}\sin^2\left(2\alpha-2\breve{b}(\boldsymbol{\sigma})\right) + \frac{4kb(\boldsymbol{\sigma})}{\sigma_e^k N_e}\left(a(\boldsymbol{\sigma})+b(\boldsymbol{\sigma})\cos\left(2\alpha-2\breve{b}(\boldsymbol{\sigma})\right)\right)^{k-1}\cos\left(2\alpha-2\breve{b}(\boldsymbol{\sigma})\right). \tag{A.4}$$

Evaluating the second derivative $\hat{d}''$ of the damage function $\hat{d}$ in Eq. (A.4) at $\alpha = \breve{b}(\boldsymbol{\sigma})$ we get

$$d''(\boldsymbol{\sigma}, \breve{b}(\boldsymbol{\sigma})) = \frac{4kb(\boldsymbol{\sigma})}{\sigma_e^k N_e} \left(a(\boldsymbol{\sigma}) + b(\boldsymbol{\sigma})\right)^{k-1}. \tag{A.5}$$

Inserting the value of the derivatives evaluated at $\alpha = \breve{b}(\boldsymbol{\sigma})$ into Eq. (A.2) we get the Taylor series of the damage function $\hat{d}$ at $\breve{b}(\boldsymbol{\sigma})$ as

$$\hat{d}(\boldsymbol{\sigma}, \alpha) = \hat{d}(\boldsymbol{\sigma}, \breve{b}(\boldsymbol{\sigma})) + \frac{2kb(\boldsymbol{\sigma})}{\sigma_e^k N_e} \left(a(\boldsymbol{\sigma}) + b(\boldsymbol{\sigma})\right)^{k-1} (\alpha - \breve{b}(\boldsymbol{\sigma}))^2 + O\left((\alpha - \breve{b}(\boldsymbol{\sigma}))^4\right)$$

This completes the proof. □

We define $F : \mathbb{R} \to \mathbb{R}$ for fixed stress $\boldsymbol{\sigma}$ as

$$\alpha \mapsto \sum_{i=-\infty}^{\infty} f_{\breve{a}(\boldsymbol{\sigma}),\breve{b}(\boldsymbol{\sigma}),\breve{c}(\boldsymbol{\sigma})}(\alpha - i\pi) = \breve{a}(\boldsymbol{\sigma}) \sum_{i=-\infty}^{\infty} \exp\left(-\frac{(\alpha - i\pi - \breve{b}(\boldsymbol{\sigma}))^2}{\breve{c}^2(\boldsymbol{\sigma})}\right) \tag{A.6}$$

Theorem A.1.2. *Let the function F be defined as in Eq.* (A.6)*. The Taylor series of F at $\breve{b}(\boldsymbol{\sigma})$ is given as*

$$F(\alpha) = \breve{a}(\boldsymbol{\sigma}) \sum_{i=-\infty}^{\infty} \exp\left(-\frac{i^2\pi^2}{\breve{c}^2(\boldsymbol{\sigma})}\right) + \frac{\breve{a}(\boldsymbol{\sigma})}{\breve{c}^2(\boldsymbol{\sigma})} \sum_{i=-\infty}^{\infty} \left(\frac{2i^2\pi^2}{\breve{c}^2(\boldsymbol{\sigma})} - 1\right) \exp\left(-\frac{i^2\pi^2}{\breve{c}^2(\boldsymbol{\sigma})}\right) (\alpha - \breve{b}(\boldsymbol{\sigma}))^2 + O((\alpha - \breve{b}(\boldsymbol{\sigma}))^4) \tag{A.7}$$

Proof. We want to find the Taylor series of the function F around $\breve{b}(\boldsymbol{\sigma})$ of order 4. The Taylor series is given as

$$F(\alpha) = F(\breve{b}(\boldsymbol{\sigma})) + \frac{F'(\breve{b}(\boldsymbol{\sigma}))}{1!}(\alpha - \breve{b}(\boldsymbol{\sigma})) + \frac{F''(\breve{b}(\boldsymbol{\sigma}))}{2!}(\alpha - \breve{b}(\boldsymbol{\sigma}))^2 + \frac{F^{(3)}(\breve{b}(\boldsymbol{\sigma}))}{3!}(\alpha - \breve{b}(\boldsymbol{\sigma}))^3 + O((\alpha - \breve{b}(\boldsymbol{\sigma}))^4) \tag{A.8}$$

To give the Taylor series we need to find $F(\breve{b}(\boldsymbol{\sigma}))$, $F'(\breve{b}(\boldsymbol{\sigma}))$, $F''(\breve{b}(\boldsymbol{\sigma}))$ and $F^{(3)}(\breve{b}(\boldsymbol{\sigma}))$. Evaluating the function F at $\alpha = \breve{b}(\boldsymbol{\sigma})$ yields

$$F(\breve{b}(\boldsymbol{\sigma})) = \breve{a}(\boldsymbol{\sigma}) \sum_{i=-\infty}^{\infty} \exp\left(-\frac{i^2\pi^2}{\breve{c}^2(\boldsymbol{\sigma})}\right) \tag{A.9}$$

The first derivative of the function F is

$$F'(\alpha) = -\frac{2\breve{a}(\boldsymbol{\sigma})}{\breve{c}^2(\boldsymbol{\sigma})} \sum_{i=-\infty}^{\infty} (\alpha - i\pi - \breve{b}(\boldsymbol{\sigma})) \exp\left(-\frac{(\alpha - i\pi - \breve{b}(\boldsymbol{\sigma}))^2}{\breve{c}^2(\boldsymbol{\sigma})}\right). \tag{A.10}$$

Evaluating the first derivative F' at $\alpha = \breve{b}(\boldsymbol{\sigma})$ we get

$$F'(\breve{b}_1(\boldsymbol{\sigma})) = \frac{2\pi\breve{a}(\boldsymbol{\sigma})}{\breve{c}^2(\boldsymbol{\sigma})} \sum_{i=-\infty}^{\infty} i \exp\left(-\frac{i^2\pi^2}{\breve{c}^2(\boldsymbol{\sigma})}\right) = 0. \tag{A.11}$$

The summand $i \exp\left(-\frac{i^2\pi^2}{\breve{c}^2(\boldsymbol{\sigma})}\right)$ in Eq. (A.11) is an odd function of i. So, the i^{th} and $-i^{th}$ terms cancel each other in the sum. The second derivative of the function F is

$$F''(\alpha) = \frac{2\breve{a}(\boldsymbol{\sigma})}{\breve{c}^2(\boldsymbol{\sigma})} \sum_{i=-\infty}^{\infty} \left(\frac{2(\alpha - i\pi - \breve{b}(\boldsymbol{\sigma}))^2}{\breve{c}^2(\boldsymbol{\sigma})} - 1 \right) \exp\left(-\frac{(\alpha - i\pi - \breve{b}(\boldsymbol{\sigma}))^2}{\breve{c}^2(\boldsymbol{\sigma})} \right). \tag{A.12}$$

Evaluating the second derivative F'' at $\alpha = \breve{b}(\boldsymbol{\sigma})$ yields

$$F''(\breve{b}(\boldsymbol{\sigma})) = \frac{2\breve{a}(\boldsymbol{\sigma})}{\breve{c}^2(\boldsymbol{\sigma})} \sum_{i=-\infty}^{\infty} \left(\frac{2i^2\pi^2}{\breve{c}^2(\boldsymbol{\sigma})} - 1 \right) \exp\left(-\frac{i^2\pi^2}{\breve{c}^2(\boldsymbol{\sigma})} \right). \tag{A.13}$$

The third derivative of F is

$$F^{(3)}(\alpha) = \frac{4\breve{a}(\boldsymbol{\sigma})}{\breve{c}^4(\boldsymbol{\sigma})} \sum_{i=-\infty}^{\infty} \left(3(\alpha - i\pi - \breve{b}(\boldsymbol{\sigma})) - \frac{2(\alpha - i\pi - \breve{b}(\boldsymbol{\sigma}))^3}{\breve{c}^2(\boldsymbol{\sigma})} \right) \exp\left(-\frac{(\alpha - i\pi - \breve{b}(\boldsymbol{\sigma}))^2}{\breve{c}^2(\boldsymbol{\sigma})} \right). \tag{A.14}$$

Evaluating the third derivative $F^{(3)}$ at $\alpha = \breve{b}(\boldsymbol{\sigma})$ gives

$$F^{(3)}(\breve{b}(\boldsymbol{\sigma})) = -\frac{4\breve{a}(\boldsymbol{\sigma})}{\breve{c}^4(\boldsymbol{\sigma})} \sum_{i=-\infty}^{\infty} \left(3i\pi - \frac{2i^3\pi^3}{\breve{c}^2(\boldsymbol{\sigma})} \right) \exp\left(-\frac{i^2\pi^2}{\breve{c}^2(\boldsymbol{\sigma})} \right) = 0. \tag{A.15}$$

The summand above is an odd function with respect to the variable i and therefore cancel each other out. At $i = 0$ the summand is zero. Inserting $F(\breve{b}(\boldsymbol{\sigma}))$ from Eq. (A.9), $F'(\breve{b}(\boldsymbol{\sigma}))$ from Eq. (A.11), $F''(\breve{b}(\boldsymbol{\sigma}))$ from Eq. (A.13) and $F^{(3)}(\breve{b}(\boldsymbol{\sigma}))$ from Eq. (A.15) into Eq. (A.8) gives the fourth order Taylor series of F:

$$F(\alpha) = \breve{a}(\boldsymbol{\sigma}) \sum_{i=-\infty}^{\infty} \exp\left(-\frac{i^2\pi^2}{\breve{c}^2(\boldsymbol{\sigma})} \right) + \frac{\breve{a}(\boldsymbol{\sigma})}{\breve{c}^2(\boldsymbol{\sigma})} \sum_{i=-\infty}^{\infty} \left(\frac{2i^2\pi^2}{\breve{c}^2(\boldsymbol{\sigma})} - 1 \right) \exp\left(-\frac{i^2\pi^2}{\breve{c}^2(\boldsymbol{\sigma})} \right) (\alpha - \breve{b}(\boldsymbol{\sigma}))^2 + O((\alpha - \breve{b}(\boldsymbol{\sigma}))^4) \tag{A.16}$$

This completes the proof. □

Theorem A.1.2 gives a general result on the Taylor series of the sum of Gaussian functions about the parameter $\breve{b}(\boldsymbol{\sigma})$ for which the Gaussian functions are defined. We use this result to give Taylor series for other functions required in the proof of theorems from previous chapters.

Corollary A.1.3. *The Taylor series expansion of the approximation function $g_{\mathbb{R}}(\boldsymbol{\sigma}, \alpha)$ from Eq. (4.67) at $\breve{b}(\boldsymbol{\sigma})$ is*

$$g_{\mathbb{R}}(\boldsymbol{\sigma}, \alpha) = \breve{a}(\boldsymbol{\sigma}) \sum_{i=-\infty}^{\infty} \exp\left(-\frac{i^2\pi^2}{\breve{c}^2(\boldsymbol{\sigma})} \right) + \frac{\breve{a}(\boldsymbol{\sigma})}{\breve{c}^2(\boldsymbol{\sigma})} \sum_{i=-\infty}^{\infty} \left(\frac{2i^2\pi^2}{\breve{c}^2(\boldsymbol{\sigma})} - 1 \right) \exp\left(-\frac{i^2\pi^2}{\breve{c}^2(\boldsymbol{\sigma})} \right) (\alpha - \breve{b}(\boldsymbol{\sigma}))^2 + O((\alpha - \breve{b}(\boldsymbol{\sigma}))^4) \tag{A.17}$$

Proof. Follows directly from Theorem A.1.2 by observing that the function F and the approximation function $g_{\mathbb{R}}(\boldsymbol{\sigma}, \alpha)$ have exactly the same form. □

Corollary A.1.4. *The Taylor series of the approximation function $\tilde{g}_{\mathbb{R}}(\boldsymbol{\sigma}, \alpha)$ from Eq. (4.80) at $\breve{b}_1(\boldsymbol{\sigma})$ for $\alpha \in \hat{I}_1$ is*

$$\tilde{g}_{\mathbb{R}}(\boldsymbol{\sigma}, \alpha) = \breve{a}_1(\boldsymbol{\sigma}) \sum_{i=-\infty}^{\infty} \exp\left(-\frac{i^2\pi^2}{\breve{c}_1^2(\boldsymbol{\sigma})}\right) + \frac{\breve{a}_1(\boldsymbol{\sigma})}{\breve{c}_1^2(\boldsymbol{\sigma})} \sum_{i=-\infty}^{\infty} \left(\frac{2i^2\pi^2}{\breve{c}_1^2(\boldsymbol{\sigma})} - 1\right) \exp\left(-\frac{i^2\pi^2}{\breve{c}_1^2(\boldsymbol{\sigma})}\right) (\alpha - \breve{b}_1(\boldsymbol{\sigma}))^2 + \breve{d}_1(\boldsymbol{\sigma}) + O((\alpha - \breve{b}_1(\boldsymbol{\sigma}))^4) \quad \text{(A.18)}$$

Proof. Follows directly from Theorem A.1.2 by using parameters $\breve{a}_1(\boldsymbol{\sigma})$, $\breve{b}_1(\boldsymbol{\sigma})$ and $\breve{c}_1(\boldsymbol{\sigma})$ for the Gaussian functions in the summand of the function F and observing that $\breve{d}_1(\boldsymbol{\sigma})$ is independent of α. □

Corollary A.1.5. *The Taylor series of the approximation function $\tilde{g}_{\mathbb{R}}(\boldsymbol{\sigma}, \alpha)$ from Eq. (4.80) at $\breve{b}_2(\boldsymbol{\sigma})$ for $\alpha \in \hat{I}_2$ is*

$$\tilde{g}_{\mathbb{R}}(\boldsymbol{\sigma}, \alpha) = \breve{a}_2(\boldsymbol{\sigma}) \sum_{i=-\infty}^{\infty} \exp\left(-\frac{i^2\pi^2}{\breve{c}_2^2(\boldsymbol{\sigma})}\right) + \frac{\breve{a}_2(\boldsymbol{\sigma})}{\breve{c}_2^2(\boldsymbol{\sigma})} \sum_{i=-\infty}^{\infty} \left(\frac{2i^2\pi^2}{\breve{c}_2^2(\boldsymbol{\sigma})} - 1\right) \exp\left(-\frac{i^2\pi^2}{\breve{c}_2^2(\boldsymbol{\sigma})}\right) (\alpha - \breve{b}_2(\boldsymbol{\sigma}))^2 + \breve{d}_2(\boldsymbol{\sigma}) + O((\alpha - \breve{b}_2(\boldsymbol{\sigma}))^4) \quad \text{(A.19)}$$

Proof. Follows directly from Theorem A.1.2 by using parameters $\breve{a}_2(\boldsymbol{\sigma})$, $\breve{b}_2(\boldsymbol{\sigma})$ and $\breve{c}_2(\boldsymbol{\sigma})$ for the Gaussian functions in the summand of the function F and observing that $\breve{d}_2(\boldsymbol{\sigma})$ is independent of α. □

A.2. Convexity proofs

A.2.1. Convexity of $\mathcal{T}$ in Eq. (4.30)

In this section we show that the function $\mathcal{T}$ as defined in Eq. (4.30) is strictly convex. We have for positive constants $a \geq b > 0$ and $k \geq 1$

$$\mathcal{T}(k) = \frac{(a+b)^k - (a-b)^k}{2kb\,(a+b)^{k-1}}. \quad \text{(A.20)}$$

To prove that the function $\mathcal{T}$ is strictly convex we use the following Theorem.

Theorem A.2.1. *Let I be an open interval and suppose that f is twice differentiable on I. Then f is convex on I if and only if*

$$f''(x) \geq 0$$

for all $x \in I$.

Proof. For proof see [5]. □

Corollary A.2.2. *Let I be an open interval and suppose that f is twice differentiable on I. Then f is strictly convex on I if and only if*

$$f''(x) > 0$$

for all $x \in I$.

So if we can show that $\mathcal{T}''(k) > 0$ for all $k \in (1, \infty)$ we are done as a result of Corollary A.2.2.

Theorem A.2.3. *The function* $\mathcal{T}$ *as defined in Eq.* (A.20) *is strictly convex on the interval* $k \in (1, \infty)$.

Proof. Differentiating the function $\mathcal{T}$ once yields

$$\mathcal{T}'(k) = \begin{cases} \frac{1}{2bk^2(a+b)^{k-1}} \left((a-b)^k - (a+b)^k + k(a-b)^k \log\left(\frac{a+b}{a-b}\right)\right), & \text{if } a > b \\ -\frac{1}{k^2}, & \text{if } a = b \end{cases},$$

and differentiating again we get the second derivative of the function $\mathcal{T}$ as

$$\mathcal{T}''(k) = \begin{cases} \frac{1}{2bk^3(a+b)^{k-1}} \left(2(a+b)^k - (a-b)^k \left(2 + k \ln\left(\frac{a-b}{a+b}\right)\left(k \ln\left(\frac{a-b}{a+b}\right) - 2\right)\right)\right), & \text{if } a > b \\ \frac{2}{k^3}, & \text{if } a = b \end{cases}.$$

Next we show that $\mathcal{T}''(k) > 0$ for all $a \geq b > 0$ and $k > 1$. For the case $a = b$ we have $\mathcal{T}(k) = \frac{2}{k^3} > 0$. For the other case we start by taking $(a-b)^k$ common and rewriting $\mathcal{T}''(k)$ as

$$\mathcal{T}''(k) = \frac{(a-b)^k}{2bk^3(a+b)^{k-1}} \left(2\left(\frac{a+b}{a-b}\right)^k - \left(2 + k \ln\left(\frac{a-b}{a+b}\right)\left(k \ln\left(\frac{a-b}{a+b}\right) - 2\right)\right)\right) \tag{A.21}$$

We replace $\frac{a+b}{a-b}$ by t in Eq. (A.21) to get

$$= \frac{a+b}{2bk^3t^k} \left(2t^k - \left(2 + k \ln\left(\frac{1}{t}\right)\left(k \ln\left(\frac{1}{t}\right) - 2\right)\right)\right) \tag{A.22}$$

Using the property $\ln\left(\frac{1}{t}\right) = -\ln t$ we can further simplify Eq. (A.22) as

$$\begin{aligned} &= \frac{a+b}{2bk^3t^k} \left(2t^k - (2 - k \ln t\,(-k \ln t - 2))\right) \\ &= \frac{a+b}{2bk^3t^k} \left(2t^k - 2 - 2k \ln t - k^2 \ln^2 t\right) \end{aligned} \tag{A.23}$$

Replacing t^k by $\exp(k \ln t)$ in Eq. (A.23) we get

$$\begin{aligned} &= \frac{a+b}{2bk^3t^k} \left(2\exp(k \ln t) - 2 - 2k \ln t - k^2 \ln^2 t\right) \\ &= \frac{a+b}{bk^3t^k} \left(\exp(k \ln t) - 1 - k \ln t - \frac{k^2}{2} \ln^2 t\right) \end{aligned}$$

Finally we replace $k \ln t$ by u to get

$$= \frac{a+b}{bk^3t^k} \left(\exp(u) - 1 - u - \frac{u^2}{2!}\right) \tag{A.24}$$

In Eq. (A.24), we observe that we are taking the difference of exponential function and first three terms of its Taylor series. Since $u = k \ln t = k \ln \left(\frac{a+b}{a-b}\right) > 0$, the difference is positive

$$> 0.$$

We have proven that the second derivative of the function $\mathcal{T}$ is positive for all $a \geq b > 0$ and $k > 1$ and from Corollary A.2.2 we have that the function $\mathcal{T}$ is strictly convex on $(1, \infty)$. □

A.3. Other results

Theorem A.3.1. *For $\theta \in \left[0, \frac{\pi}{2}\right)$ the term $\sqrt{\frac{1+\sin\theta}{2}}\frac{4}{\pi+2\theta}$ is decreasing.*

Proof. For the term to be decreasing in the interval $\left[0, \frac{\pi}{2}\right)$ we have to show that the first derivative of the term is less than zero in this interval. The first derivative is given by using the product rule of differentiation

$$\frac{d}{d\theta}\left(\sqrt{\frac{1+\sin\theta}{2}}\frac{4}{\pi+2\theta}\right) = \frac{\sqrt{2}\cos\theta}{\sqrt{1+\sin\theta}(\pi+2\theta)} - \frac{4\sqrt{2}\sqrt{1+\sin\theta}}{(\pi+2\theta)^2}$$

Making the denominators of both the terms same and factoring out $\sqrt{2}\cos\theta$ yields

$$= \frac{\sqrt{2}\cos\theta\left(\pi+2\theta-\frac{4}{\cos\theta}(1+\sin\theta)\right)}{\sqrt{1+\sin\theta}(\pi+2\theta)^2}$$

The denominator and $\sqrt{2}\cos\theta$ are positive which gives us

$$\begin{aligned} &< \pi + 2\theta - \frac{4}{\cos\theta}(1+\sin\theta) \\ &= \pi + 2\theta - \frac{4}{\cos\theta} + 4\tan\theta \end{aligned}$$

$$\pi < \frac{4}{\cos\theta} \text{ and } 2\theta \leq 4\tan\theta \Rightarrow < 0.$$

Therefore, the first derivative is less than zero in the interval $\left[0, \frac{\pi}{2}\right)$ and we have proven that the term is decreasing. □

A.3.1. Proof that function is positive at a point

We prove a general result that we use to show that $\mathcal{T}\left(\frac{1}{k}\right)$ in Eq. (4.113) and $\mathcal{T}\left(\frac{1}{2k}\right)$ in Eq. (4.134) are positive.

Let us consider a function $\hat{\mathcal{T}}$ defined as

$$\hat{\mathcal{T}} : (1, \infty) \to \mathbb{R}, k \mapsto \frac{\sum_{i=-1}^{1} \left(tk - 2\pi^2 i^2 (tk)^3\right) \exp\left(-i^2\pi^2(tk)^2\right)}{\sum_{i=-1}^{1} \left(\exp\left(-i^2\pi^2(tk)^2\right) - \exp\left(-\frac{(2i+1)^2\pi^2(tk)^2}{4}\right)\right)} \tag{A.25}$$

where $t \in \mathbb{R}$ and $t \geq 1$.

We want to prove that the function $\hat{\mathcal{T}}$ is always greater than tk for $k \in \mathbb{R}$ and $k > 1$. We will use the following results in the proof:

Lemma A.3.2. *For $x \in [0, \infty)$ we have*

$$T(x) := x^2 \exp\left(-\frac{3x^2}{4}\right) < 0.5.$$

Proof. We show that the maximum value of the function T on the interval $[0, \infty)$ is less then 0.5. The first derivative of the function T is

$$T'(x) = 2x \exp\left(-\frac{3x^2}{4}\right) - \frac{3}{2}x^3 \exp\left(-\frac{3x^2}{4}\right)$$

The critical points greater than or equal to zero are at $x = \frac{2}{\sqrt{3}}, 0$. Taking the second derivative

$$T''(x) = 2 \exp\left(-\frac{3x^2}{4}\right) - \frac{15}{2}x^2 \exp\left(-\frac{3x^2}{4}\right) + \frac{9}{4}x^4 \exp\left(-\frac{3x^2}{4}\right).$$

Evaluating the second derivative at the critical points gives us $T''(0) = 2$ and $T''\left(\frac{2}{\sqrt{3}}\right) = -\frac{4}{e}$. Since, the second derivative $T''\left(\frac{2}{\sqrt{3}}\right) < 0$, point $x = \frac{2}{\sqrt{3}}$ is a point of local maximum and since $T''(0) > 0$, point $x = 0$ is a point of local minimum.

Evaluating the function T at $x = \frac{2}{\sqrt{3}}$ we get $T\left(\frac{2}{\sqrt{3}}\right) = \frac{4}{3e} < 0.5$. We have proven that the local maximum of the function T is less then 0.5 but we need to consider the asymptotic behaviour of the function T to be sure that the function T is bounded for $x \to \infty$. In this case $\lim_{x\to\infty} T(x) = 0$. Hence, $T(x) < 0.5$ for all $x \in [0, \infty)$. In Figure A.1, we see a plot of the function $T(x)$. □

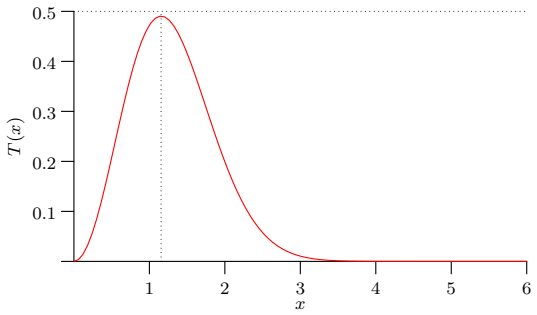

Figure A.1.: $T(x), x \in [0, 6]$

Lemma A.3.3. *For real $k > 1$ we have*

$$\sum_{i=-1}^{1} \exp\left(-\frac{(2i+1)^2 k^2 \pi^2}{4}\right) < 1.$$

Proof. The term $\sum_{i=-1}^{1} \exp\left(-\frac{(2i+1)^2 k^2 \pi^2}{4}\right)$ is a decreasing function with respect to k. Hence, the maximum value of the term is at $k = 1$. Inserting $k = 1$ in the term above we get:

$$\sum_{i=-1}^{1} \exp\left(-\frac{(2i+1)^2 k^2 \pi^2}{4}\right) < \sum_{i=-1}^{1} \exp\left(-\frac{(2i+1)^2 \pi^2}{4}\right) < 1 \tag{A.26}$$

□

Equipped with Lemma A.3.2 and Lemma A.3.3 we can show that the function $\hat{\mathcal{T}}$ from Eq. (A.25) is always more than tk.

Theorem A.3.4. *For $t \in \mathbb{R}$, $t \geq 1$ and $k \in \mathbb{R}$, $k > 1$, the function $\hat{\mathcal{T}}$ as defined in Eq.* (A.25) *is always more than tk.*

Proof. We have to show that $\hat{\mathcal{T}}$ is always more than tk. We subtract tk from $\hat{\mathcal{T}}$ and show that the result is positive. The difference after simplification yields

$$\hat{\mathcal{T}} - tk = \frac{2tk \exp\left(-\frac{\pi^2 (tk)^2}{4}\right)\left(1 - 2\pi^2 (tk)^2 \exp\left(-\frac{3\pi^2 (tk)^2}{4}\right)\right) + tk \exp\left(-\frac{9\pi^2 (tk)^2}{4}\right)}{\sum_{i=-1}^{1}\left(\exp\left(-i^2 \pi^2 (tk)^2\right) - \exp\left(-\frac{(2i+1)^2 \pi^2 (tk)^2}{4}\right)\right)}. \tag{A.27}$$

For the proof we need to show that the numerator and the denominator both are positive. The numerator is positive if $\left(1 - 2\pi^2 (tk)^2 \exp\left(-\frac{3\pi^2 (tk)^2}{4}\right)\right)$ is positive and the denominator is positive if $\sum_{i=-1}^{1}\left(\exp\left(-i^2 \pi^2 k^2\right) - \exp\left(-\frac{(2i+1)^2 \pi^2 k^2}{4}\right)\right)$ is positive.

Applying Lemma A.3.2 for $x = \pi tk$ results in the numerator being positive.

The denominator can also be written as

$$1 + 2\exp\left(-\pi^2 k^2\right) - \sum_{i=-1}^{1} \exp\left(-\frac{(2i+1)^2 \pi^2 k^2}{4}\right).$$

From Lemma A.3.3 we know that the term $\sum_{i=-1}^{1} \exp\left(-\frac{(2i+1)^2 \pi^2 k^2}{4}\right)$ is less than one. Hence, the denominator is also positive. Therefore, we have shown that for $k \in \mathbb{R}$, $k > 1$ and $t \in \mathbb{R}$, $t \geq 1$ the function $\hat{\mathcal{T}}$ is always greater than tk. □

Corollary A.3.5. *For $k \in \mathbb{R}$ and $k > 1$, the function $\mathcal{T}$ from Eq.* (4.112) *evaluated at the point $y = \frac{1}{k}$ is positive.*

Proof. We can rewrite $\mathcal{T}\left(\frac{1}{k}\right)$ as

$$\mathcal{T}\left(\frac{1}{k}\right) = \frac{1}{k}\left(\left(\frac{k\tilde{t}\sum_{i=-1}^{1}\left(k-2i^2\pi^2k^3\right)\exp\left(-i^2\pi^2k^2\right)}{\sum_{i=-1}^{1}\left(\exp\left(-i^2\pi^2k^2\right)-\exp\left(-\frac{(2i+1)^2\pi^2k^2}{4}\right)\right)}\right)^{\frac{1}{4}}-1\right).$$

We know that $\tilde{t} \in \left[\frac{1}{k}, 1\right]$. Therefore, $k\tilde{t} > 1$. Applying Theorem A.3.4 with $t = 1$ yields the result. □

Corollary A.3.6. *For $k \in \mathbb{R}$ and $k > 1$, the function $\mathcal{T}_1$ from Eq. (4.132) evaluated at the point $y = \frac{1}{2k}$ is positive.*

Proof. It can be shown that $\sum_{i=-1}^{1}\exp\left(-(2k)^2\left(\frac{\pi}{4}+\frac{\theta}{2}+i\pi\right)^2\right) > \sum_{i=-1}^{1}\exp\left(-\frac{(2i+1)^2\pi^2(2k)^2}{4}\right)$ for all $\theta \in \left[0, \frac{\pi}{2}\right)$. This gives us

$$\mathcal{T}\left(\frac{1}{2k}\right) > \frac{1}{2k}\left(\left(\frac{2k\tilde{t}_1\sum_{i=-1}^{1}\left(2k-2i^2\pi^2(2k)^2\right)\exp\left(-i^2\pi^2(2k)^2\right)}{\sum_{i=-1}^{1}\left(\exp\left(-i^2\pi^2(2k)^2\right)-\exp\left(-\frac{(2i+1)^2\pi^2(2k)^2}{4}\right)\right)}\right)^{\frac{1}{4}}-1\right).$$

We know that $\tilde{t}_1 \in \left[\frac{1}{2k}, \frac{1}{k}\right)$. Therefore, $2k\tilde{t}_1 > 1$. Applying Theorem A.3.4 with $t = 2$ yields the result. □

A.3.2. Equation (4.133) is negative

We have to show that

$$\frac{\tilde{t}_1\sum_{i=-1}^{1}\left(2^2-2i^2\pi^2\right)\exp\left(-\frac{i^2\pi^2}{2^2}\right)}{\sum_{i=-1}^{1}\left(\exp\left(-\frac{i^2\pi^2}{2^2}\right)-\exp\left(-\frac{\left(\frac{\pi}{4}+\frac{\theta}{2}+i\pi\right)^2}{2^2}\right)\right)} < 16,$$

which implies that Eq. (4.133) is negative. We subtract the term from 16 and prove that the difference is positive for $k \in \mathbb{R}$, $k > 1$ and $\tilde{t}_1 \in \left[\frac{1}{2k}, \frac{1}{k}\right)$.

$$\begin{aligned} F(\tilde{t}_1) :=& 16 - \frac{\tilde{t}_1\sum_{i=-1}^{1}\left(2^2-2i^2\pi^2\right)\exp\left(-\frac{i^2\pi^2}{2^2}\right)}{\sum_{i=-1}^{1}\left(\exp\left(-\frac{i^2\pi^2}{2^2}\right)-\exp\left(-\frac{\left(\frac{\pi}{4}+\frac{\theta}{2}+i\pi\right)^2}{2^2}\right)\right)} \\ =& \frac{16\sum_{i=-1}^{1}\left(\exp\left(-\frac{i^2\pi^2}{2^2}\right)-\exp\left(-\frac{\left(\frac{\pi}{4}+\frac{\theta}{2}+i\pi\right)^2}{2^2}\right)\right)-\tilde{t}_1\sum_{i=-1}^{1}\left(2^2-2i^2\pi^2\right)\exp\left(-\frac{i^2\pi^2}{2^2}\right)}{\sum_{i=-1}^{1}\left(\exp\left(-\frac{i^2\pi^2}{2^2}\right)-\exp\left(-\frac{\left(\frac{\pi}{4}+\frac{\theta}{2}+i\pi\right)^2}{2^2}\right)\right)} \end{aligned}$$

The terms $16\sum_{i=-1}^{1}\exp\left(-\frac{i^2\pi^2}{2^2}\right)$ and $\sum_{i=-1}^{1}\left(2^2-2i^2\pi^2\right)\exp\left(-\frac{i^2\pi^2}{2^2}\right)$ are constants. Next we prove that $\mathcal{F}(\tilde{t}_1) := \sum_{i=-1}^{1}\exp\left(-\frac{\left(\frac{\pi}{4}+\frac{\theta}{2}+i\pi\right)^2}{2^2}\right)$ is a decreasing function in the interval $\left[\frac{1}{2k},\frac{1}{k}\right)$ for $\theta = \sin^{-1}(2k\tilde{t}_1-1)$ (We have $\theta = \sin^{-1}\left(\frac{a(\boldsymbol{\sigma})}{b(\boldsymbol{\sigma})}\right)$ and $\tilde{t}_1 = \frac{a(\boldsymbol{\sigma})+b(\boldsymbol{\sigma})}{2kb(\boldsymbol{\sigma})}$.). We take the first derivative of the function $\mathcal{F}$ to get

$$\begin{aligned}\mathcal{F}'(\tilde{t}_1) &= -\frac{1}{16\sqrt{\tilde{t}_1-\tilde{t}_1^2}}\sum_{i=-1}^{1}(\pi+2\theta+4i\pi)\exp\left(-\frac{\left(\frac{\pi}{4}+\frac{\theta}{2}+i\pi\right)^2}{2^2}\right)\\ &< -\frac{1}{16}\sum_{i=-1}^{1}(\pi+2\theta+4i\pi)\exp\left(-\frac{\left(\frac{\pi}{4}+\frac{\theta}{2}+i\pi\right)^2}{2^2}\right)\end{aligned}$$

Let us insert $\theta_1 = \frac{\pi}{2}+\theta$, $\theta_1 \in [\frac{\pi}{2},\pi)$, into the equation above and expand to get

$$\begin{aligned}&= -\frac{1}{8}\left(\theta_1\exp\left(-\frac{\theta_1^2}{4^2}\right)+(-2\pi+\theta_1)\exp\left(-\frac{(-2\pi+\theta_1)^2}{4^2}\right)+(2\pi+\theta_1)\exp\left(-\frac{(2\pi+\theta_1)^2}{4^2}\right)\right)\\ &= -\frac{\exp\left(-\frac{(2\pi+\theta_1)^2}{4^2}\right)}{8}\left(\exp\left(\frac{\pi\theta_1}{2}\right)\left(\theta_1\exp\left(\frac{\pi^2-\pi\theta_1}{4}\right)-2\pi+\theta_1\right)+2\pi+\theta_1\right)\end{aligned}$$

If we can show that $\theta_1\exp\left(\frac{\pi^2-\pi\theta_1}{4}\right)-2\pi+\theta_1 > 0$ then we are done. The following lemma proves that indeed $\theta_1\exp\left(\frac{\pi^2-\pi\theta_1}{4}\right)-2\pi+\theta_1 > 0$.

Lemma A.3.7. *For* $x \in \left[\frac{\pi}{2},\pi\right]$

$$L(x) := x\left(1+\exp\left(\frac{\pi^2}{4}-\frac{\pi x}{4}\right)\right) \geq 2\pi$$

Proof. Taking the first and second derivative of the function L gives us

$$L'(x) = 1+\exp\left(\frac{\pi^2}{4}-\frac{\pi x}{4}\right)-\frac{\pi x}{4}\exp\left(\frac{\pi^2}{4}-\frac{\pi x}{4}\right),$$

$$L''(x) = \frac{\pi}{2}\left(\frac{\pi x}{8}-1\right)\exp\left(\frac{\pi^2}{4}-\frac{\pi x}{4}\right).$$

We observe that $L'(\frac{\pi}{2}) > 0$ and $L'(\pi) < 0$. This implies from the Intermediate Value Theorem that there exists at least one point c such that $L'(c) = 0$ in the interval $\left[\frac{\pi}{2},\pi\right]$. Since, the value of the first derivative at the end points of the interval are of opposite sign we have either one, three, five, etc. number of such points. However, we notice that the second derivative has just one root at $x = \frac{8}{\pi}$ in the interval $\left[\frac{\pi}{2},\pi\right]$ which implies there can be at most two sign changes for the first derivative. Hence, there exists only one c such that $L'(c) = 0$ in the interval $\left[\frac{\pi}{2},\pi\right]$.

Also, since $L'(x) > 0$ in the interval $\left[\frac{\pi}{2},c\right)$ implies the function L is increasing in this interval. Similarly the function L is decreasing in the interval $(c,\pi]$. So, it would be sufficient to show that $L(x) \geq 2\pi$ at the end points of the interval $\left[\frac{\pi}{2},\pi\right]$. We have $L(\frac{\pi}{2}) = 6.9647749 > 2\pi$ and $L(\pi) = 2\pi$. This proves our claim. □

Applying Lemma A.3.7 for $x = \theta_1$ we have shown that the first derivative of the function $\mathcal{F}$ is negative and therefore, the function $\mathcal{F}$ is a decreasing function for $\tilde{t}_1 \in [\frac{1}{2k}, \frac{1}{k})$. Using this result we can further show that $\sum_{i=-1}^{1}\left(\exp\left(-\frac{i^2\pi^2}{2^2}\right) - \exp\left(-\frac{\left(\frac{\pi}{4}+\frac{\theta}{2}+i\pi\right)^2}{2^2}\right)\right)$ is more than zero for all $\tilde{t} \in \left[\frac{1}{2k}, \frac{1}{k}\right)$. For $F(\tilde{t}_1)$ to be positive we have to show that the numerator is positive. We do this by proving that numerator is increasing. The numerator is:

$$16\sum_{i=-1}^{1}\exp\left(-\frac{i^2\pi^2}{2^2}\right) - \tilde{t}_1\sum_{i=-1}^{1}\left(2^2 - 2i^2\pi^2\right)\exp\left(-\frac{i^2\pi^2}{2^2}\right) - 16\sum_{i=-1}^{1}\exp\left(-\frac{\left(\frac{\pi}{4}+\frac{\theta}{2}+i\pi\right)^2}{2^2}\right) \tag{A.28}$$

We observe that the term $16\sum_{i=-1}^{1}\exp\left(-\frac{i^2\pi^2}{2^2}\right) - \tilde{t}_1\sum_{i=-1}^{1}\left(2^2 - 2i^2\pi^2\right)\exp\left(-\frac{i^2\pi^2}{2^2}\right)$ is a decreasing function of $\tilde{t}_1$ and we have also proven that $16\sum_{i=-1}^{1}\exp\left(-\frac{\left(\frac{\pi}{4}+\frac{\theta}{2}+i\pi\right)^2}{2^2}\right)$ is a decreasing function. Since we are adding a decreasing function and an increasing function we have to show that the rate of increase of the increasing function is more than the rate of decrease in the decreasing function. In other words we have to show after taking the first derivative of the numerator that

$$-\sum_{i=-1}^{1}\left(2^2 - 2i^2\pi^2\right)\exp\left(-\frac{i^2\pi^2}{2^2}\right) - 16\mathcal{F}'(\tilde{t}_1) > 0$$

$$\mathcal{F}'(\tilde{t}_1) < -\frac{\sum_{i=-1}^{1}\left(2^2 - 2i^2\pi^2\right)\exp\left(-\frac{i^2\pi^2}{2^2}\right)}{16}$$

$$\mathcal{F}'(\tilde{t}_1) < -0.083154375$$

We can prove similar to the proof in Lemma A.3.7 that $\mathcal{F}''$ is also negative for all $\tilde{t}_1 \in \left[\frac{1}{2k}, \frac{1}{k}\right)$. Hence, $\mathcal{F}'$ is a decreasing function on this interval. Evaluating $\mathcal{F}'$ at $\tilde{t}_1 = \frac{1}{2k}$ and finding the maximum value for all $k > 1$ we get

$$\max_{k>1, k\in\mathbb{R}} \mathcal{F}'\left(\frac{1}{2k}\right) = -0.0840917 < -0.083154375.$$

Hence, the numerator is positive and we have shown that Eq. (4.133) is negative.

B. Images

B.1. Approximation around the maximum

In this section, we compare the damage function $\hat{d}$ from Eq. (4.4) and its approximation around the maximum developed in Section 4.2.

B.1.1. Case $a(\boldsymbol{\sigma}) \geq b(\boldsymbol{\sigma})$

In Figure B.1, we compare the approximation function g from Eq. (4.5) and the damage function $\hat{d}$ in the case of $\frac{b(\boldsymbol{\sigma})}{a(\boldsymbol{\sigma})} \approx 0$. In Figure B.2, we compare the approximation function g from Eq. (4.5) and the damage function $\hat{d}$ in the case of $\frac{b(\boldsymbol{\sigma})}{a(\boldsymbol{\sigma})} = 0.5$. In Figure B.3, we compare the approximation function g from Eq. (4.5) and the damage function $\hat{d}$ in the case of $\frac{b(\boldsymbol{\sigma})}{a(\boldsymbol{\sigma})} = 1$. In all the figures the horizontal axis is given by the plane angle α which is centered around the maximum value.

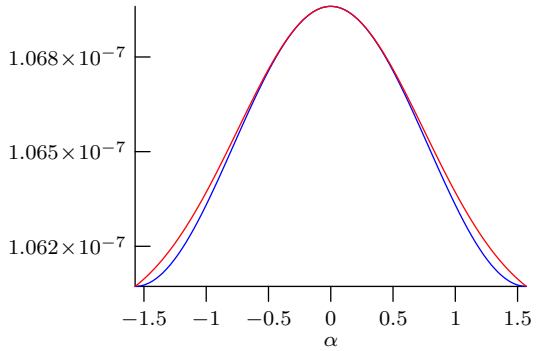

(a) Approximation (red) and actual (blue) damage.

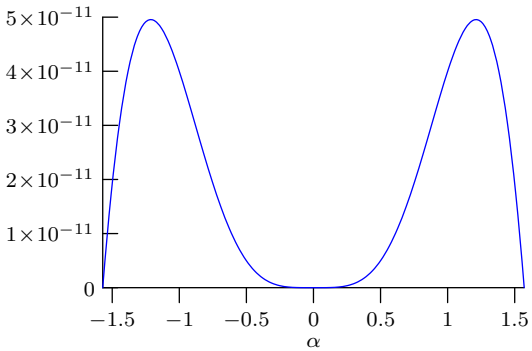

(b) Error $|\hat{d}(\boldsymbol{\sigma}, \alpha) - g(\boldsymbol{\sigma}, \alpha)|$.

Figure B.1.: Approximation around maximum when $\frac{b(\boldsymbol{\sigma})}{a(\boldsymbol{\sigma})} \approx 0$.

We see that the error in Figure B.1(b) is small compared to the maximum damage. Also, since $b(\boldsymbol{\sigma}) \approx 0$, damage is almost constant over the entire interval.

In Figure B.2(b) and Figure B.3(b) the error is also small compared to the maximum damage but the relative error in these cases is greater than the relative error displayed in Figure B.1(b). In general, the approximation function g approximates the damage function exactly at the point of maximum as seen in the plot for the error functions in Figure B.1(b), Figure B.2(b) and Figure B.3(b).

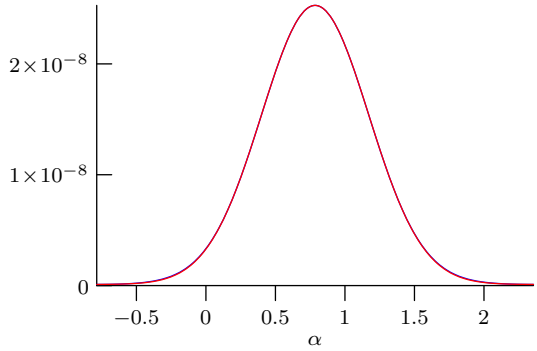

(a) Approximation (red) and actual (blue) damage.

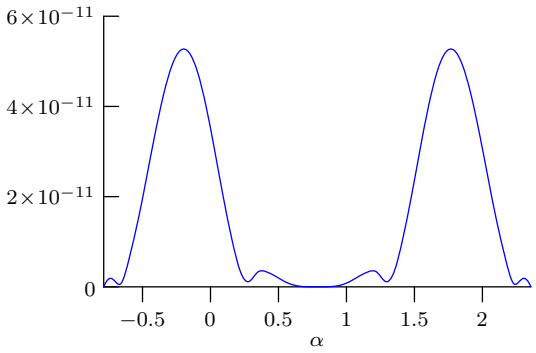

(b) Error $|\hat{d}(\boldsymbol{\sigma}, \alpha) - g(\boldsymbol{\sigma}, \alpha)|$.

Figure B.2.: Approximation around maximum when $\frac{b(\boldsymbol{\sigma})}{a(\boldsymbol{\sigma})} = 0.5$.

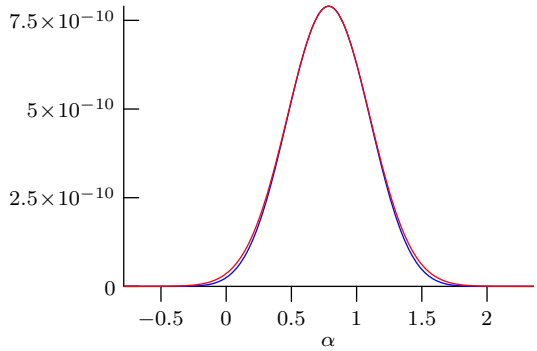

(a) Approximation (red) and actual (blue) damage.

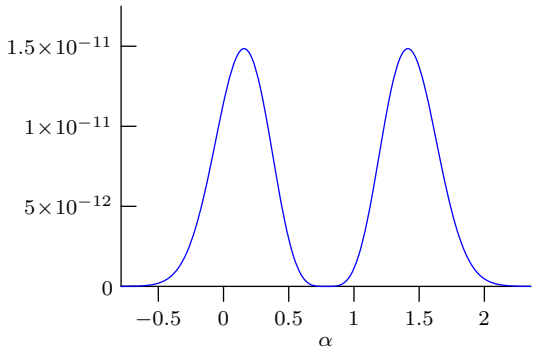

(b) Error $|\hat{d}(\boldsymbol{\sigma}, \alpha) - g(\boldsymbol{\sigma}, \alpha)|$.

Figure B.3.: Approximation around maximum when $\frac{b(\boldsymbol{\sigma})}{a(\boldsymbol{\sigma})} = 1$.

B.1.2. Case $a(\boldsymbol{\sigma}) \geq b(\boldsymbol{\sigma})$

In Figure B.4, we compare the approximation function $\tilde{g}$ from Eq. (4.36) and the damage function $\hat{d}$ in the case of $\frac{a(\boldsymbol{\sigma})}{b(\boldsymbol{\sigma})} = 0$. In Figure B.5, we compare the approximation function $\tilde{g}$ from Eq. (4.36) and the damage function $\hat{d}$ in the case of $\frac{a(\boldsymbol{\sigma})}{b(\boldsymbol{\sigma})} = 0.128$.

In Figure B.4, we have $a(\boldsymbol{\sigma}) = 0$ which implies that the two peaks in the damage profile have the same height. Again, we observe that as soon as the ratio $\frac{a(\boldsymbol{\sigma})}{b(\boldsymbol{\sigma})}$ increases to 0.128 the height of the smaller peak is less than half of the height of the larger peak. Therefore, with increasing value of the ratio $\frac{a(\boldsymbol{\sigma})}{b(\boldsymbol{\sigma})}$ the contribution of the peak with smaller height becomes negligible.

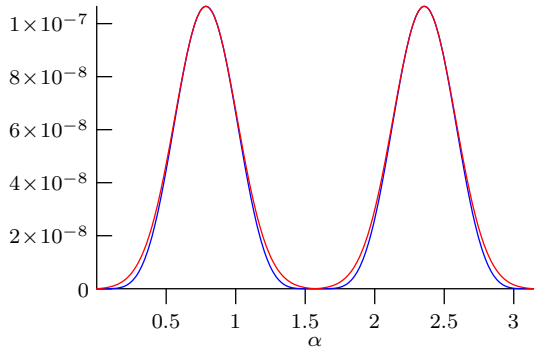

(a) Approximation (red) and actual (blue) damage.

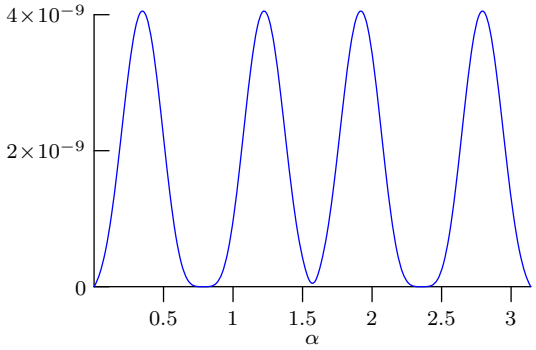

(b) Error $|\hat{d}(\boldsymbol{\sigma}, \alpha) - \tilde{g}(\boldsymbol{\sigma}, \alpha)|$.

Figure B.4.: Approximation around maximum when $\frac{a(\boldsymbol{\sigma})}{b(\boldsymbol{\sigma})} = 0$.

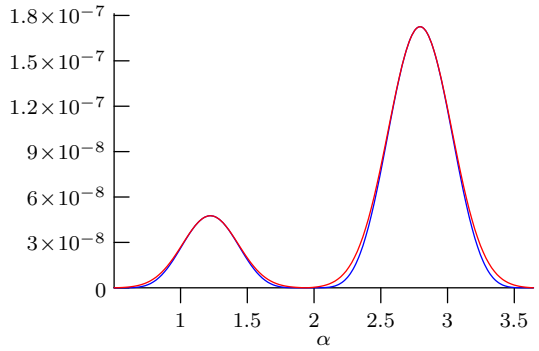

(a) Approximation (red) and actual (blue) damage.

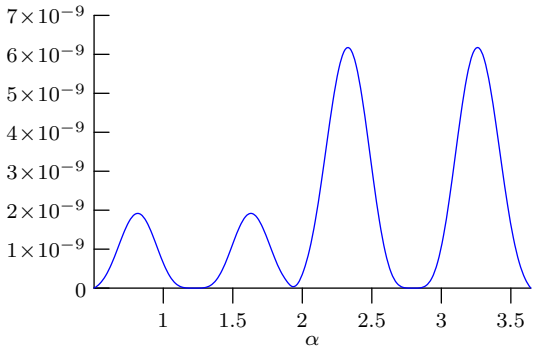

(b) Error $|\hat{d}(\boldsymbol{\sigma}, \alpha) - \tilde{g}(\boldsymbol{\sigma}, \alpha)|$.

Figure B.5.: Approximation around maximum when $\frac{a(\boldsymbol{\sigma})}{b(\boldsymbol{\sigma})} = 0.128$.

C. Algorithms

C.1. 4-Point algorithm

We present in this section the 4-point algorithm as given in [17]. For more information about 4-point algorithm and Rainflow counting in general look at Chapter 3 in [17].

We work with only turning points, which are the local maximum and minimums in a given stress time series. We then discretize these turning points. This sequence of discretized turning points z_i, for $i = 1, \cdots, N$, taking values $1, \cdots, n$, that is the min/max filtering and discretization has already been done. The rainflow matrix RFM has all zeros as its entries and the residual set RES is empty at the beginning. The algorithm as the name suggests works with a stack of 4 points, which is initialized with the first 4 points of the signal $s = [s_1 = z_1, s_2 = z_2, s_3 = z_3, s_4 = z_4]$ and the number of elements in the residual set RES, r is set to zero, $r = 0$. After the initialization step we apply the following counting rule

(c) if $\min(s_1, s_4) \leq \min(s_2, s_3)$ and $\max(s_2, s_3) \leq \max(s_1, s_4)$, then the pair (s_2, s_3) is a cycle,

that is provided s_2, s_3 are contained between s_1, s_4. If this is the case we store the cycle in the matrix $RFM(s_2, s_3) = RFM(s_2, s_3) + 1$. We delete the points s_2, s_3 from the stack. The stack has to be refilled now. The way this is done reflects the memory rules from the hysteresis model. We fill the stack with the points from the residual if possible. In detail, this means (k denotes the next point of the signal z):

(r1) if $r = 0$, then $[s_1 = s_1, s_2 = s_4, s_3 = z_k, s_4 = z_{k+1}]$, and $k = k + 2$

(r2) if $r = 1$, then $[s_1 = RES_r, s_2 = s_1, s_3 = s_4, s_4 = z_k]$, $k = k + 1$ and $r = 0$

(r3) if $r = 2$, then $[s_1 = RES_{r-1}, s_2 = RES_r, s_3 = s_1, s_4 = s_4]$, and $r = r - 2$

Then the counting rule is applied again. If the counting condition (c) is not fulfilled, then

(r4) $r = r + 1, RES_r = s_1, [s_1 = s_2, s_2 = s_3, s_3 = s_4, s_4 = z_k]$, and $k = k + 1$.

This is repeated until the last point of the time signal is reached and (c) does not apply any more. The result of this procedure is the rainflow matrix RFM, containing all close cycles, and the residual RES, containing the remaining sequence of turning points.

C.1.1. The Residual

The residual consists of an increasing part followed by a decreasing part. The residual is very important when short signals are used repeatedly for testing or simulation. If the signal is applied once on the component, some hysteresis cycles result. If we now apply the signal a second time, some other cycles are created. But, if the signal is applied further, the same cycles are created as during the second run.

The *4-point algorithm* gives us RFM which contains all the cycles closing in the first as well as in the second run through the signal. We can study the Residual also by using Rainflow Counting algorithm with an additional counting condition (c1):

(c1) if $u_{s_2} \cdot u_{s_3} < 0$ and $|u_{s_4}| \leq |u_{s_2}| \leq |u_{s_3}|$ then (s_2, s_3) is a cycle,

where u_{s_2} and u_{s_3} are the physical values of the stress corresponding to the bin values s_2 and s_3, respectively.

We start with the 4-point stack $s = [RES_1, RES_2, RES_3, RES_4]$, we check the counting condition (c1). If (c1) is fulfilled, then we remove s_2, s_3 from the stack which is then refilled in similar way as explained above. This gives us only those cycles which close in the first run. We can also get the cycles which close in the second run and all following runs by constructing an intermediate signal y by doubling the residual in the form $y = (RES, RES)$ and applying the 4-point algorithm.

We do not consider the damage due to all cycles closing in only the first run, as they have very negligible influence on the final damage value when we have large number of runs.

C.1.2. Example of Rainflow Counting using 4-Point algorithm

Figure C.1 shows the signal, with discretized turning points, considered for the example. The stress time series is

$$(3, 9, 7, 10, 1, 4, 2, 9, 3, 8, 5, 10, 2, 4, 1)$$

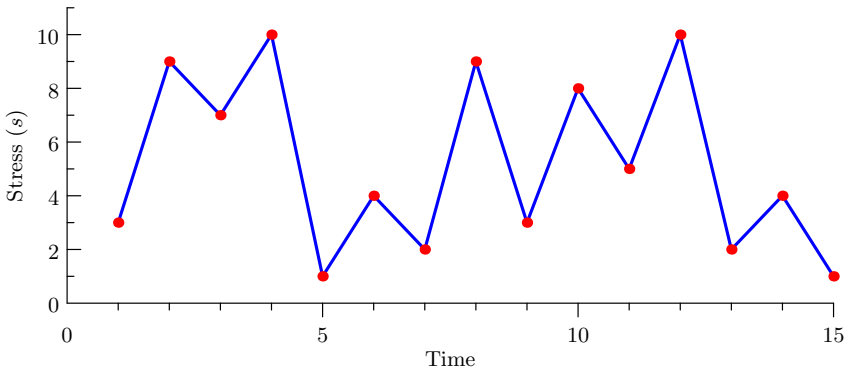

Figure C.1.: A simple stress time series for explaining 4-point method

Applying 4-point algorithm gives the following closed cycles

$$\{(9,7),(4,2),(8,5),(9,3),(2,4)\}$$

and the residual is

$$(3,10,1,10,1)$$

As we can see, the largest load cycle is in the residual, and thus needs to be treated. As explained in the previous section we can compute the cycles in the residual by doubling the residual and making a rainflow count. The 4-point algorithm gives the following cycles in the residual:

$$\{(1,10),(1,10)\}$$

These cycles are formed each time we repeat the load signal.

List of Symbols

Chapter 2	
$D^{(ref)}$	reference damage at some point of the surface
A	the number of available attachment points
A_f	index of the fixation point
A_a	index of the attachment points where actuators are installed
n_a	number of actuators
$\mathcal{TC}$	testrig configuration
$\mathcal{F}$	set of 2-tuples with all the forces/moments acting at attachment points
$\mathbf{x}_i$	location of hotspot with index i
$D_{\mathbf{x}_i}$	total damage at hotspot $\mathbf{x}_i$
$\mathfrak{F}$	the location and direction of forces/moments acting on the component
n	total number of forces/moments acting on the component
$\mathbf{L}$	general load time series
$\mathbf{l}_i$	loads at i-th point of time series
N	the number of points in the load time series
$\mathbf{l}'_j$	the load time series acting at j-th actuator
$\mathbf{0}_n$	vector of size n with all elements zero
ν	the number of times a single unit of the block load is repeated
$\mathscr{B}$	block loading
m	the number of blocks
$\mathscr{L}$	the amplitudes of all the blocks
$\mathcal{V}$	the number of times the single unit of block loads are repeated
$\mathbf{L}_b$	load time series with block loads
$\boldsymbol{\sigma}_\mathbf{x}$	stress at hotspot $\mathbf{x}$
$\tilde{\boldsymbol{\sigma}}_\mathbf{x}$	stress tensor at hotspot $\mathbf{x}$
$\boldsymbol{\Sigma}_\mathbf{x}$	stress time series at hotspot $\mathbf{x}$
s	scalar stress
$\mathbf{n}$	transformation vector to transform stress $\boldsymbol{\sigma}$ to scalar stress s
$\hat{a}(\boldsymbol{\sigma})$	non oscillating component of scalar stress
$b(\boldsymbol{\sigma})$	oscillating component of scalar stress
$a(\boldsymbol{\sigma})$	absolute value of $\hat{a}$
$\mathbf{S}_a$	tuple of alternating stress amplitudes
d	damage from a single alternating stress
$\mathbf{l}_{b,j}$	the amplitudes of the j-th block at each actuator
$\mathbf{L}_{b,a}$	matrix of amplitudes of block loads
$\mathbf{S}_\mathbf{x}$	set of scalar stresses at point $\mathbf{x}$
$\hat{\mathbf{L}}$	vector of amplitudes in $\mathbf{L}_b$
$\hat{\mathbf{S}}_\mathbf{x}$	the scalar stresses at point $\mathbf{x}$ for $\hat{\mathbf{L}}$

$\mathbf{N}$	the matrix with block diagonal entries as $\mathbf{n}$
$\hat{\mathbf{\Sigma}}_{\mathbf{x}}$	the matrix with block diagonal entries given by $\tilde{\boldsymbol{\sigma}}_{\mathbf{x}}$
$\hat{D}_{\mathbf{x}}$	Damage computed from $\hat{\mathbf{L}}$
k	slope in the S-N curve
α	the plane angle

Chapter 3

$\mathfrak{X}$	set of all hotspots
$\sigma^{(ref)}$	reference stress time series
n_h	number of hotspots
N_f	number of points in the reference stress time series
(TSOP)	testrig stress optimization problem
(BOINCQP)	convex quadratic optimization problem with box and inequality constraints
$\mathscr{D}_{\boldsymbol{\sigma}}$	design space of the testrig stress optimization problem
l_{min}	the minimum load that can be applied through the actuators
l_{max}	the maximum load that can be applied through the actuators
$\mathcal{S}$	the vector of scalar stresses
$\widetilde{\Sigma}$	a block row matrix with elements $\mathbf{x}_i$ for all hotspots
$\mathcal{L}_{\boldsymbol{\sigma}}$	set of all feasible solutions for testrig stress optimization problem
η	objective function for testrig stress optimization problem
$\mathscr{D}_D$	the design space of the testrig damage optimization problem
σ_{max}	the maximum stress allowed to develop in the component
$(WSDP)$	testrig damage optimization problem
$Z_{\mathcal{Z},W}$	weighted sum objective function for the (WSDP)
ζ_i	the objective function in the testrig optimization problem
$\widetilde{D}_{\mathbf{x}_i}$	maximum total damage at hotspot $\mathbf{x}_i$

Chapter 4

$f_{\breve{a},\breve{b},\breve{c}}$	Gaussian function with parameters $\breve{a}$, $\breve{b}$ and $\breve{c}$
$\breve{a}$	the maximum value of the Gaussian function
$\breve{b}$	the point of maximum of the Gaussian function
$\breve{c}$	such that $\breve{b} \pm \frac{\breve{c}}{\sqrt{2}}$ are inflexion points
$\mathbb{R}_+$	positive real numbers
σ_e	the stress at any point on the S-N curve
N_e	the number of cycles for the component to fail for alternating stress σ_e
$\hat{d}$	the damage from a single block
g	the approximation of damage for the case $a(\boldsymbol{\sigma}) \geq b(\boldsymbol{\sigma})$
$\tilde{g}$	the approximation of damage for the case $a(\boldsymbol{\sigma}) < b(\boldsymbol{\sigma})$
$\hat{g}$	simplified approximation of damage for the case $a(\boldsymbol{\sigma}) < b(\boldsymbol{\sigma})$

Chapter 5

$\mathcal{G}$	sum of Gaussian functions
φ	the fixed point operator for finding critical points
p_{ij}	measure of closeness of the i-th and the j-th Gaussian functions in the sum $\mathcal{G}$
n_g	number of Gaussian functions

$\mathfrak{C}$	a general cluster
$\hat{\mathscr{C}}$	a general clustering
$\mathfrak{D}_{\mathfrak{C}}$	within-cluster distance
$\mathscr{C}$	Gaussian clustering
$\mathfrak{D}_{\mathfrak{C}_i,\mathfrak{C}_j}$	between-cluster distance
$\hat{m}^*$	number of maxima of sum $\mathcal{G}$
$\alpha_{\mathfrak{C}}$	approximate maximum of cluster $\mathfrak{C}$

Chapter 6

G	total damage as sum of Gaussian functions
$\mathcal{I}_g$	the set of indices of block loads with $a(\boldsymbol{\sigma}) \geq b(\boldsymbol{\sigma})$
$\mathcal{I}_l$	the set of indices of block loads with $a(\boldsymbol{\sigma}) < b(\boldsymbol{\sigma})$

Bibliography

[1] A. Ahmadi, H Mauch, and G. Bremer. Entwicklung von prfszenarien mittels der numerischen betriebsfestigkeitssimulation. *33.VDI Jahrestagung Schadensanalyse, Wrzburg 2007*.

[2] WAJ Albert. Über treibseile am harz. *Archiv für Mineralogie, Geognosie, Bergbau und Hüttenkunde*, 10:215–234, 1837.

[3] N. N. Aprausheva, N. Mollaverdi, and S. V. Sorokin. Bounds for the number of modes of the simplest gaussian mixture. *International Conference on Pattern Recognition and Image Analysis: New Information Technologies*, 7:677–681, 2004.

[4] Stefan Banach. Sur les opérations dans les ensembles abstraits et leur application aux équations intégrales. *Fund. Math.*, 3:133–181, 1922.

[5] K. G. Binmore. *Mathematical Analysis: A Straightforward Approach*. Cambridge University Press, Cambridge, United Kingdom, 1982.

[6] Martin Brokate, Klaus Dressler, and Pavel Krejci. Rainflow counting and energy dissipation for hysteresis models in elastoplasticity. *European Journal of Mechanics A/Solids*, 15(4):705–737, 1996.

[7] M. A. Carreira-Perpiñán. Mode-finding for mixtures of gaussian distributions. *IEEE Transactions on Pattern Analysis and Machine Intelligence*, 22:1318–1323, 2000.

[8] J. A. Collins. *Failure of Materials in Mechanical Design: Analysis, Prediction, Prevention*. Wiley-Interscience publication. Wiley, 1993.

[9] JB De Jonge. *The analysis of load-time histories by means of counting methods*. Nationaal Lucht-en Ruimtevaartlaboratorium, 1982.

[10] John Draper. *Modern metal fatigue analysis*. EMAS, 2008.

[11] M. Ehrgott. *Multicriteria Optimization*. Springer, 2006.

[12] T. Endo, K. Mitsunaga, H. Nakagawa, and K. Ikeda. Fatigue of metals subjected to varying stress–low cycle, middle cycle fatigue. In *Preliminary Proceedings of the Chugoku-Shikoku District Meeting*, pages 41–44, 1967.

[13] Ali Fatemi and Darrell F. Socie. A critical plane approach to multiaxial fatigue damage including out-of-phase loading. *Fatigue & Fracture of Engineering Materials & Structures*, 11(3):149–165, 1988.

[14] I. M. Gelfand and M. E. Saul. *Trigonometry*. Gel'fand School Outreach Program Series. Birkhäuser Boston, 2001.

[15] Lalit Gupta and Thotsapon Sortrakul. A gaussian-mixture-based image segmentation algorithm. *Pattern Recognition*, 31(3):315–325, 1998.

[16] Christian Hennig. Methods for merging gaussian mixture components. *Advances in Data Analysis and Classification*, 4(1):3–34, 2010.

[17] P. Johannesson and M. Speckert. *Guide to Load Analysis for Durability in Vehicle Engineering*. Automotive Series. John Wiley & Sons, 2013.

[18] W. H. Kim and C. Laird. Crack nucleation and stage I propagation in high strain fatigue—II. mechanism. *Acta Metallurgica*, 26(5):789 – 799, 1978.

[19] Konrad Knopp. *Infinite Sequences and Series*. Dover Publications, New York, United States, 1956.

[20] Y. L. Lee, J. Pan, R. Hathaway, and M. Barkey. *Fatigue Testing and Analysis: Theory and Practice*. Elsevier Science, 2011.

[21] T. H. Lin. Fatigue crack initiation. Technical report, DTIC Document, 1991.

[22] M. Matsuishi and T. Endo. Fatigue of metals subjected to varying stress. *Japan Society of Mechanical Engineers, Fukuoka, Japan*, pages 37–40, 1968.

[23] Milton A. Miner. Cumulative damage in fatigue. *Journal of applied mechanics*, 12(3):159–164, 1945.

[24] H. Naunheimer. *Automotive Transmissions: Fundamentals, Selection, Design and Application*. Springer, 2010.

[25] T. Nicholas and J. R. Zuiker. On the use of the goodman diagram for high cycle fatigue design. *International Journal of Fracture*, 80(2-3):219–235, 1989.

[26] A. Z. Palmgren. Die lebensdauer von kugellagern. *Zeitschrift des Vereins Deutscher Ingenieure*, 68:339–341, 1924.

[27] Jinsoo Park and Drew Nelson. Evaluation of an energy-based approach and a critical plane approach for predicting constant amplitude multiaxial fatigue life. *International Journal of Fatigue*, 22(1):23–39, 2000.

[28] A. D. Polyanin and A. I. Chernoutsan. *A Concise Handbook of Mathematics, Physics, and Engineering Sciences*. Taylor & Francis, 2010.

[29] William John Macquorn Rankine. On the causes of the unexpected breakage of the journals of railway axles; and on the mean of preventing such accidents by observing the law of continuity in their construction. *Journal of the Franklin Institute*, 36(3):178–180, 1843.

[30] Surajit Ray and Bruce G Lindsay. The topography of multivariate normal mixtures. *Annals of Statistics*, pages 2042–2065, 2005.

[31] Douglas Reynolds. Gaussian mixture models. *Encyclopedia of Biometric Recognition*, 2008.

[32] Douglas A. Reynolds. Speaker identification and verification using gaussian mixture speaker models. *Speech communication*, 17(1):91–108, 1995.

[33] Douglas A. Reynolds, Thomas F. Quatieri, and Robert B Dunn. Speaker verification using adapted gaussian mixture models. *Digital signal processing*, 10(1):19–41, 2000.

[34] D. Roylance. Transformation of stresses and strains. Lecture Notes for Mechanics of Materials, May 2001.

[35] Igor Rychlik. A new definition of the rainflow cycle counting method. *International journal of fatigue*, 9(2):119–121, 1987.

[36] Walter Schütz. A history of fatigue. *Engineering Fracture Mechanics*, 54(2):263 – 300, 1996.

[37] Luca Susmel. A simple and efficient numerical algorithm to determine the orientation of the critical plane in multiaxial fatigue problems. *International Journal of Fatigue*, 32(11):1875–1883, 2010.

[38] Antonio Vecchio, Reinhold Carmine, Renaud De Voghel, Geert Van Der Linden, and Patrick Guillaume. Numerical evaluation of damage distribution over a slat track using flight test data. *Proc. IMAC XXI, Orlando, FL, USA*, 2003.

[39] Y. Zhang and Q. Liu. Reliability-based design of automobile components. *Proceedings of the Institution of Mechanical Engineers, Part D: Journal of Automobile Engineering*, 216(6):455–471, 2002.

Lebenslauf des Verfassers

Oct 2010–Dec 2013	Promotionsstudent in Mathematik an der Technischen Universität Kaiserslautern (Stipendiat des DAAD und des Fraunhofer ITWM).
Oct 2008–Sep 2010	Master in Technomathematik an der Technischen Universität Kaiserslautern. Master in Industriemathematik an der Johannes Kepler Universität, Linz, Österreich. Titel der Masterarbeit: Generalized Penalty Methods for the Signorini's problem. Double-Degree-Programm gefördert durch ein Erasmus Mundus Stipendium.
Jul 2004–Jul 2008	Bachelor of Engineering in Mechanical Engineering am Delhi College of Engineering Titel of Bachelorarbeit: Quality Improvement through Reengineering

The Author's Scientific Career

Oct 2010–Dec 2013	PhD candidate in Mathematics at the Technical University of Kaiserslautern (funded by a scholarship of the DAAD and Fraunhofer ITWM).
Oct 2008–Sep 2010	Master in Industrial Mathematics at the Technical University of Kaiserslautern, Germany. Master in Industrial Mathematics at the Johannes Kepler University, Linz, Austria. Title of Master Thesis: Generalized Penalty Methods for the Signorini's problem. Double masters program funded by the Erasmus Mundus Scholarship.
Jul 2004–Jul 2008	Bachelor of Engineering in Mechanical Engineering at Delhi College of Engineering Title of Bachelor Thesis: Quality Improvement through Reengineering

ee